



Dietz, Jonathan David (2018) *Lithofacies architecture and facies models of volcanic, volcanoclastic and sedimentary rocks in the Hreppar Formation, Iceland: understanding hydrocarbon prospects in volcanic rifted margins*. PhD thesis.

<https://theses.gla.ac.uk/30927/>

Copyright and moral rights for this work are retained by the author

A copy can be downloaded for personal non-commercial research or study, without prior permission or charge

This work cannot be reproduced or quoted extensively from without first obtaining permission in writing from the author

The content must not be changed in any way or sold commercially in any format or medium without the formal permission of the author

When referring to this work, full bibliographic details including the author, title, awarding institution and date of the thesis must be given

Enlighten: Theses

<https://theses.gla.ac.uk/>  
[research-enlighten@glasgow.ac.uk](mailto:research-enlighten@glasgow.ac.uk)

# **Lithofacies architecture and facies models of volcanic, volcanoclastic and sedimentary rocks in the Hreppar Formation, Iceland: understanding hydrocarbon prospects in volcanic rifted margins**

**Jonathan David Dietz**

BSc (Hons), University of Glasgow  
MSc, University of Aberdeen

Submitted in fulfilment of the requirements for the Degree of Doctor of Philosophy

School of Geographical and Earth Sciences

College of Science and Engineering

University of Glasgow

October 2018

©Jonathan Dietz, 2018

---

## Abstract

Predicting the geometry and continuity of clastic units within lava-dominated sequences in volcanic margin settings is problematic as they are typically laterally discontinuous, relatively thin and often poorly imaged in the subsurface. Although such sequences are well known, detailed studies of their lithofacies architecture are rare and poorly constrained, which can result in major challenges to hydrocarbon exploration in these settings. As the demand for hydrocarbons increases, exploration is being focussed on more challenging stratigraphic and tectonic settings, such as volcanic margins. Consequently, it is necessary we enhance our understanding of how petroleum systems interact with volcanic-prone sequences, in order to maximise recovery of hydrocarbons. Using a field analogue in conjunction with remote sensing datasets is fundamental to understanding these complicated systems. This study utilises the Hreppar Formation (HF) in SW Iceland as an analogue to understand elements of petroleum systems to reduce the challenges and risk associated with hydrocarbon exploration within volcanic-dominated basins.

The HF at Flúðir, comprises basaltic lavas and interbasaltic sedimentary rocks of Plio-Pleistocene age (3.3-0.7Ma) and provides excellent 3D exposure. This study provides a comprehensive evaluation of the geology in this area and its relevance and importance to hydrocarbon exploration.

Detailed field mapping and graphic logging have been combined with field panoramas and photogrammetry to characterise the sequence in detail and to identify the lateral (dis)connectivity of the clastic units, the main lithofacies, the different facies architectures, structural elements and drainage pathways within the HF.

The detailed field data presented here are generally all below seismic resolution. In an offshore setting, with currently available technology, it is highly unlikely this level of detail can be captured using remote sensing tools alone. The advantage of using a field analogue such as that of the HF is the level of detail which can be captured. This enables the gap in scale, between field-scale and seismic/well-scale to be bridged. It allows models to be ground truthed, which reduces uncertainty and risk, essential to hydrocarbon exploration.

This research identifies complex interaction between volcanic, glacial and fluvial systems, underpinned by a strong tectonic influence. >60% of the HF is dominated by sub-aerial basaltic lavas and predicting where lithofacies occur in these types of environments is challenging, however through initial quantitative analysis of volcanic and sedimentary units in the HF, basic prediction in similar settings is possible.

The field data collected in the HF can inform every stage of the development of a hydrocarbon field in a volcanic margin, from determining the architecture of a potential reservoir to defining the main structures and potential fluid pathways as well as deciding how to produce the field.

Abstract .....	II
List of Figures .....	IX
List of tables .....	XI
Acknowledgements .....	XII
Author's Declaration.....	XIV
Definitions/Abbreviations.....	XV
<b>1 Introduction .....</b>	<b>1</b>
1.1 Research Rationale .....	1
1.2 Research aims and objectives .....	3
1.3 Project outline .....	5
<b>2 Regional setting.....</b>	<b>7</b>
2.1 Introduction.....	7
2.2 Iceland .....	7
2.2.1 Plume or non-plume origin for Iceland .....	9
2.2.2 Onshore Iceland .....	9
2.3 Glaciation in Iceland.....	11
2.4 South Iceland and the Hreppar Formation.....	12
<b>3 Geological terms and nomenclature.....</b>	<b>15</b>
3.1 Introduction.....	15
3.2 Lava types .....	15
3.2.1 'A'ā lava flows .....	16
3.2.2 Pāhoehoe lava flows.....	17
3.2.3 Effusion rates and emplacement mechanisms.....	18
3.3 Volcaniclastic rocks.....	22
3.3.1 Fisher (1961).....	23
3.3.2 Cas and Wright (1987).....	23
3.3.3 McPhie et al (1993) .....	25
3.3.4 White and Houghton (2006) .....	25
3.3.5 Sub-divisions of volcaniclastic rocks .....	25
3.3.6 Volcaniclastic deposits in the Hreppar Formation .....	28
<b>4 Methodology and maps .....</b>	<b>31</b>

<b>4.1</b>	<b>Introduction</b> .....	<b>31</b>
<b>4.2</b>	<b>Field methods</b> .....	<b>31</b>
4.2.1	Field mapping .....	31
4.2.2	Logging .....	37
<b>4.3</b>	<b>Laboratory methods</b> .....	<b>38</b>
4.3.1	Samples and petrography .....	38
4.3.2	Photogrammetry .....	38
4.3.3	Synthetic seismic .....	39
<b>5</b>	<b>Lithofacies and descriptions</b> .....	<b>41</b>
<b>5.1</b>	<b>Introduction</b> .....	<b>41</b>
<b>5.2</b>	<b>Ignimbrites</b> .....	<b>45</b>
5.2.1	Lava-like ignimbrite (A1) .....	47
5.2.2	Massive lapilli tuff (A2) .....	51
<b>5.3</b>	<b>Sub-aerial basaltic lavas</b> .....	<b>53</b>
5.3.1	Pāhoehoe basalt lava with clinker top (B1) .....	55
5.3.2	Pāhoehoe basalt lava; large columnar jointing (B2) .....	59
5.3.3	Pāhoehoe basalt lava; poorly defined tops and bottoms (B3) .....	64
5.3.4	Pāhoehoe lava with colonnade and entablature (B4) .....	66
<b>5.4</b>	<b>Primary hyaloclastite and pillow breccia</b> .....	<b>70</b>
5.4.1	Primary hyaloclastite and pillows (C1) .....	73
5.4.2	Primary hyaloclastite and pillow fragments (C2) .....	77
<b>5.5</b>	<b>Reworked hyaloclastite</b> .....	<b>80</b>
5.5.1	Massive reworked hyaloclastite (D1) .....	82
5.5.2	Stratified reworked hyaloclastite (D2) .....	84
<b>5.6</b>	<b>Conglomerate</b> .....	<b>87</b>
5.6.1	Fluvial derived conglomerate (E1) .....	88
5.6.2	Glacial derived conglomerate (E2) .....	92
5.6.3	Mass flow derived conglomerate (E3) .....	95
<b>5.7</b>	<b>Sandstone</b> .....	<b>98</b>
5.7.1	Stratified sandstone (F1) .....	98
<b>5.8</b>	<b>Sandstone and siltstone</b> .....	<b>102</b>
5.8.1	Alternating siltstone and sandstone units (G1) .....	102
<b>5.9</b>	<b>Conclusions</b> .....	<b>108</b>
<b>6</b>	<b>Lithofacies successions</b> .....	<b>109</b>
<b>6.1</b>	<b>Introduction</b> .....	<b>109</b>
<b>6.2</b>	<b>Sub-aerial lava, hyaloclastite and re-worked hyaloclastite</b> .....	<b>113</b>
6.2.1	Description of panorama 1 .....	113
6.2.2	Interpretation of panorama 1 .....	116
<b>6.3</b>	<b>Sub-aerial lava, conglomerate and fluvial sandstone</b> .....	<b>117</b>

6.3.1	Description of panorama 2 .....	117
6.3.2	Interpretation of panorama 2 .....	120
<b>6.4</b>	<b>Sub-aerial lavas, hyaloclastite, conglomerate and fluvial sandstone.....</b>	<b>121</b>
6.4.1	Description of panorama 3 .....	121
6.4.2	Interpretation of panorama 3 .....	124
<b>6.5</b>	<b>Conglomerate, hyaloclastite and sub-aerial lava .....</b>	<b>125</b>
6.5.1	Description of panorama 4 .....	125
6.5.2	Interpretation of panorama 4 .....	128
<b>6.6</b>	<b>Sub-aerial lava, fluvial sandstone and conglomerate.....</b>	<b>129</b>
6.6.1	Description of panorama 5 .....	129
6.6.2	Interpretation of panorama 5 .....	132
<b>6.7</b>	<b>Sub-aerial lava, sandstone/siltstone and hyaloclastite.....</b>	<b>133</b>
6.7.1	Description of panorama 6 .....	133
6.7.2	Interpretation of panorama 6 .....	136
<b>6.8</b>	<b>Sub-aerial lava, conglomerates, hyaloclastite and fluvial sandstone.....</b>	<b>137</b>
6.8.1	Description of panorama 7 .....	137
6.8.2	Interpretation of panorama 7 .....	141
<b>6.9</b>	<b>Sub-aerial lava, fluvial sandstone, conglomerate and ignimbrites.....</b>	<b>142</b>
6.9.1	Description of panorama 8 .....	142
6.9.2	Interpretation of panorama 8 .....	145
<b>6.10</b>	<b>Conclusions.....</b>	<b>146</b>
<b>7</b>	<b>Stora Laxa case study .....</b>	<b>147</b>
<b>7.1</b>	<b>Introduction.....</b>	<b>147</b>
<b>7.2</b>	<b>Field relationships and environments of deposition.....</b>	<b>149</b>
7.2.1	Stora Laxa section 1 .....	149
7.2.2	Stora Laxa section 2 .....	152
7.2.3	Stora Laxa section 3 .....	157
7.2.4	Stora Laxa section 4 .....	161
7.2.5	Stora Laxa section 5 .....	171
7.2.6	Stora Laxa section 6 .....	177
7.2.7	Stora Laxa section 7 .....	180
7.2.8	Stora Laxa section 8 .....	184
7.2.9	Stora Laxa section 9 .....	187
7.2.10	Stora Laxa section 10.....	197
<b>7.3</b>	<b>Stora Laxa summary.....</b>	<b>199</b>
<b>7.4</b>	<b>Conclusions.....</b>	<b>201</b>
<b>8</b>	<b>Integrated stratigraphic and structural model .....</b>	<b>202</b>
<b>8.1</b>	<b>Introduction.....</b>	<b>202</b>
<b>8.2</b>	<b>Evidence of tectonic setting in the HF .....</b>	<b>205</b>

<b>8.3</b>	<b>Cross sections of the Hreppar Formation .....</b>	<b>212</b>
8.3.1	Cross section 1 (E7, F7, E8, F8).....	212
8.3.2	Cross section 2 (F6).....	216
8.3.3	Cross section 3 (C9, D9).....	218
8.3.4	Cross section 4 (E9, F9) .....	220
<b>8.4</b>	<b>Tectonic evolution of the Hreppar Formation .....</b>	<b>223</b>
<b>8.5</b>	<b>Koehn / Bubeck model .....</b>	<b>223</b>
<b>8.6</b>	<b>Passerini, 1997 model .....</b>	<b>228</b>
<b>8.7</b>	<b>Clifton and Kattenhorn, 2006 model.....</b>	<b>230</b>
<b>8.8</b>	<b>Tectonic summary of the Hreppar Formation.....</b>	<b>233</b>
<b>8.9</b>	<b>Conclusions.....</b>	<b>235</b>
<b>9</b>	<b>Discussion .....</b>	<b>236</b>
<b>9.1</b>	<b>Introduction.....</b>	<b>236</b>
<b>9.2</b>	<b>Volcano-sedimentary settings away from the HF.....</b>	<b>236</b>
9.2.1	Höfðasandur, Iceland.....	236
9.2.2	Blue Nile and Afar region, Ethiopia .....	242
<b>9.3</b>	<b>Modern analogues; Iceland.....</b>	<b>250</b>
9.3.1	Proglacial lakes.....	250
9.3.2	Braided fluvial systems .....	255
9.3.3	Lava extrusion in the Hreppar Formation .....	259
<b>9.4</b>	<b>Spatial distribution of lithofacies in the HF .....</b>	<b>262</b>
9.4.1	Normalised log data .....	262
9.4.2	Actual log data .....	263
9.4.3	Lavas and fluvial sediment thickness .....	265
<b>9.5</b>	<b>HF model .....</b>	<b>272</b>
<b>9.6</b>	<b>Hydrocarbon implications .....</b>	<b>275</b>
9.6.1	General issues surrounding hydrocarbon exploration in volcanics .....	277
9.6.2	Sub basalt imaging.....	277
9.6.3	Drilling through volcanics (basalt) .....	284
9.6.4	Connectivity in volcanic dominated environments .....	286
<b>9.7</b>	<b>The Hreppar Formation as an analogue .....</b>	<b>290</b>
<b>9.8</b>	<b>Future exploration within volcanic dominated settings .....</b>	<b>293</b>
<b>9.9</b>	<b>Conclusions.....</b>	<b>294</b>
<b>10</b>	<b>Conclusions and further work.....</b>	<b>295</b>
<b>10.1</b>	<b>Main findings of this work.....</b>	<b>295</b>
<b>10.2</b>	<b>Further work.....</b>	<b>297</b>

---

11	Appendix .....	299
12	References .....	304

## List of Figures

Figure 1-1 Map of the world, indicating large igneous .....	2
Figure 2-1 Location map of Iceland after (Thordarson et al, 2014).....	7
Figure 2-2 Simplified geological map of Iceland. ....	8
Figure 2-3 General structure of the Icelandic crust (after, Thordarson and Höskuldsson, 2014). ..	11
Figure 2-4 Glacial ice extent in Iceland. ....	12
Figure 2-5 Location of the Hreppar Formation. ....	13
Figure 3-1 Sketch diagram of compound and simple lava flows .....	16
Figure 3-2 Summary figure of lava types. ....	18
Figure 3-3 Development of a pāhoehoe lava flow over time.....	20
Figure 3-4 Summary of the main volcanioclastic nomenclature schemes .....	24
Figure 3-5 Summary figure of volcanioclastic rocks. ....	28
Figure 3-6 Approach to volcanioclastic nomenclature in the HF.....	30
Figure 4-1 Selection of maps, .....	33
Figure 4-2 Geological map of the HF at Flúðir (situated 2 km WSW of the map).....	34
Figure 4-3 Part 1 lithofacies key and codes.....	35
Figure 4-4 Part 2 lithofacies key and codes.....	36
Figure 4-5 Example log section. ....	37
Figure 4-6 Example workflow and how the drone is flown in the field.....	40
Figure 5-1 The main lithofacies of the Hreppar Formation and their associated sub-facies. ....	42
Figure 5-2 Graph demonstrating the frequency of certain thicknesses of lavas .....	44
Figure 5-3 Lava-like ignimbrites of the Hreppar Formation. ....	49
Figure 5-4 Petrography of A1. ....	50
Figure 5-5: Massive lapilli tuff. ....	52
Figure 5-6 Petrography of A2. ....	52
Figure 5-7 Typical large and small scale features of B1. ....	58
Figure 5-8 Petrography of B1.....	59
Figure 5-9 Typical features of B2 lavas.....	62
Figure 5-10 Petrography of B2. ....	63
Figure 5-11 Typical large and small scale features of B3.....	65
Figure 5-12 Petrography of B3 .....	66
Figure 5-13 Typical features of B4 lavas .....	68
Figure 5-14 Petrography of B4. ....	69
Figure 5-15 Features of C1 primary hyaloclastite.....	75
Figure 5-16 Petrography of C1 .....	76
Figure 5-17 Features of C2 primary hyaloclastite.....	78
Figure 5-18 Petrography of C2. ....	79
Figure 5-19 Features of D1 re-worked hyaloclastite.....	83
Figure 5-20 Petrography of D1. ....	84
Figure 5-21 Features of D2 re-worked hyaloclastite.....	86
Figure 5-22 Features of E1 conglomerate .....	91
Figure 5-23 Characteristics of E2 conglomerates .....	94
Figure 5-24 Features of E3 conglomerates.....	97
Figure 5-25 Characteristics of F1 sandstones.....	100
Figure 5-26 Petrography of F1. ....	101
Figure 5-27 Characteristics of G1 sedimentary rocks .....	105
Figure 5-28 Petrography of G1.....	106
Figure 5-29 Petrography of tuff/sand injectite horizon. ....	107
Figure 6-1 Geological map of the Hreppar Formation at Flúðir. ....	110
Figure 6-2 Lithofacies codes of the Hreppar Formation. ....	111
Figure 6-3 Lithofacies codes of the Hreppar Formation .....	112
Figure 6-4 Location of panorama 1.....	113
Figure 6-5 Details of panorama, highlighting the relationships between D2, C2 and B3. ....	115
Figure 6-6 Location of panorama 2,.....	117
Figure 6-7 Panorama 2 highlights the main relationship between lithofacies B1, E3 and F1. ....	119
Figure 6-8 Location of panorama 3.....	121
Figure 6-9 Details of panorama 3.....	123
Figure 6-10 Location of panorama 5 .....	125
Figure 6-11 Panorama 4 documents the relationship between lithofacies E2, C2 and B3. ....	127
Figure 6-12 Location of panorama 5 .....	129
Figure 6-13 Panorama 5 documents the relationship between lithofacies B1, F1, E3 and B2. ...	131

Figure 6-14 Location of panorama 6 .....	133
Figure 6-15 Panorama 6 documents the relationship between lithofacies B2, G1 and C1. ....	135
Figure 6-16 Location of panorama 7 .....	137
Figure 6-17 Details of panorama 7 .....	140
Figure 6-18 Location of panorama 8 .....	142
Figure 6-19 Details of panorama 8 .....	144
Figure 7-1 Inset map of the Stora Laxa river section.....	148
Figure 7-2 Sketch illustration of the main units within the section.....	150
Figure 7-3 Panorama of section 1 .....	151
Figure 7-4 Panorama of section 2 .....	153
Figure 7-5 Block diagram of fissure eruptions.....	154
Figure 7-6 Block diagram of the development of a braided fluvial system. ....	155
Figure 7-7 Block diagram of sub-aerial lavas entering a water body .....	156
Figure 7-8 Sketch illustration of section 3 .....	158
Figure 7-9 Panorama of section 3 .....	159
Figure 7-10 Panorama of section 4.....	162
Figure 7-11 Details of sub-aerial lavas filling pre-existing topography. ....	164
Figure 7-12 Block diagram of a braided fluvial system.....	165
Figure 7-13 Block diagram of sub-aerial lavas following a pre-existing drainage network. ....	166
Figure 7-14 Block diagram of continued extrusion of lava. ....	167
Figure 7-15 Block diagram of the development of debris flow deposits .....	168
Figure 7-16 Block diagram of the re-establishment of a fluvial system. ....	169
Figure 7-17 Block diagram of a braided fluvial system.....	170
Figure 7-18 Faulting within section 5. ....	172
Figure 7-19 Panorama of section 5.....	175
Figure 7-20 Panorama of section 6.....	178
Figure 7-21 Panorama of section 7.....	182
Figure 7-22 Rotational landslide.....	183
Figure 7-23 Panorama of section 8.....	185
Figure 7-24 Panorama of section 9.....	188
Figure 7-25 Details of the lacustrine unit featured in Figure 7 19. ....	190
Figure 7-26 Block diagram of the extrusion of sub-aerial lavas .....	191
Figure 7-27 Block diagram of the development of small water bodies. ....	192
Figure 7-28 Block diagram of coalesced water bodies. ....	193
Figure 7-29 Block diagram of coalesced water bodies. ....	194
Figure 7-30 Block diagram of a lacustrine setting dominated by sub-aerial lavas.....	195
Figure 7-31 Panorama of section 10 .....	198
Figure 7-32 Generalised vertical section of the Stora Laxa river section. ....	200
Figure 8-1 Iceland structural map with the main direction of plate movement highlighted. ....	203
Figure 8-2 Geomorphology of the Hreppar Formation with Flúðir and Hrúni marked.....	204
Figure 8-3 Uninterpreted photogrammetry model and interpreted model, .....	207
Figure 8-4 Uninterpreted photogrammetry model and interpreted model .....	208
Figure 8-5 Uninterpreted photogrammetry model and interpreted model .....	209
Figure 8-6 Photogrammetry model, highlighting the main faults within the Stora Laxa river section .....	210
Figure 8-7 Looking SW in the HF at Flúðir with the main rivers (Stora Laxa and Lita Laxa) highlighted. ....	211
Figure 8-8 HF geological map with grid square location of cross sections .....	213
Figure 8-9 Faulted relationships between different outcrops. ....	214
Figure 8-10 Faulted relationships of outcrops D and E.....	217
Figure 8-11 Faulted relationships between outcrops F and G.....	219
Figure 8-12 Complex faulted relationships in the Stora Laxa river. ....	222
Figure 8-13 Conceptual diagrams of the Koehn and Bubeck et al models. ....	224
Figure 8-14 Koehn 2008/ Bubeck et al model. ....	226
Figure 8-15 Koehn 2008/ Bubeck et al model. ....	227
Figure 8-16 Passerini et al 1991, 1997 model. ....	229
Figure 8-17 Clifton and Kattenhorn modelled faults and fractures applied to the HF. ....	232
Figure 8-18 Summarised models of Koehn/Bubeck, Passerini and Clifton and Kattenhorn.....	234
Figure 9-1 Lava field development around Höfðasandur. ....	237
Figure 9-2 Continued lava field development around Höfðasandur.....	239
Figure 9-3 Final stages of lava field development around Höfðasandur.....	241
Figure 9-4 Lava field development in Ethiopia. ....	243
Figure 9-5 Lava field development of the Afar region, Ethiopia. ....	245

Figure 9-6 Continued lava field development of the Afar region, Ethiopia.....	246
Figure 9-7 Final stages of lava field development in the Afar region.....	249
Figure 9-8 Aerial images of examples of lake bodies.....	251
Figure 9-9 Aerial panorama of the mouth of the Sólheimajökull glacier.....	253
Figure 9-10 Photogrammetry model of the Sólheimajökull glacier mouth.....	254
Figure 9-11 Two examples of braided river systems in Iceland.....	257
Figure 9-12 Overview images of braided river systems in Iceland. ....	258
Figure 9-13 Modern day landscape .....	260
Figure 9-14 Looking NW in the Hreppar Formation to the Icelandic Highlands. ....	261
Figure 9-15 Hreppar Formation area map with normalised percentages of units.....	264
Figure 9-16 Non-normalised log data from the HF.....	267
Figure 9-17 Thickness of sub-aerial lavas and fluvial sandstones. ....	268
Figure 9-18 Palaeoflow directions from the HF. ....	269
Figure 9-19 Average fluvial sediment grain size. ....	270
Figure 9-20 Thickness of lava flows within the HF.....	271
Figure 9-21 Thickness of sandstone units within the HF.....	271
Figure 9-22 Thickness of mass flows units within the HF. ....	272
Figure 9-23 Distinctive B3 lava unit.....	273
Figure 9-24 Conceptual development of the HF at Flúðir. ....	274
Figure 9-25 Map of the world, indicating large igneous .....	276
Figure 9-26 Volcanic and volcanoclastic cover in the FSB.....	278
Figure 9-27 Seismic images across the Faroe-Shetland Basin. ....	279
Figure 9-28 Synthetic seismic images.....	282
Figure 9-29 Synthetic seismic images.....	283
Figure 9-30 Caliper log responses of various volcanic facies.....	286
Figure 9-31 Large dyke within the HF compartmentalising the system. ....	288
Figure 9-32 Outcrop within the HF to be considered in the subsurface.....	289
Figure 9-33 Comparison of scale.....	292
Figure 9-34 Integration of data. ....	293
Figure 11-1 Graphic logs of the HF, 1-10.....	299
Figure 11-2 Graphic logs of the HF, 11-20. ....	300
Figure 11-3 Graphic logs of the HF, 21-30. ....	301
Figure 11-4 Graphic logs of the HF, 41-50. ....	302
Figure 11-5 Graphic logs of the HF, 51-62. ....	303

## List of tables

Table 5-1 Quantitative lithofacies data within the HF.....	43
--	----

---

## Acknowledgements

This research has been funded by Statoil UK through the Volcanic Margins Research Consortium. I would like to thank Statoil UK for sponsoring this project and the associated opportunities I have been given.

Firstly, I would like to thank Davie Brown for giving me this fantastic opportunity to travel the world, studying geology, I really have enjoyed it. Thank you for encouraging me when I needed it, for all of the field trips and the associated craic, the wisdom you have imparted and for making me a better geologist, I really appreciate it.

I would like to thank Brian Bell, Dave Ellis and Simon Passey for fieldwork discussions, stories, support and guidance and general field work comradery. Nick Schofield for helping me to learn the intricacies of picking seismic and general support and advice. Rich Walker for helping to find structural evidence in the field, even though there was very little. Rich Brown for everything VMRC related. Thank you also to Thor Thordarson for fieldwork advice and some great conversations in the field.

Thank you to everyone who has been involved with the Volcanic Margins Research Consortium for their positive discussions on fieldtrips, feedback on presentations and the opportunity to run a field trip. Thanks, in particular to Pete Reynolds, Heather Rawcliffe, Tim Watton, Clayton Grove, Liam Holt, Ben Hedley and Kirstie Wright. Finally, thanks to Niall Mark and Douglas Watson for their help in preparing the field guide for the VMRC field trip and presenting on it.

Sapphire, Charlotte, Elisha, Johnny, Pamela, Romain and Dougie for being the best field assistants; not giving up when the rain was sideways and enjoying the delights of Iceland with me. I had a great time. In particular I'd like to thank Charlotte for the debates we had in the field, they really helped my understanding of the area.

I'd also like to thank the members of VO@G (Heather, Charlotte, Sapphire, Pamela and Iain) for the great trips and meals. A special mention to all the other staff at Glasgow (the department wouldn't be the same without you!); Margaret and Jackie for always having the answers to my questions; John for preparing my thin

sections and all the great conversations. Daniel, Rod, Tim, Martin, Nick, Cristina, Amanda, Iain, John, Robert and Peter; for the invaluable advice you have given me, the enjoyable conversations and discussions on field trips, helping me learn how to teach students and answering all of my questions, I really appreciate everything.

Elisha, thank you for your continued support, your unwavering belief in me, listening to my ideas and discussing them, putting up with my moaning, logging in the rain, our adventures outside of a PhD, the list is endless... I wouldn't have been able to do it without you.

Finally, I would like to thank my family; Mum, Dad, Andrew, Auntie Jen and Uncle Steve you have encouraged me throughout this project and have supported me every step of the way, have put up with me whilst writing and fully believed that I could do it. Thank you. To my grandparents, who I wish I could be celebrating with.

## Author's Declaration

I declare that this thesis, except where acknowledged to others, represents my own work carried out in the School of Geographical and Earth Sciences, University of Glasgow. The research submitted here has not been submitted for any other degree at the University of Glasgow, nor at any other institution. Any published or unpublished work by authors has been given full acknowledgement in the text.



Jonathan Dietz

---

## Definitions/Abbreviations

BBOE-Billions of Barrels of Oil Equivalent

EARS- East African Rift System

FSB- Faroe Shetland Basin

HF - Hreppar Formation

NAIP - North Atlantic Igneous Province

VMRC - Volcanic Margins Research Consortium

# 1 Introduction

Hydrocarbon exploration within volcanic dominated basins can present numerous challenges as well as opportunities compared to conventional sedimentary basins. Volcanically dominated basins are generally poorly understood due to the heterogeneity involved in volcanic systems and their relationship with sedimentation. This project uses the Hreppar Formation (HF) in Iceland as a field analogue to better understand how elements of petroleum systems are affected by volcanism.

This project is part of the Volcanic Margins Research Consortium (VMRC), an industry funded consortium consisting of five oil and gas companies (Statoil, Dong, JX Nippon, ENI and Siccar Point Energy) and four universities (Universities of Glasgow, Aberdeen, Durham and Leicester) as well as CASP. The consortium is now at the end of the 2<sup>nd</sup> phase and has funded three other projects. The consortium is a collaboration between industry and academia to better understand the effects and processes of volcanism on petroleum systems and hydrocarbon exploration. This particular study aims to provide a more detailed understanding of the lithofacies architecture of interbedded volcanic, volcanoclastic and sedimentary rocks and their role in potential volcano-sedimentary petroleum systems.

## 1.1 Research Rationale

Large volumes of volcanic rocks are often associated with rifted margins and continental breakup and are found all over the world (Figure 1-1) (e.g. northern, central and southern Atlantic Ocean, southern Red Sea, East Africa, east and west coasts of Australia and India, as well as Antarctica; Menzies et al, 2002). As a result of their association with rifted margins and continental breakup, volcanic rocks are commonly found within sedimentary basins. They can comprise a significant volume of them (Menzies et al, 2002; Geoffroy, 2005). This can present numerous challenges to hydrocarbon exploration in these offshore basins.

Hydrocarbon exploration within frontier basins, dominated by volcanic rocks, such as that of the Faroe-Shetland Basin of the NE Atlantic Margin can be problematic

due to the significant extent of subaerial lava impeding seismic imaging (Poppit et al, 2016).

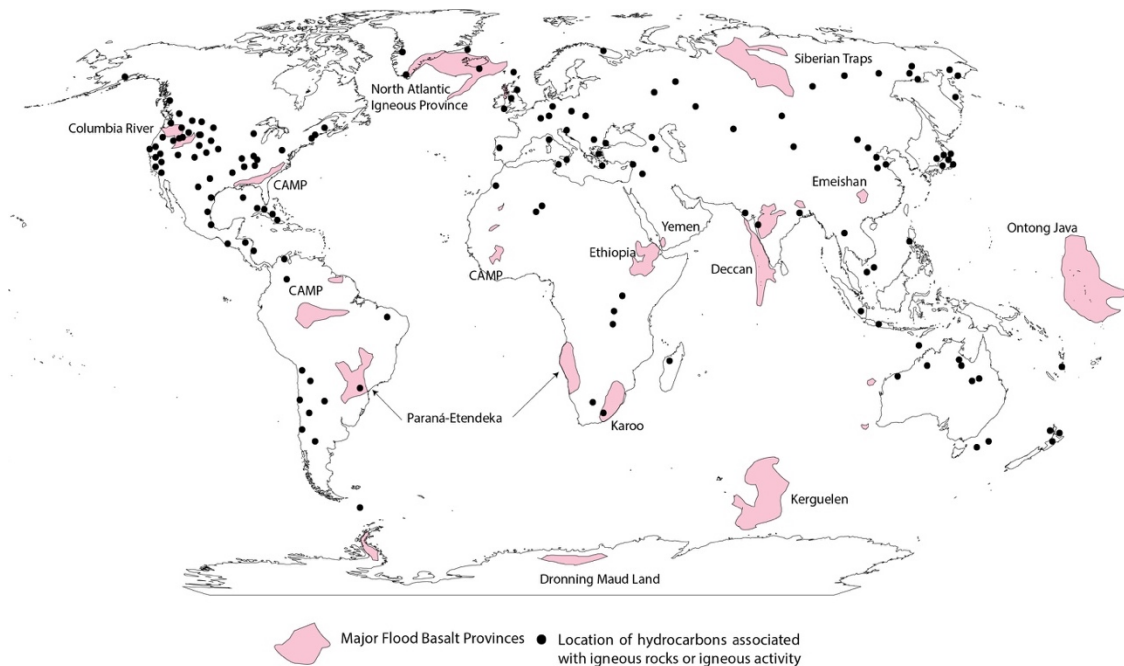


**Figure 1-1 Map of the world, indicating large igneous provinces in pink and black dots signify the presence of hydrocarbons associated with igneous rocks. (After Jerram and Widdowson, 2005; Bryan and Ferrari, 2013; Wright, 2013).**

The FSB and other volcanic dominated basins have proven, large oil and gas discoveries (e.g. the Rosebank, Schiehallion, Clare and Cambo fields are all significant fields in the FSB; Schofield and Jolley, 2013; Muirhead et al, 2017). Within the Rosebank Field, the main reservoir intervals are fluvial clastic sequences which are interbedded with basaltic lavas, hyaloclastites and volcanoclastic sedimentary units (Schofield and Jolley, 2013; Poppit et al, 2016). These types of sequences record the complex interaction of competing volcanic and sedimentary systems; however, even with continued exploration, development and production, these systems remain poorly understood.

Predicting the continuity and lateral extent of clastic units in lava-dominated settings is difficult due to the typically, laterally discontinuous nature of the units. Additionally these units are generally relatively thin and are often poorly imaged in the subsurface due to the overlying lava cover (Woodburn et al, 2014). Although these types of sequences are well known, detailed studies of their lithofacies architecture are rare and poorly constrained, which can result in numerous challenges to hydrocarbon exploration.

Historically, hydrocarbon exploration has targeted petroleum systems in siliciclastic and carbonate rocks, as generally these systems have been easier to explore and produce. However, with the demand for hydrocarbons remaining high, dwindling reserves, and an increasing world population, hydrocarbon exploration has had to focus on more challenging areas (Deloitte, 2015; Biscardini et al, 2017) in order to maintain and increase reserves. These include exploration in to unconventional (coal bed methane, shale gas, shale oil) and in to more complex geology such as sub-salt and sub-basalt exploration. The latter is the primary driver of this project.

Understanding of challenging geological areas such as those affected by volcanism in terms of hydrocarbon exploration are relatively limited as evidenced by the Rosebank Field in the FSB (Poppit et al, 2016). It was discovered in 2004, yet due to the challenges associated with the volcanic cover (e.g. seismic imaging within and beneath the basalt cover, interpretation of petrophysical data), the field is still within the appraisal phase, with no definitive date for coming on stream (Poppit et al, 2016). The timeline of the Rosebank Field highlights the complexity of exploring for hydrocarbons within volcanic dominated margins. Some of the biggest issues surrounding exploration in these types of areas is predicting where reservoir units may occur and the connectivity between these units. Typically, within volcanically dominated environments, reservoir intervals are discontinuous, mostly due to volcanic and sedimentary systems competing for the same available accommodation space and structural controls on deposition, resulting in inter-fingering relationships (Schofield and Jolley, 2013). The term accommodation space, within this project, is defined as the space available for units to accumulate within. To better understand these challenging geological areas, it is important to understand them from a field perspective. In doing so, detailed information can be obtained which can be used to populate models where data is lacking, e.g in offshore hydrocarbon exploration. Fieldwork has been a necessary, large component of this project in order to improve understanding of these areas.

## 1.2 Research aims and objectives

The interaction of volcanic and sedimentary systems can produce very heterogeneous deposits and very little is actually known about these systems. It

is particularly useful therefore to understand how these differing systems compete for accommodation space and evolve with time in terms of being able to better understand hydrocarbon exploration in volcanic dominated settings.

The project aims to advance the current understanding of volcano-sedimentary settings in order to target similar offshore sequences for hydrocarbon exploration by utilising the Hreppar Formation (HF) as an analogue that has similar characteristics to the offshore fields mentioned previously. As with any analogue study, there needs to be some caution in directly comparing onshore analogue data with offshore field data, as it is likely there will be discrepancies between the two, the HF is no different. There is no “perfect analogue” for any offshore field; however, continued work on onshore analogues allows us to develop “end member” models, which may be used to inform future appraisal and exploration.

The main objectives of this project are;

- To develop a detailed understanding of lithofacies architecture of interbedded volcanic, volcanoclastic and sedimentary rocks in the HF and apply this to potential volcano-sedimentary systems.
- To create detailed maps and logs of representative sections of lavas, volcanoclastic and sedimentary rocks from the HF.
- To generate a detailed facies scheme and to develop general facies models of the HF, which may also be applicable to other volcano-sedimentary settings.
- To combine all these datasets (maps, lithological logs, photogrammetry models, facies models and conceptual models) in to a coherent case study of how volcanic and sedimentary rocks interact in the HF and how these data may be applied offshore.
- To compare the collected data with modelled remote sensing data, in order to better understand how these systems may appear in the sub-surface.

It is important to note that this is predominantly a field based study in order to understand the detailed nature of volcano-sedimentary settings and is not an exhaustive comparison with offshore remote sensing data. This is beyond the scope of this project, however a study of offshore data compared with HF data would be complimentary to this work.

### **1.3 Project outline**

Chapters 2-10 are summarised below. The chapters follow a logical order of analysis of the HF from large scale features to detailed descriptions and the implications of the work. Individual chapters build on the previous chapters main points and are not meant to be stand-alone pieces of work. Much of the work focusses around the geological map of the HF which is referred to throughout.

Chapter 2: An introduction to the regional geological history of Iceland and the HF. It focusses on the timing of events in Iceland that led to the formation of the HF and gives a brief description of the units found in the HF.

Chapter 3: A description of the terminology used throughout the project, with images of key examples.

Chapter 4: Focusses on the main methods used within the project and an introduction to the various maps that were created of the HF.

Chapter 5: A detailed description of the main lithofacies found within the HF at Flúðir, including field examples. This chapter also describes the environments of deposition of the main lithofacies. 7 main lithofacies have been identified, with 15 further sub-facies in the HF area. This is not an exhaustive lithofacies description, but instead the lithofacies have been genetically grouped in order to make identification simple.

Chapter 6: A detailed investigation of the main lithofacies successions in the HF, which builds upon the main lithofacies in chapter 5. It focusses on using log data and interpreted panoramas to determine the most common associations. These are often genetic, however in areas where volcanics and sediments interact, the associations are frequently non-genetic.

Chapter 7: A case study from the Stora Laxa river section within the HF at Flúðir. It is the largest continually exposed section within the HF at Flúðir making it an ideal section to examine lateral and vertical facies changes as well as gaining an insight in to the underlying structure of the area. This chapter utilises, photogrammetry, panoramas and logs to determine the nature of the relationships between the various units.

Chapter 8: A detailed investigation in to the underlying structure of the HF at Flúðir and how this controls deposition of volcanic rocks and sediments. The structural relationships between key outcrops are investigated, as well as different models for the overall complex structure of the HF.

Chapter 9: Focusses on the positive and negative general aspects of volcano-sedimentary systems on hydrocarbon exploration. It uses examples from the HF as well as forward modelling and published data.

Chapter 10: Provides a tentative step towards understanding geospatial relationships within the volcano-sedimentary settings. It also provides comprehensive discussion and conclusions of the main findings from the field studies, highlighting the main characteristics of volcano-sedimentary settings and their importance in hydrocarbon exploration.

## 2 Regional setting

### 2.1 Introduction

The following chapter provides an overview of the geological history of Iceland and in particular, that of the HF. This is intended to be a brief description of the regional context of the project and not an in-depth review, which is outside the scope of the project. For a detailed geological history of Iceland, see Thordarson and Höskuldsson (2014) and references therein.

### 2.2 Iceland

Iceland is situated in the North Atlantic Ocean between Greenland to the west and Norway to the east and covers an area of ~350,000 km<sup>2</sup> (Thordarson and Höskuldsson, 2014). It lies on the junction between the Reykjanes and Kolbeinsey Ridge (Mid Atlantic Ridge) and the Greenland-Iceland-Faroes Ridge (Ellis and Stoker, 2004; Thordarson and Höskuldsson, 2014) (Figure 2-1).

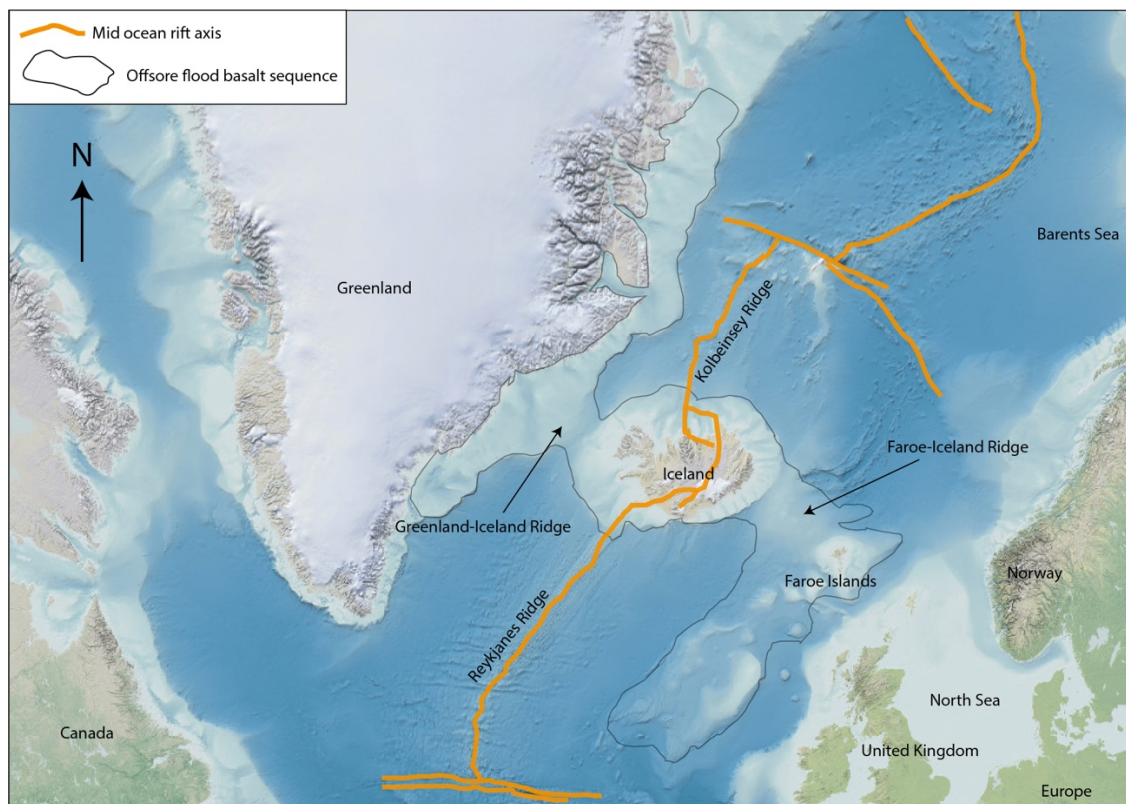


**Figure 2-1** Location map of Iceland after (Thordarson et al, 2014). Iceland is situated in the middle of the North Atlantic at the junction between the Reykjanes and Kolbeinsey Ridges and the Greenland-Iceland-Faroe Ridge.

The Icelandic land mass is part of the oceanic crust which forms the floor of the Atlantic Ocean and there is an approximately 50-200 km wide shelf around Iceland, with water depths of up to 400 m (Thordarson and Höskuldsson, 2014). Iceland is the only place on Earth where a mid-ocean ridge rises above sea level. Iceland began to form ~ 24 Ma however the oldest exposed rocks in Iceland are ~14-16 Ma which are predominantly found in the east and west (Figure 2-2) (Thordarson and Höskuldsson, 2014).

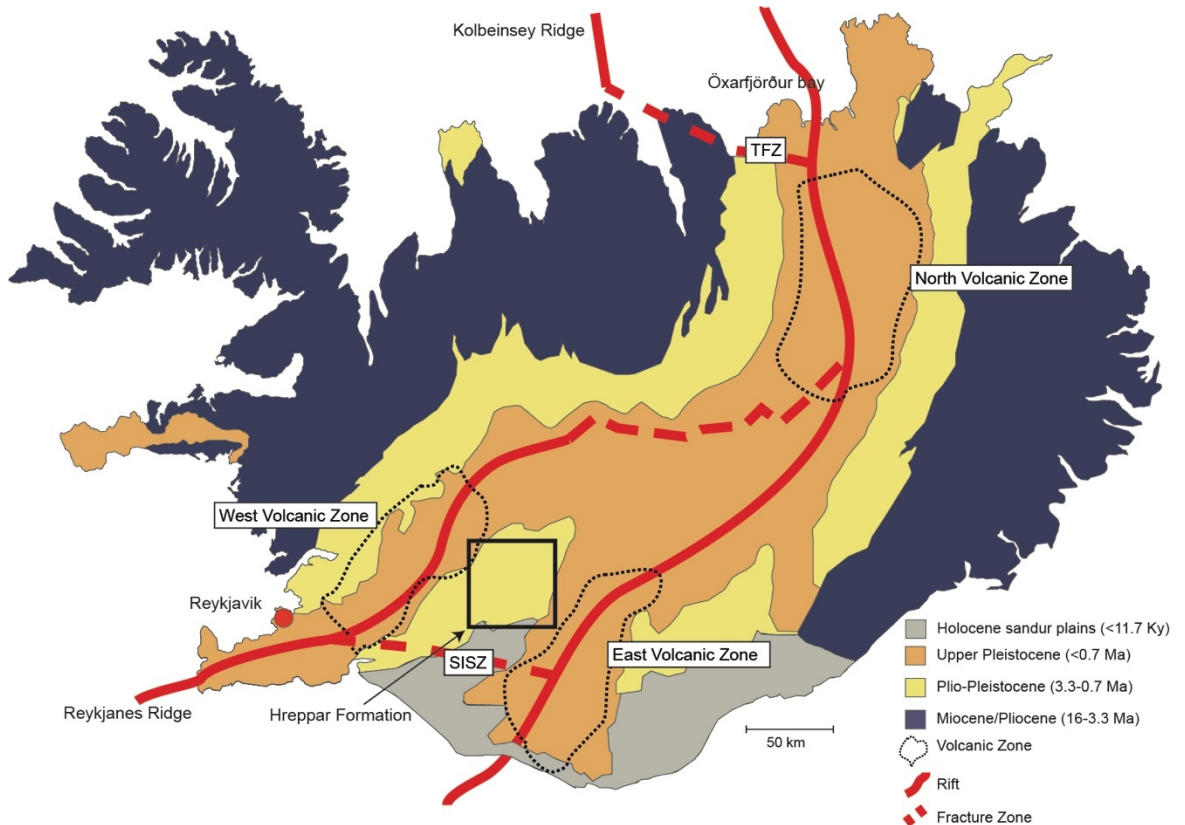


**Figure 2-2 Simplified geological map of Iceland. The main ages of the rocks found within Iceland and their distribution are highlighted. East, West and North Volcanic Zones are indicated by black dashed lines. General location of the Hreppar Formation is highlighted. After Thordarson and Höskuldsson (2014).**

There is some debate as to how Iceland has developed in the last 60Ma, with some authors suggesting that Iceland is the result of interaction between a spreading ridge and a mantle plume (an upwelling of lower mantle material) (Thordarson and Larsen, 2007; Mjelde et al, 2008; Thordarson and Höskuldsson, 2014; Smallwood and White, 2014), whilst others propose a non-plume, plate tectonic origin for the formation of Iceland (Lundin and Doré, 2005; Ellis and Stoker, 2014).

### 2.2.1 Plume or non-plume origin for Iceland

Plume protagonists suggest that the most obvious feature of the presence of a plume underneath Iceland is the elevation of Iceland over the surrounding sea floor (Thordarson and Larsen, 2007; Mjelde et al 2008; Thordarson and Höskuldsson, 2014). The mantle plume provides the material for the volcanic zones observed in Iceland (Thordarson 2012). According to Mjelde et al (2008) a large plume developed west of Greenland and coincided with NE-SW extension, which allowed dykes to develop from Greenland to Britain. The plume moved beneath central Greenland at 55 Ma and hot material flowed beneath the thinnest parts of the lithosphere, which generated extensive margin magmatism, coinciding with rifting (Mjelde et al, 2008). The plume head and associated magma had become exhausted and much reduced in size. At 23 Ma there was increased activity at the Kolbeinsey Ridge, which is presumed to be a result of direct interaction between plume and ridge (Mjelde et al 2008) and resulted in the beginning of the formation of Iceland.

Non-plume protagonists suggest that Iceland formed as a result of opposing rifts-propagating in different directions; a SW propagating rift from the North Atlantic and the other a NE propagating rift from the central Atlantic, which began ~48 Ma (Lundin and Doré, 2005; Ellis and Stoker 2014). Non-plume protagonists dispute the spherical nature of the positive geoid centred beneath Iceland, and instead they identify a linear shape not centred beneath Iceland, which poses problems for the plume model. The Greenland-Iceland Faroe-Ridge is proposed to have formed as a result of linear rifting, lithospheric thinning and decompressive melting to create this anomalously thick area of oceanic crust (Ellis and Stoker, 2014) (Figure 2-1) which is symmetrical in age about Iceland (disputing it as a hotspot track) (Lundin and Doré, 2005). Non-plume protagonists suggest that the two opposing rifts and simple plate tectonics are enough to justify the development of the North Atlantic.

### 2.2.2 Onshore Iceland

Narrow belts of active volcanism and faulting define the Kolbeinsey and Reykjanes ridges in onshore Iceland. These are seen from Reykjanes in the southwest to Öxarfjörður bay in the north (Figure 2-2). The North American and Eurasian Plates

are spreading at a rate of ~18 mm per year at a trend of N105°E and 285°W (Thordarson and Höskuldsson, 2014). Generally speaking, the eastern side of Iceland sits on the Eurasian Plate, whereas the western side of Iceland sits on the North American Plate (Einarsson, 2008).

In the subsurface, associated with the continued spreading at the ridges, large vertical dykes form. The surface expression of these dykes is swarms of linear volcanic fissures that are confined to narrow belts. These narrow belts are referred to as volcanic zones and they are connected by large transform faults (Thordarson 2012). There are three main volcanic zones within Iceland each of which are ~20-50 km in width (Figure 2-2): they are the North Volcanic Zone (NVZ); East Volcanic Zone (EVZ); and the West Volcanic Zone (WVZ). Connecting these different rift zones are two major transform zones: the Tjörnes Fracture Zone (TFZ) in the north of Iceland and the South Iceland Seismic Zone (SISZ) in the south of Iceland. These fracture zones accommodate the uneven movement generated by the eastwards shift of the spreading zone which results in a complex fracture network (Clifton and Kattenhorn, 2006; Einarsson, 1991). The SISZ is ~15-20 km wide (N-S) and 70 km long (E-W) (Bergerat and Angelier, 2000; Einarsson, 1991).

Magma produced within the volcanic zones generally accumulates in the centre of the zone, rather than at the margins (Figure 2-3). As a result the volcanic units formed in the centre of the rifts tend to experience rapid burial and follow a steep burial curve as they move away from the rift (Thordarson and Höskuldsson, 2014). Units found at the margins of the rift zones are buried much more slowly and undergo shallower burial. As a result of volcanic activity and spreading, a low angle (5-10°) syncline forms (Figure 2-3), with beds dipping towards the spreading centre (Thordarson and Höskuldsson, 2014).

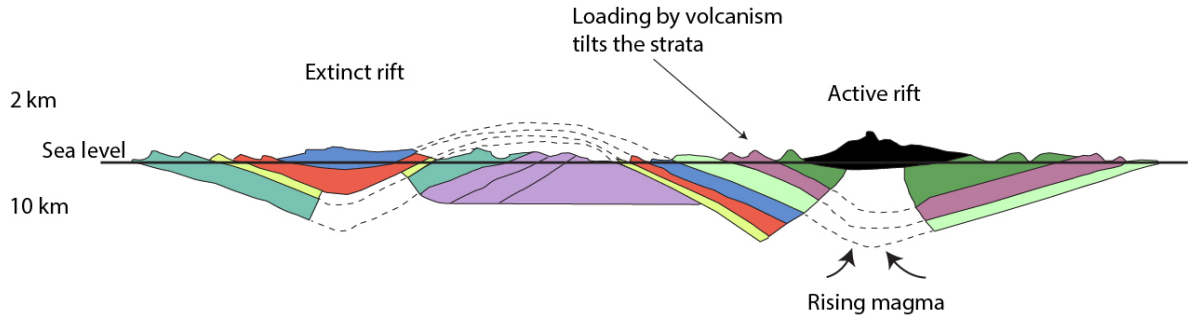


**Figure 2-3** General structure of the Icelandic crust (after, Thordarson and Höskuldsson, 2014).

## 2.3 Glaciation in Iceland

Modern day Iceland is classed as having a cold, temperate/maritime climate in the lowlands and a low arctic climate in the highlands (Syvitski et al, 1999). There are currently 6 main glaciers in Iceland, the largest being Vatnajökull. Prior to and during the Plio-Pleistocene and the formation of the HF, there were significant glacial/interglacial periods which affected the sedimentary units deposited within the HF (chapter 5) (Figure 2-4). In Plio-Pleistocene sequences such as that of the HF, there are repetitions of glaciated and ice-free deposits ((Eiríksson and Geirsdóttir, 1991). During the Plio-Pleistocene there were approximately 9 glacial/interglacial cycles with each one lasting between 100,000-200,000 years (Thordarson and Höskuldsson, 2014). As a result of these glacial/interglacial cycles, there are significantly more volcanoclastic and clastic sedimentary rocks higher up in the stratigraphy of the Plio-Pleistocene sequences (Thordarson and Höskuldsson, 2014).

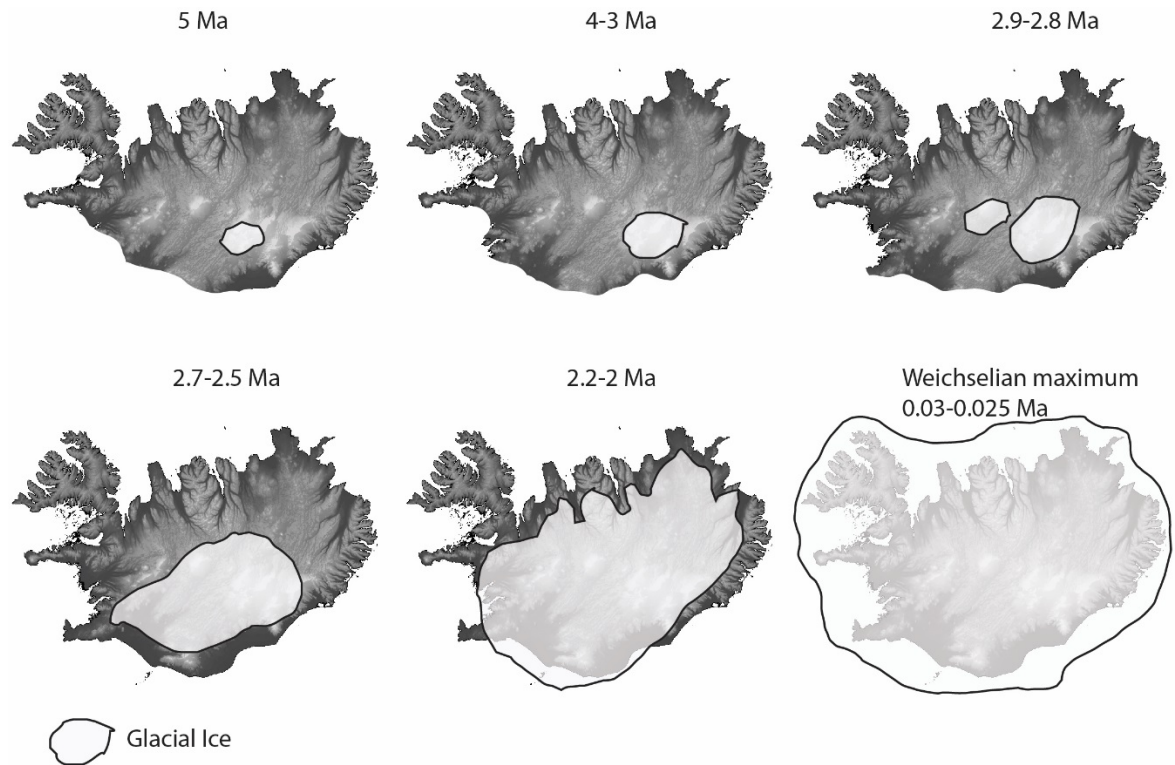


**Figure 2-4** Glacial ice extent in Iceland. Glacial ice reached a maximum during the Weichselian, as did much of North America and Europe at this time. During these glacial cycles, there were also interglacial periods also. Up to nine glacial/interglacial periods occurred during the Plio-Pleistocene. After (Eiríksson and Geirsdóttir, 1991).

In the last 0.7 Ma, there have been 5 glacial/interglacial cycles with the greatest extent of ice in Iceland occurring during the Weichselian stage (Figure 2-4) at its maximum extent between 30Kyr to 25 Kyr, which coincided with extensive glaciation in North America and Europe (Thordarson and Höskuldsson, 2014). During the Holocene the climate in Iceland became like it is today.

## 2.4 South Iceland and the Hreppar Formation

The HF is situated in between the WVZ and the EVZ, just north of the SISZ (Figure 2-2). This area is neither part of the North American Plate or the Eurasian Plate, but is instead a separate plate, called the Hreppar Microplate (Clifton and Kattenhorn, 2006; Einarsson, 2008).

The HF is Pleistocene in age (2.5 Ma-10 Kyr) with the majority of lavas in the HF forming between 0.2 Ma and 2.2 Ma (Kristjánsson et al, 1998). In the eastern HF, west of the Þjórsá river, the formation has an age of 2.4 Ma (Figure 2-5). The Þjórsárdalur (Thjorsardalur) and Gljúfurleit areas in the north part of the HF are

thought to be 1.5 Ma (Kristjánsson et al 1998). The youngest units are to be found in Búrfel and Búðarháls (Figure 2-5). The HF forms an anticline with the axis striking NE-SW due to the surrounding east and west volcanic zones. The large load created in the centre of the volcanic zones causes subsidence of the crust. This occurs on both sides of the main Hreppar Formation (south west Iceland) and therefore results in an anticlinal structure in the centre (Thordarson 2012).

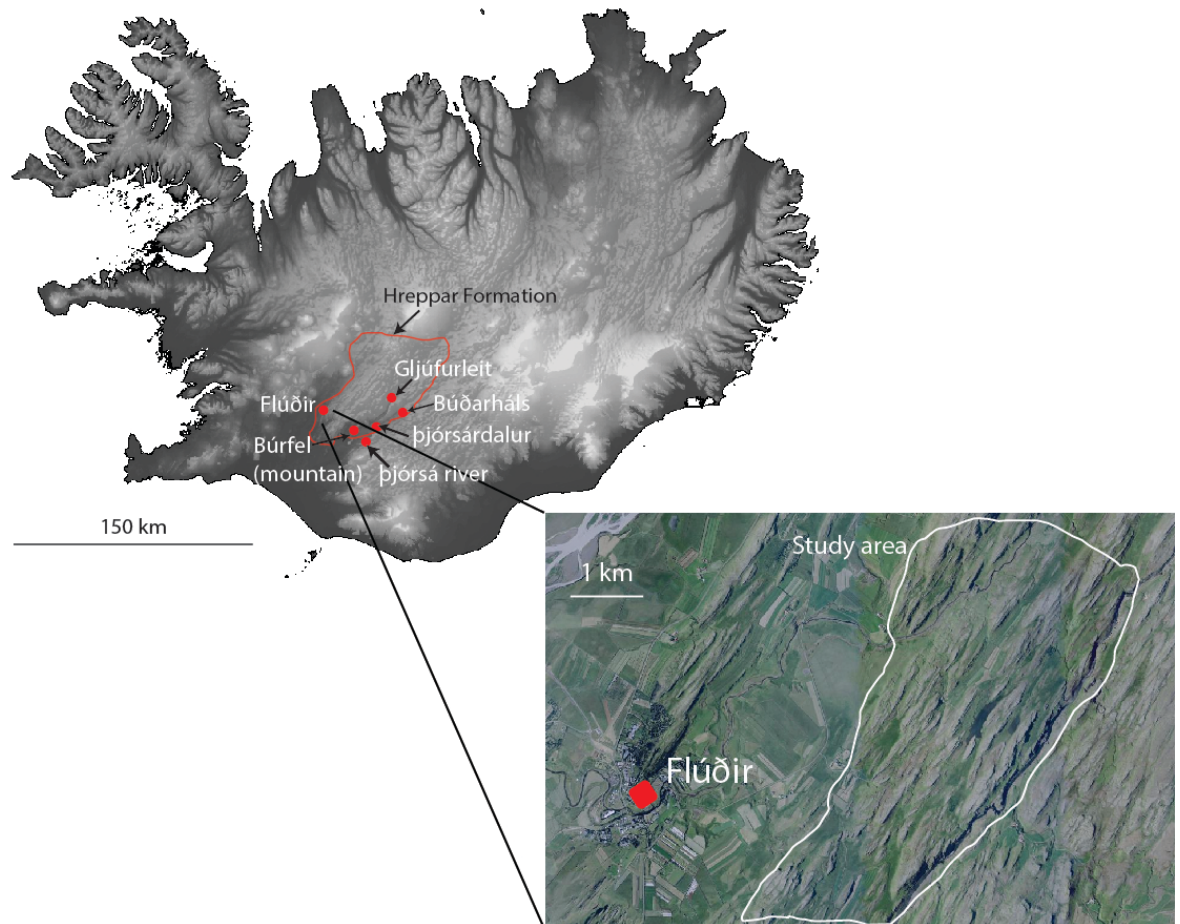


**Figure 2-5** Location of the Hreppar Formation. Key localities that have previously been studied in the Hreppar Formation have been highlighted with red dots. Inset map is of the Hreppar Formation just outside Flúðir (the area of study) which is ~16 km<sup>2</sup> and is situated within the red outlined area on the map.

The majority of previous work on the HF has been carried out in the east around Þjórsárdalur and Þjórsá (Figure 2-5) and generally focusses on broad scale mapping and age dating (Kristjánsson et al 1998). Furthermore, much of the work on the HF has been published in Icelandic, making it difficult to obtain. Previous studies document interbedded lavas and sedimentary rocks, with the sedimentary rocks generally having a glacial and volcanic origin. Individual units exhibit considerable lateral variations in thickness and extent due to the topography of the area and

various periods of glaciation. The total thickness of the area is estimated to be ~500 m (Kristjánsson et al 1998). Individual units vary in thickness from 1-50 m thick. In the area around Flúðir (focus of this study), there has been little to no work carried out in the HF. The HF at Flúðir is very similar geologically to the east of Iceland and is predominantly composed of interbedded basaltic lavas, volcanoclastic and fluvial/glacial sedimentary rocks.

## 3 Geological terms and nomenclature

### 3.1 Introduction

The interaction between sedimentary and volcanic systems can produce a vast range of rock types, which is a key challenge in fully understanding volcano-sedimentary settings. These settings are well known, however, their lithofacies architectures are poorly understood. Understanding all elements of these systems is key to exploiting volcano-sedimentary environments for hydrocarbon exploration. It is important to therefore understand some of the key geological terminology and nomenclature associated with these systems.

This chapter introduces the main basaltic lava types and their mode of emplacement as well as the nomenclature surrounding volcanoclastic rocks. This chapter aims to provide a brief description of these terms and is not intended to be an exhaustive source, with subsequent chapters building upon these basic concepts.

### 3.2 Lava types

There are two main types of lava morphologies; compound lava flows and simple lava flows, which are both found within flood basalt provinces (Walker 1971). Basalt lavas can be further divided into two main structural types; 'a'ā and pāhoehoe lavas (Walker, 1993). Lavas are comprised of flow units (smaller divisible lava bodies), which consist of the top of the flow, which has cooled and solidified before another flow unit is formed (Nichols 1936).

The term compound applies to lavas, which are divisible into flow units, and simple applies to lavas, which are non-divisible (Figure 3-1) (Walker 1971). Compound lavas typically have a shield-like morphology and tend to form when lava extrusion rates are low (Walker 1971), whereas simple lavas typically tend to form when the extrusion rate of the lava is relatively high (Walker 1971). Passey and Bell (2007) proposed that simple lavas they examined within the Faroe Island Basalt Group are the result of a continuous supply of lava; however, they suggest that the supply rate would not have been constant (waxes and wanes). The main difference between the two lava morphologies is the supply of magma, with

simple lavas being relatively constantly fed, and compound lavas being more punctuated.

The terms compound and simple can be difficult to apply in the field (Self et al, 1997) as it can appear as if one outcrop is a simple lava flow, but when it is traced out over its length, it is often the case that it has a contact with another flow lobe of the same lava flow (Figure 3-1).

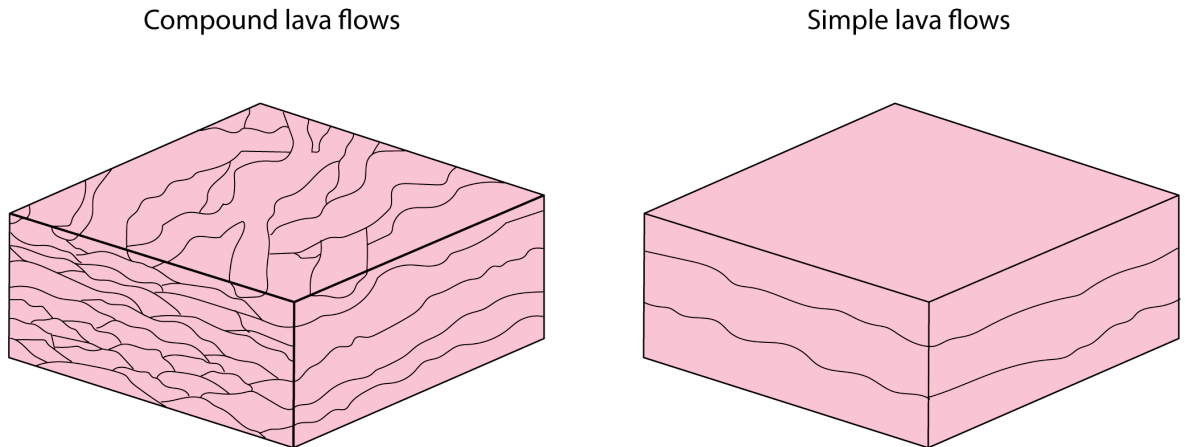


Figure 3-1 Sketch diagram of compound and simple lava flows (after Jerram et al, 2016).

### 3.2.1 'A'ā lava flows

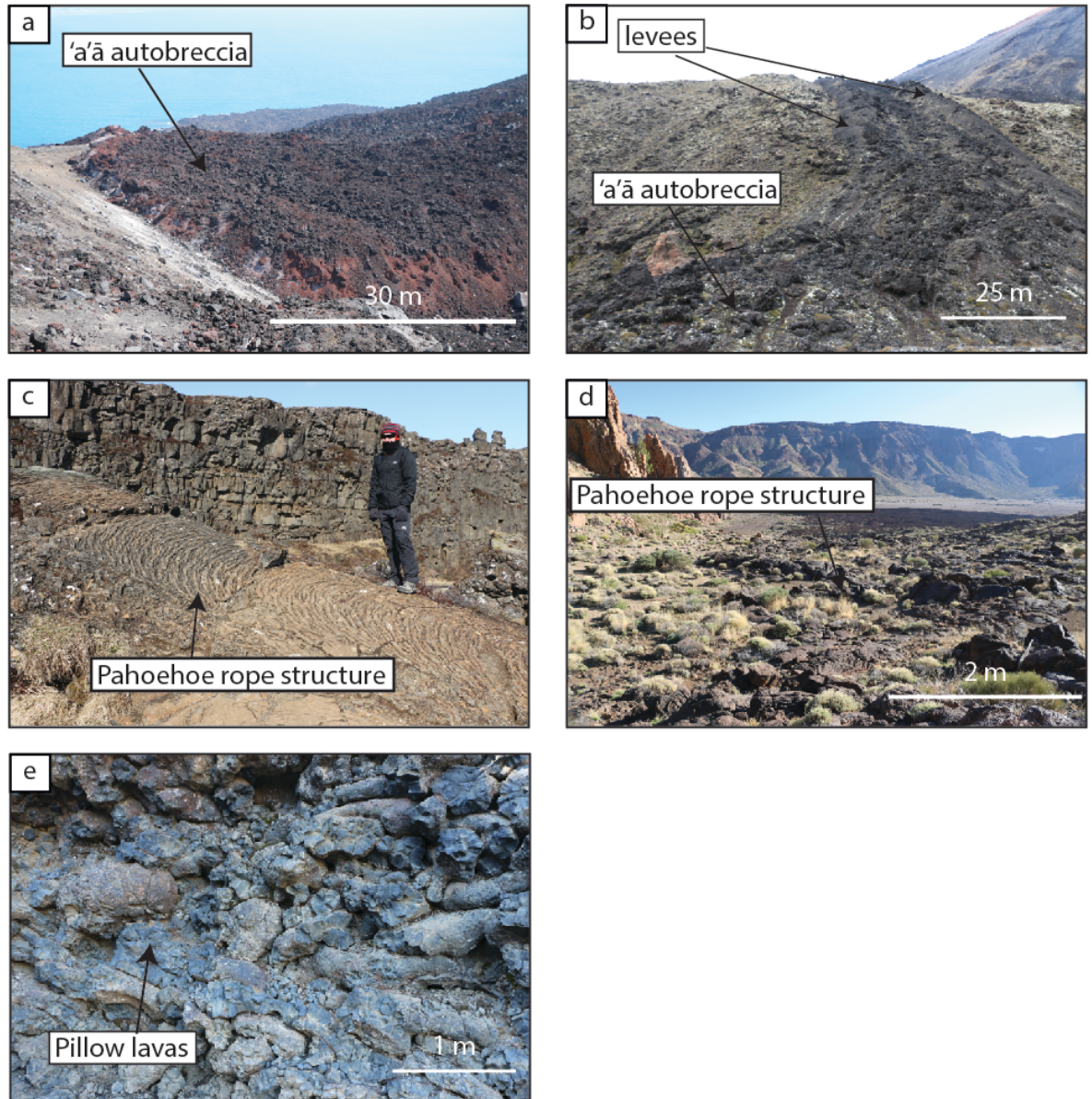
'A'ā lavas typically have a compound morphology, however, unlike pāhoehoe lava, it is often difficult to determine the individual flow units (Walker 1971). 'A'ā lavas are characterised by a rough flow top autobreccia, composed of clinker, a dense interior and often a rough, basal autobreccia composed of clinker (

Figure 3-2). Clinker is formed as a resulting of internal shearing and twisting as the lava flows. The individual flow units are on average 1-10 m, and typically demonstrate a more tabular shape in cross section. Determining the boundary between the top of one flow unit and the base of another is particularly difficult, if not impossible (Walker 1971).

### 3.2.2 Pāhoehoe lava flows

Pāhoehoe lava flows typically have a compound morphology (Walker 1971). Pāhoehoe lavas are characterised by a very smooth surface, in contrast to an 'a'ā autobreccia (

Figure 3-2). Commonly, rope structures are also observed within pāhoehoe lava flows and other small-scale features such as vesicle banding (Self et al, 1998). The individual flow units range from 5cm->10m thick and in cross-section can be tabular to bun-like. They typically demonstrate a large concentration of vesicles in the upper third of the flow unit and pipe vesicles along the bottom of the flow unit. There can be a significant difference in phenocryst content between differing flow units and even individual flow units, reflecting the lower viscosity of pahoehoe compared to 'a'a (Walker 1971). Pāhoehoe lavas typically advance through a series of individual lava tubes (Rowland and Walker, 1990).



**Figure 3-2 Summary figure of lava types. a) Large 'a'ā lava flow with distinctive upper autobreccia formed as a result of high effusion rates, Anak Krakatau, Indonesia. b) Channelised 'a'ā lava flow with clear levees on either side. This is the typical way in which and 'a'ā lava flow rapidly advances, Tongariro National Park, New Zealand. c) Preserved rope structures on the surface of a pāhoehoe lava flow in Þingvellir national park, Iceland. d) Preserved pāhoehoe rope structures and pāhoehoe lobes, Tenerife. e) Coherent pillow structures, with very little disarticulation, Þingvellir national park, Iceland.**

### 3.2.3 Effusion rates and emplacement mechanisms

The difference between 'a'ā and pāhoehoe is largely down to effusion rates and whether or not a certain viscosity threshold has been reached. Generally, if effusion rates are high, typically 'a'ā lavas form and if effusion rates are low ( $< 5\text{--}10\text{ m}^3/\text{s}$ ) then pāhoehoe lavas form (Rowland and Walker, 1990). The differences between 'a'ā and pāhoehoe can also be complicated by composition, temperature,

crystallinity, volatile content and vesicularity, which all affect the viscosity (Peterson and Tilling, 1980; Hon et al, 1993). Peterson and Tilling (1980) also identified that shear stress and the rate of shear strain will also affect the transition from 'a'ā to pāhoehoe.

'A'ā lava flows tend to advance rapidly in open channels, surrounded by levees of cooled lava either side due to high emplacement rates. This generates a narrow channel in which the lava can advance rapidly at rates of between 0.08-10 km/h (Rowland and Walker, 1990; Kesztheyli and Self, 1998; Hon et al, 2003). As the lavas travel at such great velocities, a carapace over the advancing lava will not form; this leads to a huge loss in heat via radiation and air cooling, causing the lava to become significantly more viscous (Rowland and Walker, 1990). When clots begin to develop in the advancing lava as it cools, this leads to the development of the typical 'a'ā autobreccia. 'A'ā lava flows are typically short lived (Self et al, 1998).

Pāhoehoe lavas tend to advance much slower than 'a'ā lava flows. They typically advance in a series of individual flow units (lobes). As they advance much slower they develop a carapace which insulates the flow from air cooling. Individual flow lobes can advance at a rate of ~0.12 km/h whereas the lava flow front advances at a rate of ~0.01 km/h (Rowland and Walker, 1990). The insulated nature of advancing pāhoehoe lava flow allows them to travel large distances >100 km whilst remaining at a similar temperature (Rowland and Walker, 1990; Self et al, 1998). These lava flows can continue to inflate and flow for months (Self et al, 1997; Self et al, 1998).

Pāhoehoe lavas were originally thought to form rather small accumulations of lava, but through the work of Hon et al (1994) and Self et al (1996) it was demonstrated that large flood basalt provinces such as that of the Columbia River Flood Basalts (CRFBs), are formed predominantly of pāhoehoe lava flows.

Hon et al (1994) developed a model for the emplacement of sheet lava flows (Figure 3-3). The model is based upon the supply of lava in to the centre of lobes. Inflated pāhoehoe sheet flows are initially emplaced as thin sheets of lava, but with sustained input of fresh lava they become thick inflated flows, which develop as a series of lobes (Hon et al 1994). Pāhoehoe toes (0.2-0.3 m thick) inflate and

coalesce in to 3-5m thick sheets with lateral dimensions of hundreds of metres over a period of days to weeks. The upper crust of the lava flow rises, as fresh lava is continuously fed in to the molten core of the flow, mainly through tube fed pāhoehoe lava flows (Self et al 1996).

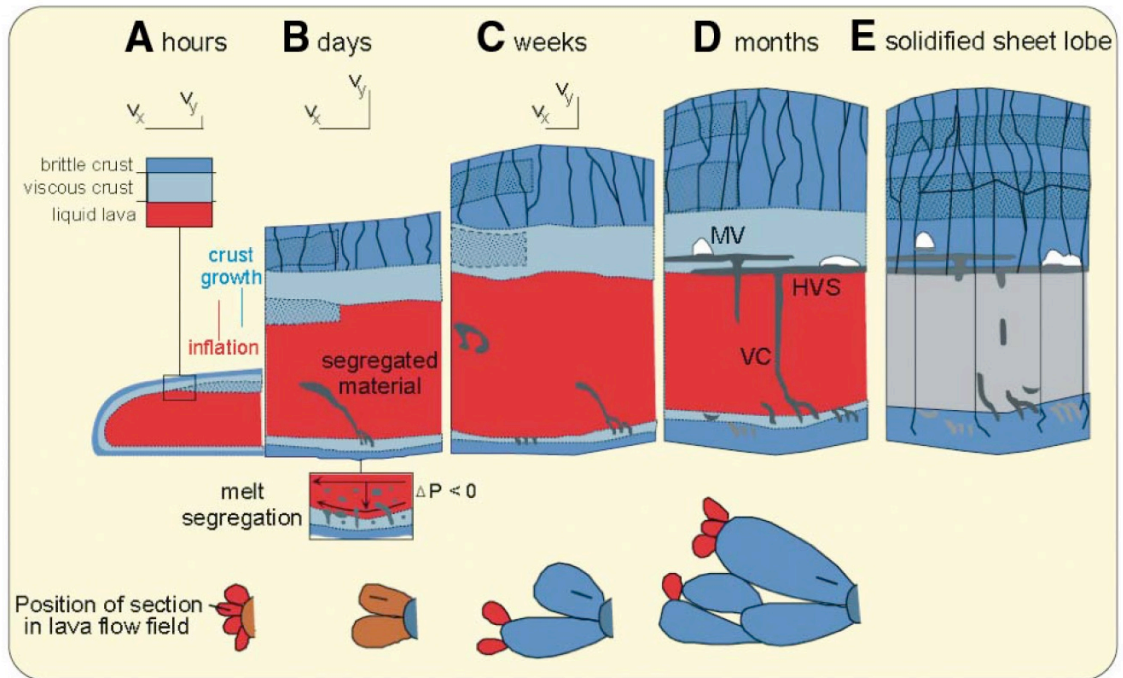


**Figure 3-3** Development of a pāhoehoe lava flow over time. With continued input of fresh lava, lobes grow through inflation, eventually coalescing and creating thick lateral sheets. The diagram at the base of the figure indicates how the lava flow advances. The lava flow can continue to grow over a period of months (after Thordarson and Self, 1998; Self et al, 2014).

Initially, individual lobes originate from outbreaks at the front of an already inflated sheet, and then rapidly move away from this point (Figure 3-3). As they move away from the point, they spread out radially and lose velocity, which allows cooling to occur, and this promotes rapid crustal growth of a thin viscoelastic skin (Hon et al 1994, Self et al 1997). The thin skin acts like a balloon, where it contains incoming lava, creating toes at the front of the flow (Hon et al, 1994, Self et al 1997). A brittle crust will develop over the top of the viscoelastic skin, which will become extensively fractured due to contraction during cooling. These fractures grow larger, allowing for the movement of the viscoelastic skin (Self et al 1997). The skin behaves plastically, allowing the toe to contain the incoming lava, which causes the toe to inflate (Hon et al 1994). The core of pāhoehoe lava flows only cool and crystallise once the sheet has stagnated (Self et al 1997). If the inflation

rates are too quick, the toes will burst creating new lobes (Hon et al 1994, Self et al 1997). As the flow front moves the crust develops and becomes thicker behind it, which provides an insulating cover for the continued supply of lava moving beneath it and an increase in the hydrostatic head at the flow front (Hon et al 1994). With the continued supply of lava, the hydrostatic pressure increases evenly throughout the core of the lava flow, producing uniform uplift (Hon et al 1994). The inflation process for pāhoehoe lava bodies is the same, regardless of the size of the body (Self et al, 1997).

### 3.3 Volcaniclastic rocks

In simplest terms, a volcaniclastic rock is a clastic rock that contains a significant volume of clasts of volcanic origin. The British Geological Survey (BGS) use the definition of 10% by volume to determine if a rock is volcaniclastic (British Geological Survey, 1999) whereas the International Ocean Drilling Programme (IODP) use a figure of >60% of volcaniclastic grains to be called volcaniclastic. In this project, a common-sense approach has been adopted to determine if the deposits are volcaniclastic: in the HF (an obviously volcanic setting) volcanic rocks, and specifically basalt is the dominant rock type and clearly dominates the environment. The approach taken in this project has been to describe volcaniclastic rocks in the HF using aspects of Cas and Wright (1987) and White and Houghton (2006).

Volcaniclastic rocks are found in most geological settings. There have been various attempts to classify volcaniclastic rocks, from an initial descriptive classification in the field, with later genetic identification, to genetic identification in the field. Currently there is no, agreed upon classification scheme for volcaniclastic rocks, but rather a series of classification schemes by numerous authors (Fisher, 1961; Cas and Wright, 1987; McPhie et al, 1993; White and Houghton, 2006). Additionally, there is a lot of debate surrounding each of these schemes, (e.g. Waitt, 2007; and White and Houghton, 2007).

Volcaniclastic rocks can be separated in to two main categories; rocks that are formed by the direct action of volcanic eruptions (primary volcaniclastic) and those that form through the process of reworking of eroded volcanic material (becoming sedimentary rock) (White and Houghton, 2006).

Within the HF, there are a significant number of different types of volcaniclastic rocks, therefore it is important to fully understand the different nomenclature schemes and which elements of these have been incorporated in to this project. Brief overviews of each scheme follow and are summarised in Figure 3-4.

### **3.3.1 Fisher (1961)**

Fisher (1961) created the first scheme to describe volcanoclastic rocks as existing schemes were woefully inadequate. Three categories of volcanoclastic rock were determined by Fisher. These were autoclastic, pyroclastic and epiclastic and were primarily divided based upon the origin of their particles (Fisher, 1961). Fisher also included a purely descriptive term for volcanoclastic materials, which have an unknown origin, based entirely on the presence of volcanic particles and their respective sizes. It is important to differentiate between instantly formed fragments and longer developed ones, due to the fundamental differences in energy required to form them. Fisher's 1961 scheme has now been built upon by numerous volcanoclastic nomenclature schemes, (e.g. Cas and Wright, 1987; McPhie et al, 1993; White and Houghton, 2006).

### **3.3.2 Cas and Wright (1987)**

Cas and Wright's scheme primarily focusses on the depositional mode of the rock to differentiate between volcanoclastic rocks, unlike Fisher's scheme which focussed on the origin of particles in the rock. Cas and Wright's scheme describes primary volcanoclastic rocks well and uses clastic sedimentology terms for all other volcanoclastic rocks. However, all rocks that are formed by normal sedimentary processes are defined as being non-primary volcanoclastic. The scheme does not differentiate between syn-eruptive and post eruptive processes. The scheme can be useful, when describing rocks where the genesis is difficult to determine. For example, Cas and Wright use clastic sedimentary terms with a volcanic modifier, (e.g. basaltic sandstone) to name these deposits.

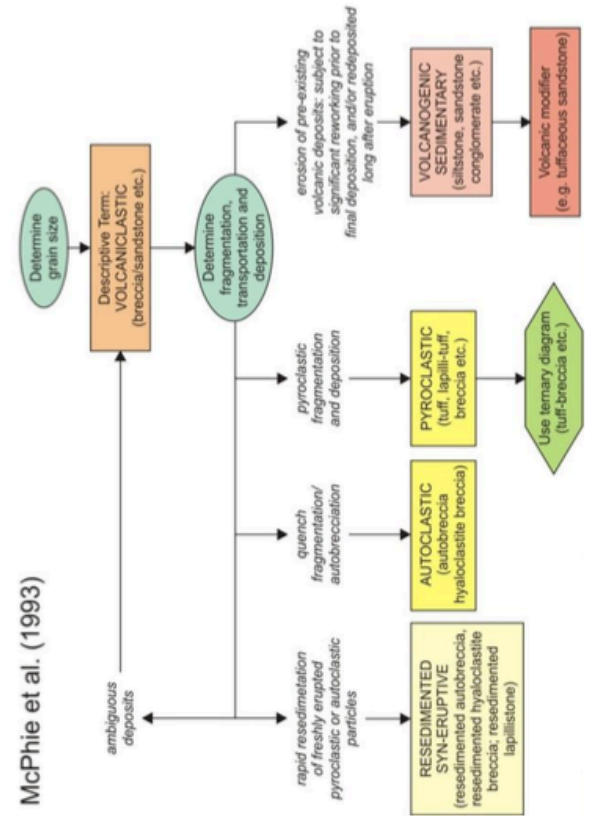
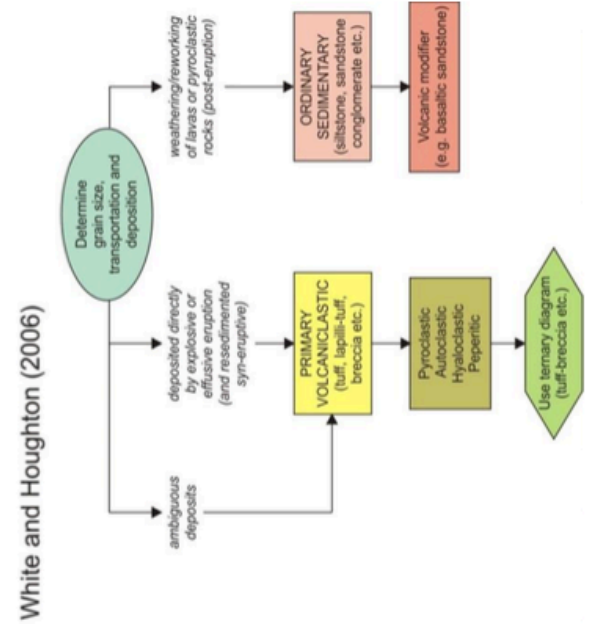
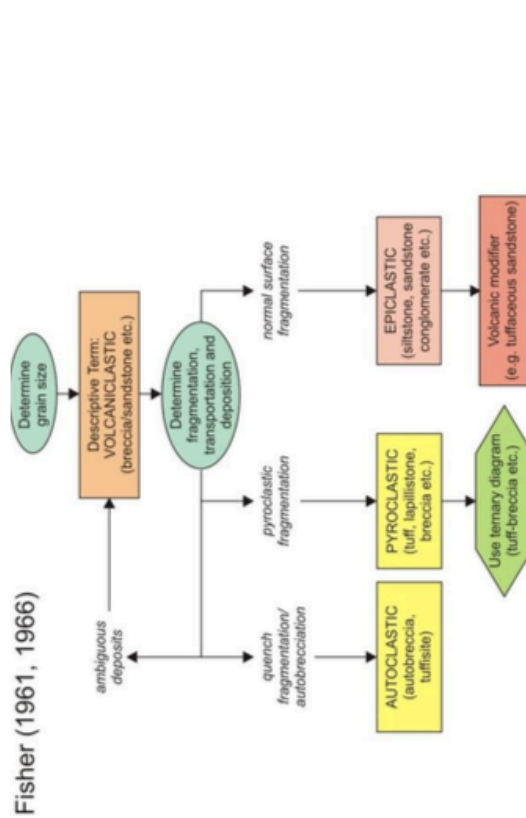
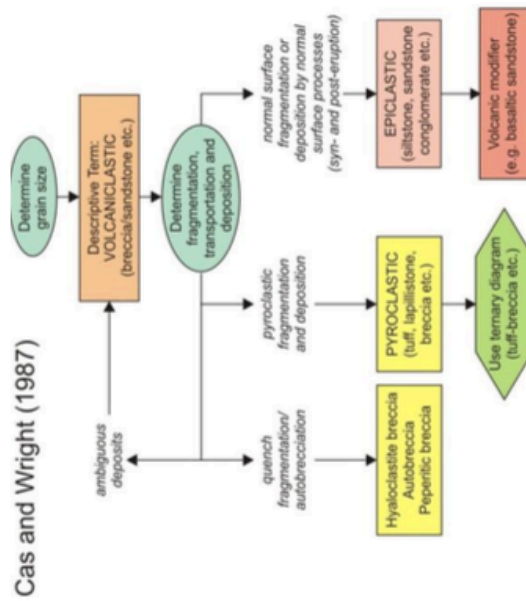


Figure 3-4 Summary of the main volcanoclastic nomenclature schemes described in this project. These schemes are generally quite similar with a few key differences. See text for detailed descriptions.

### **3.3.3 McPhie et al (1993)**

McPhie et al's scheme focusses on using clast origin, transport and deposition mechanisms to classify volcanoclastic rocks, but they also made the decision to separate deposits based on post emplacement/ syn-volcanic processes. The scheme identifies four main volcanoclastic rock types; autoclastic, pyroclastic, resedimented syn-eruptive volcanoclastic and volcanogenic sedimentary. The term resedimented syn-eruptive volcanoclastic, refers to deposits that formed as a result of the primary eruption, yet were modified by external agents, such as wind, water or gravity. Both Cas and Wright (1987) and McPhie et al (1993) proposed using lithological and lithofacies terms to describe volcanic and volcanoclastic rocks, before applying terms that have genetic implications. A difficulty with the McPhie et al, 1993 scheme is that it is extremely complicated and uses awkward terminology which may be difficult to apply.

### **3.3.4 White and Houghton (2006)**

White and Houghton's nomenclature scheme builds upon the previous schemes mentioned and employs different elements of each. For instance, White and Houghton use clastic sedimentary nomenclature for rocks that have been produced as a result of weathering of primary volcanoclastic units or lavas. The scheme focusses on the primary transport and deposition of particles and identifies, four primary volcanoclastic end members. These are; pyroclastic, autoclastic, hyaloclastite and peperite. Initial depositional mechanism is used to describe the deposits and then further detail comes from observation of the grain size classes. When using White and Houghton's scheme, it is useful to have young, fresh deposits that are easily characterised. If exposure is poor and deposits are difficult to determine, it can be challenging to use this scheme.

### **3.3.5 Sub-divisions of volcanoclastic rocks**

#### **3.3.5.1 Pyroclastic**

A pyroclastic deposit is composed of discrete particles from a volcanic vent (Fisher, 1961) although this is not always the case. They typically form as a result of volcanic plumes, jets or pyroclastic density currents (White and Houghton,

2006). The resultant deposits include ignimbrites, scoria and spatter and pumice (Fisher, 1966; Cas and Wright, 1987) (Figure 3-5).

### **3.3.5.2 Autoclastic**

Formed from the contact with air, for example during effusive volcanism when a dome or lava flow cools and fragments in contact with air, it produces an autobreccia (Figure 3-5). The fragments are deposited under continued lava or dome flowage (White and Houghton, 2006).

### **3.3.5.3 Hyaloclastite**

Hyaloclastite forms as a result of extruding magma or flowing lava cooling and fragmenting as it comes in to contact with water or ice. The resultant fragments are deposited with continued lava emplacement (White and Houghton, 2006). The deposits mainly consist of angular lava fragments, basalt/sideromelane glass shards, zeolites, clay and calcite (Smellie and Skilling, 1994; Walton and Schiffman, 2003) (Figure 3-5). In the HF, hyaloclastite is the most abundant volcanoclastic rock. The term hyaloclastite has been used here in the same way as Watton (2013) used it; it represents a passive fragmentation process with a limited active component. The term reworked hyaloclastite has been used to describe deposits that have seen a second phase of deposition.

### **3.3.5.4 Peperite**

Peperite is formed when magma fragments and interacts with a generally wet, unconsolidated sediment component (Skilling et al, 2002; White and Houghton, 2006), which could be at the base of lava flows or at the margins of intrusions (Figure 3-5). Peperite can be useful in field studies to understand the relative chronology of that area (Skilling et al, 2002).

### **3.3.5.5 Epiclastic/sedimentary**

Epiclastic processes are normal surface processes involving weathering and erosion. Epiclastic deposits therefore are rocks that were produced by normal surface fragmentation processes and contain material from previous volcanic modes of fragmentation (Cas and Wright, 1987) (Figure 3-5). White and Houghton

(2006) would prefer the use of sedimentary to describe these deposits. In this project, sedimentary has been used instead of the term epiclastic.

#### **3.3.5.6 Pillow lavas**

Underwater eruptions can be effusive or explosive and this is determined by depth of the water column, composition of magma, and the interaction between water column and magma (Fisher, 1984). Pillow lavas and compound pahoehoe lavas can be easily confused, but in reality, pillow lava is actually a type of compound lava flow (

Figure 3-2, Figure 3-5), with pillows representing individual flow units (Walker 1971). In the HF, the pillows are typically disarticulated and form hyaloclastite-pillow breccias. The lavas would have fragmented in contact with water producing pillow clasts and interstitial hyaloclastite material (Figure 3-5). In this format and within the context of this project, pillow lavas have been classed as primary volcanoclastic rocks as they typically form pillow breccias.

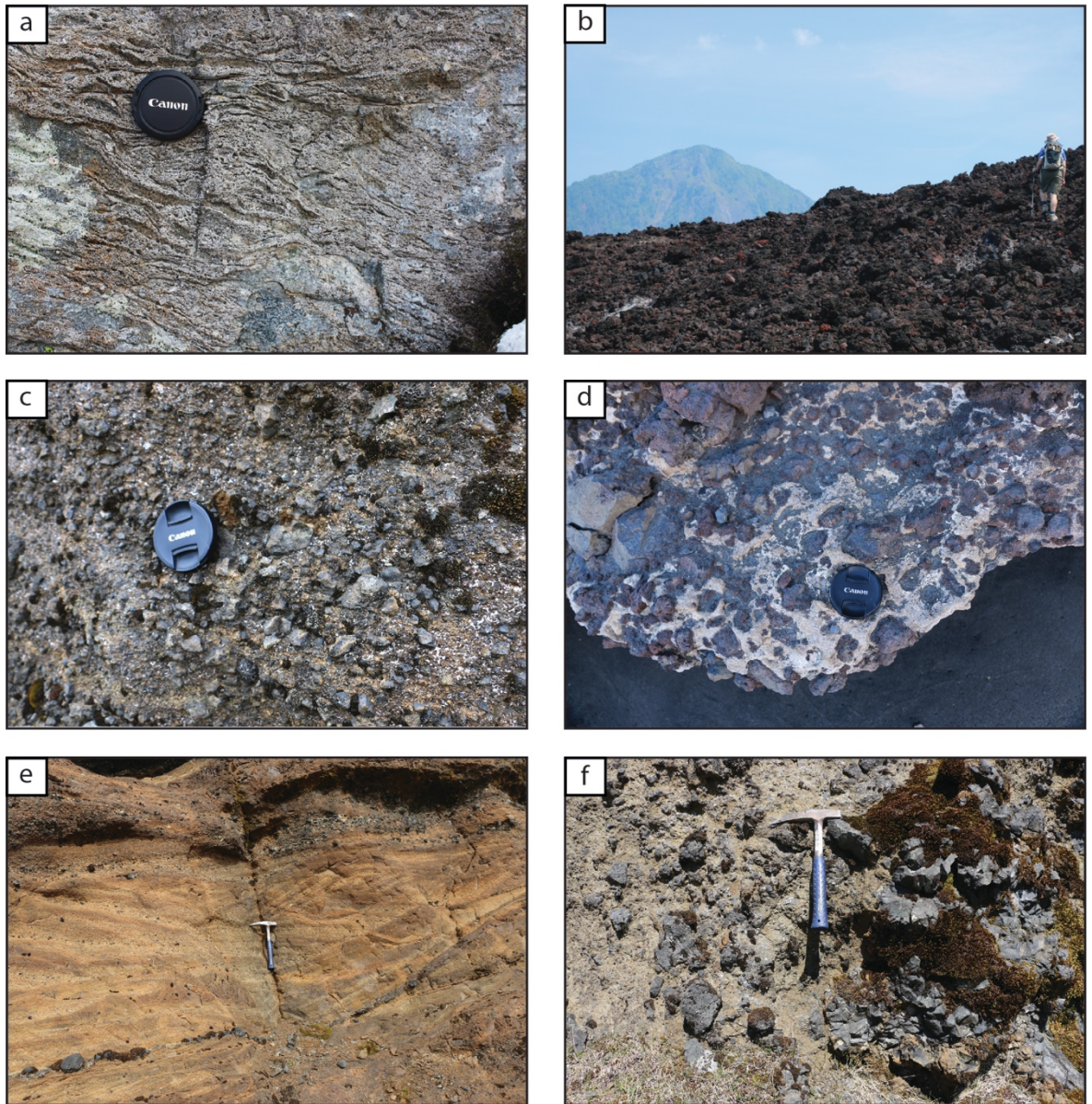


**Figure 3-5 Summary figure of volcanoclastic rocks. a) Welded ignimbrites, with weathered out fiamme, Glencoe, Scotland. b) Autobreccia on an 'a'ā lava flow from Anak Krakatau, Indonesia. c) Hyaloclastite with angular shards of basalt and glass, clay and calcite, Hreppar Formation, Iceland. d) Peperite formed from the interaction of a lava flow with wet, unconsolidated sediment, Tenerife. e) Reworked, cross bedded, volcanoclastic material. In this project, this is referred to as sedimentary after White and Houghton (2006). From the Hreppar Formation, Iceland. f) Disarticulated pillows in a hyaloclastite matrix. This is typical of the HF.**

### 3.3.6 Volcanoclastic deposits in the Hreppar Formation

As each nomenclature scheme has positive and negative aspects to it, the approach that has been employed within the HF is to use different elements of Cas and Wright 1987 (descriptive terminology) and White and Houghton (2006). This has primarily been done as the exposure within the HF can be poor in places, leading to ambiguous units, making it very difficult to apply genetic terminology

without further detailed analysis (Passey, 2009). The focus of the project was to understand the architectures of different units, so genetic histories were not the primary focus, and therefore initial descriptive volcanoclastic terminology was used in the field, similar to Cas and Wright, 1987 (Figure 3-6). Where primary volcanoclastic units could be identified within the field, White and Houghton's genetic terminology was employed. Clastic sedimentary nomenclature has been applied to deposits that have been weathered/reworked, after White and Houghton (2006), with one exception; reworked hyaloclastite. The term reworked hyaloclastite has been employed as it is difficult to determine to what degree the hyaloclastite has been reworked in the HF and the term basaltic breccia/conglomerate is not favourable.

In order to fully describe and compare and contrast different volcanoclastic rock types in different parts of the world, a simpler, widely applicable nomenclature scheme has to be developed. This will help in hydrocarbon exploration in these areas, as often petroleum geoscientists have not experienced volcanic/volcanoclastic rocks and the difficulties of the associated nomenclature.

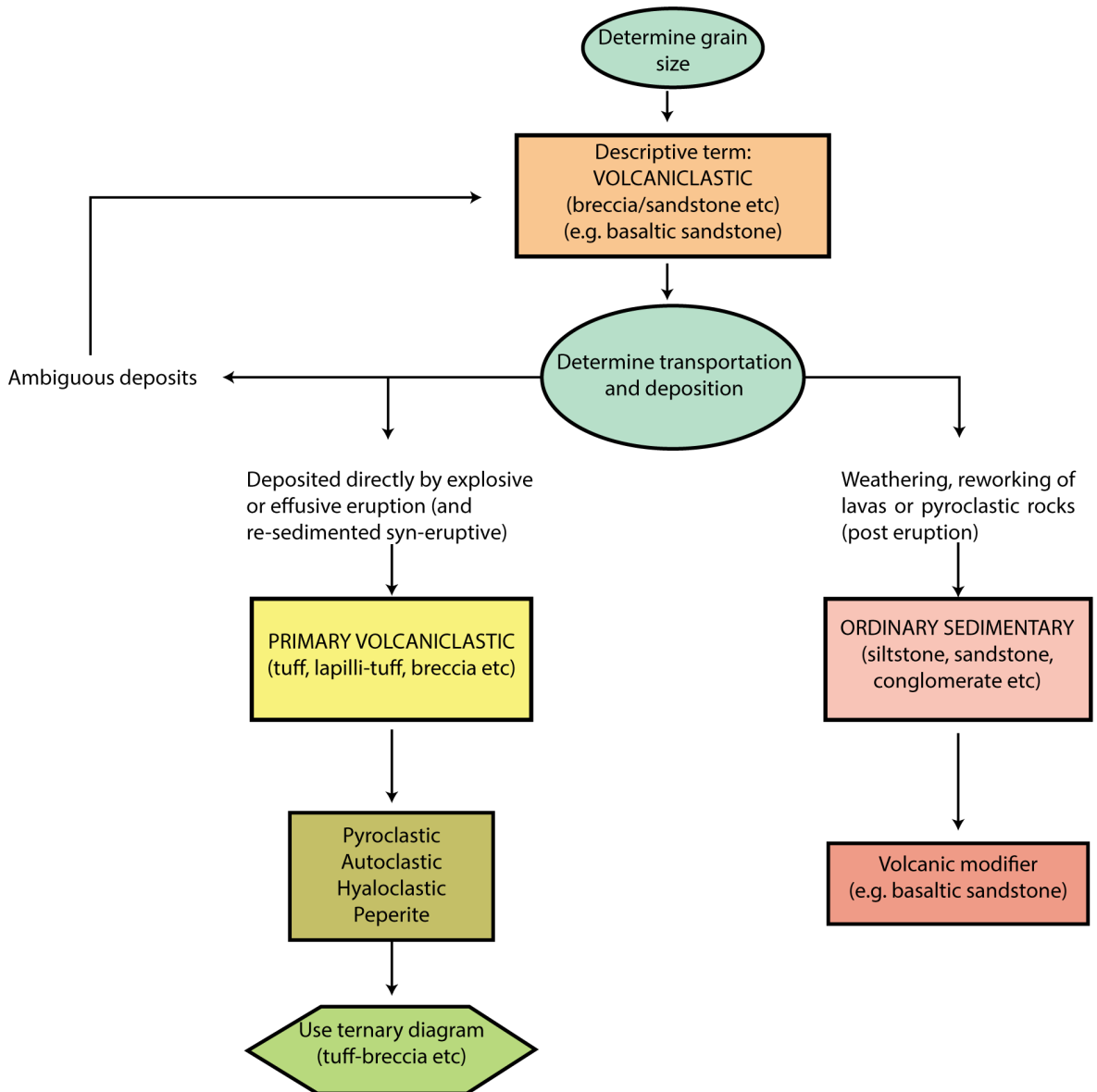


**Figure 3-6 Approach to volcaniclastic nomenclature in the HF. This is primarily based upon the schemes of Cas and Wright (1987) and White and Houghton (2006). The differences between Cas and Wright and the approach that has been employed here is that ambiguous deposits are given descriptive volcaniclastic terms opposed to genetic primary volcaniclastic terms. Additionally, weathered and reworked rocks are referred to as sedimentary opposed to epiclastic, used by Cas and Wright (1987).**

## 4 Methodology and maps

### 4.1 Introduction

This project is based primarily on detailed field mapping and logging of volcanic, volcanoclastic and sedimentary units. The HF around Flúðir has previously been mapped at a very large scale (1:600,000), and no detailed relationships of units in the HF were available from this. The ~16 km<sup>2</sup> study area is geologically, very diverse with clear evidence of numerous geological systems (volcanic, fluvial, glacial) having interacted throughout its history, leading to complex relationships between units. Detailed field mapping and logging was required to capture these relationships effectively. The project was primarily field based, however, in addition to the mapped and logged field data, samples were collected for petrographical and XRF analysis to support interpretations made based on field mapping and logging.

To gain an understanding of what some of the outcrops may look like in the subsurface, IKON's RokDoc programme was used to create synthetic seismic images.

### 4.2 Field methods

#### 4.2.1 Field mapping

The main purpose of the field mapping and logging was:

- to establish how the different units in the HF at Flúðir fit with the regional geology
- to determine the relationships between different units in the HF and their overall architectures
- to understand the intricate details of how different geological systems interact through time, with a specific focus on the HF
- To develop palaeogeographies and facies models of specific areas in the HF based on the detailed relationships between units

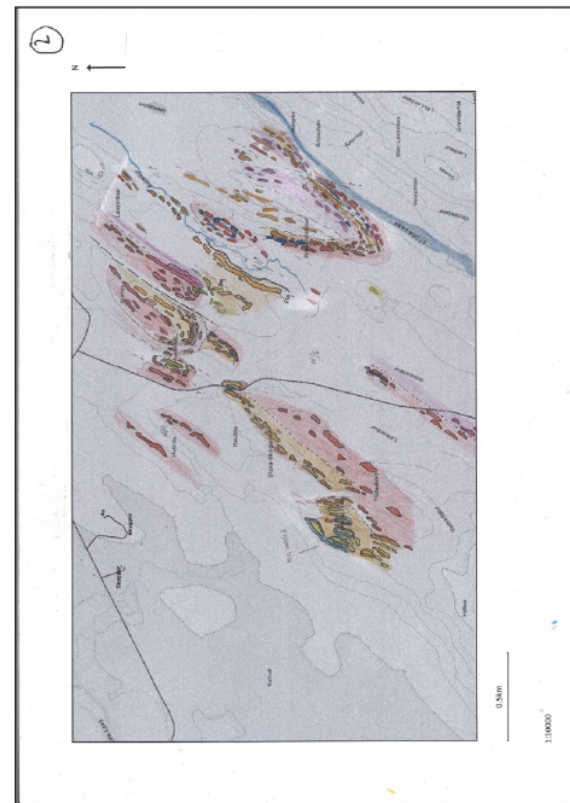
Geological field mapping was conducted using a combination of topographic maps from Landmælingar Islands in Iceland (1: 50,000) and aerial imagery from [www.map.is](http://www.map.is) (Figure 4-1). The resultant base maps were then digitised using Adobe Illustrator (Figure 4-2).

The mapped area is ~2.5 km ENE of Flúðir and covers an area of ~16 km<sup>2</sup> between two rivers- the Stora Laxá in the east of the area and the Litla Laxá in the west (Figure 4-2). Overlying the map is a grid, split in to 1 km<sup>2</sup> with letters and numbers for easy location identification. Localities are referred to in the following chapters using this grid system. This chapter features the A3 geological map for reference, there is also an A0 map (map insert) that should be used in conjunction with the following chapters for detailed locality information.

The geological map that has been produced for this project is primarily an outcrop based map (Figure 4-2). Where it is possible to predict the subsurface geology, this has been done, however this is only possible in limited locations in the HF at Flúðir. An outcrop map has been employed in the HF at Flúðir as there is an abundance of vertical exposure (cliffs), however the exposure between these cliffs is typically poor, and predicting the geology between is very challenging. The only place where the entire stratigraphy of the HF at Flúðir can be observed is within the Stora Laxá river section (map insert), however predicting the geology away from this locality in to the interior of the study area is near impossible, due to the underlying complex structure of the HF. In addition to the geological map, there is a part 1 and part 2 key (Figure 4-3, Figure 4-4) which is also applicable to all maps, logs and digitised images. A larger version of the key is found on the A0 geological map insert.



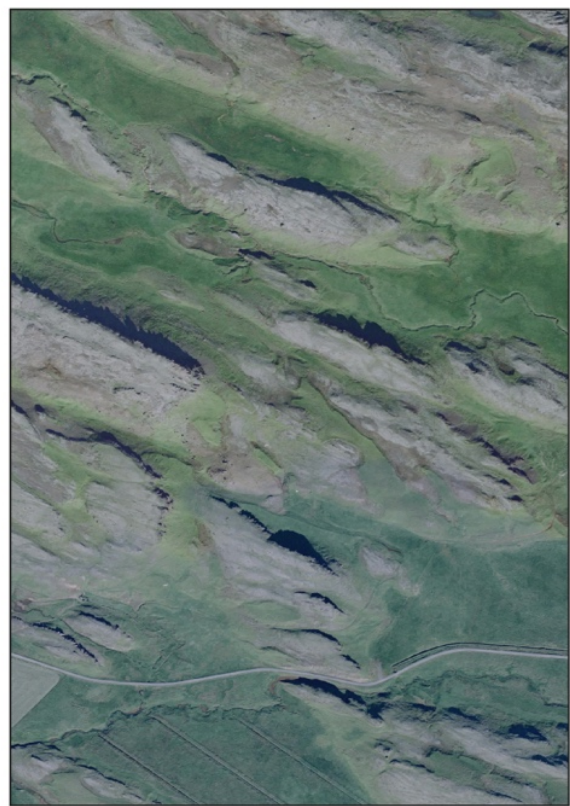
Broad scale aerial imagery (www.map.is)



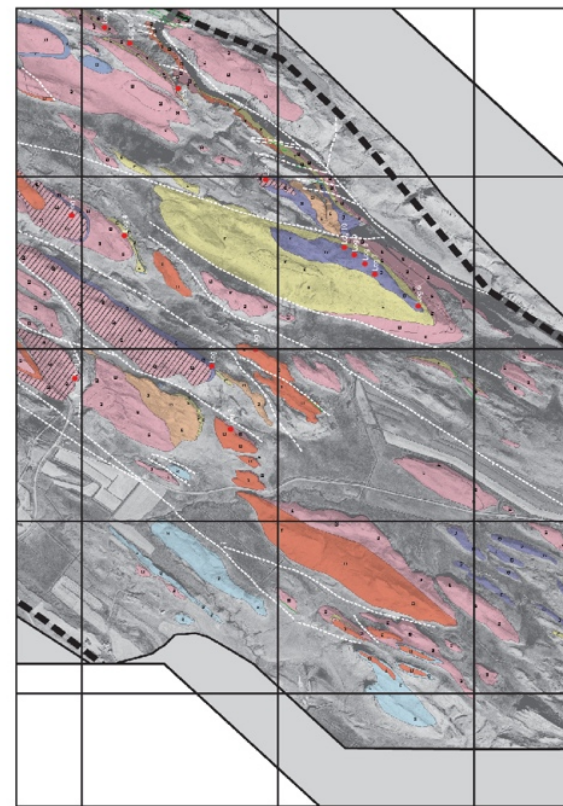
Base maps



Contour maps, with place names (www.lmi.is/)



Detailed aerial imagery (www.map.is)



Final geological outcrop map

Figure 4-1 Selection of maps, that were used in combination to create the final geological outcrop map. The aerial images used from [www.map.is](http://www.map.is) provide a much higher resolution than other products

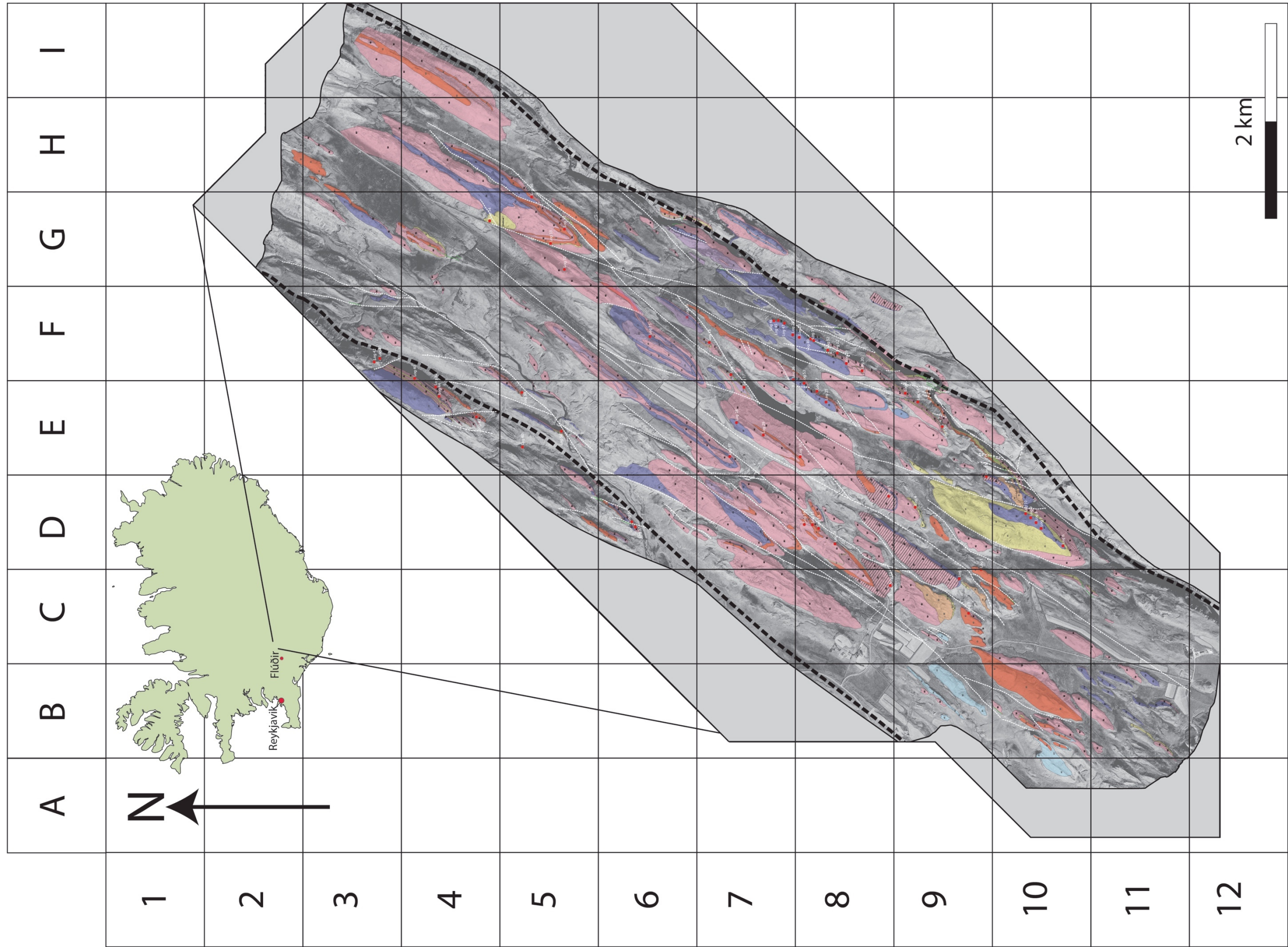


Figure 4-2 Geological map of the HF at Flúðir (situated 2 km WSW of the map). Greyed areas on the map indicate where no data has been collected, these areas are beyond the scope of the project. Red circles indicate log positions. The map is predominantly an exposure map, however, where possible to infer geology this has been done. The A0 scale map in APPENDIX 1, should be used in conjunction with the text for locating localities.

<b>A</b>	<p><b>Ignimbrite</b></p> <p><b>A1</b> Lava-like ignimbrite with well-developed fold structures on mm-m scale. Folds are highlighted by alternating dark and light bands. Very fine-grained (&lt;0.125 mm) and rarely glassy. Spherulites at the base of the unit is common. Laterally extensive &gt;0.5-1 km and ~5-10 m thick.</p> <p><b>A2</b> Massive lapilli tuff. Lithic lapilli range from 5-15 mm, pumice lapilli and weathered-out pumice commonly present. Typically grades in to C1. Laterally continuous &gt;0.5-1 km, to, 1-3 m thick.</p>
<b>B</b>	<p><b>Sub-aerial, basaltic lava</b></p> <p><b>B1</b> Local development of 'a'a, commonly with a clinker top facies. Typically the clinker top is irregular in its lateral extent and filled with sediment. These lavas are ~5-10m thick and laterally continuous. Often the entablature facies not always present.</p> <p><b>B2</b> Pahoehoe with obvious, well-developed colonnade. Laterally extensive dark grey/ pink and fine-grained (0.125 mm). Commonly the entablature is absent. Columnar joint spacing 1.5-2.5m with well defined chisel marks spaced 20-40 mm.</p> <p><b>B3</b> Pahoehoe with obvious core, poorly distinguishable top and bottom. Tops and bottoms vesicle-rich. Generally 5-10 individual units stacked together, with individual units ~1-3m in thick. Locally, thin columnar-jointed units transition in to, and have irregular boundaries with, hyaloclastite. Dark grey/ black, generally medium-grained (0.25 mm), locally fine (0.125 mm) and coarse (0.5 mm). Where laterally and vertically discontinuous, indicated by B3*.</p> <p style="text-align: center;"> <b>B3</b></p> <p><b>B4</b> Pahoehoe with obvious colonnade and entablature. Lower crust dominated by chilled margin, pseudo pillows and peperite development. Columns are frequently smaller than B2, ~1 m in width. Often found to laterally transition to hyaloclastite. Dark grey/black, fine to medium grained (0.125- 0.250 mm), aphyric.</p>
<b>C</b>	<p><b>Primary hyaloclastite and pillow breccia</b></p> <p><b>C1</b> Typically this unit has irregular contacts and has variable thickness, laterally can be quite extensive, up to 0.5 km. Dark grey/-black on fresh surfaces, brown/orange on weathered surfaces. Massive, poorly sorted, glassy juvenile clasts range from fine (0.125 mm) to coarse (64 mm); angular/sub-angular clasts; fine-grained (&lt;0.125 mm) matrix, dominated by glassy shards.</p> <p><b>C2</b> Typically this unit has irregular contacts and has variable thickness, laterally can be quite extensive, up to 0.5 km. Dark grey/-black on fresh surfaces, brown/orange on weathered surfaces. Massive, poorly sorted, glassy juvenile clasts range from fine (0.125 mm) to coarse (64 mm); angular/sub-angular clasts; fine-grained (&lt;0.125 mm) matrix, dominated by glassy shards. Additionally pillow fragments up to pebble size (64 mm) with an obvious glassy outer crust and pipe vesicles are present.</p>
<b>D</b>	<p><b>Reworked hyaloclastite</b></p> <p><b>D1</b> Unit is typically up to ~10 m thick and laterally discontinuous. Poor to moderately sorted, typically sub-rounded, rarely sub-angular, glassy juvenile clasts up to pebble (64 mm) in a fine grained (&lt;0.125 mm) matrix dominated by glassy shards. Grey/ black on fresh surfaces, brown/ orange on weathered surfaces. Unit is massive, with no apparent structure.</p> <p><b>D2</b> Unit is typically up to ~10 m thick and laterally discontinuous. Poor to moderately sorted typically sub-rounded, rarely sub-angular, glassy juvenile clasts up to pebble (64 mm) in a fine grained (&lt;0.125 mm) matrix dominated by glassy shards. Grey/ black on fresh surfaces, brown/ orange on weathered surfaces. Normal and reversely graded beds up to 2 m thick are characteristic of this unit.</p>

**Figure 4-3 Part 1 lithofacies key and codes with brief description of each lithofacies. See Chapter 5 for detailed descriptions and interpretations. Maps, logs and digitised panoramas use this same key.**

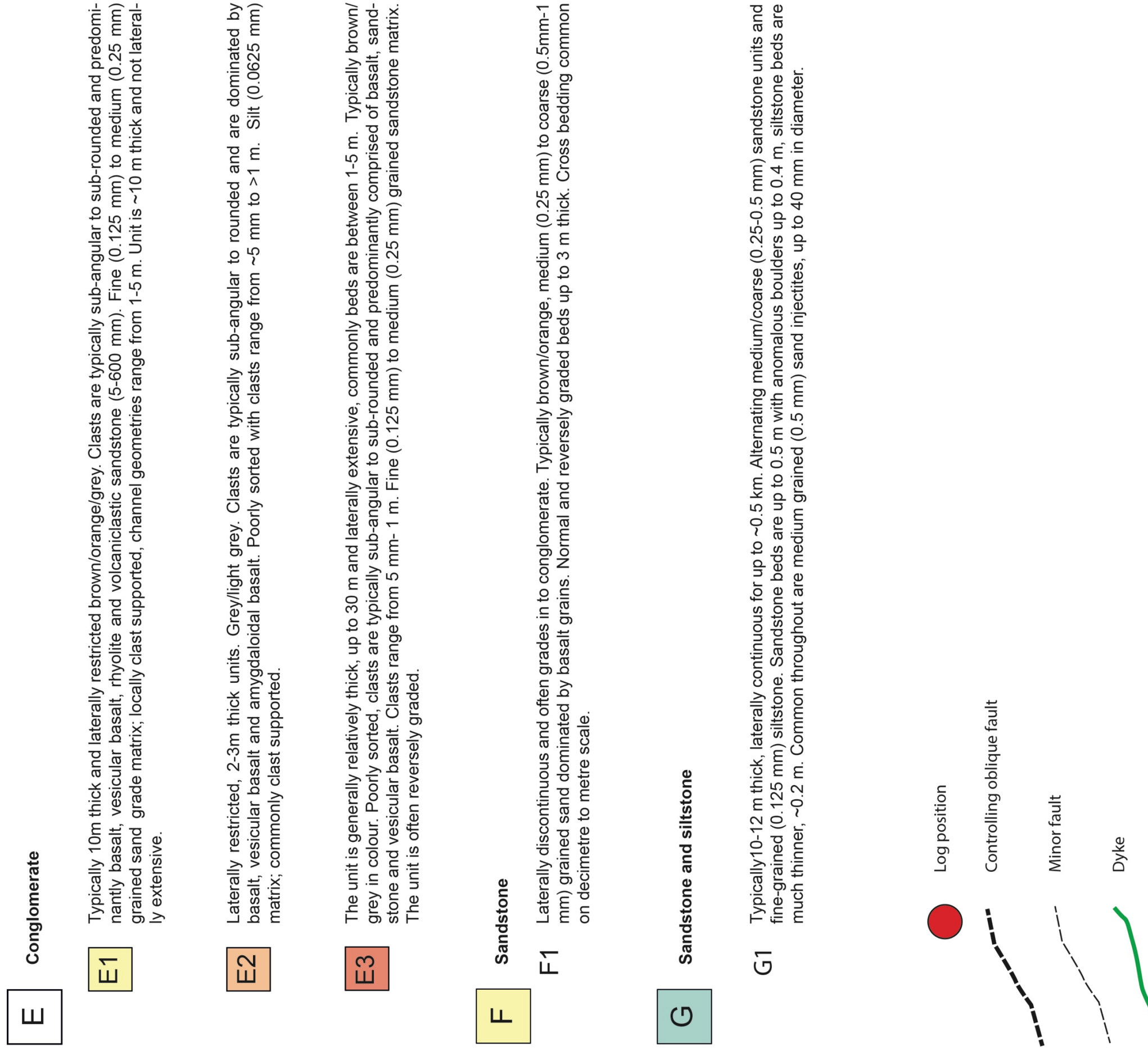
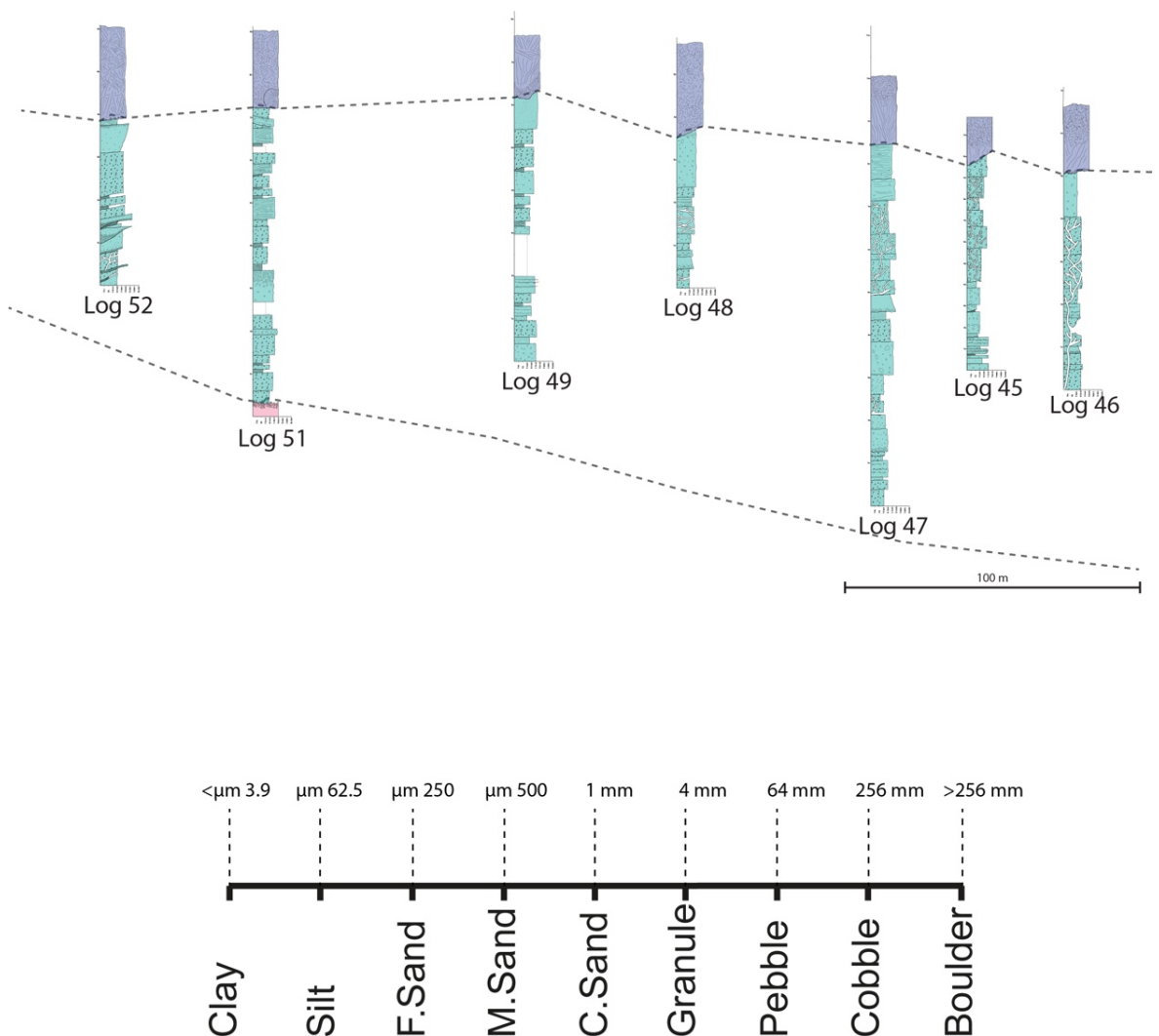


Figure 4-4 Part 2 lithofacies key and codes with brief description of each lithofacies. See Chapter 5 for detailed descriptions and interpretations. Maps, logs and digitised panoramas use this same key.

## 4.2.2 Logging

Field logging was employed to understand the relationships between different outcrops and to determine the lateral facies changes associated with volcano-sedimentary settings (e.g. the transition from sub-aerial lava in to lacustrine sediments, hyaloclastite and reworked hyaloclastite) (Figure 4-5). Approximately 60 logs at various scales (0.05m-0.5 m) and various heights (~2m-141m), were completed throughout the HF, with grain sizes based on the Udden-Wentworth scale (Figure 4-5). As well as determining relationships between different outcrops, logging allowed detailed information to be collected about the contacts between individual units (e.g. lava-sediment, lava-lava, lava-volcaniclastic etc).



**Figure 4-5 Example log section.** An example of a logged section consisting of 7 logs that have been correlated, to understand the interaction between different units and the palaeogeography of the section. The second image shows the logging scale that was used in the field.

## 4.3 Laboratory methods

### 4.3.1 Samples and petrography

Samples were collected of the main lithofacies in the field for petrographical analysis. Each lithofacies was sampled to understand on a microscopic level and to determine differences/similarities that may not be apparent in the field. The thin sections are a mixture of large and standard format, 30 µm thick unpolished sections, and were prepared by John Gilleece (University of Glasgow). The thin sections were analysed using a polarizing microscope and photomicrographs were taken with an Olympus DP25 camera.

### 4.3.2 Photogrammetry

Agisoft's PhotoScan was used to create 3D photogrammetry models of difficult to reach cliff sections, utilising images collected by a DJI Phantom 2 drone and GoPro Hero 4 camera (Figure 4-6). These models allow the reader to fully understand the complexity and intricacies of the more challenging sections.

To create the models, the drone had to be flown next to the outcrops to take photos and video. The drone was flown along the section being analysed by the author and field assistants. It was flown ~20-30 m away from the cliff, so the modelling software could recognise features to correlate. If the drone was flown too close the photos would be very detailed and prevent an accurate correlation in the modelling software. The drone was flown at various altitudes, so that the entire section would be covered (Figure 4-6). The GoPro camera was programmed to take a photo at 5 second intervals and to take continuous video. Continuous video was useful for analysis away from the field as it allowed, for example, lateral continuity of units to be determined more easily, especially when correlating logs. This method of image collection produces between 150-250 photos per section being analysed.

Away from the field, the images were selected for the modelling software. This involved ensuring that there was ~50% overlap between each image, no duplicate images, and if any images were not suitable (e.g. the drone's propellers were in the image) they were deleted. The aim was to have ~50-80 images per model. The images were then loaded to Agisoft PhotoScan to create the model. This involved

aligning the images, building a point cloud, building a polygon mesh, and generating a texture for the model. For an in-depth review of this process, see Tavani et al (2014).

### **4.3.3 Synthetic seismic**

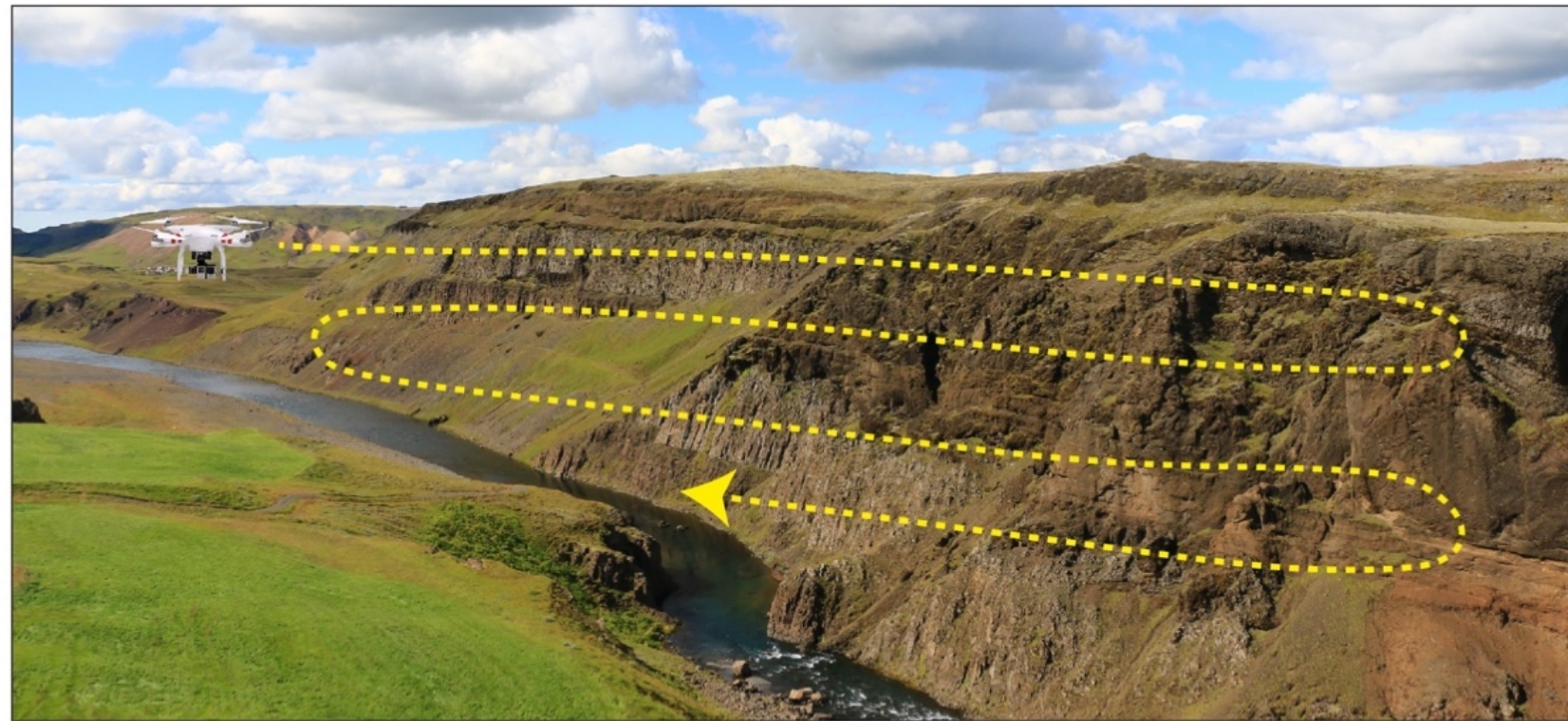
To understand how some of the sections in the HF may appear in the subsurface, synthetic seismic images were created at the University of Aberdeen. The images were created using IKON's RokDoc programme. This involved digitising the sections and assigning different subsurface properties to each unit. Chapter 9 provides a detailed description of this process.



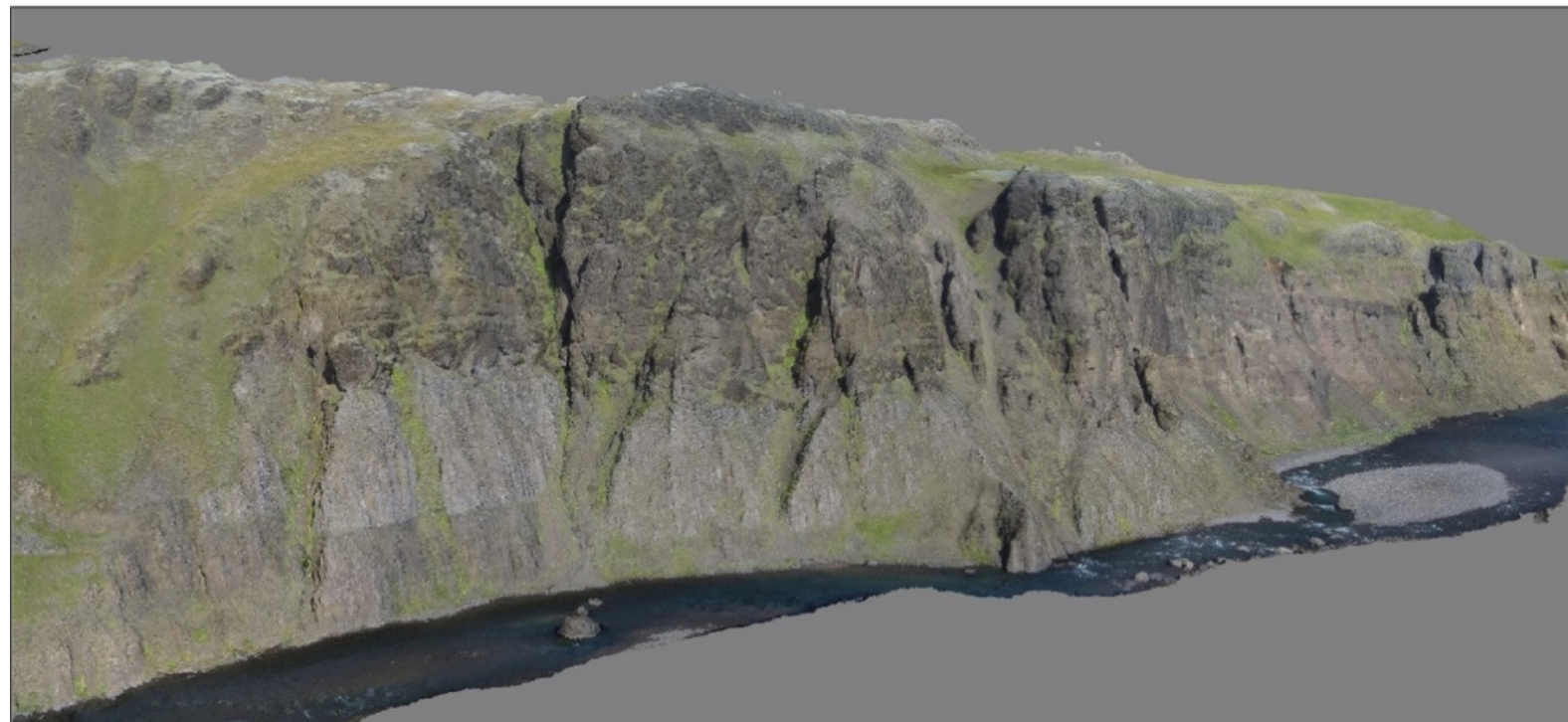
DJI Phantom 2 drone



Author and field assistant flying drone



Flight path of the drone, ensuring that every aspect of the section is covered. Flown at a distance of approximately 20-30 m from the cliff.



Resultant 3D photogrammetry model compiled in Agisoft PhtoScan. This is a 2D image of the 3D model, which allows the viewer to gain a better understanding of the intricacies and geomorphology of the section.

Figure 4-6 Example workflow and how the drone is flown in the field. The photos are then collated and processed using Agisoft PhotoScan to create a 3D photogrammetry model

## 5 Lithofacies and descriptions

### 5.1 Introduction

This chapter defines the main lithofacies within the HF (Figure 5-1). Systematic field documentation of; grain size, bedding and sedimentary structures forms the basis for lithofacies description (Eyles et al 1983) and has been employed here to characterise the geology of the HF in a quick and logical manner in the field.

The exposure within the HF is generally very good with units often continually being exposed for up to ~2 km. Detailed field mapping and logging has identified seven main lithofacies based upon the main characteristics of each unit, including grain size, structure, genetic origin and clast lithology. Whilst this is a simplification of the geology in the HF, this was essential, otherwise a different lithofacies could have been created for almost every outcrop. The seven main lithofacies are sub-divided in to fifteen sub-facies. These sub-facies further characterise the main lithofacies and allow subtleties within the units to be identified easily. The logged lithofacies within the HF have also been quantitatively analysed to determine the most dominant lithofacies (Table 5-1), as expected, sub-aerial lavas dominate the HF (60.3%). The average thickness of sub-aerial lavas within the HF is 6.7 m (Figure 5-2). Sandstones and hyaloclastites are potentially underrepresented within Table 5-1 (in comparison with the map) due to inaccessibility with logging these particular lithofacies within certain areas of the HF. It is clear from the quantitative data (Table 5-1) that volcanic systems and conglomerates (fluvial, glacial and mass) are the biggest competitors of accommodation space within the HF.

The lithofacies codes and colour (Figure 5-1) correspond to the geological map of the study area and should be used together. The lithofacies and sub-facies follow a simple layout. They have been given purely field based descriptions as far as possible, and based upon these descriptions, an interpretation of the unit has been determined.

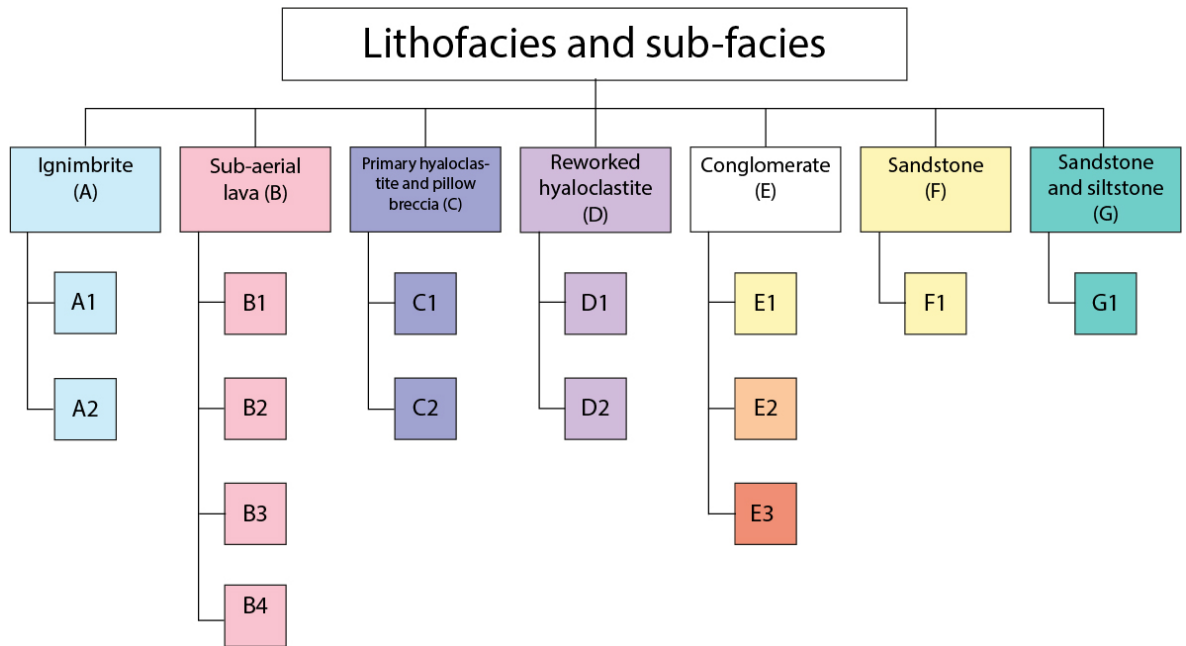
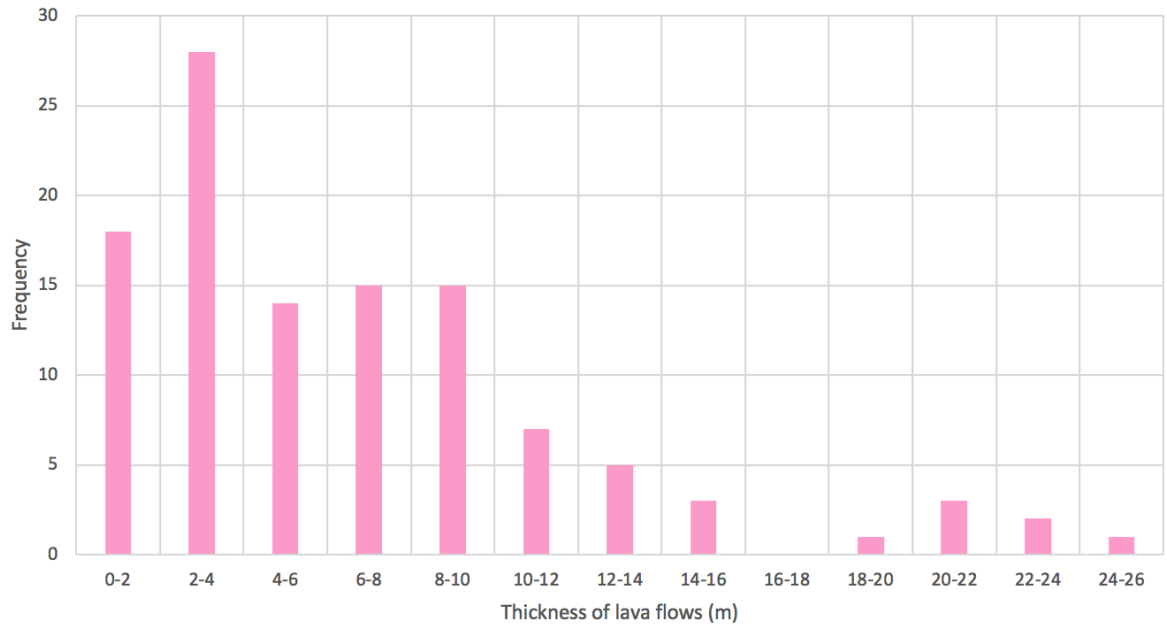


Figure 5-1 The main lithofacies of the Hreppar Formation and their associated sub-facies.

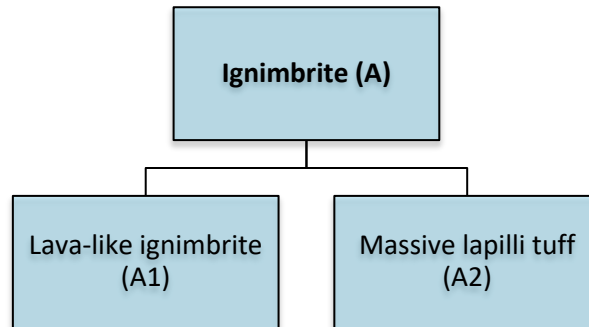
Lithofacies	% in logged data	Grouped %
B1	22.6 %	Sub-aerial lavas (B)  60.3%
B2	18.6 %	
B3	12.8 %	
B4	6.3 %	
C1	6.2 %	Primary hyaloclastite and pillow breccia (C)  8.8%
C2	2.6 %	
D1	2.1 %	Reworked Hyaloclastite (D)  2.8%
D2	0.7 %	
E1	3.3 %	Conglomerate (E)  15.6%
E2	1.2 %	
E3	11.1 %	
F1	8.1 %	Sandstone (F)  8.1%
G1	4.4 %	Sandstone and siltstone (G)  4.4%

**Table 5-1 Quantitative lithofacies data within the HF and the relative % of each in the field area. Sub-aerial lavas dominate the environment within the HF. No ignimbrite lithofacies were logged and therefore don't feature within the data. Additionally, sandstone is under represented here due to accessibility issues with logging sandstone.**



**Figure 5-2 Graph demonstrating the frequency of certain thicknesses of lavas within the HF logged data. The overall average thickness of a lava within the field area is 6.7 m.**

## 5.2 Ignimbrites



Lithofacies	Description (Field based)	Interpretation
Ignimbrite 	<p><i>Lithology:</i></p> <p>Dark grey/ black, with dark and light flow bands. Extremely fine grain size means that determination of lithology is very difficult. Towards the base of the unit, lithic lapilli (5-15 mm), pumice lapilli and weathered out pumice are present and became increasingly rare towards the top.</p> <p><i>Structure:</i></p> <p>At the base of this unit, there is an obvious eutaxitic texture, which is observed for roughly 1-2 m. At the base of the unit, spherulites up to 5 mm in diameter are present (Figure 5-3). They are particularly abundant within the bottom 0.4 m of the unit. Above the spherulites</p>	<p>The transition from a eutaxitic texture at the base of the unit in to well-developed curvilinear folds is indicative that welding has occurred. The curvilinear folds within the unit are indicative of lava-like ignimbrite, as there is clear evidence of agglutination/coalescence and ductile flow in addition to almost no original clast outlines being present (Andrews and Branney, 2011).</p> <p>Initially the eruption would have been more explosive (Plinian) with slightly lower temperatures and numerous lithics</p>

	<p>and eutaxitic texture, obvious curvilinear fold structures are observed within the unit and these range in size from mm scale to m scale (Figure 5-3). They are highlighted by the obvious difference in colour between dark and light flow bands.</p> <p><i>Geometry:</i></p> <p>Laterally extensive, however only observed within one valley in the field area. Continues for ~1 km and where exposed is ~5-10 m thick.</p>	<p>incorporated, before transitioning into a low fountaining boil-over eruption where temperatures would have been hotter, allowing coalescence and agglutination to occur.</p> <p>The spherulites towards the base of the unit are most likely the result of devitrification of original glass (Breitkreutz, 2013) and typically occur in large super-cooling events where liquids are quenched to crystalline solids (Gránásy et al, 2005).</p> <p>The difference in colour between dark and light bands within the curvilinear folds is most likely the result of compositional and textural differences within the unit (Breitkreutz, 2013), exacerbated by weathering and alteration.</p>
--	--	--

### 5.2.1 Lava-like ignimbrite (A1)

Lithofacies	Description	Interpretation
<div style="border: 1px solid black; padding: 2px; display: inline-block; background-color: #e0f0ff;">A1</div>	<p><i>Lithology:</i></p> <p>Dark grey/black and very fine grained/glassy. Obvious bands of lighter material are present but are also glassy (Figure 5-4).</p> <p><i>Structure:</i></p> <p>Eutaxitic texture at the base of the unit, transitioning in to the obvious curvilinear folded texture. Small spherulites (&lt;5 mm) are abundant and found at the contact with the underlying strata (Figure 5-3), before disappearing after 0.4 m. At this height the obvious curvilinear fold texture becomes apparent. Within the curvilinear section of the unit there is a lack of obvious fiamme.</p> <p>Fold structures on mm to m scale. Evidence of symmetrical,</p>	<p>Silicic eruptive event that was very explosive in comparison with the more effusive basaltic eruptions in the surrounding area. There are numerous volcanic centres nearby that have documented silicic events.</p> <p>Initially an explosive Plinian eruption occurred, depositing the eutaxitic ignimbrite observed at the base of the unit. This likely transitioned in to a boil-over type eruption producing a pyroclastic density current (PDC) which deposited this high-grade, lava-like ignimbrite (Branney and Kokelaar, 1992). These eruptions are incredibly hot; within the PDC there is extreme welding and ductile flow occurs, before cooling, causing mm-m scale folds to develop within the unit (Figure 5-3) (Schminke and Swanson, 1967; Branney and Kokelaar, 1992). During deposition of the unit, agglutination and coalescence occurred (Figure 5-4), causing clasts to become streaked out and difficult to identify (Branney and Kokelaar, 2002).</p>

	<p>asymmetrical, isoclinal and recumbent folds.</p> <p><i>Geometry:</i></p> <p>Laterally discontinuous. The unit is found at 3 main localities. Each individual outcrop is &lt;100 m in length and stands out from the surrounding landscape. These outcrops cover a distance of ~ 1 km and appear to demonstrate a linear trend (Figure 4-2).</p> <p><i>Petrography:</i></p> <p>Well defined flow banding, partial coalescence of lithic fragments and ‘swallow tails’ are defining characteristics of A1 (Figure 5-4).</p>	<p>The absence of upper and lower autobreccias indicates that the unit is not a lava.</p> <p>The linear trend of the outcrops suggests that the eruption was directed down a palaeo valley. The ignimbrites being much more resistant to weathering than the surrounding strata, have been preserved as upstanding topography. Laterally discontinuous most likely due to a combination of faulting/erosion and the nature of deposition (the unit thins).</p>
--	--	--

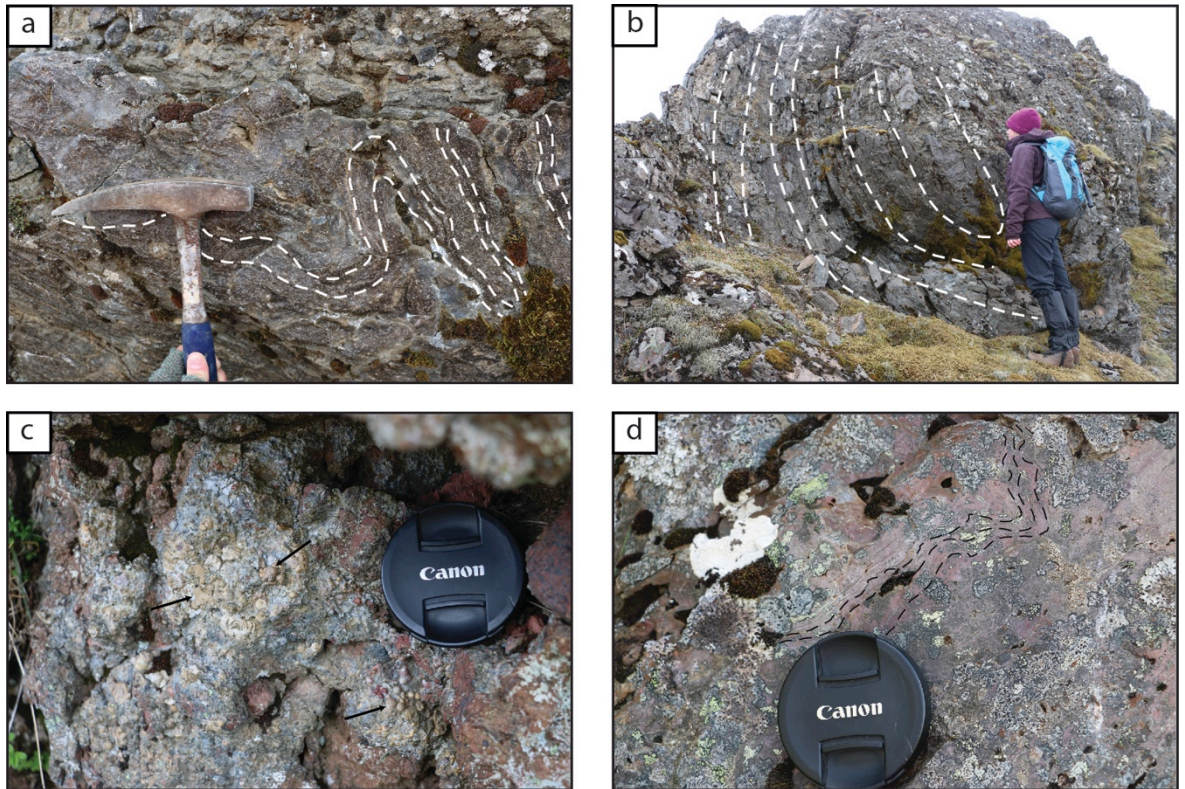


**Figure 5-3** Lava-like ignimbrites of the Hreppar Formation. a) Isoclinal and asymmetrical folds, with little evidence of clasts, due to agglutination and coalescence (hammer is 150 mm across). b) Large scale (>1 m) symmetrical folding. c) mm scale spherulites at the base of A1 (Lens cap is 67mm across). d) Chaotic recumbent and isoclinal folds on a mm scale.

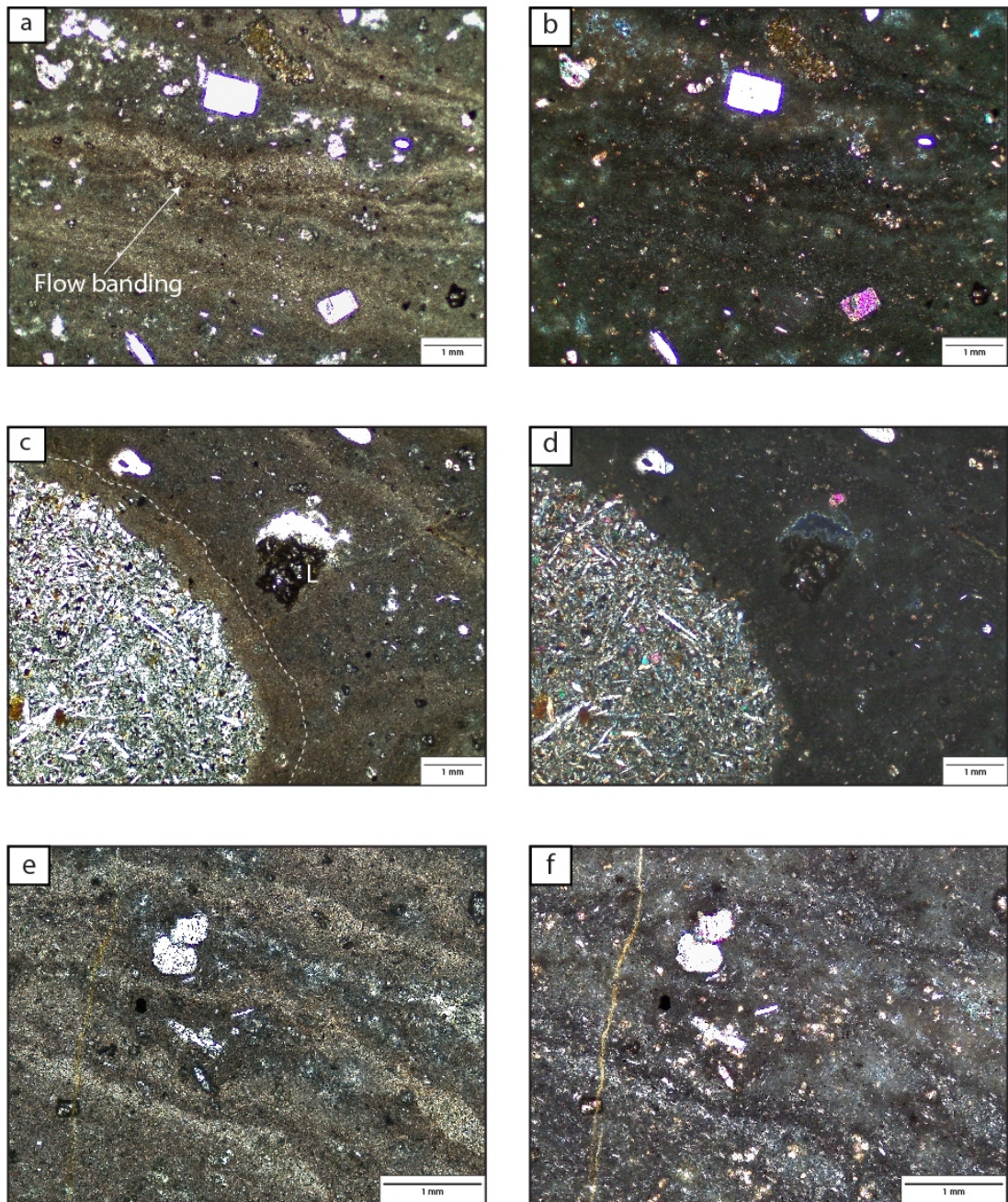


**Figure 5-4 Petrography of A1. a,b) PPL and XPL view of the overall texture of A1, with clearly defined flow banding present, formed as the result of compositional differences. c,d) PPL and XPL of a basalt lithic that has gone through partial coalescence (white dashed line). e/f) PPL and XPL images of flow banding. The flow banding occurs at different scales within the section.**

### 5.2.2 Massive lapilli tuff (A2)

Lithofacies	Description	Interpretation
A2	<p><i>Lithology:</i></p> <p>Blue/grey, fine grained tuff matrix. Non-welded, poorly sorted. Lithic fragments are composed of pumice, lapilli tuff and basalt. They are predominantly sub-angular, although locally, sub-rounded clasts are present, ranging in size from 1-40 mm (Figure 5-5). Generally matrix supported, but locally clast supported.</p> <p><i>Structure:</i></p> <p>The unit is massive with no obvious structure.</p> <p><i>Geometry:</i></p> <p>Poorly exposed along the entirety of the outcrop. Laterally discontinuous unit.</p> <p><i>Petrography:</i></p> <p>Sub-angular, predominantly altered basalt clasts, found within an ash rich matrix. A2,</p>	<p>Silicic eruptive event generating an explosive Plinian eruption. This caused lithics to be incorporated in to the unit due to explosive fragmentation processes within the eruption (Branney and Kokelaar, 2002).</p> <p>The unit is very poorly sorted and lacks any structure, indicating that the unit was deposited in a fluid escape-dominated flow boundary zone (Branney and Kokelaar, 2002).</p> <p>There is very little evidence of welding (Figure 5-6) within the unit, suggesting that no rheomorphism took place during this eruptive event.</p>

	shows no evidence of welding (Figure 5-6)	
--	--	--

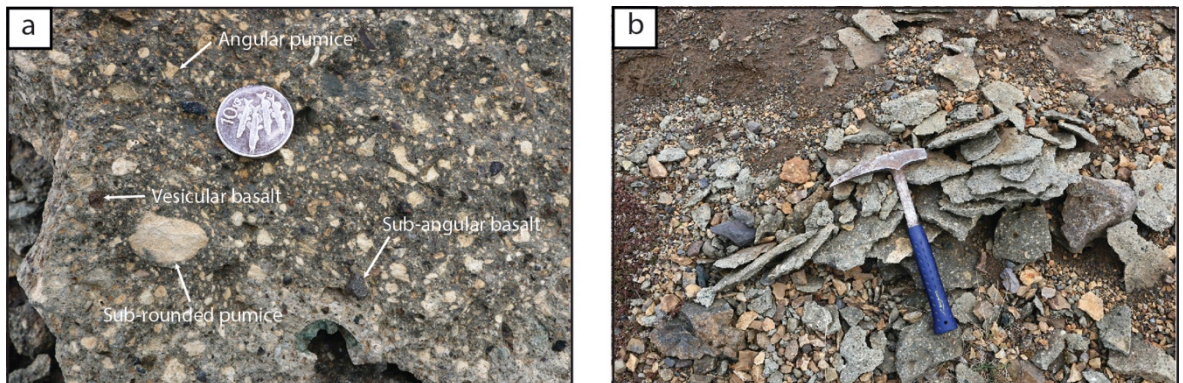


**Figure 5-5: Massive lapilli tuff.** a) Matrix supported, poorly sorted lapilli of predominantly pumice. These are sub-angular to angular and are <2 mm. Some larger pumice lapilli are sub-rounded, most likely due to transport within the PDC. Lithic country rock lapilli are also present, dominantly basalt (10 ISK coin is 27.5 mm across). b) The unit is very poorly exposed, with only 2-3 in-situ outcrops of A2, and typically appears as weathered scree.

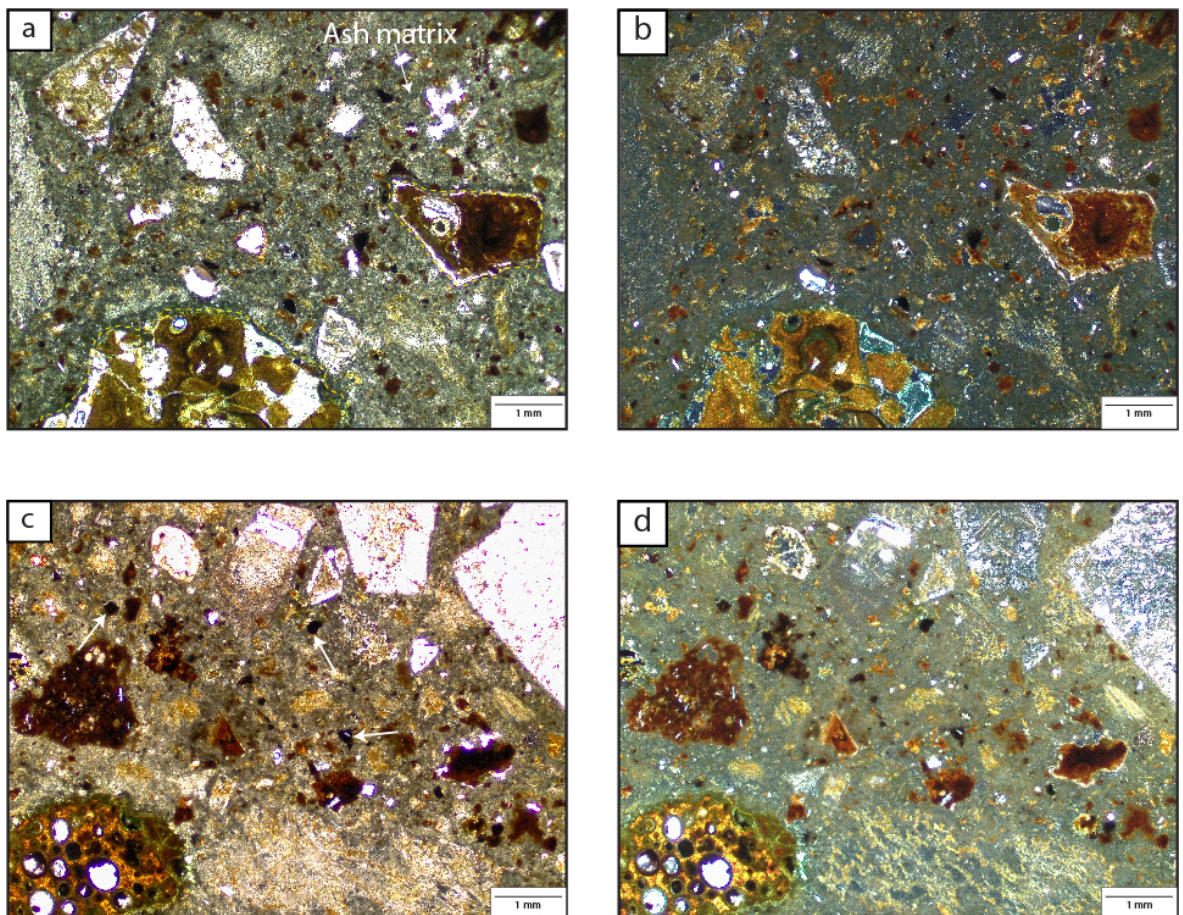
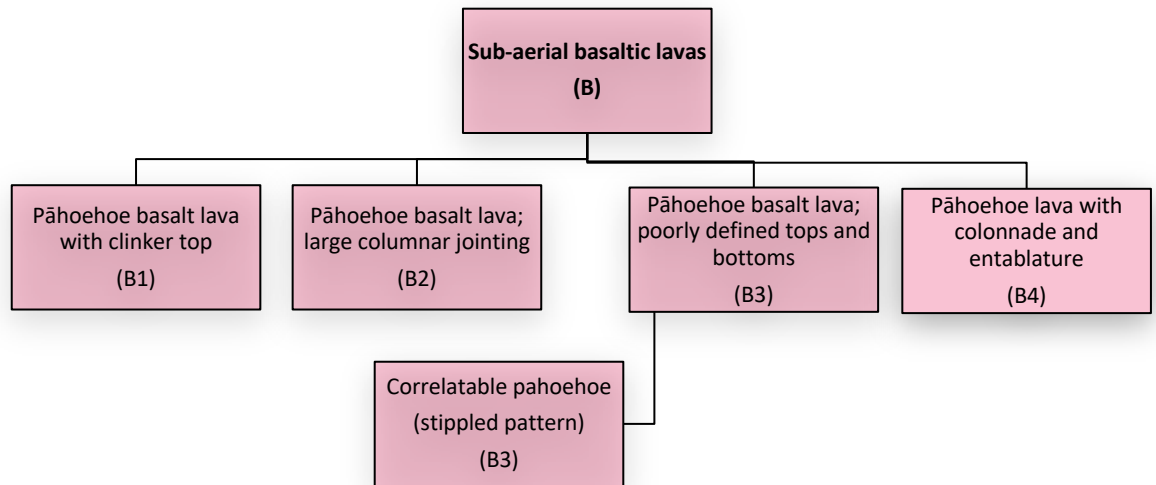


**Figure 5-6 Petrography of A2.** a/b) PPL and XPL photomicrographs highlighting the overall texture of A2. Clasts are angular and predominantly composed of altered basalt, within an ash rich matrix. c/d) Lower left of image highlights altered vesicular basalt clasts.

## 5.3 Sub-aerial basaltic lavas



Lithofacies	Description	Interpretation
Sub-aerial basaltic lavas <div style="border: 1px solid black; width: 40px; height: 40px; margin: 10px auto; text-align: center; line-height: 40px; font-size: 24px; font-weight: bold;">B</div>	<p><i>Lithology:</i></p> <p>Dark grey, brown, grey/pink in the field. Generally fine grained (0.125mm); however, occasionally medium grained (up to 0.5 mm). Typically aphyric although where coarser grained, pyroxene and plagioclase are distinguishable.</p> <p><i>Structure:</i></p> <p>Typically demonstrate three divisions; lower crust, core and upper crust. Colonnade can be observed in the core and entablature in the upper crust. The thickness of each of these varies and occasionally</p>	<p>These lavas are likely to be fissure-fed with localised central vents. The lavas may have begun along the length of the fissure, however they become localised to a few point sources (Cas and Wright, 1987). The fissure fed eruptions can initially begin with fire fountaining of a gas-rich magma, before giving way to an eruption of gas-poor lava, although these can also happen concurrently (Cas and Wright, 1987). Fissure</p>

	<p>the lower crust is not distinguishable. Where lower crust is distinguishable it is characteristically vesicle rich, with vesicles &lt;1mm. The core is often structureless with sparsely populated vesicles up to 5mm. Chisel marks are very common on the colonnade within the core of the lava. These are horizontal and generally up to 20 mm apart. Where a colonnade is present, columns range in size from 0.5-2 m wide. The upper crust is commonly dominated by vesicles &lt;1 mm in size. The upper crust, locally grades from highly vesicular in to brecciated lava. This commonly occurs over a scale of ~1m. It can often be very hackly in nature. The vesicles within the upper crust often demonstrate discrete banding on a ~50mm scale. The upper crust is also frequently dominated by an irregular clinker top/flow-top breccia which locally inter-fingers, comprising irregular shaped clasts (some appear relatively rounded), up to 400 mm that are vesicle rich, with the vesicles generally being rounded. This clinker top is usually filled with overlying sediment, which is often observed to have sedimentary structures within.</p>	<p>fed eruptions have been well documented, famously in relation to the 1783-1784 Laki eruption (Thordarson and Self, 1991) however the lavas observed in the Hreppar Formation are on a smaller scale than that of the Laki eruption. The Laki vents typically consist of scoria cones, spatter cones and tuff cones (Thordarson and Self, 1991). No obvious features of the fissures in the Hreppar Formation appear to have been preserved due to subsequent eruptions covering any evidence (Walker 1993).</p> <p>Pāhoehoe lavas are dominant in the HF. Pāhoehoe lavas are characterised by smooth billowy surfaces, with rope structures occasionally present. 'A'ā lavas are characterised by having very rough, fragmented surfaces (Cas and</p>
--	--	--

	<p><i>Geometry:</i></p> <p>Thickness of individual lavas varies from 2-3 m up to 15-20 m. They typically extend laterally for &gt;100 m. Commonly demonstrate sheet-like geometries although they do fill underlying topography, resulting in an irregular nature to the lavas.</p>	<p>Wright, 1987). These are end member lavas and within the HF there is evidence for lavas transitioning between the two (Figure 5-7, Figure 5-9, Figure 5-11, Figure 5-13).</p>
--	---	--

### 5.3.1 Pāhoehoe basalt lava with clinker top (B1)

Lithofacies	Description	Interpretation
<p><b>B1</b></p> <p>Represents 22.6% of the lithofacies within the HF (Table 5-1).</p>	<p><i>Lithology:</i></p> <p>Dark grey, fine grained (0.125 mm) (Figure 5-8), aphyric. Very vesicular towards the top of each flow, with vesicles up to 20 mm in diameter.</p> <p><i>Structure:</i></p> <p>The base of these units are not commonly observed, although where visible, it is rarely brecciated (rubbly?) and highly vesicular. This is on a relatively</p>	<p>Pāhoehoe and ‘a‘ā commonly form in the same lava flow, with pāhoehoe lava changing to ‘a‘ā as a result of the critical relationship between viscosity and the rate of shear strain being reached (Cas and Wright, 1987; Peterson and Tilling, 1980).</p> <p>The presence of a rubbly base at the bottom of the unit is uncommon in the HF. This suggests that only very locally has pāhoehoe transitioned to an ‘a‘ā lava, and a rubbly top is commonly observed (Figure 5-7)</p> <p>The rubbly top to the lava is not an in-situ weathering product as the highly vesicular clasts which compose the clinker top, do not fit together in a jigsaw fit as described by Passey and</p>

	<p>small scale (&lt;1 m). Typically, this transitions in to a very hackly core to the lava flow, with very poorly developed colonnade rarely present. These columns are typically 0.5-1 m wide. Hackly core of the lava typically transitions in to a rubbly top, with an increase in vesicles upwards. The rubbly top is highly irregular and often it is not present, but where it is, it can be up to ~6 m thick, although typically ~1-2 m thick. The rubbly top, where present, is always filled with overlying sediment, which gives the appearance of matrix supported clinker.</p> <p>Clinkers clasts are highly irregular in their shape and size, and range from 10-400 mm. They are vesicular and often</p>	<p>Bell (2007). The sedimentary infill also demonstrates sedimentary structures within. The roundness of the vesicles within the clinkers are typical of pahoehoe lava (Macdonald 1953; Cas and Wright, 1987). Typical pahoehoe inflation features such as vesicle banding are rarely present within the lava, (Duraiswami et al 2008; Self et al, 1998).</p> <p>Pahoehoe lavas that have a rubbly top/flow top breccia are referred to as rubbly pahoehoe (Keszthelyi and Thordarson, 2001; Bondre et al, 2004; Guilbaud et al, 2005). The rubbly pahoehoe forms as a result of a sudden increase in effusion rate, potentially from a pulse at the vent (Harris et al, 2017). An inflating pahoehoe sheet flow is subjected to a flux in lava which overpowers the strength of the crust and causes it to rupture, break and brecciate. Continued flux of lava transports the brecciated material and repeating cycles of inflation and surface crust brecciation cause the rubbly top to become thicker (Keszthelyi et al 2004; Guilbaud et al, 2005; Duraiswami et al 2008, Marshall et al, 2016).</p> <p>These lavas have a smooth basal crust but have varying degrees of disruption within their upper crusts, which locally</p>
--	--	---

	<p>found within lows within the lava surface.</p> <p><i>Geometry:</i></p> <p>Units are laterally extensive for up to 300 m. Typically it is 5-10 m thick.</p> <p><i>Petrography:</i></p> <p>Thin section is dominated by basalt alteration to palagonite, with clearly defined palagonite banding present (Figure 5-8).</p>	<p>grade in to a flow top breccia (Guilbaud et al, 2005; Duraiswami et al 2008, Marshall et al, 2016). They are thought to occur in various continental flood basalt provinces such as Deccan Volcanic Province, Faroe Islands and the Etendeka (Bondre et al, 2004).</p> <p>The grading of highly vesicular core into flow top breccia is typical of rubbly pāhoehoe flows (Guilbaud et al, 2005; Duraiswami et al 2008). Marshall et al, 2016 document a similar transition from a massive core to matrix supported rubble and finally clast supported rubble. In addition, the roundness of some of the clasts within the flow top breccia are suggestive of syn-emplacement shearing, rotation and grinding of fragments (Duraiswami et al 2008).</p> <p>Where the flow top breccia is irregular and found to inter-finger the underlying coherent lava, the rubbly material is thought to have formed and piggybacked on top of the flow. This material fills in cracks and depressions within the lava flow (Figure 5-7) (Guilbaud et al, 2005; Duraiswami et al, 2008).</p> <p>The presence of sedimentary structures and sediments within the clinker tops in the HF are indicative of</p>
--	---	--

		<p>a sedimentary system having developed after the deposition of the lava. This sediment has been transported over the clinker top, filling in the cracks and the majority of void space between the clinkers (Figure 5-7). Similarly, Marshall et al, 2016 document well sorted, sub-rounded quartz sand grains occupying the matrix between basaltic clasts within rubbly pāhoehoe in Antrim Plateau Volcanics of Northern Australia.</p>
--	--	---

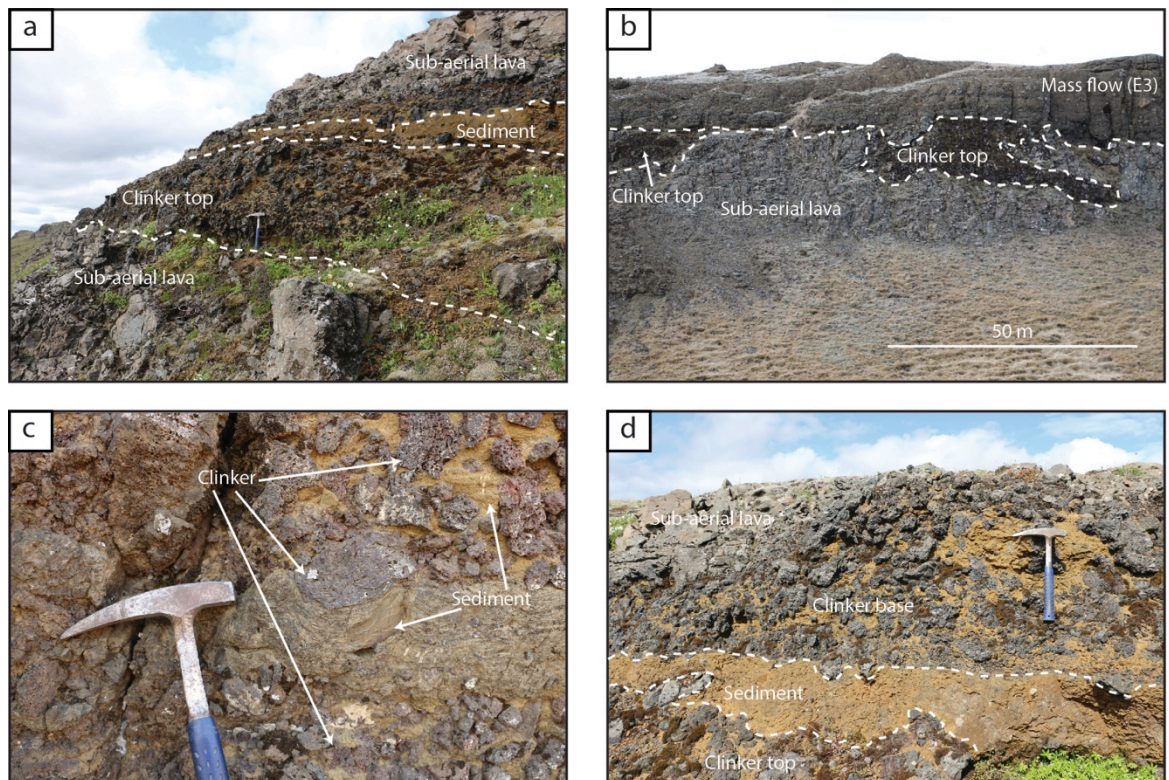


**Figure 5-7 Typical large and small scale features of B1. a) The transition from coherent, sub-aerial lava in to a clinker top, sediment package and then another lava. The sediment package is relatively small, but there has been enough quiescence in volcanic activity for it to develop. b) Clinker top of the underlying sub-aerial lava is highly irregular, in places it is not present. It appears to be preserved in “lows” within the upper surface of the lava flow. The unit seen here is overlain by E3 conglomerate. c) Detailed view of a clinker top. Clinker appears to be supported by a sandstone matrix. This matrix is laminated on a mm scale, indicating that there must have been a lot of water present to wash sediment in the clinker top and deposit it there. Clinker is highly vesicular. d) Clinker base to sub-aerial lava flows are very irregular in their nature too. The lava appears to be much more coherent towards the left of the figure.**

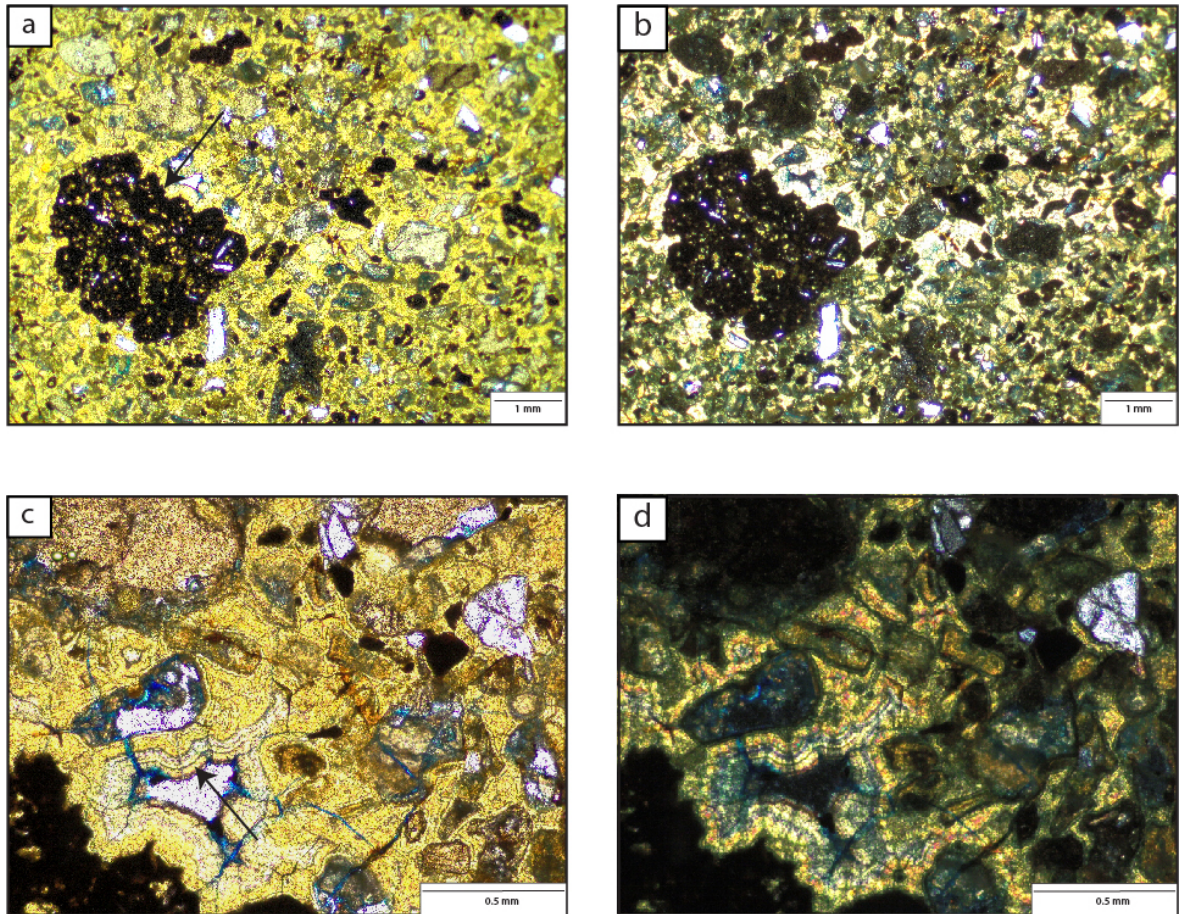


Figure 5-8 Petrography of B1. a/b) PPL and XPL photomicrographs highlight the replacement of original basalt, texture (arrow). The sample is dominated by palagonite alteration, indicating that this sample represents a relatively weathered section of B1, this could be close to clinker unit. c/d) PPL and XPL photomicrographs of fine, concentric palagonite banding (arrow).

### 5.3.2 Pāhoehoe basalt lava; large columnar jointing (B2)

Lithofacies	Description	Interpretation
<b>B2</b> Represents 18.6% of the lithofacies within the	<p><i>Lithology:</i></p> <p>Dark grey/pink, fine grained (0.125 mm), aphyric (Figure 5-10).</p> <p><i>Structure:</i></p> <p>Very well developed colonnade, with wide</p>	Well defined chisel marks are an obvious feature of this unit. These form as the result of an upwards propagating cooling front in the colonnade and therefore represent the thermal gradient and cooling rate and successive growth (DeGraff and Aydin, 1987; Lyle, 2000; Phillips et al, 2013).

<p>HF (Table 5-1).</p>	<p>(~1.5-2.5 m) columnar jointing, is the defining characteristic of this unit. Entablature is rarely present. Commonly, 20-40 mm spaced chisel marks are present.</p> <p><i>Geometry:</i></p> <p>Units are laterally continuous for up to ~150 m. Individual lavas are relatively thick at up to ~20 m and they often appear to fill lows. In areas where lavas have filled lows, columnar jointing appears to be wider at ~2-3 m.</p> <p><i>Petrography:</i></p> <p>B2 demonstrates a well defined ophitic texture with clear replacement of pyroxene (Figure 5-10).</p>	<p>The spacing of these chisel marks, remains relatively consistent within the columns, indicating a constant cooling rate (Phillips et al, 2013).</p> <p>Evidence presented from Hawaii suggests that ancient lava flows have a lack of entablature, even though there may be significant volumes of rainfall (&gt;250 cm/yr). This implies that there has to be more water than average heavy rainfall totals to generate an entablature (Long and Wood, 1986). In these units there is rarely any evidence of an entablature.</p> <p>The entablature of a lava flow forms as a result of the lava flow being subjected to large volumes of water (Long and Wood, 1986). Long and Wood (1986) suggest that the entablature has formed through quenching, whereas the colonnade has experienced a much slower cooling rate. Often lavas demonstrate multiple sets of colonnade and entablature, which can be attributed to different flooding events. The lack of an entablature in this unit (Figure 5-9) can therefore be attributed to the fact that the lava has not</p>
------------------------	--	---

		<p>been subjected to extensive flooding and therefore rapid cooling as a result of it disrupting pre-existing drainage (Long and Wood, 1986; DeGraf and Aydin, 1987; DeGraf et al, 1989; Lyle and Preston, 1998).</p> <p>The unit appears to fill lows within the palaeotopography, potentially where water would dam. The lack of an entablature in these lavas and no obvious water interaction facies suggests that the existing drainage networks would have been diverted elsewhere, meaning no water could inundate the cooling lava flow.</p>
--	--	--

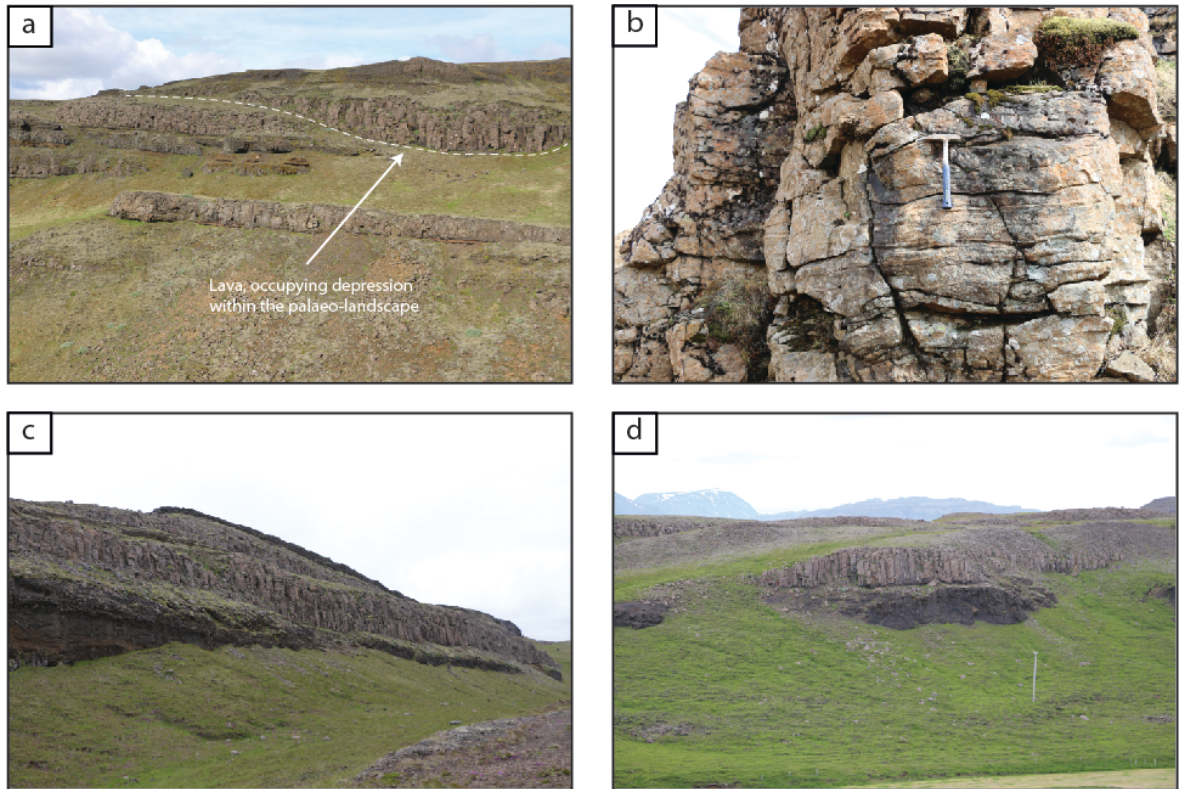


**Figure 5-9 Typical features of B2 lavas a) B2 filling a low within the topography, at this point, columnar joints appear to be more widely spaced indicating that the lava has ponded within a low. b) Close up view of one of the individual columns, highlighting how thick these columns are. Chisel marks are well defined on a 20-40 mm scale. c) Laterally extensive nature of B3. d) Highlights the massive nature of B3, with widely spaced columns, phone line pole for scale (~9 m).**

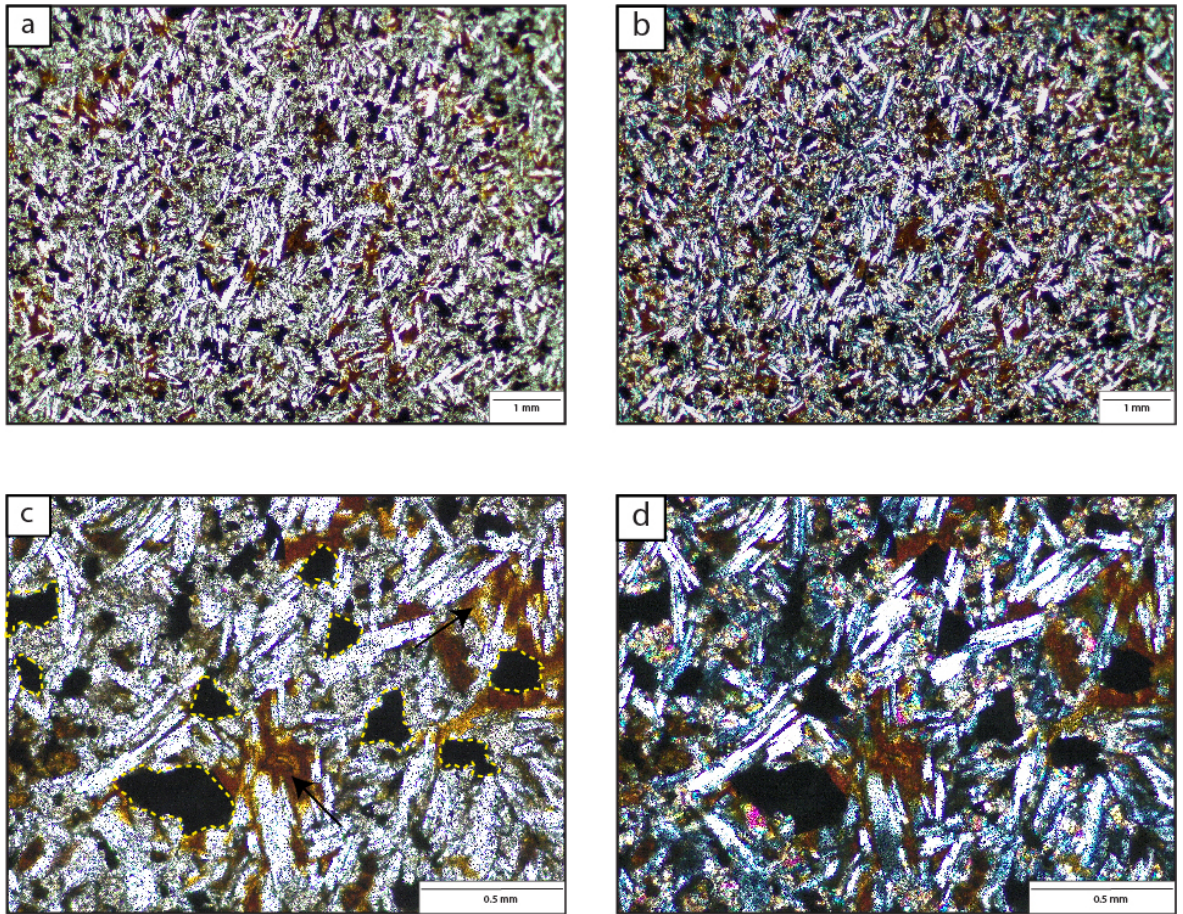


**Figure 5-10 Petrography of B2. a/b) PPL and XPL photomicrographs highlighting the fine grained, ophitic texture within B2. c/d) PPL and XPL photomicrographs of detailed ophitic texture, with pyroxenes being replaced (brown mineral). Fe-Ti oxides are common within B2, highlighted (yellow dashed lines).**

### 5.3.3 Pāhoehoe basalt lava; poorly defined tops and bottoms (B3)

Lithofacies	Description	Interpretation
<p data-bbox="320 342 411 427"><b>B3</b></p> <p data-bbox="320 499 520 752">Represents 12.8% of the lithofacies within the HF (Table 5-1).</p>  <p data-bbox="320 992 520 1525">** Certain units of B3 appear to be correlatable across the field area. Typically transitions from hyaloclastite.</p>	<p data-bbox="544 342 695 376"><i>Lithology:</i></p> <p data-bbox="544 443 1050 528">Dark grey/pink, fine grained (0.125 mm), aphyric (Figure 5-12).</p> <p data-bbox="544 600 922 633">Vesicle and amygdale rich</p> <p data-bbox="544 701 695 734"><i>Structure:</i></p> <p data-bbox="544 801 1050 1895">Vesicles dominate the lower crust of this unit, they are largest and most abundant towards the base of the unit. At the base the vesicles are up to 20 mm in diameter, becoming finer upwards to ~1 mm. The unit has a well-defined core, where a colonnade is frequently present. Columns are much smaller than in B2, and vary from ~1-2 m in width. An entablature is rarely present. The upper crust of the unit is dominated by vesicles, becoming larger towards the top, (up to 20 mm). Differentiating between flows can be difficult as the lower and upper crusts have very similar characteristics and rarely have a weathering profile between.</p> <p data-bbox="544 1962 1050 2047">This unit is commonly found to stratigraphically overly sub-</p>	<p data-bbox="1082 342 1441 925">This unit is characterised by its sheet-like architecture. This type of architecture indicates that the lava was erupted with a relatively continual supply of magma over a long period (Passey and Bell, 2007).</p> <p data-bbox="1082 992 1441 1525">The lack of sedimentary units (boles, soils or weathering profiles) between lava flows indicates that volcanism was relatively continuous throughout this period and a sedimentary system could not establish.</p> <p data-bbox="1082 1592 1441 2074">The presence of vesicle banding (Figure 5-12) and the transition from pillow lavas (see Figure 5-11) indicates that this unit is composed of inflated pāhoehoe lobes and has resulted in a compound sheet flow</p>

	<p>aqueous facies, such as C1 and C2 (Figure 5-15, Figure 5-17).</p> <p><i>Geometry:</i></p> <p>Unit is laterally continuous for up to 0.7 km, more commonly it is 200-300 m. Lavas appear to form sheets.</p> <p><i>Petrography:</i></p> <p>B3 is very fine grained with prevalent fractures throughout. Chlorite amygdales with palagonite banding are common (Figure 5-12).</p>	<p>(Figure 5-11) (Hon et al, 1994; Self et al, 1997).</p> <p>Prevalent columnar jointing, suggests that the environment was particularly wet at the time of emplacement of the lavas (Lyle, 200).</p>
--	--	---

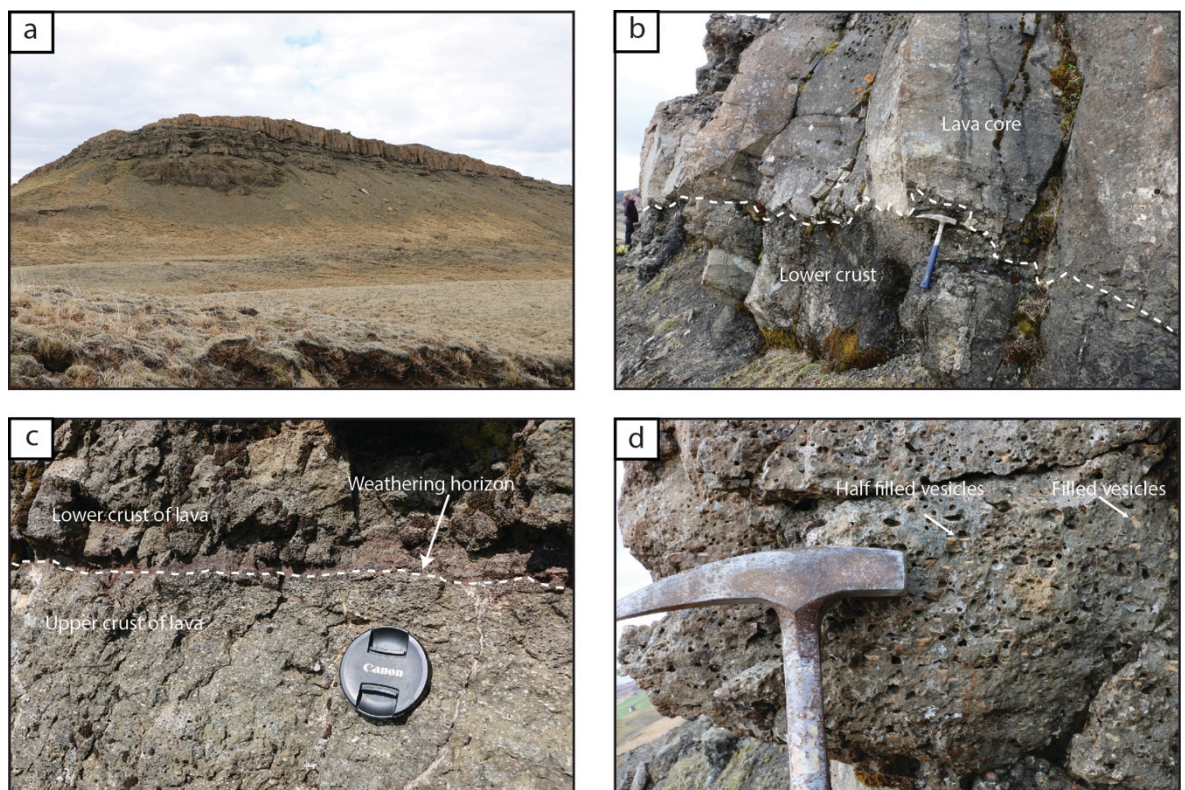


**Figure 5-11** Typical large and small scale features of B3 hammer head is (150 mm across). a) 7 to 8 individual lavas are found on top of one another. Cores of the lavas are what makes them stand out. b) Close up image of A, demonstrating the contrast between the lower crust and core of the lava flow. c) Upper crust of lower lava and lower crust of upper lava. These lavas are separated by a red weathering horizon, indicating that there has been a period of time between these individual lava flows. Often no weathering horizon is present, making

differentiation between lavas much more difficult. d) Diffusely aligned vesicles within the upper crust of a lava flow, are indicative of. Inflation of pāhoehoe lobes. Some vesicles are half filled with calcite, indicating that they are the correct way up.

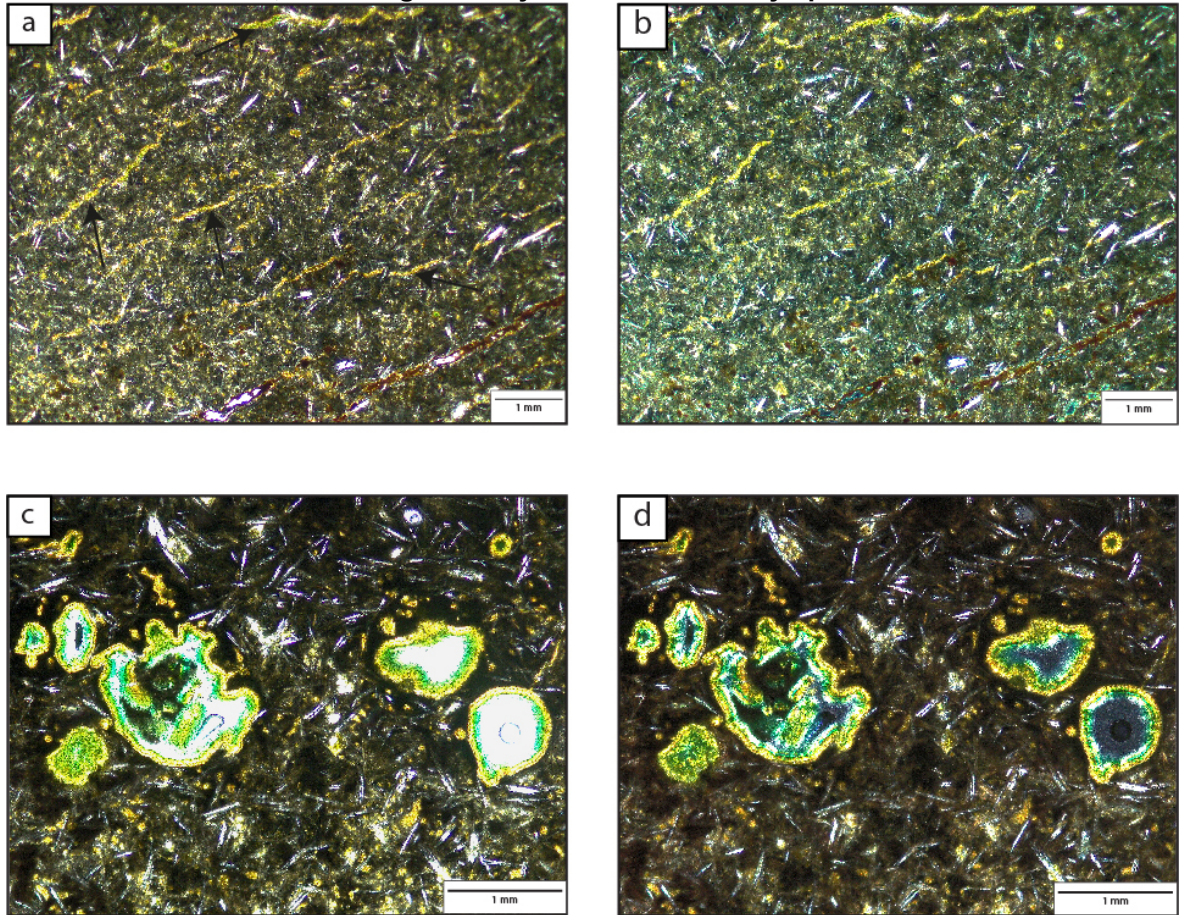
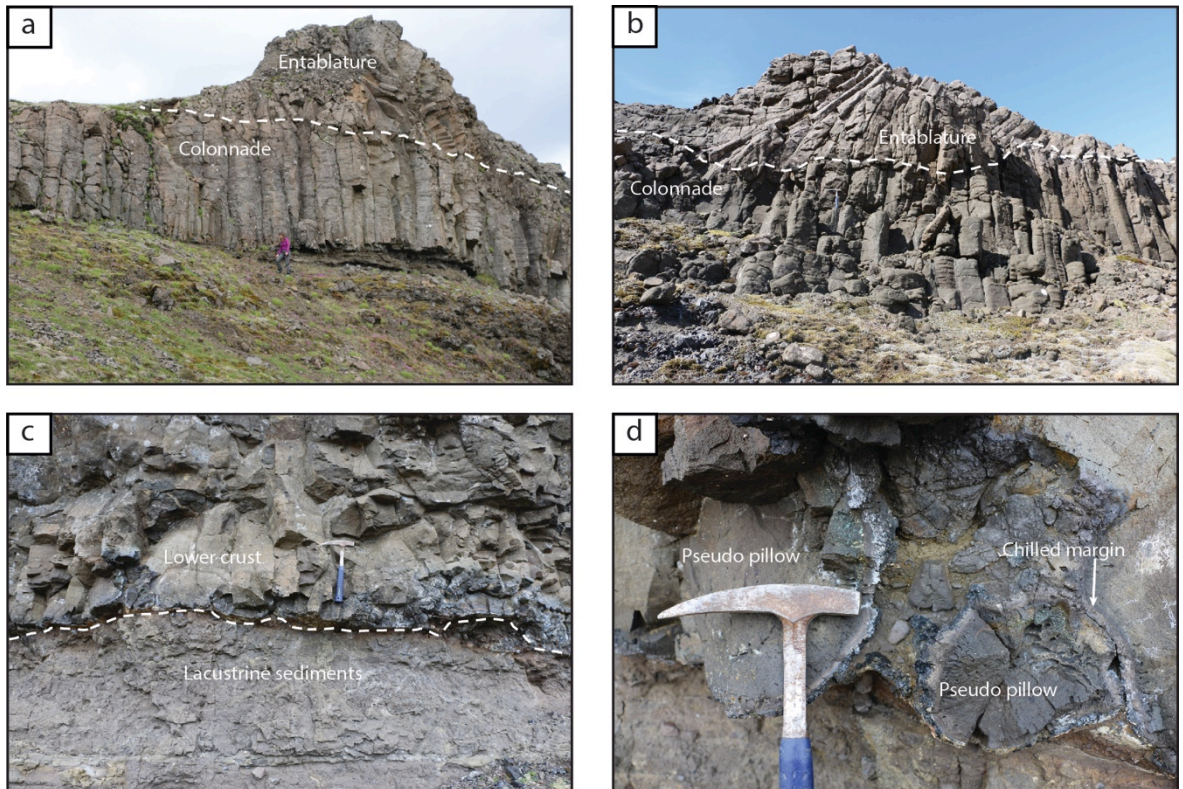


Figure 5-12 Petrography of B3 . a/b) PPL and XPL photomicrographs highlight the fine grained nature of B3. Throughout B3, there are prevalent fractures, that have been filled with a later fluid. c/d) PPL and XPL photomicrographs of chlorite amygdales with concentric palagonite banding on the interior.

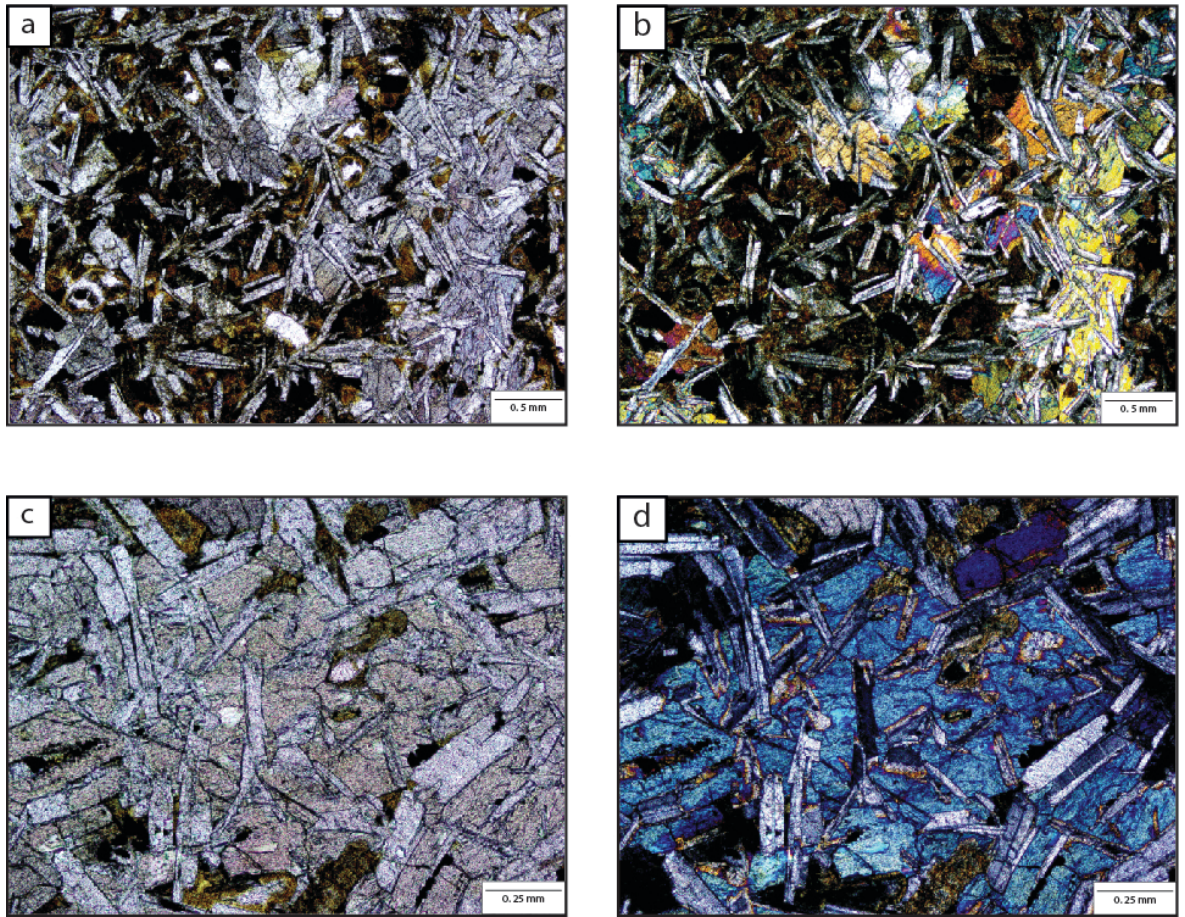
### 5.3.4 Pāhoehoe lava with colonnade and entablature (B4)

Lithofacies	Description	Interpretation
B4	<p><i>Lithology:</i></p> <p>Dark grey/black, fine to medium grained (0.125- 0.250 mm), aphyric (Figure 5-14).</p> <p><i>Structure:</i></p>	<p>This unit is characterised by its well-developed colonnade and entablature. The presence of an entablature (Figure</p>
Represents 6.3% of the lithofacies within the		

<p>HF (Table 5-1).</p>	<p>The lower crust is characterised by a chilled margin, with pseudo pillow and peperite development (Figure 5-13). The unit has a well-defined core, where a colonnade is frequently present. Columns are much smaller than in B2 and vary from ~1-2 m in width. Entablature is common with well developed curvilinear jointing present (Figure 5-13). This unit is found to transition laterally and vertically in to hyaloclastite facies (C1 and C2) and typically overlies lacustrine sedimentary units (G1). Where there is a contact with G2, there is occasionally limited, peperite development (Figure 5-13).</p> <p><i>Geometry:</i></p> <p>Unit is laterally continuous for up to 200-300 m. Lavas appear to form sheets.</p> <p><i>Petrography:</i></p> <p>Well developed ophitic texture with prevalent replacement of pyroxene (Figure 5-14).</p>	<p>5-13) indicates that the unit was subjected to large volumes of water during cooling (Long and Wood, 1986). Other lavas at a similar stratigraphic height do not have an entablature, indicating that they were not subjected to this water ingress.</p> <p>The transition from sub-aerial lava in to hyaloclastite facies suggests that this unit was emplaced in a topographical low where water collected. Evidence of blocky clasts with a jigsaw fit at the interface between the two units suggests that fragmentation occurred in situ and by quenching or mechanical stress (Skilling et al, 2002; Rawcliffe and Brown, 2014).</p>
------------------------	--	---

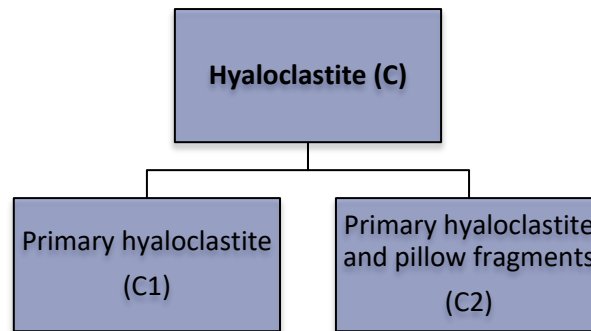


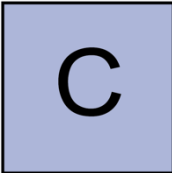
**Figure 5-13 Typical features of B4 lavas** a) Well developed colonnade and entablature present, with evidence of some of the entablature having been removed through erosion. b) Gradual transition of colonnade in to entablature, columns have well defined chisel marks. Columns within the entablature curve to a specific point indicating this is where water ingress occurred. c) Contact between B4 and underlying G1 unit. Little interaction between the two units is recorded. d) Detailed interaction of B4 with G1 indicates on a cm scale, some interaction has occurred with the generation of small <150 mm pseudo pillow structures and jigsaw-fit peperite development. There is a well-defined chilled margin present on the lower crust of the lava.



**Figure 5-14 Petrography of B4. a/b) PPL and XPL photomicrographs displaying a well developed ophitic texture with areas of the section having clearly undergone replacement (brown areas in A). c/d) PPL and XPL photomicrographs of detailed ophitic texture.**

## 5.4 Primary hyaloclastite and pillow breccia



Lithofacies	Description	Interpretation
Primary hyaloclastite and pillow breccia  	<p><i>Lithology:</i></p> <p>Dark grey on fresh surfaces, whereas weathered surfaces are distinctively brown/orange. Where brown/-orange suggests that the volcanic glass has been converted to palagonite. Poorly sorted, basalt clasts are angular to sub angular and range in grain size from fine sand (0.125 mm) to pebble (64 mm). Generally the unit is matrix supported. The matrix is composed of finer grained (&lt;0.125 mm) hyaloclastite material and glassy shards.</p> <p><i>Structure:</i></p> <p>Generally massive, however locally patches up to 1-4 m dominated by</p>	<p>The presence of a hyaloclastite matrix surrounding pillows confirms that non explosive processes, quenching and thermal granulation, have occurred (Fisher 1984; White et al, 2000; Gill 2010). Hyaloclastite can be generated by the flow of sub-aerial lava in to a water body and the subsequent interaction (Schminke et al, 1997). The transition from hyaloclastite in to sub-aerial lava is indicative of this process occurring.</p>

	<p>fine-grained hyaloclastite and fragmented pillows.</p> <p>Often the hyaloclastite is found occupying space between pillow lavas and broken pillows. This typically becomes just hyaloclastite towards the top of each individual unit. Fragmented pillow structures are often present within the hyaloclastite, and are identifiable from their obvious glassy rim, transitioning in to coarser grained basalt. These fragments can be up to 0.2-0.3 m, although are generally smaller (~20-50 mm). Where fragments of pillows are present, typically these are matrix supported, however dense clast supported areas are also present.</p> <p>Distinct pillow morphologies are common. These are either isolated or are found in clusters; however, pillows are often fragmented and broken. Where the pillows are coherent they are up to 0.7 m in diameter. The pillows typically demonstrate a distinct structure. Within some pillows, vesicles (including pipe vesicles) have been filled with hydrothermal minerals; (quartz and calcite).</p>	<p>Where pillow clumps are isolated it suggests that kinetic processes, such as tumbling and slumping, have occurred. These processes would have taken place on steep slopes and led to the further breakdown of hyaloclastite clasts (White et al, 2000).</p> <p>Where pillows lava are densely clustered, this is most likely, a relatively proximal location to where the sub-aerial lavas entered the sub-aqueous environment.</p> <p>The presence of a cusp or teardrop at the base of individual pillows confirms that the sequence is the correct way and up and has not been folded. This morphology occurs when new pillows settle in to underlying pillows (Gill, 2010).</p> <p>The typical orange/brown colour</p>
--	--	---

	<p><i>Geometry:</i></p> <p>Thickness of units is typically up to ~10-15 m. Towards the top of an individual unit, the pillow density is generally a lot lower and pillows are isolated. These units typically extend laterally for ~50-100 m.</p>	<p>associated with weathered areas indicate that sideromelane has been converted to palagonite due to the unstable nature of this volcanic glass (Gill, 2010).</p> <p>Where basalt slivers are present, it has been suggested by Bergh and Sigvaldason (1991) that the lava was erupted from a sub-aqueous fissure at high extrusion rates. This created a large, heterogeneous mass, which would flow downslope as a result of gravitational instability. Further fragmentation would occur with increasing distance from the vent, whilst the heterogeneous mass of hyaloclastite would enclose the lava. As a result, slivers of lava would align to the direction of transport (Bergh and Sigvaldason, 1991).</p>
--	---	---

### 5.4.1 Primary hyaloclastite and pillows (C1)

Lithofacies	Description	Interpretation
<p><b>C1</b></p> <p>Represents 6.2% of the lithofacies within the HF (Table 5-1).</p>	<p><i>Lithology:</i></p> <p>Dark grey/black on fresh surfaces, brown/orange on weathered surfaces. The unit is poorly sorted, with angular to sub-angular clasts of basaltic hyaloclastite that range from fine sand (0.125 mm) to pebble (64 mm). Matrix surrounding hyaloclastite is typically fine grained (&lt;0.125 mm). Areas within the unit are commonly dominated by pillow structures. Pillows are typically up to 0.7 m in diameter and have obvious pillow morphologies. They have an outer glassy rim (Figure 5-15), which is generally up to 5 mm in thickness. This passes in to a vesicle rich zone (Figure 5-15), in which the vesicles are typically &lt;1 mm. Towards the core of the pillow, large pipe vesicles up to 50 mm radiate from the core of the pillow. Within the core of the pillow vesicles are often present and are up to 10 mm. Each pillow often demonstrates teardrop or cusp morphology at its base, where it has formed with the surrounding pillows. Where pillows are isolated, they are generally in a</p>	<p>Hyaloclastite can be generated in numerous environments such as submarine volcano growth, Surtseyan eruptions, lacustrine, fluvial and sub-glacial settings (White et al, 2000; Watton et al, 2013). This typically occurs when sub-aerial lavas encounter these differing water bodies.</p> <p>The presence of pillows and the general observation that sub-aerial lavas transition in to pillow lavas laterally, is indicative of sub-aerial basaltic lavas entering a relatively shallow sub-aqueous environment (Fisher 1984). The presence of pillows in this unit, indicates the lavas entered the water body had relatively low flow rates (White et al, 2000).</p>

	<p>matrix of hyaloclastite and have no obvious tear drop morphology.</p> <p><i>Structure:</i></p> <p>Typically the unit is found in massive patches up to 4 m thick, frequently intercalated with C2. Often laterally, the unit is found to grade in to pillow rich areas and coherent, sub-aerial lavas. The unit has highly irregular contacts with the underlying and overlying strata. Often at the base of the unit, clusters of pillows are common, which typically transition to isolated pillows within a primary hyaloclastite matrix, before becoming solely primary hyaloclastite.</p> <p><i>Geometry:</i></p> <p>The units can be up to 15 m thick and laterally extensive (&gt; 0.5 km), although they can be laterally confined (&lt;20 m). Commonly they are 100-200 m in lateral extent, thickness is highly variable over this distance.</p> <p><i>Petrography:</i></p> <p>Dominated by palagonite, amygdales and vesicles, with a palagonite and clay matrix. Some vesicles are</p>	<p>Where pillows are densely clustered (Figure 5-15), this is most likely, a relatively proximal location to where the sub-aerial lavas entered the sub-aqueous environment. Where pillows are found in isolation, this indicates that these have travelled further down the hyaloclastite delta (Cas and Wright, 1987), which can form as a result of sub-aerial lavas entering a water body.</p> <p>Where irregular contacts are observed with underlying strata this is interpreted as the result of sub-aerial lava interacting with small bodies of standing water. These standing bodies of water are most likely the result of fluvial drainage systems being disrupted by lava flows, causing water to accumulate (Jones and Nelson, 1970). This would generate small</p>
--	---	---

	partially filled and therefore act as geopetal indicators. Basaltic clasts typically have a well developed palagonite rim (Figure 5-16).	areas of the unit apparently surrounded by a sub-aerial lava.
--	--	---

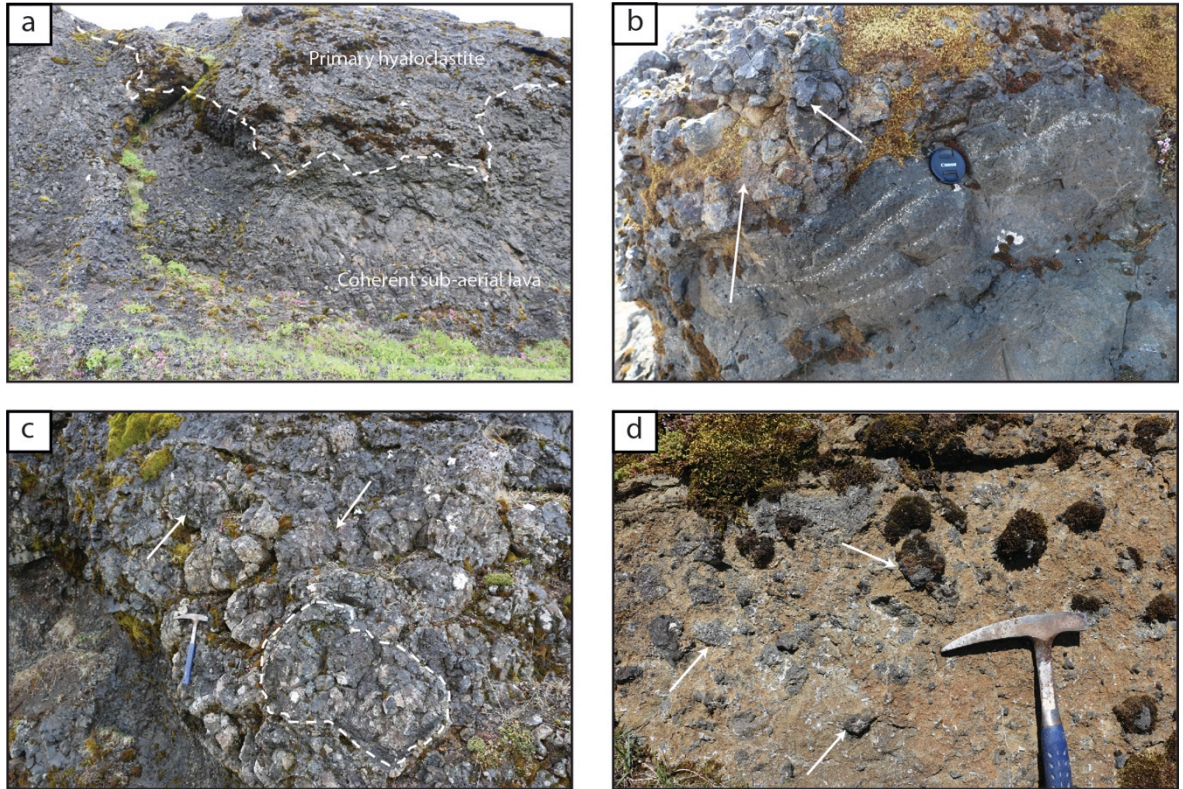


**Figure 5-15 Features of C1 primary hyaloclastite** a) Irregular contact between sub-aerial lava and C1. Vertical scale of the image is ~10 m. b) Clasts of hyaloclastite up to 80 mm, clustered together, clast supported. Vesicle banding within the sub-aerial lava, indicating inflation has occurred. c) Cluster of pillows up to ~1 m across. The density of these pillows is relatively high. d) Smaller clasts of hyaloclastite within a glassy, basaltic matrix. Hammer is ~300 mm.

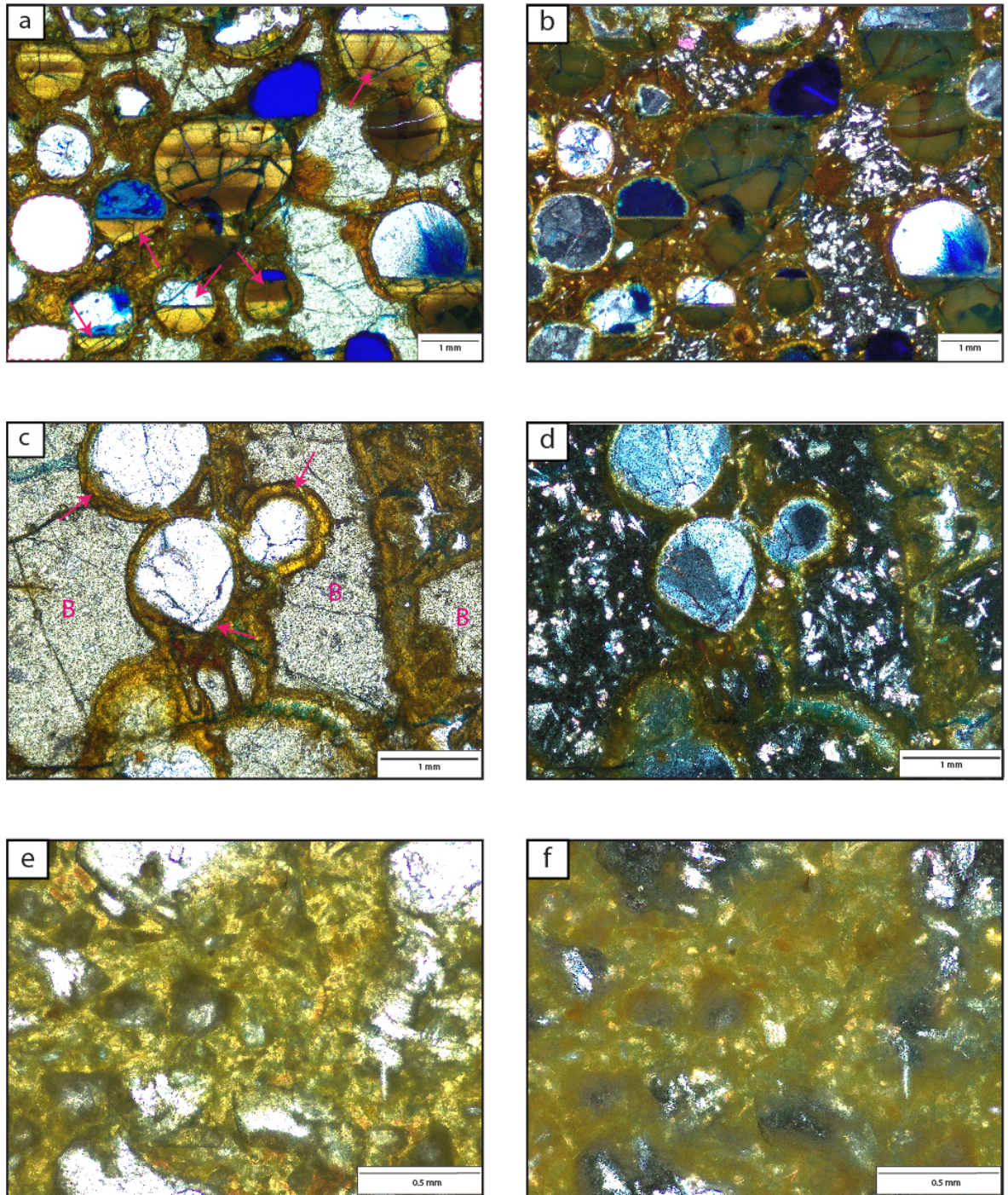


**Figure 5-16 Petrography of C1 . a/b) PPL and XPL photomicrographs of basalt clasts, palagonite, amygdales, vesicles and partially filled vesicles (the section has been stained with blue dye). The partially filled vesicles (indicated with pink arrows) are geopetal indicators and highlight the unit is the correct way up. c/d) PPL and XPL photomicrographs of amygdales with concentric palagonite banding (pink arrows). Basalt clasts (B) have a well developed palagonite rind. e/f) PPL and XPL photomicrograph of detailed matrix, primarily composed of palagonite and clay.**

### 5.4.2 Primary hyaloclastite and pillow fragments (C2)

Lithofacies	Description	Interpretation
<p><b>C2</b></p> <p>Represents 2.6% of the lithofacies within the HF (Table 5-1).</p>	<p><i>Lithology:</i></p> <p>Dark grey/black on fresh surfaces, brown/orange on weathered surfaces. The unit is poorly sorted, with angular to sub-angular clasts of basaltic hyaloclastite, lava fragments and pillow fragments, which range from fine sand (0.125 mm) to pebble (64 mm). Matrix is typically fine grained (&lt;0.125 mm) (Figure 5-18). Pillow fragments are easy to identify due to their distinct morphologies; glassy rims, pipe vesicles and distribution of regular vesicles. The unit is often found in close proximity to C1.</p> <p><i>Structure:</i></p> <p>The unit is typically massive and is frequently found intercalated with C1. Often laterally, the unit is found to grade in to pillow rich areas, coherent sub-aerial lavas and re-worked hyaloclastite. The unit has highly irregular contacts</p>	<p>As in C1, irregular contacts with under and overlying strata indicate that sub-aerial lavas came in to contact with standing bodies of water, such as dammed fluvial systems and lake bodies. This interaction generated hyaloclastite and pillows (Fisher, 1984; White et al, 2000; Watton et al, 2013).</p> <p>The presence of broken pillow fragments (Figure 5-17) suggests that the lavas have encountered a sub-aqueous slope and have started to prograde down it. The fragmentation of the lavas is through quenching and deformation of brittle lava crusts. Continued breakage occurs through movement down slope (White et al, 2000).</p> <p>Isolated pillows (Figure 5-17) within a fine matrix indicate that they have</p>

	<p>with the under and overlying strata.</p> <p><i>Geometry:</i></p> <p>The unit can be up to 15 m thick and laterally extensive (&gt; 0.5 km), although it can be laterally confined (&lt;20 m). Commonly it is found to be 1-200 m in lateral extent, thickness is highly variable over this distance.</p> <p><i>Petrography:</i></p> <p>Dominated by palagonite, the sections display a large degree of alteration (Figure 5-18).</p>	<p>encountered syn-sedimentary movement down a slope, such as the hyaloclastite delta front (Cas and Wright, 1987). This movement occurs as a sub-aqueous debris flow, resulting in pillows and glassy matrix material, moving together (Watton et al, 2013).</p>
--	---	---

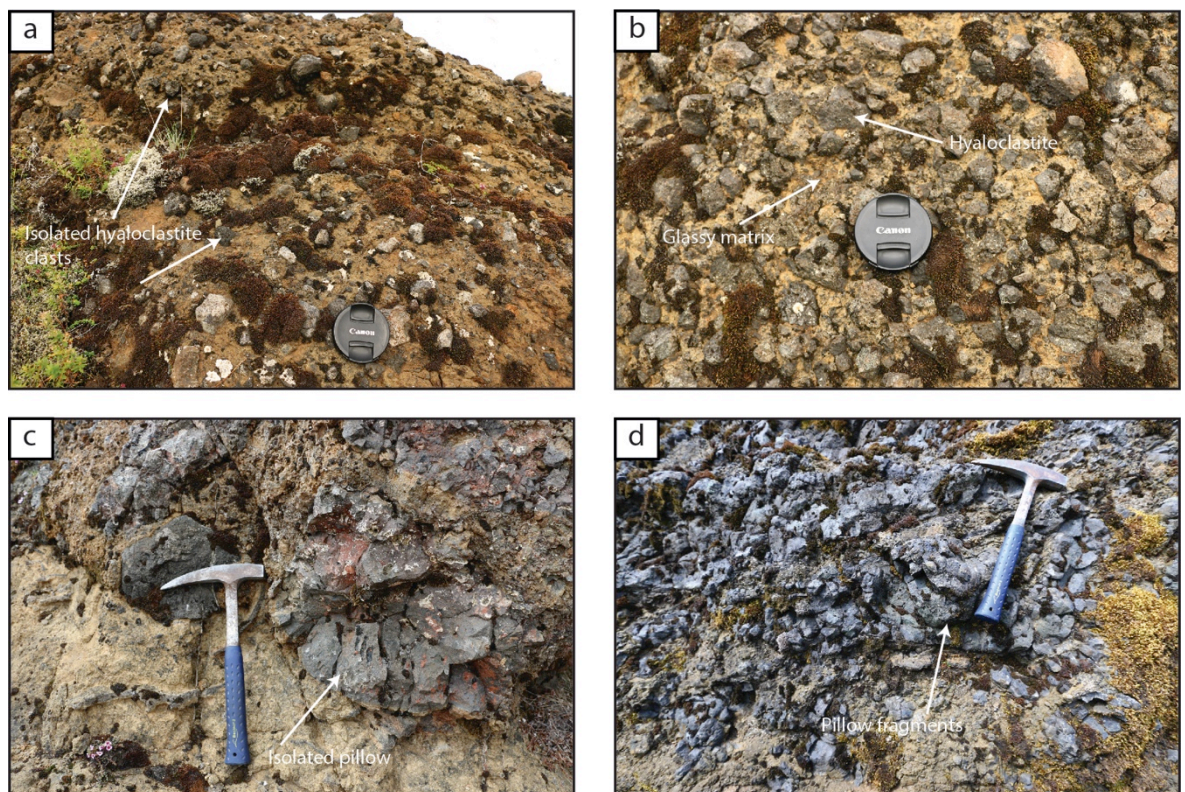


**Figure 5-17 Features of C2 primary hyaloclastite a) Matrix supported clasts of hyaloclastite within a fine/medium, glass rich matrix. b) Clast supported hyaloclastite and small pillow fragments within a fine/medium, glassy matrix. c) Isolated pillows within a glass rich matrix,**

indicating they have moved down a slope in a debris rich, flow. d) Densely grouped clasts of hyaloclastite and pillow fragments with obvious features such as pipe vesicles present.

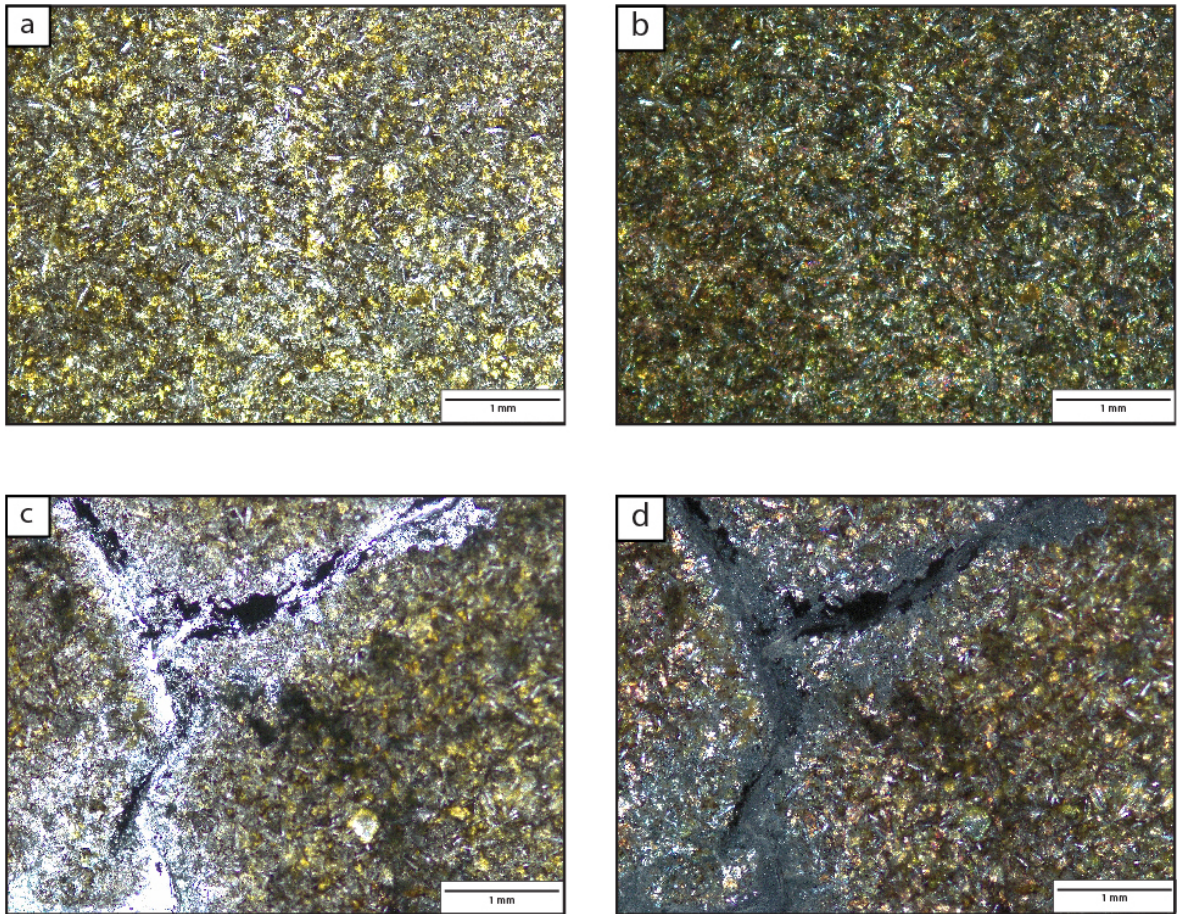
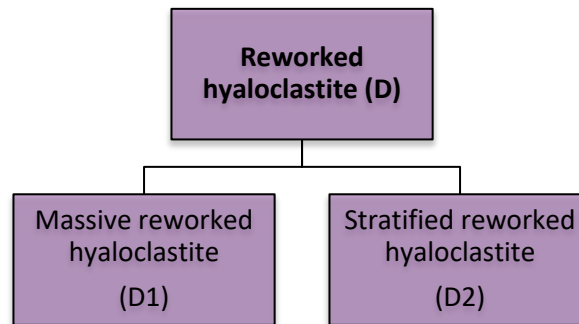


**Figure 5-18 Petrography of C2. a/b) PPL and XPL photomicrographs highlighting the altered fine grained texture of the unit. The unit is dominated by palagonite. c/d) PPL and XPL images highlighting fractures within the unit, these act as pathways for fluids to move through.**

## 5.5 Reworked hyaloclastite



Lithofacies	Description	Interpretation
<b>D</b>	<p><i>Lithology:</i></p> <p>Dark grey/black on fresh surfaces, distinctively brown/orange on weathered surfaces. Where brown/orange this suggests that the volcanic glass has been converted to palagonite. Clasts are of basalt and range from fine sand (0.125 mm) to pebble (64 mm). Individual clasts are glassy/ very fine grained. Clasts are sub angular to sub-rounded, however they are dominantly sub-rounded. Generally the unit is matrix supported and monomict. The matrix is composed of finer grained (&lt;0.125mm) hyaloclastite material and glassy shards.</p> <p><i>Structure:</i></p> <p>Grading is absent, however, locally, reverse grading is present.</p>	<p>Reversely graded hyaloclastite beds are characteristic of grain flow deposits (McPhie et al, 1993), which are common within prograding deltaic facies (Williamson and Bell 2012). Together in combination with the large foresets this indicates that the hyaloclastite could have been prograding down a hyaloclastite delta front/ slope (Watton et al 2013). Clasts move downslope due to gravity and are independent of the interstitial fluid (McPhie et al, 1993). Where cross bedding is present within the unit this is likely the</p>

	<p>Metre scale foresets are observed to have a steep angle of ~35-40° and cross-bedding is present on ~m scale.</p> <p><i>Geometry:</i></p> <p>Individual beds are up to 2 m thick, units are up to 10 m thick. Units typically pass laterally and vertically in to primary hyaloclastite units and coherent sub-aerial basalt lavas. Where it passes from primary hyaloclastite this comprises very broken hyaloclastite/pillow material. Laterally continuous for ~20-40 m.</p>	<p>result of the hyaloclastite being reworked by strong currents within the water body (Reading, 2002).</p> <p>The range of clast roundness implies that reworking was an active process where hyaloclastite formed and prograded down the slope. As a result of these processes older material is subsequently more rounded in comparison with fresh, younger hyaloclastite, as the older material has been present longer and has experienced considerable movement and reworking,- rounding the clasts further (Tucker, 2011).</p> <p>The presence of sedimentary structures and other cross-bedding structures, indicates reworking by tractional currents within the water body the lavas entered.</p>
--	---	---

### 5.5.1 Massive reworked hyaloclastite (D1)

Lithofacies	Description	Interpretation
<p><b>D1</b></p> <p>Represents 2.1% of the lithofacies within the HF (Table 5-1).</p>	<p><i>Lithology:</i></p> <p>Dark grey/black on fresh surfaces. Brown/orange on weathered surfaces. Poorly sorted, angular to sub-rounded (Figure 5-20), dominantly sub-rounded clasts of basalt ranging from fine (0.125 mm) to pebble (64 mm). Monomict.</p> <p>Units are matrix supported, matrix is fine grained (&lt;0.125 mm) (Figure 5-20).</p> <p><i>Structure:</i></p> <p>The units are typically massive and structureless. Often found to grade laterally in to D2.</p> <p><i>Geometry:</i></p> <p>The units are usually ~10 m thick, although this is highly variable along outcrops. Laterally continuous for ~20-40 m.</p> <p><i>Petrography:</i></p> <p>The unit is dominated by altered basaltic clasts and volcanic glass set</p>	<p>Rounding of fragments indicates that they have undergone mechanical abrasion (Figure 5-19, Figure 5-20) (Werner and Schmincke, 1999). This rounding process suggests that mass flow or current action have re-worked primary hyaloclastite deposits down slope, causing them to become rounded (Bergh and Sigvaldson, 1991). The massive nature of the unit indicates that these processes were very common as they produce a lot of material. Additionally a lack of structure within the unit could indicate that there were very little tractional processes, or bottom currents occurring.</p>

	within a palagonite matrix (Figure 5-20).	
--	---	--

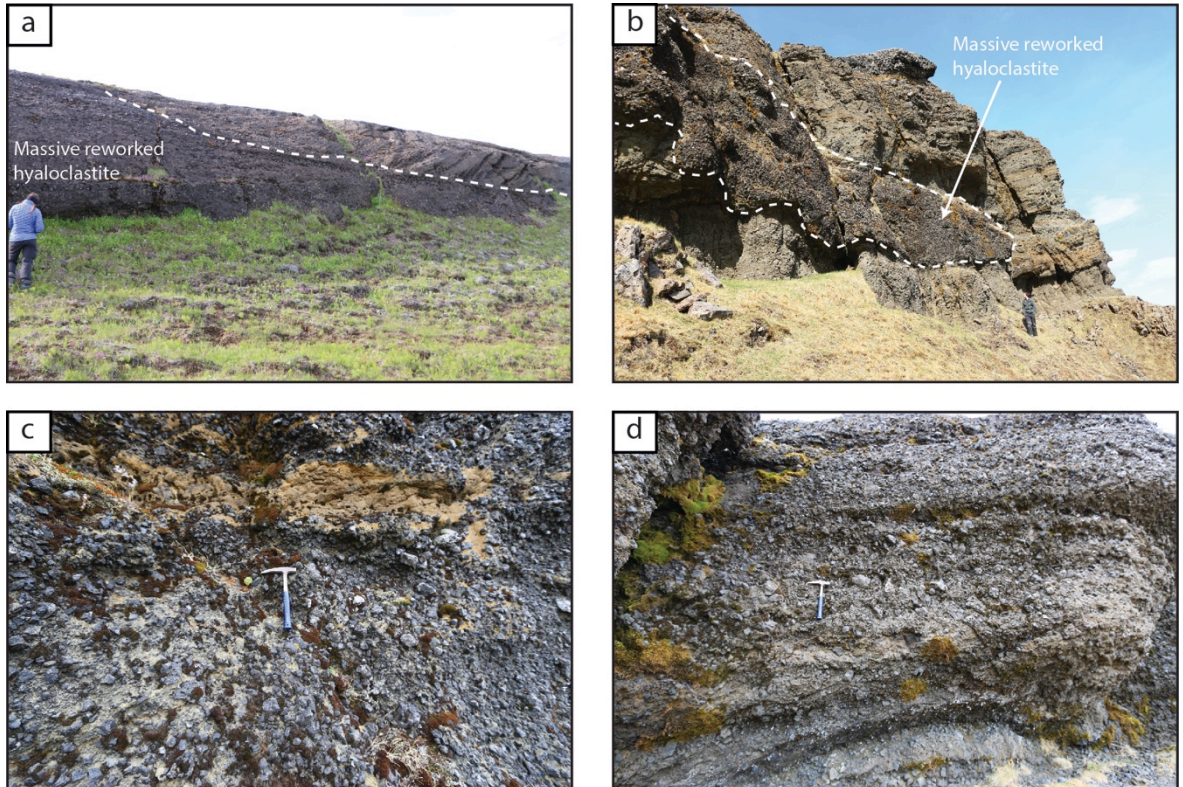


**Figure 5-19 Features of D1 re-worked hyaloclastite a) Transition from massive reworked hyaloclastite in to stratified reworked hyaloclastite (D2). b) Massive reworked hyaloclastite transitions in to sub-aerial lava (out of shot). c) Detail of the unit, highlighting the rounding of clasts and matrix. d) Some clasts can be ~64 mm, yet still sub-rounded. Hammer is ~300 mm.**

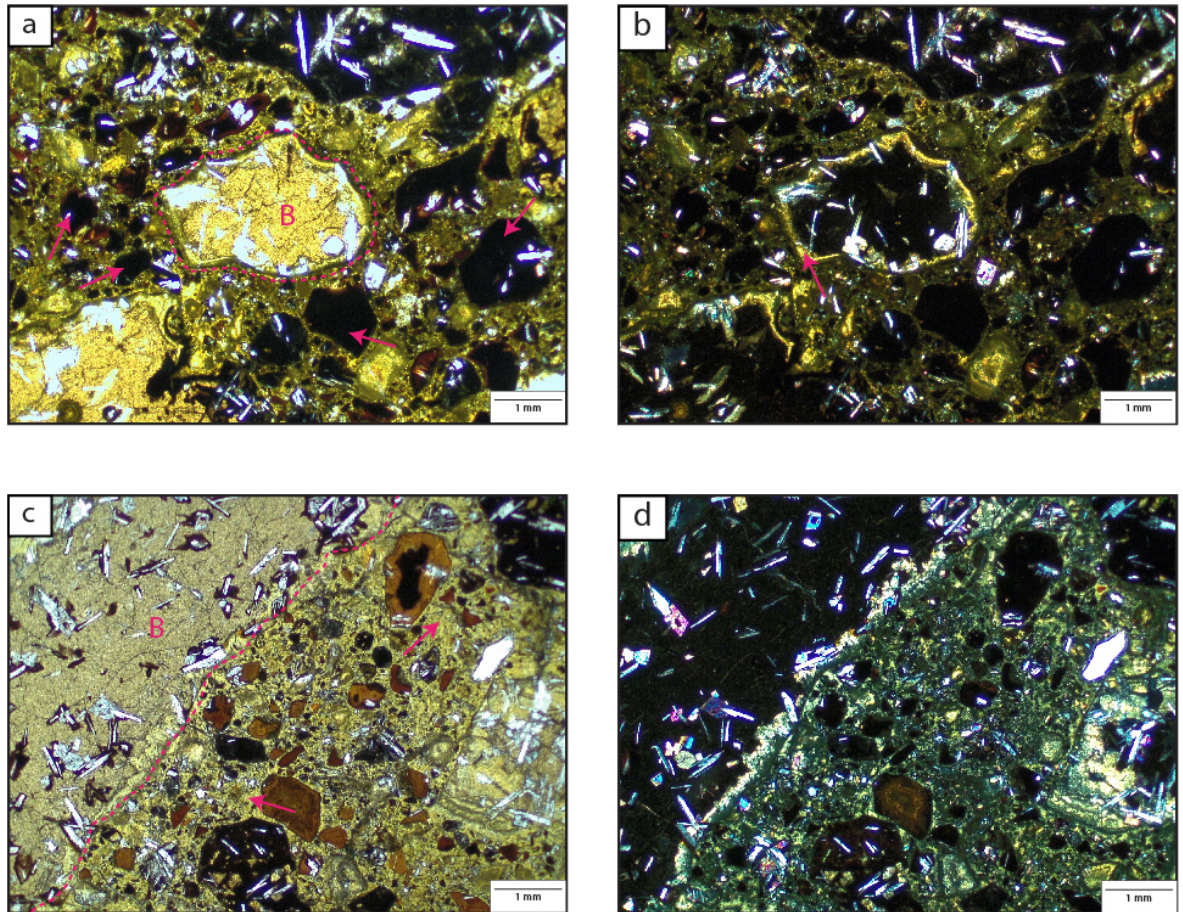
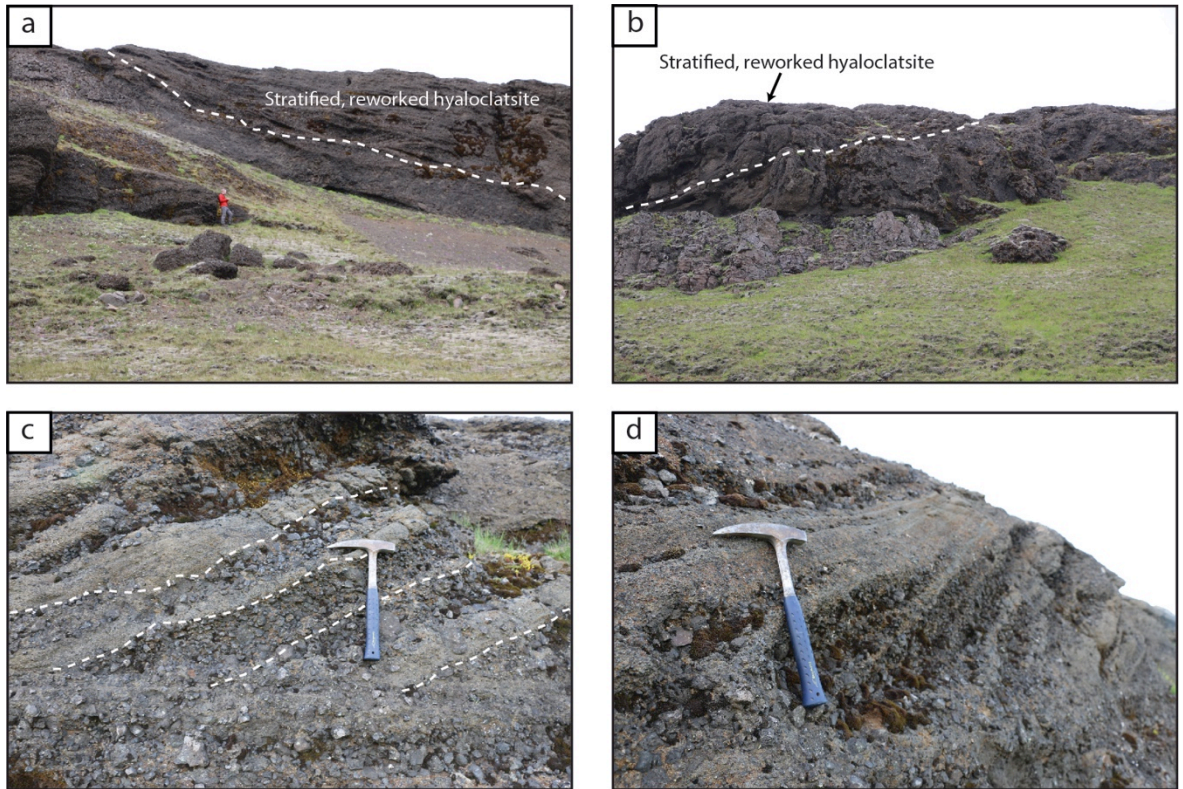


Figure 5-20 Petrography of D1. a/b) PPL and XPL photomicrograph highlighting the chaotic nature of the unit. The unit is dominated by basalt clasts within a palagonite matrix. The clasts are typically sub-rounded and composed of basaltic glass (pink arrows). Large basalt clasts with palagonite rind (B and dashed pink line). c/d) PPL and XPL photomicrographs highlighting a large basalt clast (b) with palagonite rind and palagonite matrix (pink arrows).

### 5.5.2 Stratified reworked hyaloclastite (D2)

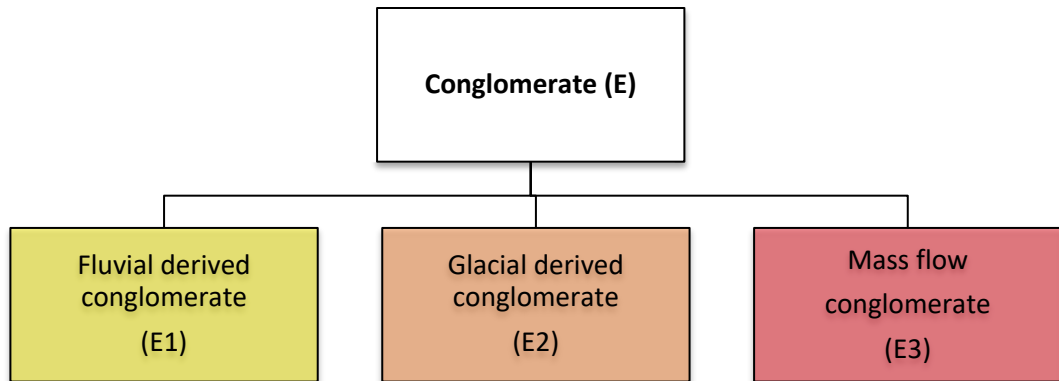
Lithofacies	Description	Interpretation
D2	<p><i>Lithology:</i></p> <p>Dark grey/black on fresh surfaces. Brown/orange on weathered surfaces. Poorly sorted, angular to sub-rounded, dominantly sub-rounded clasts of basalt range from fine (0.125 mm) to pebble (64 mm). Monomict. Units are matrix</p>	<p>Reworking by strong currents within a water body and various other processes such as grain flow result in large foresets, inverse graded units and large cross-bedding. These are very</p>

<p>HF (Table 5-1).</p>	<p>supported, matrix is fine grained (&lt;0.125 mm)</p> <p><i>Structure:</i></p> <p>Reversely graded, normally graded and massive beds are all present. Metre scale foresets and cross-bedding present</p> <p><i>Geometry:</i></p> <p>Individual beds are up to 2 m thick, units ~10 m thick and laterally continuous for ~20-40 m.</p>	<p>distal to the edge of the water body.</p> <p>Metre scale cross bedding observed within the bedded hyaloclastites (Figure 5-21) indicates that reworking and re-deposition has occurred by traction currents (Bergh and Sigvaldason, 1991). Watton et al (2013) state that high angle cross bedding in the unit could represent Gilbert style delta deposition. They form as a result of flank collapse within the deposited hyaloclastite pile. Stratification of the hyaloclastites indicates that mass flow processes and bottom currents have reworked and sorted the primary hyaloclastite (Fisher, 1984; Reading, 2002).</p>
------------------------	---	--



**Figure 5-21 Features of D2 re-worked hyaloclastite** a) Transition from sub-aerial lava and massive reworked hyaloclastite in to stratified reworked hyaloclastite. Notice the large structures within the unit. b) Similar transition from sub-aerial lava in to primary hyaloclastite and stratified reworked hyaloclastite. This represents the lava transitioning in to the water body and becoming reworked due to mass flow processes or bottom current reworking. c) Reversely graded beds of reworked stratified hyaloclastite. d) Normal and inverse graded beds of stratified reworked hyaloclastite. Hammer is ~300 mm.

## 5.6 Conglomerate



Lithofacies	Description	Interpretation
<b>E</b>	<p><i>Lithology:</i></p> <p>Typically the units are grey/brown/orange in colour. Clasts range in size from ~2 mm to &gt;256 mm. Clasts are dominated by basalt, vesicular basalt, amygdaloidal basalt, rhyolite and volcanoclastic sandstone. They are rounded to sub-angular, but predominantly sub-rounded. Clasts are generally supported by a matrix, ranging in grain size from silt (0.0625 mm) to coarse sand (0.5 mm). Locally units are clast supported. Units range from monomict to polymict.</p> <p><i>Structure:</i></p> <p>Units are normally graded, inversely graded, well stratified, diffusely stratified and massive,</p>	<p>In the HF there is considerable variation in the conglomerate lithofacies. This has been categorised into three main sub-facies.</p> <p>Fluvial systems, glaciers and gravity all play a large role in the formation of conglomerates within the HF. E1 conglomerates are most abundant, whereas E2 are least abundant. This suggests that the HF was dominated by fluvial systems and ice played a minor role in the area.</p>

	<p>depending on the genetic origin of each unit.</p> <p><i>Geometry:</i></p> <p>Unit thickness is highly variable although generally &gt;2 m to ~25 m thick. Laterally units are continuous for up to 0.5 km, although locally, 10-50 m.</p>	
--	--	--

### 5.6.1 Fluvial derived conglomerate (E1)

Lithofacies	Description	Interpretation
<p><b>E1</b></p> <p>Represents 3.3% of the lithofacies within the HF (Table 5-1).</p>	<p><i>Lithology:</i></p> <p>Typically brown/orange with lighter and darker areas present. Dominated by moderately sorted and relatively immature clasts of basalt, volcanoclastic sandstone, vesicular basalt, amygdaloidal basalt and rhyolite with the dominant clast type being basalt. The unit varies between matrix and clast supported. Where matrix supported, generally medium (0.25-0.5 mm)</p>	<p>Channel features, gravel lags, gravel and the relatively immature nature of the deposit (Figure 5-22) are all suggestive of being formed in a braided fluvial environment (Collinson, 1996). The environment would have been very similar to modern day Iceland, with large volumes of gravel, sand and suspended load being transported by high energy fluvial systems.</p> <p>Gravel bar bedforms are common within the HF and these represent deposition within a braided fluvial system. As in modern day Iceland, braided fluvial systems develop as the result of having a heavy load of coarse sediment and rapid discharge fluctuations. This rapid</p>

	<p>to coarse (0.5-1 mm) grained sand. Clasts are typically sub-angular to sub-rounded and range from 5-600 mm.</p> <p><i>Structure:</i></p> <p>Beds demonstrate normal and reverse grading on a metre scale. Some horizons within beds demonstrate imbrication of basalt pebbles, although this is relatively uncommon. Small gravel lags are present at the base of coarser beds, and these are dominated by basalt pebbles (up to 64mm). Individual beds can appear very heterogeneous with very little structure apparent.</p> <p><i>Geometry:</i></p> <p>Beds are typically between 1-3 m in thickness and commonly laterally discontinuous. These units tend to pass</p>	<p>discharge is associated with seasonal melt water (the reduction in flow causes the sediment to deposit, this could be a result of lower gradient downstream, shallowing of the water depth and lateral expansion) (Collinson, 1996). The largest clasts are only transported during peak flooding, typically in the spring when melt water is greatest (Collinson, 1996). During peak flow rates, imbrication occurs, effectively indicating the palaeoflow direction (Bluck, 1974).</p> <p>Bar forms grow during high water and sediment discharge, they are typically normally graded, as seen in the HF (Figure 5-22). Sand is deposited during falling flow rates, as it settles out of suspension (Ashley et al, 1985). This sand typically infills pore spaces and accumulates on the bar surface (Figure 5-22) (Miall, 1985; Collinson, 1996).</p> <p>These systems would have been heavily influenced by glaciers and the emplacement of lavas. This would potentially alter the course of the rivers and with time the rivers would have become less confined to valleys and pre-</p>
--	---	---

	<p>in to sandstone facies. Within units, channel features are found with an axis width of between 1-2 m and a depth of ~0.3-0.5 m. Typically these channel features tend to cut in to the underlying and adjacent channels. Gravel bar bedforms are also common tabular features, these vary in size depending on which axis is being observed. These are typically clast supported and often interbedded with sandstone (Figure 5-22).</p>	<p>existing drainage networks (Schofield and Jolley, 2013).</p> <p>Where basalt pebbles are present in a definable horizon, this is likely a result of an erosional surface at the base of a channel, bar or dune (Ebinghaus et al 2013). There are a lot of entrained pebbles within the cross bedding, suggesting that this was a very dynamic environment where channels formed and frequently had large inputs of sediment in to them, resulting in an abundance of basalt pebbles within.</p> <p>The change in angularity of clasts from sub-angular to sub-rounded and the presence of numerous lithologies indicates that there have been multiple sources of sediment input in to the system. Imbrication of the clasts infer the direction of palaeoflow, which has been measured and is generally from the NE to the SW.</p>
--	---	--

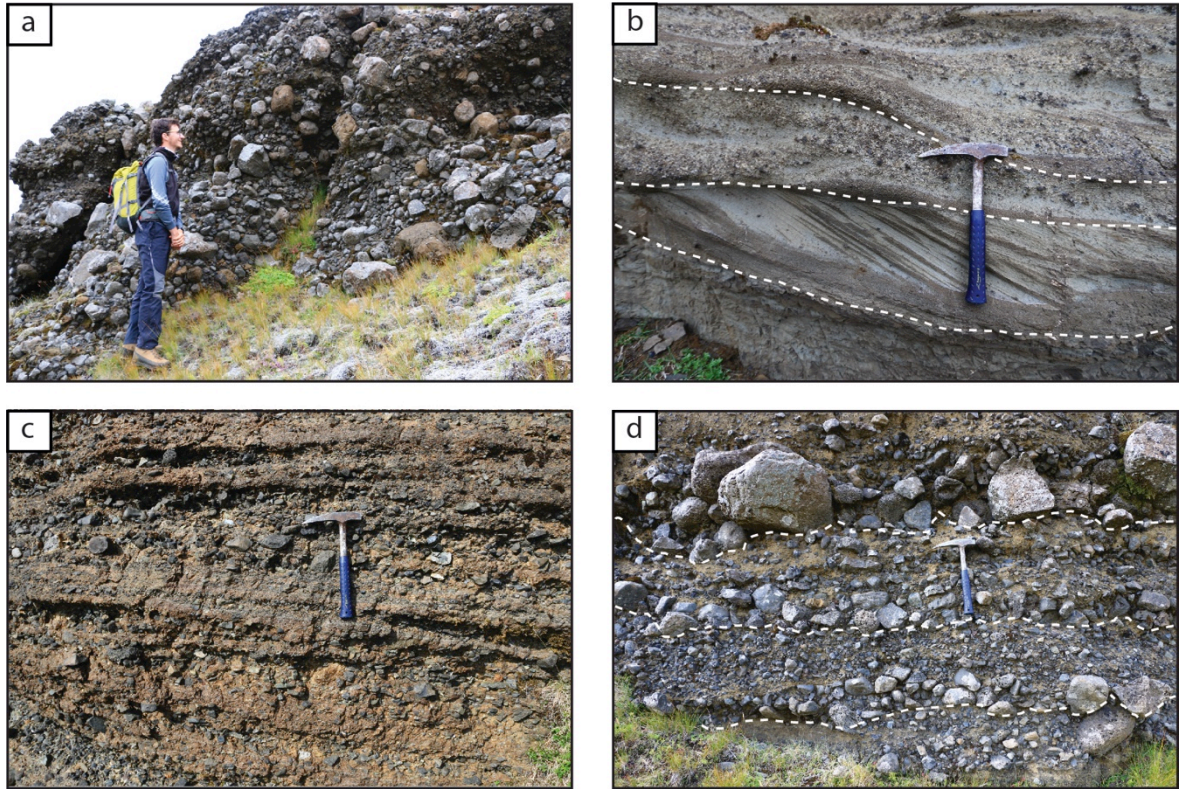


**Figure 5-22 Features of E1 conglomerate** a) Heterogeneous nature of the unit in places. Clast sizes can be ~600 mm in diameter, indicating these were deposited within a very high energy environment. b) Matrix supported conglomerate (bar) (E1) overlain by small foresets, indicating palaeo-flow direction to the right of the image. Another bar deposit overlies this sequence. c) Repeating bars, demonstrating normal grading. Imbrication of clasts can be observed. d) Normally graded bar deposits, represent the waxing and waning of water level within the river system- associated with spring snow melt. Discrete imbrication of clasts can be observed. Hammer is ~300 mm.

### 5.6.2 Glacial derived conglomerate (E2)

Lithofacies	Description	Interpretation
<p><b>E2</b></p> <p>Represents 1.2% of the lithofacies within the HF (Table 5-1).</p>	<p><i>Lithology:</i></p> <p>Typically very chaotic with a large range of clast sizes supported by a predominantly fine grained sand matrix. Clasts are typically basaltic, sub angular to sub rounded, and range in size from fine sand (0.125 mm) to boulder (&gt;256 mm). Some individual clasts demonstrate striations on their surfaces. The matrix can vary in colour and grain size from grey/ white to orange/ brown and clay (0.0039mm) to fine sand (0.125mm). Clasts comprise ~ 70% of the unit.</p> <p><i>Structure:</i></p> <p>Diffuse bedding and lenticular beds are occasionally present and often reverse grading is observed within beds. Where this is present,</p>	<p>The poorly sorted, chaotic nature of the unit combined with the unit being matrix supported, indicates that it was deposited by a high energy event (Figure 5-23).</p> <p>Rounded basaltic clasts with striations indicate that these have been affected by glacial action. The presence of striated clasts and predominantly mature clasts indicates that the clast population was previously affected by glacial action before/after transportation.</p> <p>Debris flow deposits commonly display extremely poor sorting, lack of internal stratification, reverse to normal grading and the largest clasts being supported by a matrix (Smith, 1986). They typically form as a result of high rainfall, floods and snowfall, (Innes, 1983; Costa, 1984; Sassa and Wang, 2005) although it is also possible to generate debris flows from glacial lake outbursts (Costa, 1984).</p> <p>The dominance of clasts derived from glacial action within the unit</p>

	<p>typically the unit is clast supported. Individual beds, frequently demonstrate small horizons (0.2-0.3 m), which are dominated by pebbles (64 mm) of sub-angular basalt. Within the matrix, small mm scale cross bedding is locally observed.</p> <p><i>Geometry:</i></p> <p>Occurs as beds, which are generally massive, up to 15-20 m thick as a package and laterally extend for 30-40 m. Individual beds are difficult to identify, although where possible are between ~1-3 m. Typically only locally present and laterally discontinuous, and thus difficult to correlate.</p>	<p>indicate that the source area was a relatively glacial proximal, environment.</p> <p>It is likely that a debris flow occurred as the result of a glacial lake outburst (jökulhlaup). This could have occurred as the result of rising spring temperatures, leading to excess glacial and snow melt (Breien et al, 2008). G1 lithofacies indicate that there were glacial lakes within the HF environment making this scenario a possibility. The debris flow would have followed pre-existing drainage pathways for up to several kilometres before depositing the sediment within a structurally (?) confined area. Breien et al (2008) document a debris flow resulting from a glacial outburst flood in Norway, which incorporated primarily glacial till.</p> <p>E2 has been deposited by a debris flow, composed of glacially derived material. The process is the same between E2 and E3 lithofacies however, the provenance of clasts is different between the two units.</p>
--	---	---

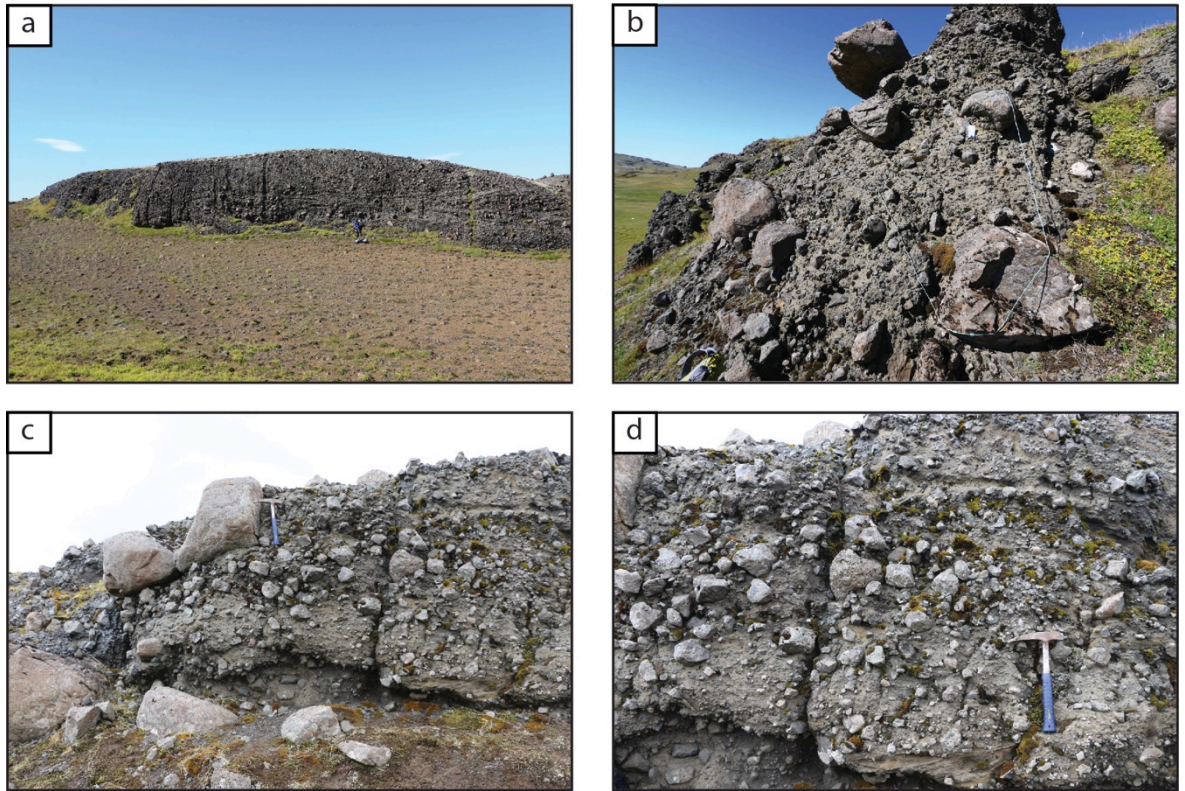


**Figure 5-23 Characteristics of E2 conglomerates** a) Large scale outcrop of conglomerate, with diffuse bedding structures present. b) Chaotic nature of the unit, with large > 1 m clasts of sub-rounded basalt and <10 mm clasts of basalt indicating the very poorly sorted nature of the unit, all within a grey, fine sand to clay matrix. c) Highlights the poorly sorted nature of the matrix. There is an apparent reverse grading structure, however this is uncommon within the unit. d) Some of the smaller, cobble to boulder sized clasts within the unit. At the base of the outcrop, there is a lens of fine-grained sandstone demonstrating small cross bedding. Hammer is 300 mm.

### 5.6.3 Mass flow derived conglomerate (E3)

Lithofacies	Description	Interpretation
<p><b>E3</b></p> <p>Represents 11.1% of the lithofacies within the HF (Table 5-1).</p>	<p><i>Lithology:</i></p> <p>Frequently dark brown/dark grey. Clasts are typically sparsely distributed and set in a medium/coarse (0.25-0.5 mm) sand, locally silt grade matrix. Clasts are predominantly sub-angular to sub-rounded and range in size from 4mm - 150 mm. The unit is relatively poorly sorted. Clast types consist of basalt, vesicular basalt, amygdaloidal basalt, hyaloclastite and altered basalt. Basalt clasts are dominant and tend to be largest (~150 mm although locally &gt;500 mm).</p> <p><i>Structure:</i></p> <p>Generally massive with occasional mm scale laminae. Discontinuous 0.4-0.5 m scale cross bedding is occasionally present within the matrix. Locally clasts demonstrate diffuse bedding. Reverse</p>	<p>The poorly sorted and matrix supported nature of the unit combined with the often, common transition in to sand rich units such as F1, indicate that the unit formed as a result of periodically high energy events (Figure 5-24). Debris flow deposits commonly display extremely poor sorting, lack of internal stratification, reverse to normal grading and the largest clasts being supported by a matrix (Smith, 1986).</p> <p>The presence of sub-rounded and sub-angular clasts (Figure 5-24) indicate that there is potentially two populations of clast types within the unit that have seen different histories. Brown and Bell (2006, 2007) observe similar populations within deposits from Palaeogene lava fields in Ardnamurchan, Scotland. They attribute the difference in rounding of clasts to the fact that one population (sub-rounded) has already gone through a weathering and transport cycle before becoming incorporated in</p>

	<p>grading is common within the unit.</p> <p><i>Geometry:</i></p> <p>Generally observed to be between ~ 5-20 m thick beds. Laterally continuous &gt;100 m tabular bodies.</p>	<p>to the deposit. This is highly likely in the HF as there is abundant evidence for widespread fluvial systems (F1).</p> <p>Normal faulting, uplift and intrusions are all possible candidates for generating debris flows in LIP's (Reubi et al, 2005). Additionally, high rainfall, floods and snowfall, all contribute to the development of debris flows (Innes, 1983; Costa, 1984; Sassa and Wang, 2005). The presence of a strong tectonic control in the HF would have generated faulting and uplift, creating a possible mechanism for the generation of debris flows.</p> <p>The transition from sand rich beds in to conglomerate rich beds and back, suggests that a sudden, high-energy event produced the deposit (Figure 5-24).</p>
--	---	--

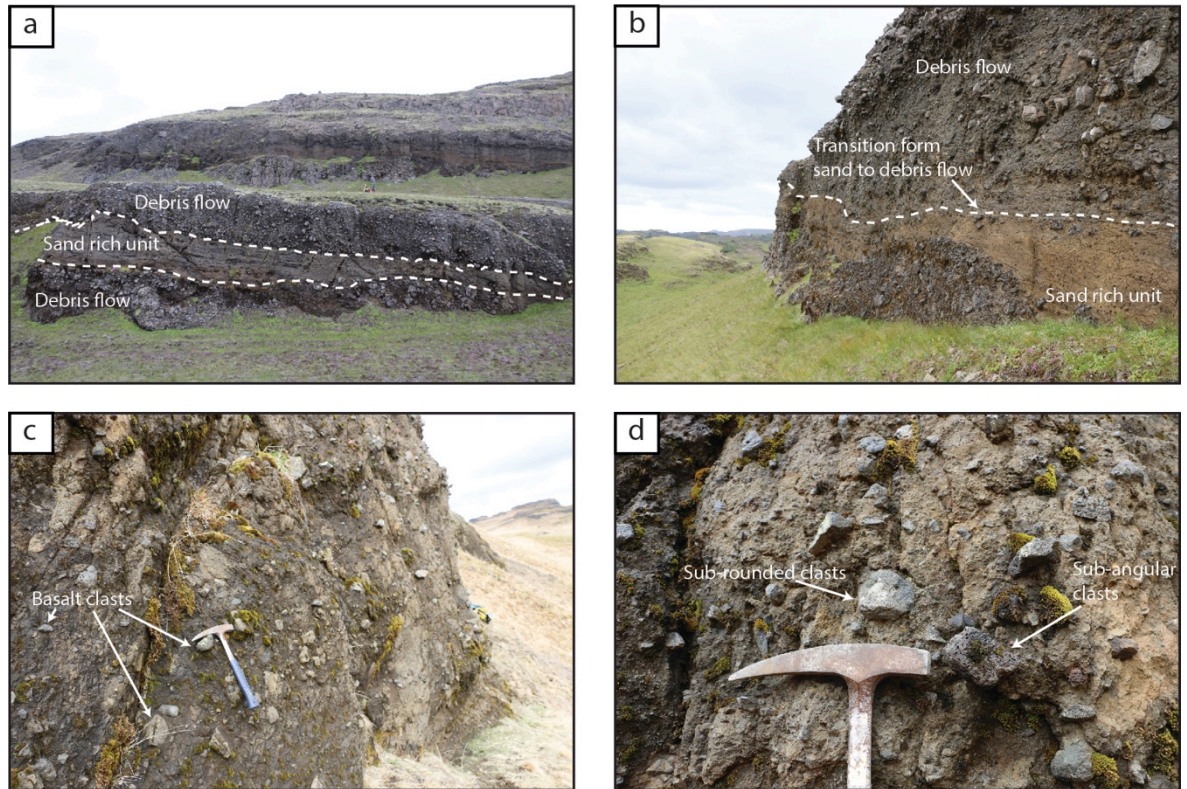
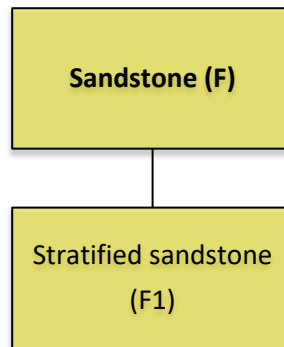


**Figure 5-24 Features of E3 conglomerates** a) Transition from poorly sorted conglomerate in to sand rich unit and back in to conglomerate. This transition indicates that these deposits are the result of sudden, high-energy events such as faulting. Notice the reverse grading to the unit. b) Close up transition of the two units. The transition is very small, again indicating that this was a sudden event. c) The unit is dominated by basaltic clasts set within a sandy matrix. d) Clasts are typically sub-rounded and sub-angular, suggesting that there is two clast populations to this unit. Hammer is 300 mm.

## 5.7 Sandstone



### 5.7.1 Stratified sandstone (F1)

Lithofacies	Description	Interpretation
<div style="border: 1px solid black; background-color: yellow; width: 40px; height: 40px; display: flex; align-items: center; justify-content: center; margin-bottom: 5px;"> <span style="font-size: 24px; font-weight: bold;">F</span> </div> <div style="border: 1px solid black; background-color: yellow; width: 40px; height: 20px; display: flex; align-items: center; justify-content: center; margin-bottom: 5px;"> <span style="font-size: 18px; font-weight: bold;">F1</span> </div> <p>Represents 8.1% of the lithofacies within the HF (Table 5-1).</p>	<p><i>Lithology:</i></p> <p>Typically, brown/orange with lighter and darker areas present. Generally medium (0.25-0.5 mm) to coarse (0.5-1 mm) grained sand, which is dominated by basalt grains (Figure 5-26). Glass grains are typically sub-angular, whereas vesicular basalt grains are sub-rounded. Composition of the clasts is variable and includes; basalt, volcaniclastic sandstone, vesicular basalt, amygdaloidal basalt and rhyolite. The units are typically moderately sorted and relatively immature.</p>	<p>Cross bedded sand primarily composed of sub-angular to sub-rounded medium sand grain sized, basalt clasts, suggest reworking of older lava flows has occurred to produce the deposit (McPhie et al, 1993).</p> <p>Glass fragments (&lt;1 mm) appear to be sub-angular in comparison with sub-rounded basalt clasts, suggesting these did not come from the same source. Potentially the basaltic clasts have come from a relatively more distal source.</p> <p>Where basalt pebbles are present within larger cross beds, this is likely a result of an erosional surface at the base of</p>

	<p><i>Structure:</i></p> <p>Beds demonstrate normal and reverse grading on a 1 m scale. Cross bedding is present on a 1-1.5 m scale and smaller scale (0.3-0.5 m) trough cross bedding is also present. Some horizons within beds demonstrate imbrication of basalt pebbles, although this is not widespread. Small gravel lags are present at the base of coarser beds, and these are dominated by basalt pebbles (up to 64mm).</p> <p><i>Geometry:</i></p> <p>Beds are typically between 1-3 m in thickness and generally are laterally discontinuous. These units tend to pass in to E1 (Figure 5-25). Within the unit, bars are found with an axis of between 1-2 m and a depth of ~0.3-0.5 m. Typically these bars tend to cut in to the underlying and adjacent channels.</p> <p><i>Petrography:</i></p>	<p>a channel, bar or dune (Ebinghaus et al 2011). There are numerous entrained pebbles within the cross beds, suggesting that this was a very dynamic environment where channels formed and frequently had large inputs of sediment in to them, resulting in an abundance of basalt pebbles within.</p> <p>Bars, gravel lags, large scale cross bedding, gravel and the relatively immature nature of the deposit are all suggestive of being formed in a braided fluvial environment (Figure 5-25) (Reading, 2002). The unit commonly transitions in to E1 (Figure 5-25) indicating that the two are intrinsically linked with F1 being the deposit from the waning braided fluvial system.</p> <p>The environment in which this unit was deposited would have been very similar to modern day Iceland, with large volumes of gravel, sand and suspended load being transported by these high-energy fluvial systems. Glaciers and the presence of lavas would have heavily</p>
--	--	--

	Dominated by basaltic and sandstone clasts within a clay/palagonite matrix. The section has been blue dyed, indicating a lack of porosity within the unit (Figure 5-26).	influenced these systems, potentially altering the course of the rivers. With time the rivers would have become less confined to valleys and pre-existing drainage networks (Schofield and Jolley, 2013).
--	--	---

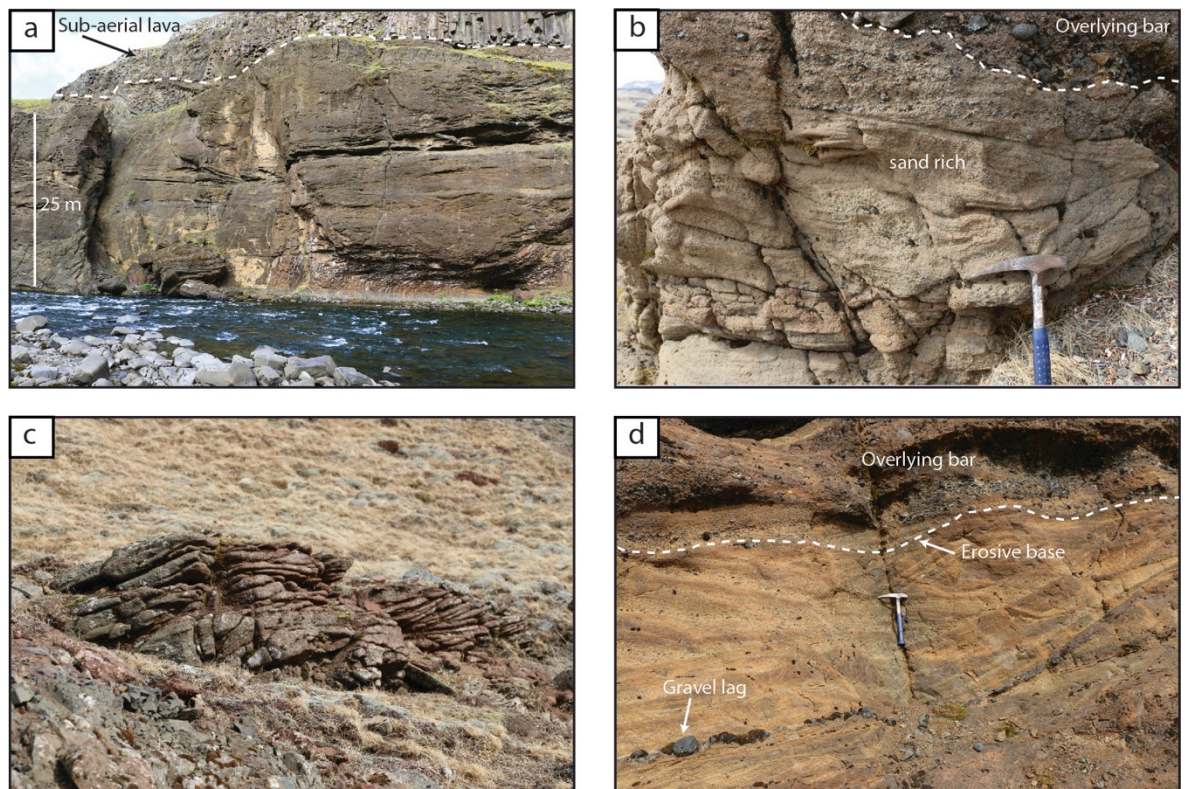


**Figure 5-25 Characteristics of F1 sandstones** a) Large package of F1 and E1. On close inspection, E1 typically cuts in to underlying F1 and commonly there is a transition from E1 to F1, representing the waning of fluvial energy. b) Close up image of what is described in (a). The overlying bar (E1) has an erosive contact with the underlying sandstone. c) Cross bedded, medium grained sandstone highlighting varying palaeoflow directions. d) Cross bedded sandstone with a gravel lag at its base, indicating an erosional surface.

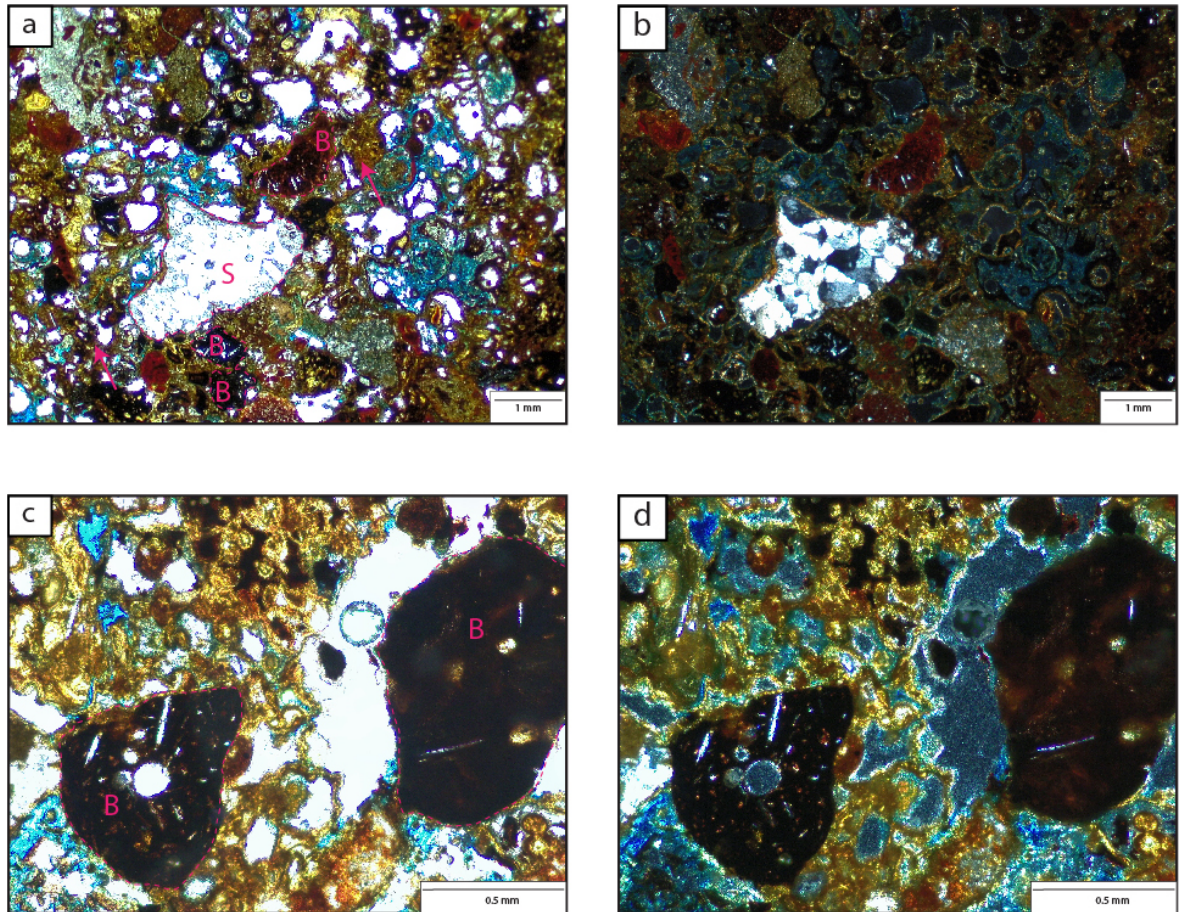
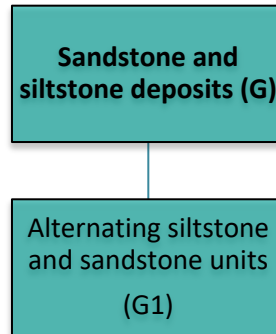


**Figure 5-26 Petrography of F1. a/b) PPL and XPL photomicrographs highlighting the range of clast types within F1 and the lack of porosity (the section has been stained with blue dye). Basalt clasts are sub-rounded (B) and the unit contains clasts of sandstone (S). Matrix is composed of clays and palagonite (pink arrows). c/d) PPL and XPL photomicrographs of basalt clasts (B), highlighting the sub-rounded nature of each.**

## 5.8 Sandstone and siltstone



### 5.8.1 Alternating siltstone and sandstone units (G1)

Lithofacies	Description	Interpretation
<p style="text-align: center;"><b>G</b></p> <p style="text-align: center;"><b>G1</b></p> <p>Represents 4.4% of the lithofacies within the HF (Table 5-1).</p>	<p><i>Lithology:</i></p> <p>Alternating brown/beige fine grained (up to 0.25mm) sand and laminated siltstone layers with obvious recessed dark brown siltstone layers. Clasts within sandstone are predominantly basaltic, sub-rounded and are small pebble size (64mm). These clasts are often aligned. Some larger clasts are observed within the sandstone, and these are predominantly basaltic, sub-rounded to rounded and are small cobble in size (65 - 100 mm).</p> <p>Small, white/grey horizons of claystone up to 50 mm are present within the unit, locally</p>	<p>Interbedded silt and sandstone with larger clasts and faint bedding is indicative of being deposited within a glaciolacustrine setting (Figure 5-27) (Livingstone et al, 2015). The cyclical nature of the inter-bedding could possibly represent seasonal variations in sediment input. Where siltstone is present this is most likely to be formed during a period of quiescence in winter months when meltwater and therefore sediment, is less available (Bennett and Glasser, 2009).</p>

	<p>between the siltstone and sandstone layers.</p> <p>Small, concordant and discordant horizons of medium grained, orange/brown sandstone are present within the unit. These are obvious due to the difference in colour with the surrounding sandstone and siltstone.</p> <p><i>Structure:</i></p> <p>Parallel bedded layers. Typically sandstone layers are ~0.5-1 m thick and these are punctuated by much thinner layers, ~0.1-0.2 m, of siltstone. Within the siltstone, mm scale laminations are present and are occasionally observed to be deformed around clasts, which have been entrained in the layer. Within the sandstone layers, larger clasts are present. Faint bedding is present on a ~50-100mm scale within the sandstone layers due to the rough alignment of clasts.</p> <p><i>Geometry:</i></p> <p>Parallel tabular bodies, laterally continuous and extending for up to ~40m. Typically passes in to hyaloclastite and pillow material.</p>	<p>The presence of larger clasts (Figure 5-28) within the sandstone layers and deformation of siltstone layers around clasts could potentially be the result of rain out from rafted ice with a low clast concentration, that have calved within a lake (Livingstone et al, 2015; Bennett and Glasser, 2009; Ashley et al, 1985).</p> <p>The concordant and discordant sandstone structures within the unit are interpreted as sand injectites (Figure 5-27 based on the fact that the structures appear to be connected and traceable downwards until there is no exposure. Above the units, there are only lavas and hyaloclastite, indicating that the sand must have come from depth. Sand injectites form due to the elevation of pore pressure, hydrofracture of the sealing unit, fluidisation and injection of sand (Hurst et al, 2011). Numerous trigger mechanisms are</p>
--	---	--

	<p>White/grey claystone horizons are laterally continuous for 3-4 m.</p> <p>Concordant and discordant sandstone horizons are laterally continuous for up to 30 m. Over that distance they demonstrate a complex relationship with the sandstone and siltstone.</p> <p><i>Petrography:</i></p> <p>The unit is dominated by small, sub-rounded basaltic clasts within a silt/clay grade matrix (Figure 5-28). Where the tuff horizons are present, cusped glass shards dominate (Figure 5-29). Sand injectites are dominated by small, sub rounded, altered clasts of basalt (Figure 5-29).</p>	<p>suggested for the formation for sand injectites- seismicity, thermal pressurisation, overpressuring caused by rapid loading, fluid migration and igneous intrusion (Hurst et al, 2011 and references therein). In the HF the most likely trigger mechanism is overpressure caused by rapid loading by lavas above the unit.</p> <p>Analysis of the white/grey horizons has revealed vesicle structures within the claystone (Figure 5-29). This is most likely to be an ash fall deposit. The preservation of this horizon is in keeping with the unit representing a quiescent lacustrine setting.</p>
--	---	--

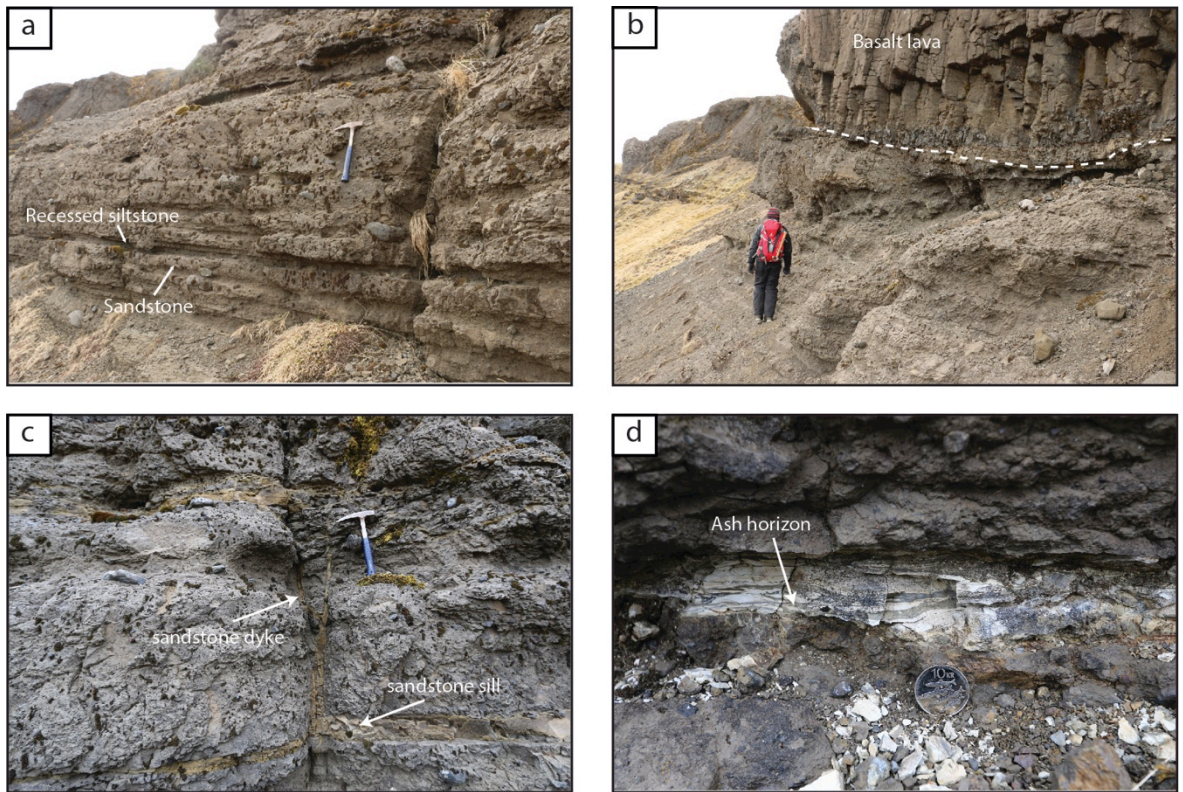


**Figure 5-27 Characteristics of G1 sedimentary rocks a) Alternating beds of siltstone and sandstone, with dropstones present. Alternating beds highlights the seasonal input of sediment in to the lacustrine body. b) Lava overlying the alternating siltstone and sandstone unit. c) Sand injectites that most likely formed as a result of the emplacement of the overlying lava. d) White/grey ash horizon preserved within the unit, indicating that the environment was relatively quiescent.**

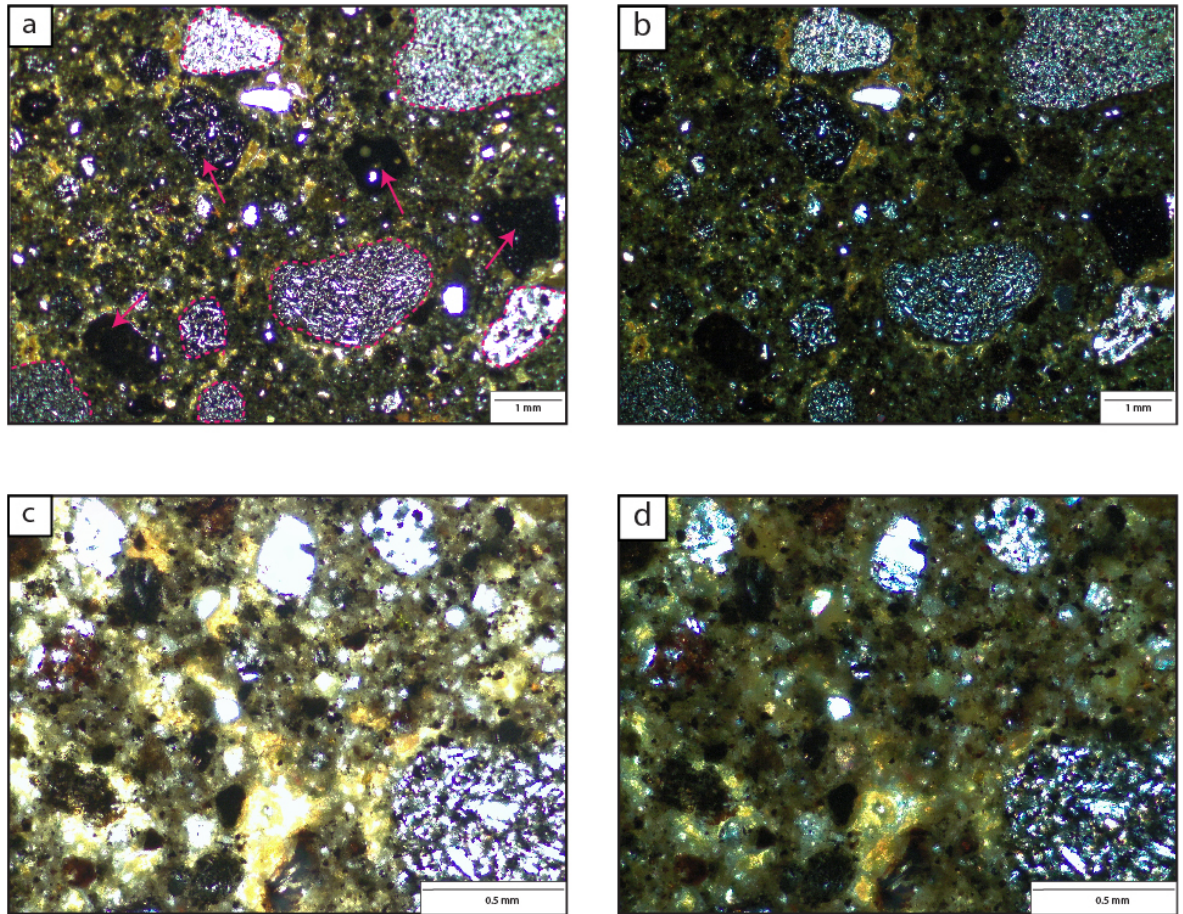


**Figure 5-28 Petrography of G1. a/b) PPL and XPL photomicrographs of the texture of unit G1. The unit has sub-rounded basalt clasts (dashed pink line) and basaltic glass (pink arrows). The matrix is composed of silt grade sediment. c/d) PPL and XPL photomicrographs of the matrix, highlighting the fine grained nature.**

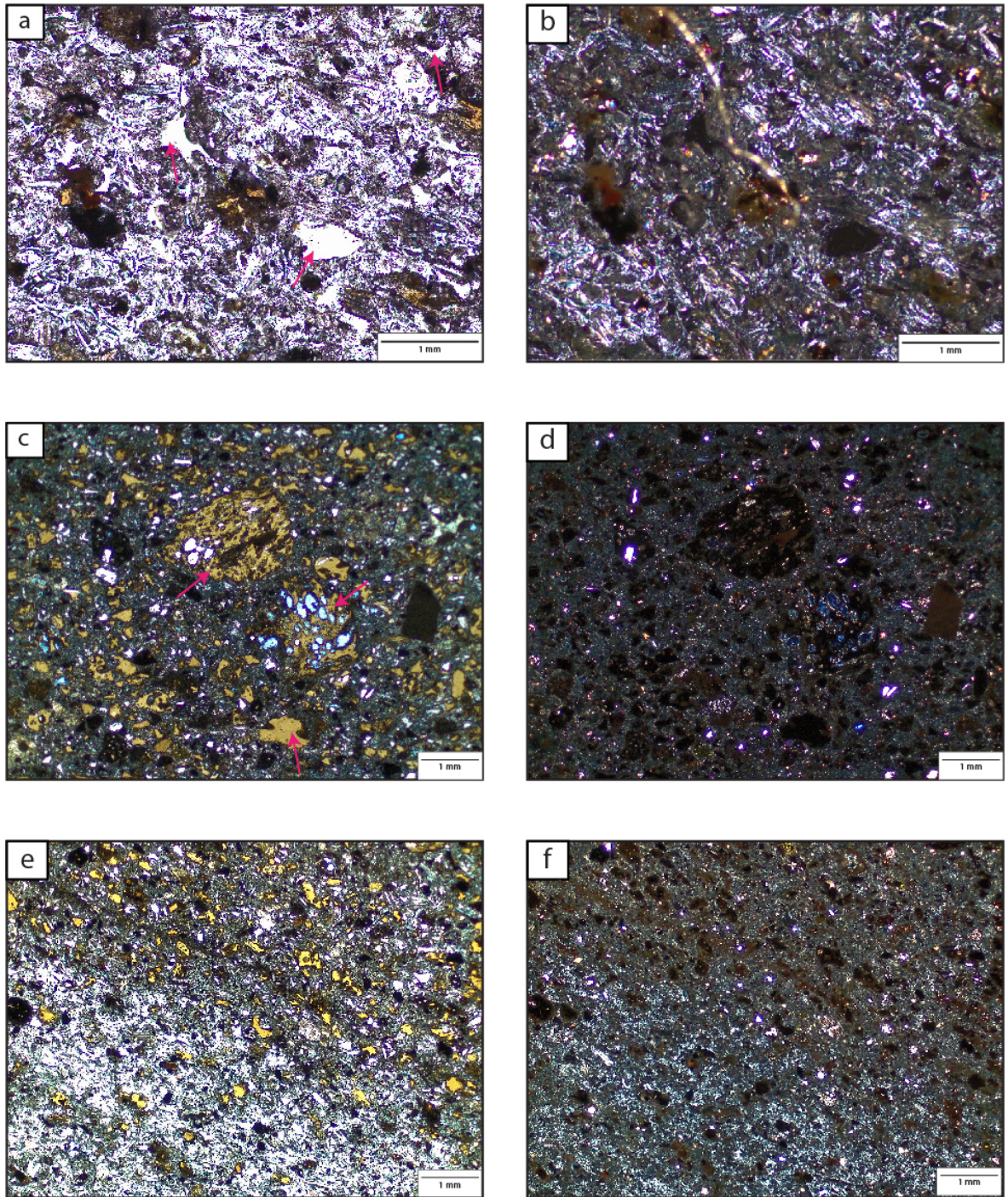


**Figure 5-29** Petrography of tuff/sand injectite horizon. a/b) PPL and XPL photomicrograph highlighting the general texture of the tuff horizon. Cusped glass shards dominate this area of the section (pink arrows). c/d) PPL and XPL photomicrographs of the sand injectite area of the thin section. This is dominated by altered, sub-rounded, vesicular basalt clasts (pink arrows). e/f) This area of the thin section represents the interaction of the sand injectite (top right) and the tuff (bottom right).

## 5.9 Conclusions

- Seven main lithofacies have been identified within the HF. These have been subdivided in to 15 sub-lithofacies.
- The dominant lithofacies within the HF is B1. Sub-aerial lavas dominate the HF, with >60% of lithofacies being sub-aerial lava, this is unsurprising given the location of the HF in SW Iceland.
- Based on the lithofacies data from the HF, the most dominant system is the volcanic system. The most dominant sedimentary unit in the HF is mass flow units. These indicate there was frequent, high energy events associated with high rainfall and loose regolith, these would typically wane to normal fluvial processes. The volcanic and sedimentary systems in the HF have interacted to produce complex outcrops throughout the HF.
- The lithofacies presented here are end members and often within the field it is difficult to apply a specific lithofacies to an outcrop as there is often overlap between different lithofacies. This is particularly the case with E1, E2 and E3 as well as C1,C2, D1 and D2.

## 6 Lithofacies successions

### 6.1 Introduction

This chapter focuses on understanding some of the key lithofacies successions within the Hreppar Formation. The HF comprises a variety of palaeo-environments, highlighted by the complex relationships between the main lithofacies. Example lithofacies successions are described in detail here, enabling the environments of deposition to be fully understood.

The lithofacies successions are depicted through the use of annotated logs and field panoramas. The field location of each panorama can be identified through the use of the grid system on the main geological map (Figure 6-1, map insert) and each lithofacies association description has an inset map, highlighting the location and geology in detail. The lithofacies successions build on the descriptions of the lithofacies in the previous chapter. Lithofacies successions in volcano sedimentary settings demonstrate genetic associations as well as non-genetic associations.

The environment in which these lithofacies were formed was heterogeneous, with evidence for competing volcanic, glacial and fluvial systems, controlled by tectonics, volcanism and climate with tectonics being the primary driver. These different systems can be observed actively competing for available accommodation space in modern day Iceland and provide helpful analogues for the HF.

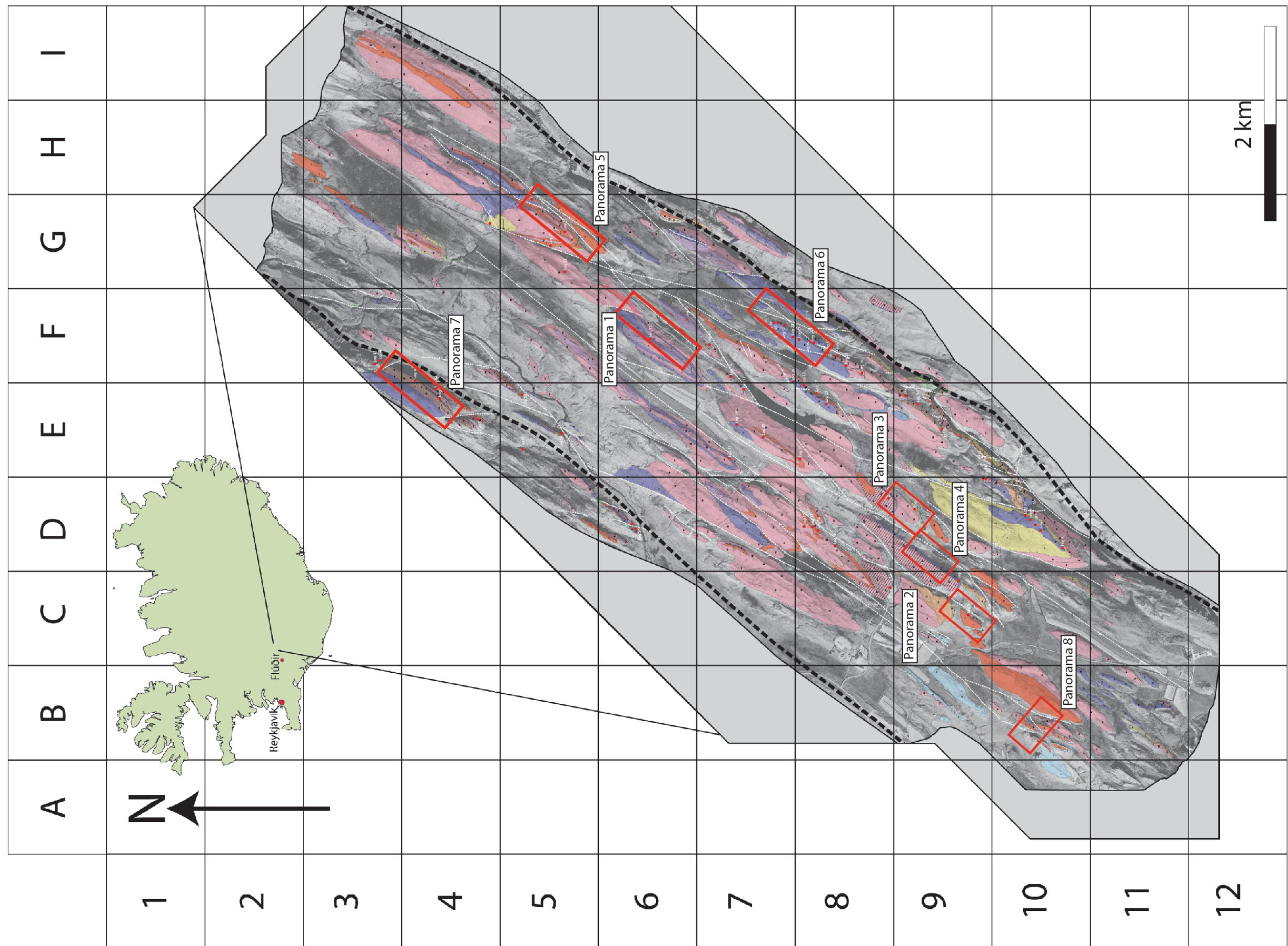
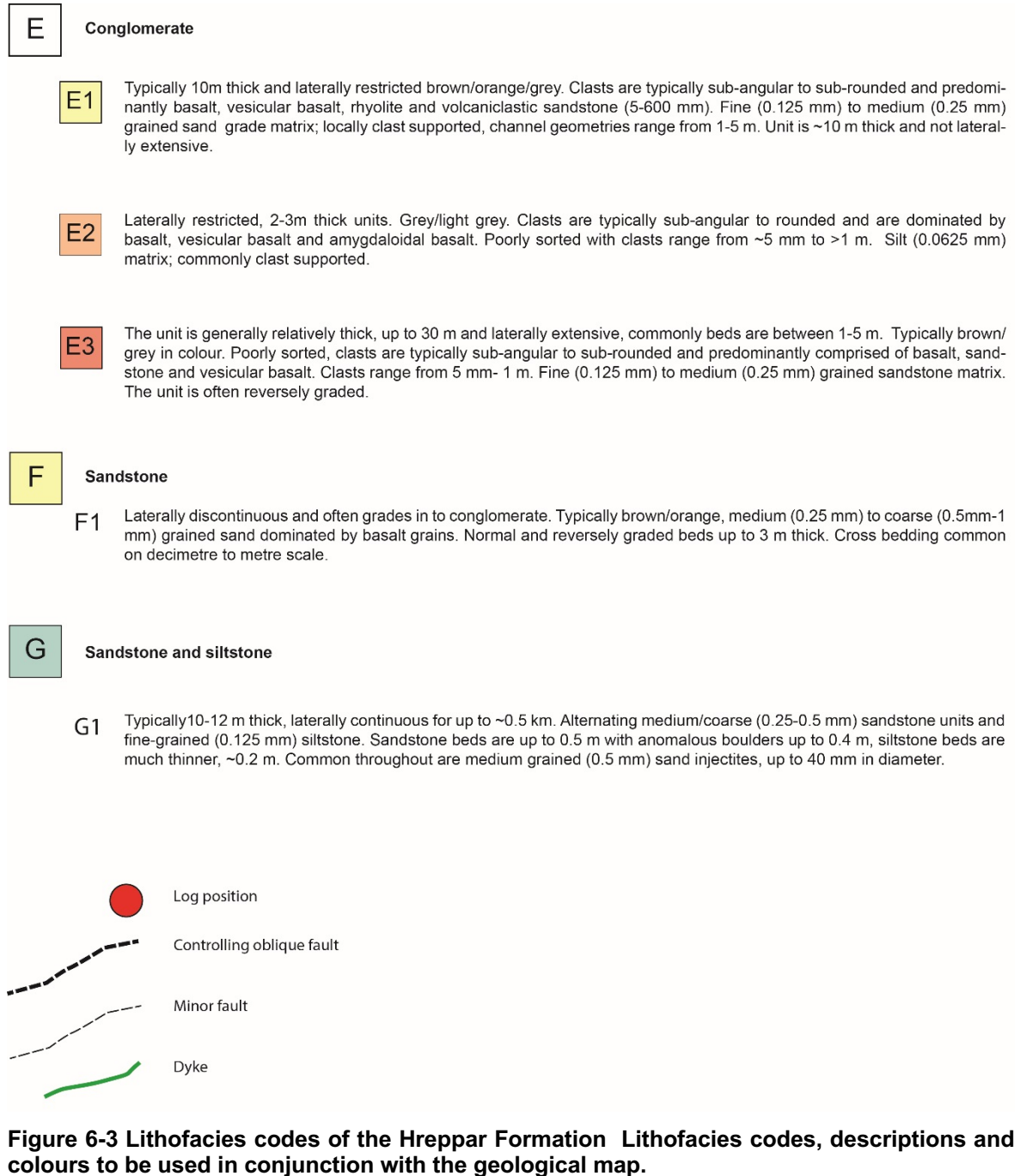


Figure 6-1 Geological map of the Hreppar Formation at Flúðir. The area has been divided in to a grid system, to easily identify where the panoramas are located.

- A** **Ignimbrite**
- A1 Lava-like ignimbrite with well-developed fold structures on mm-m scale. Folds are highlighted by alternating dark and light bands. Very fine-grained (<0.125 mm) and rarely glassy. Spherulites at the base of the unit is common. Laterally extensive >0.5-1 km and ~5-10 m thick.
- A2 Massive lapilli tuff. Lithic lapilli range from 5-15 mm, pumice lapilli and weathered-out pumice commonly present. Typically grades in to C1. Laterally continuous >0.5-1 km, to, 1-3 m thick.
- B** **Sub-aerial, basaltic lava**
- B1 Local development of 'a'a, commonly with a clinker top facies. Typically the clinker top is irregular in its lateral extent and filled with sediment. These lavas are ~5-10m thick and laterally continuous. Often the entablature facies not always present.
- B2 Pahoehoe with obvious, well-developed colonnade. Laterally extensive dark grey/ pink and fine-grained (0.125 mm). Commonly the entablature is absent. Columnar joint spacing 1.5-2.5m with well defined chisel marks spaced 20-40 mm.
- B3 Pahoehoe with obvious core, poorly distinguishable top and bottom. Tops and bottoms vesicle-rich. Generally 5-10 individual units stacked together, with individual units ~1-3m in thick. Locally, thin columnar-jointed units transition in to, and have irregular boundaries with, hyaloclastite. Dark grey/ black, generally medium-grained (0.25 mm), locally fine (0.125 mm) and coarse (0.5 mm). Where laterally and vertically discontinuous, indicated by B3\*.
-  B3\* Correlatable pahoehoe with obvious core poorly distinguishable top and bottom. Weathers pink/orange. Individual units 1-3 m thick and laterally extensive. Typically fine-grained (0.125 mm). Commonly found to transition with hyaloclastite.
- C** **Primary hyaloclastite and pillow breccia**
- C1 Typically this unit has irregular contacts and has variable thickness, laterally can be quite extensive, up to 0.5 km. Dark grey/black on fresh surfaces, brown/orange on weathered surfaces. Massive, poorly sorted, glassy juvenile clasts range from fine (0.125 mm) to coarse (64 mm); angular/sub-angular clasts; fine-grained (<0.125 mm) matrix, dominated by glassy shards.
- C2 Typically this unit has irregular contacts and has variable thickness, laterally can be quite extensive, up to 0.5 km. Dark grey/black on fresh surfaces, brown/orange on weathered surfaces. Massive, poorly sorted, glassy juvenile clasts range from fine (0.125 mm) to coarse (64 mm); angular/sub-angular clasts; fine-grained (<0.125 mm) matrix, dominated by glassy shards. Additionally pillow fragments up to pebble size (64 mm) with an obvious glassy outer crust and pipe vesicles are present.
- D** **Reworked hyaloclastite**
- D1 Unit is typically up to ~10 m thick and laterally discontinuous. Poor to moderately sorted, typically sub-rounded, rarely sub-angular, glassy juvenile clasts up to pebble (64 mm) in a fine grained (<0.125 mm) matrix dominated by glassy shards. Grey/ black on fresh surfaces, brown/ orange on weathered surfaces. Unit is massive, with no apparent structure.
- D2 Unit is typically up to ~10 m thick and laterally discontinuous. Poor to moderately sorted typically sub-rounded, rarely sub-angular, glassy juvenile clasts up to pebble (64 mm) in a fine grained (<0.125 mm) matrix dominated by glassy shards. Grey/ black on fresh surfaces, brown/ orange on weathered surfaces. Normal and reversely graded beds up to 2 m thick are characteristic of this unit.

**Figure 6-2 Lithofacies codes of the Hreppar Formation. Lithofacies codes, descriptions and colours to be used in conjunction with the geological map.**



**Figure 6-3 Lithofacies codes of the Hreppar Formation Lithofacies codes, descriptions and colours to be used in conjunction with the geological map.**

## 6.2 Sub-aerial lava, hyaloclastite and re-worked hyaloclastite

A typical transition from sub-aerial lava in to hyaloclastite and re-worked hyaloclastite within the HF. Panorama 1 depicts the relationships between each of these lithofacies.

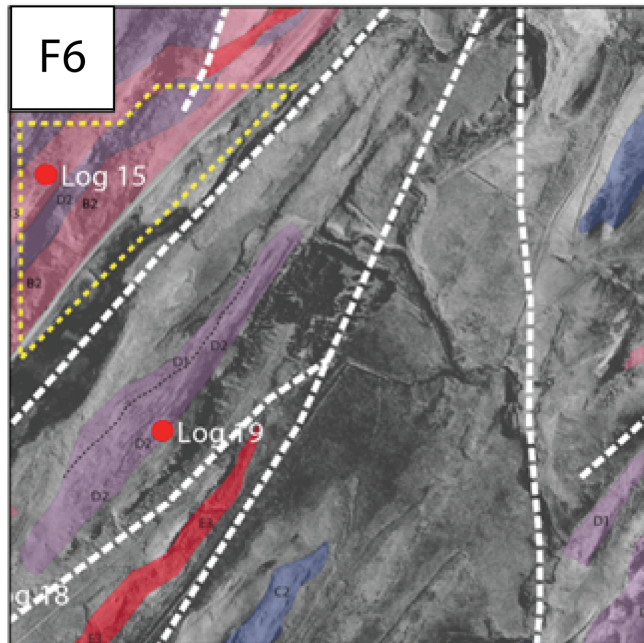


Figure 6-4 Location of panorama 1. Indicated by the dashed yellow line.

### 6.2.1 Description of panorama 1

Panorama 1 is situated in grid square F6 (Figure 6-1, Figure 6-4) in the centre of the field area. Lithofacies B3, D2 and C2 are represented in this panorama (Figure 6-5). The base of the outcrop consists of stratified reworked hyaloclastite (D2), primarily consisting of beds of sub-angular to sub-rounded hyaloclastite. These beds are ~1 m thick and display inverse grading. Laterally, D2 is not exposed.

Overlying D2 there is a lateral transition from left-right, of pāhoehoe basalt lava (B3) in to primary hyaloclastite and pillow fragments (C2). Two outcrops of B3 are observed with one having a direct contact with C2. At the contact, there is a transition over 0.5 m from coherent basalt in to hyaloclastite. Here, there is a mingling of the two lithofacies (Figure 6-5).

A sequence of B3, C2 and D2 is found at the top of the outcrop. B3 transitions laterally and vertically in to C2, which also transitions laterally and vertically in to D2. C2 is relatively thin in comparison with D3, which is >7 m.

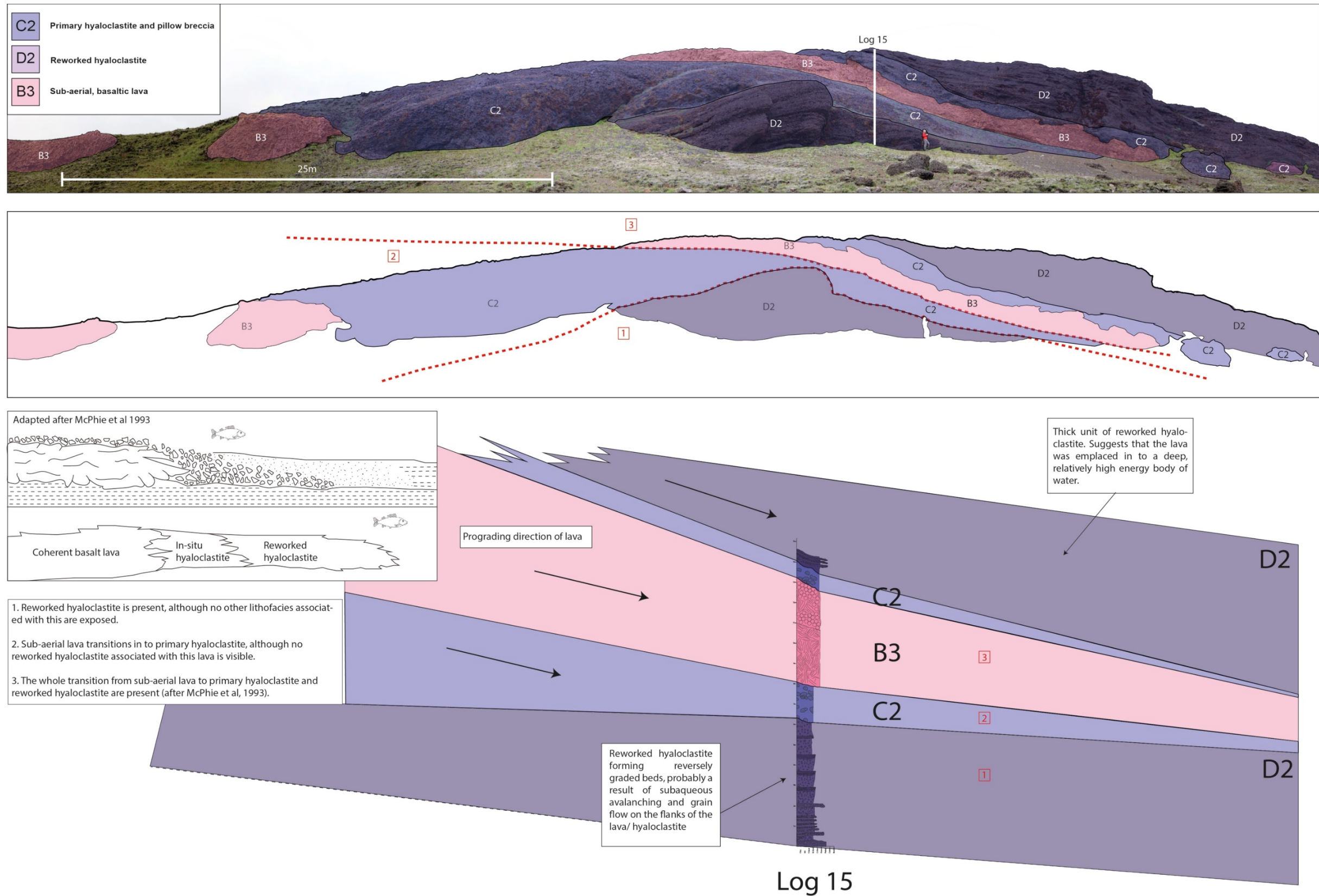


Figure 6-5 Details of panorama, highlighting the relationships between D2, C2 and B3. The panorama documents the transition from sub-aerial volcanism to sub-aqueous volcanism and the subsequent reworking of hyaloclastite.

### 6.2.2 Interpretation of panorama 1

The transition from B3 in to C2 and D3 is of sub-aerial lava entering a water body, (most likely a lake) which generated primary hyaloclastite and pillows (Fisher 1984; White et al, 2000; Gill 2010), before becoming re-worked by lake bottom currents and grain flow (Fisher, 1984; Reading, 2002). The water body in this example, is at least 6m deep based on the hyaloclastite and pillow thicknesses, in other areas within the study area the lacustrine facies indicate water depths of up to 16m, suggesting that lake bottom currents would have played an active role in reworking these deposits. Watton et al (2013) suggest that high angle cross bedding could represent Gilbert style delta deposition as the lavas entered the water body. The repetition of lithofacies B3, C2 and D2 indicate that this process has occurred repeatedly. The outcrop demonstrates evidence of this process having occurred at least three times. The lowest exposure of D2 in the outcrop has no associated exposure of sub-aerial lava or primary hyaloclastite exposed; however, it represents the first instance of sub-aerial lava entering a water body at this locality.

The second occurrence is only partially represented as there is no associated D2, exposed. During the first and second sequence, the position of the water body moved more basin-ward (right) due to a possible reduction in the volume of water in the lake. This is highlighted by C2, directly overlying D2, as C2 typically forms in shallower water.

The full sequence (B3-C2-D2) (Figure 6-5) exposed at the top highlights the whole process described by McPhie et al (1993)(inset diagram on Figure 6-5), of sub-aerial lava entering a water body, producing in-situ primary hyaloclastite and pillows before being reworked. The position/depth of the lake changed between sequence two and three, indicated by B3 directly overlying C2.

This sequence of lithofacies indicates that the volcanism was dominant at this point in time, with no development of sedimentary interbeds between sequences indicating that there was insufficient quiescence for the sediments to develop or there was a lack of preservation of sediments (?). The presence of sub-aqueous facies C2 and D2 demonstrate that there was an abundance of water in this depositional environment. This water could have potentially come from

volcanically dammed fluvial systems, producing lake bodies within the upstream confined valleys (Costa and Schuster, 1988; Schofield and Jolley, 2013; van Gorp et al, 2013). These dams could also have been produced as a result of landslides, glaciers and alluvial fans (Costa and Schuster, 1988) blocking fluvial systems.

### 6.3 Sub-aerial lava, conglomerate and fluvial sandstone

A typical transition from a sub-aerial lava in to debris flow conglomerates and fluvial sediments. Panorama 2 highlights the relationships between these different lithofacies.

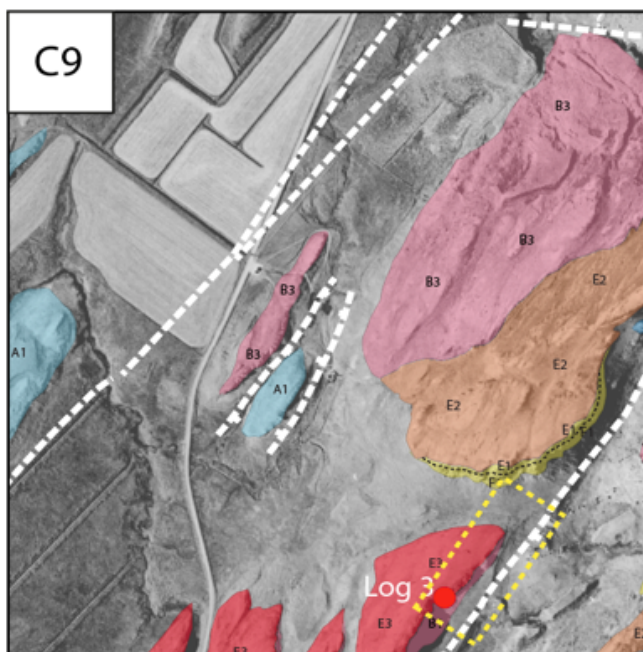


Figure 6-6 Location of panorama 2, Indicated by the dashed yellow line

#### 6.3.1 Description of panorama 2

Panorama 2 is situated in grid square C9 (Figure 6-1, Figure 6-6) of the field area. Three lithofacies are represented in this panorama; 'a'ā basalt lava with clinker top (B1), debris flow conglomerates (E3) and fluvial sandstones (F1) (Figure 6-7).

At the base of the outcrop ~6 m of B1 is present, but the base of lithofacies B1 is not exposed. The upper 2 m of B1 is highly irregular, with pockets of rubbly top preserved in depressions within the lava. The depressions are irregular and inter finger with the coherent core of the lava. Where these pockets of rubbly top are preserved, a matrix of fine/ medium sandstone surrounds the clinker that comprises the rubbly top.

B1 grades in to lithofacies E3 over ~1.5 m. Contacts of coherent basalt with E3 are present as are contacts of rubbly top and E3. Within the first metre of E3, isolated clinker clasts are present, but these become rarer higher in the unit. The unit is approximately ~7 m thick with the top 1.5 m being dominated by large boulders of up to ~1 m. The unit is inversely graded. E3 transitions over ~1 m in to F1, with the very top of E3 comprising medium sand. F1 is ~3 m thick and is dominated by small cross bedded horizons.

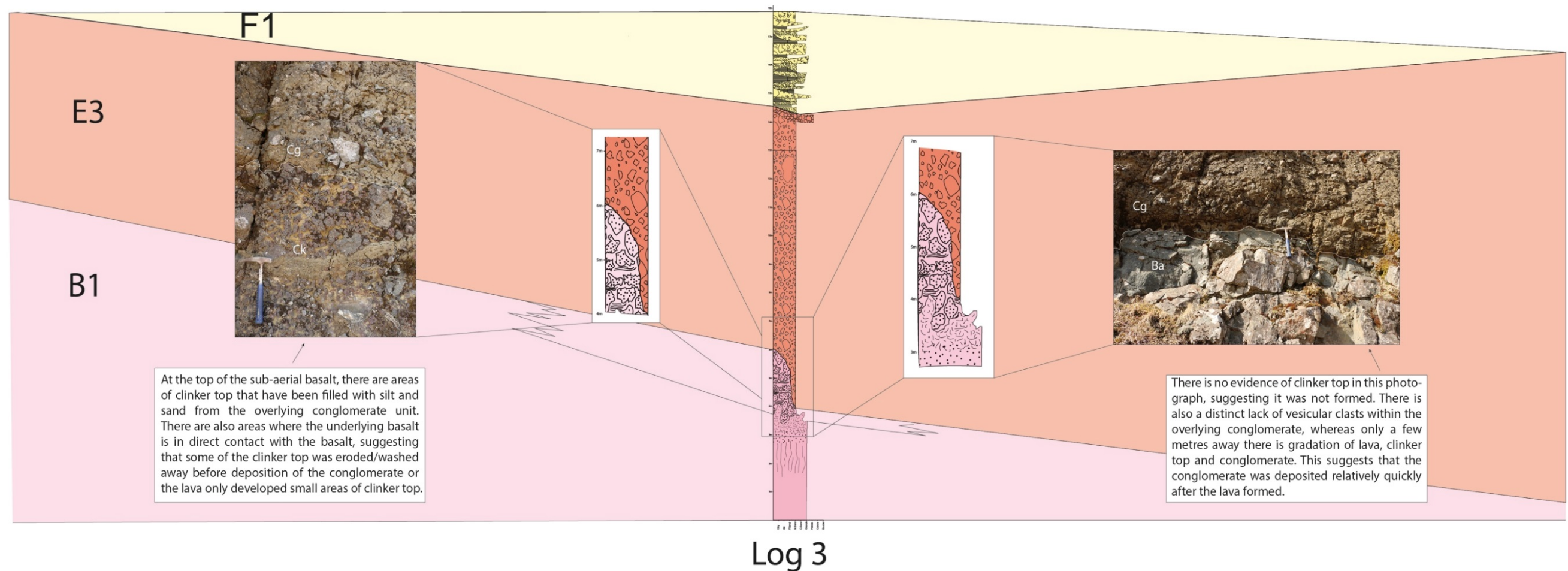
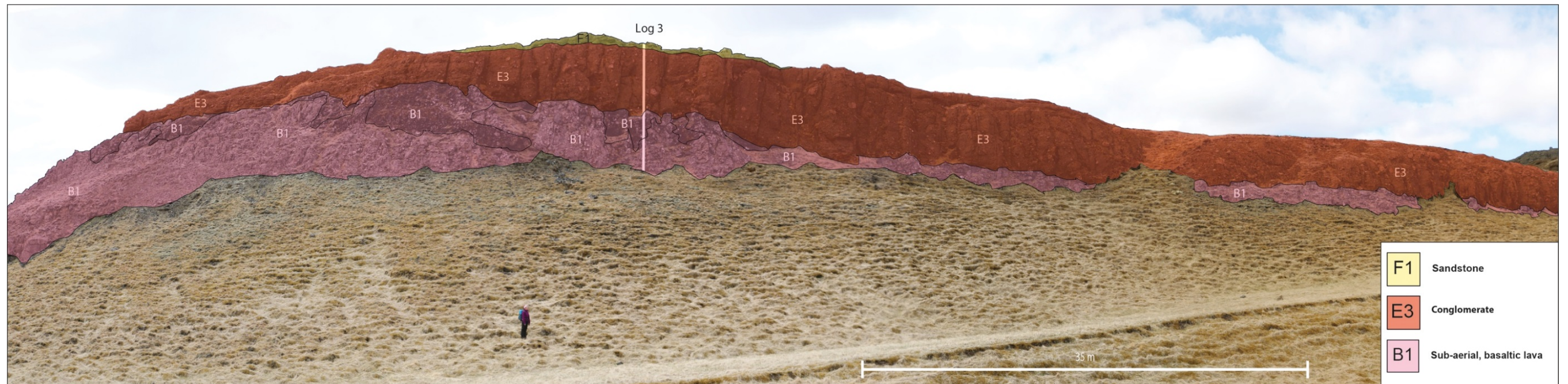


Figure 6-7 Panorama 2 highlights the main relationship between lithofacies B1, E3 and F1. The panorama documents the role of tectonics in the HF and the deposits associated with faulting

### 6.3.2 Interpretation of panorama 2

The lithofacies association represents a change in the dominant system at that time (Figure 6-7). B1 dominates before there is volcanic quiescence, allowing sedimentary systems to fully develop. A rubbly top has formed on the surface of B1 as a result of increased effusion rate from the fissure. Kestzthelyi et al (2000) suggest surging and autobrecciation as mechanisms of emplacement that can generate rubbly flow tops with smooth, pahoehoe like bases. The rubbly top has only been preserved within lows of the lava surface (Figure 6-7), as it is very susceptible to weathering and erosion; this is why it is not observed along the entire length of the contact with E3.

The transition between B1 and E3 highlights a hiatus in volcanic activity. In the area there was active faulting occurring at the time of deposition. This, combined with heavy rainfall, saturated ground and loose debris from erosion, are likely triggers for generating debris flows (Costa, 1984; Hungr et al, 2001). The area would have been very wet with an abundance of rain and snowmelt. Furthermore, there would have been a lack of vegetation cover and an abundance of loose eroded material, primarily from fluvial systems and weathering. All these factors could have combined to generate a debris flow such as E3. It most likely stopped within a low in the palaeo-topography. The debris flow would have likely been confined to a channel, allowing a relatively large flow depth to be maintained (Hungr et al, 2001). This would have been utilised more than once by debris flows. Areas of much coarser grained clasts within the unit evidence this. Reverse grading is typical of these deposits (Costa, 1984).

The gradation from E3 to F1 represents a change from high-energy, debris flow events associated with faulting, heavy rainfall and loose material, to a lower energy fluvial system. Development of a fluvial system indicates that erosion rates were high and there was a lack of volcanic activity at the time of deposition. The fluvial system would have taken advantage of lows in the palaeo-topography, much like B1 and E3.

## 6.4 Sub-aerial lavas, hyaloclastite, conglomerate and fluvial sandstone

Panorama 3 depicts the transition from conglomerate in to fluvial sediment, sub-aerial lava and hyaloclastite and highlights the main relationships between the differing lithofacies.

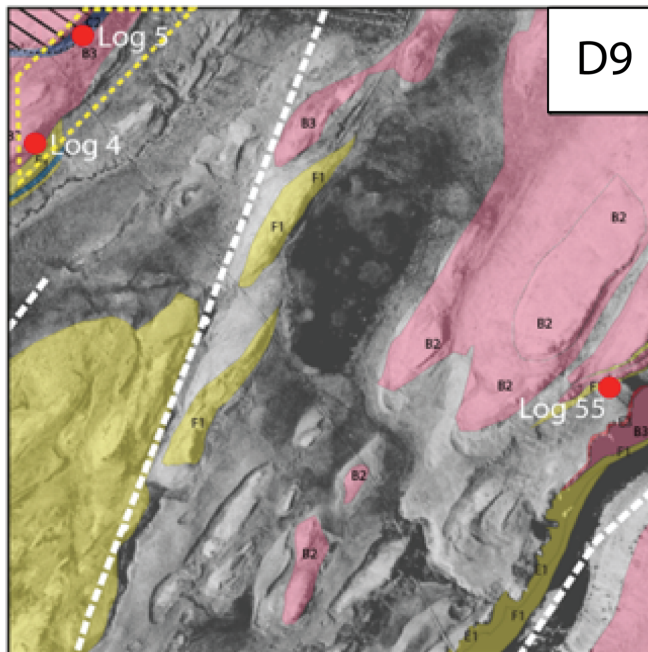


Figure 6-8 Location of panorama 3 indicated by the dashed yellow line

### 6.4.1 Description of panorama 3

Panorama 3 is situated in grid square D9 (Figure 6-1, Figure 6-8). Four lithofacies are represented in the panorama; glacial derived conglomerate (E2), fluvial sandstones (F1), pahoe-hoe basalt lava with poorly defined tops and bottoms (B3) and primary hyaloclastite and pillow breccia (C2) (Figure 6-9).

At the bottom of the panorama, E2 is exposed for ~3-4 m, although the contact with the underlying unit is not observed. E2 is dominated by boulders >1 m of basalt, with small (cm) sedimentary structures such as cross bedding observed within the clay/silt matrix. Diffuse bedding within E2 is present on a metre scale.

The contact between E2 and F1 is not observed due to lack of exposure. It is assumed that there is a gradation between the two lithofacies, over the zone of no exposure.

F1 is a small coarsening upwards sequence of sandstone with occasional pebbles of basalt. Cross bedding is observed within the unit on a 0.5 m scale. There is a relatively well defined, regular contact between F1 and B3.

B3 is a small unit with poorly developed columnar jointing up to 0.3 m wide, the top surface is not exposed. The lava weathers orange/brown.

There is no exposure between lithofacies B3 and C2. Log 5 begins higher in the stratigraphy due to the lack of exposure above B3. Areas of C2 are dominated by clusters of well-developed pillows up to 1 m in diameter. These are typically more common at the base of the unit. Towards the contact with B3, the unit is predominantly primary hyaloclastite with occasional pillow fragments. The total thickness of the unit is ~ 7 m.

The contact with B3 is irregular and varies laterally. There is no transition between the two different lithofacies, and the contact is sharp. Within B3 there are at least 5 lava flows present with a thickness of ~13 m.

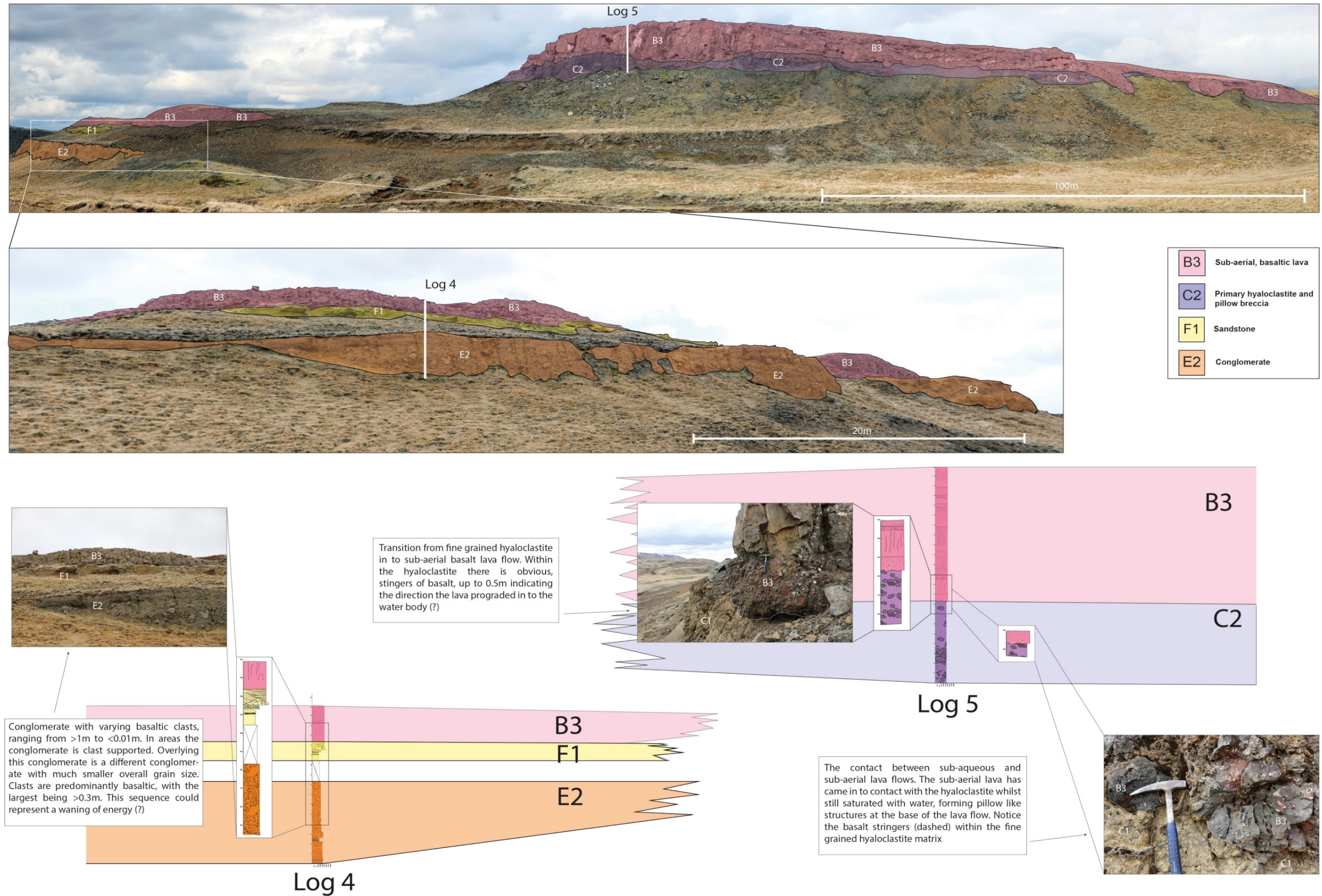


Figure 6-9 Details of panorama 3. Panorama 3 highlights the main relationships between lithofacies E2, F1, B3 and C2. It documents the interaction of fluvial, glacial, volcanic and tectonic systems and how these are related

### 6.4.2 Interpretation of panorama 3

The panorama highlights the relationship between various competing systems (Figure 6-9). E2 represents a debris flow deposit that contains glacially derived material. As the unit is not fully exposed it is difficult to understand fully. The transition from E2 to F1 most likely represents a glacial outburst event which deposited E2 and subsequent fluvial output from a glacier as the flood event waned. This would have been a very wet environment with a lot of fluvial output from the glacier in addition to frequent rainfall, much like modern day Iceland.

B3 and C2 represent a change in the system where volcanic activity dramatically increased. The increase in volcanism produced the lavas exposed in the lower outcrop of B3. C2 indicates that the sub-aerial lavas of B3 entered a water body, demonstrating that a fluvial system was still active during the increase in volcanism. This fluvial system was most likely dammed or had its course altered by sub-aerial lavas, generating a water body (Costa and Schuster, 1988; Schofield and Jolley, 2013; van Gorp et al, 2013). Subsequent lava flows entered this water body generating lithofacies C2. Lithofacies B3 above C2 indicates that the water body was no longer present when the last lavas were erupted as they mark a return to being sub-aerial as opposed to sub-aqueous.

## 6.5 Conglomerate, hyaloclastite and sub-aerial lava

A typical transition from debris flow conglomerate in to hyaloclastite and sub-aerial lava within the HF. Panorama 4 depicts the relationships between each of these lithofacies.

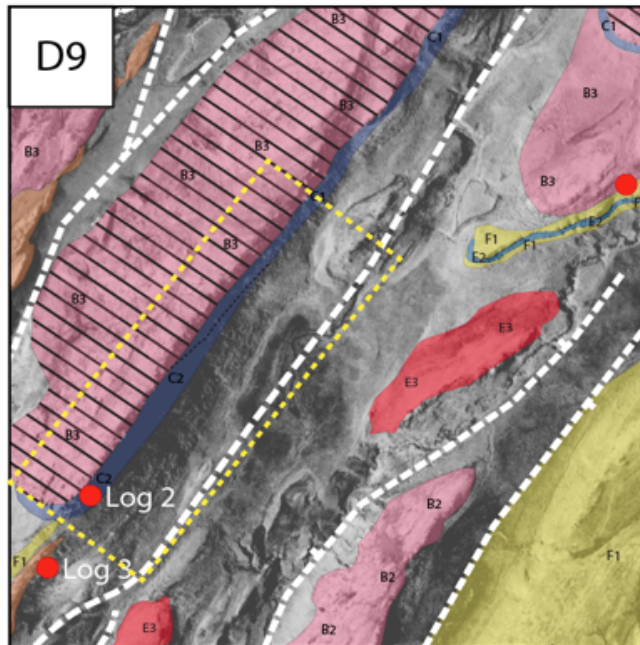


Figure 6-10 Location of panorama 5 indicated by the dashed yellow line.

### 6.5.1 Description of panorama 4

Panorama 4 is situated in grid square D9 (Figure 6-1, Figure 6-10). Three lithofacies are represented in this panorama; glacial derived conglomerate (E2), primary hyaloclastite and pillow breccia (C2) and pāhoehoe lava with poorly defined tops and bottoms (B3) (Figure 6-11).

A small exposure of E2 is found at the base of the section. This is ~7 m thick and is dominated by rounded basaltic boulders set within a clay/silt matrix. It is assumed that this unit is laterally continuous, although not exposed, based on the presence of the unit, along strike.

There is ~8 m of no exposure between E2 and C2, so it is difficult to determine where the contact would likely be. A ~10 m exposure of C2 is found overlying the area of no exposure. The lowest 4 m of the unit is dominated by pillow structures, typically 0.5 m in diameter with obvious tear drops between, confirming the

sequence is the correct way up. Moving up through the remainder of the unit, the pillow density decreases, with more pillow fragments and isolated pillows present within a hyaloclastite matrix.

C2 grades upwards in to B3, however this contact is highly irregular laterally away from the position of log 2. C2 contains at least 8 individual lavas, with a cumulative thickness of ~20 m. The lowermost six lavas are relatively thin at ~1-2 m each, whereas the upper two lavas are 4-8 m thick.

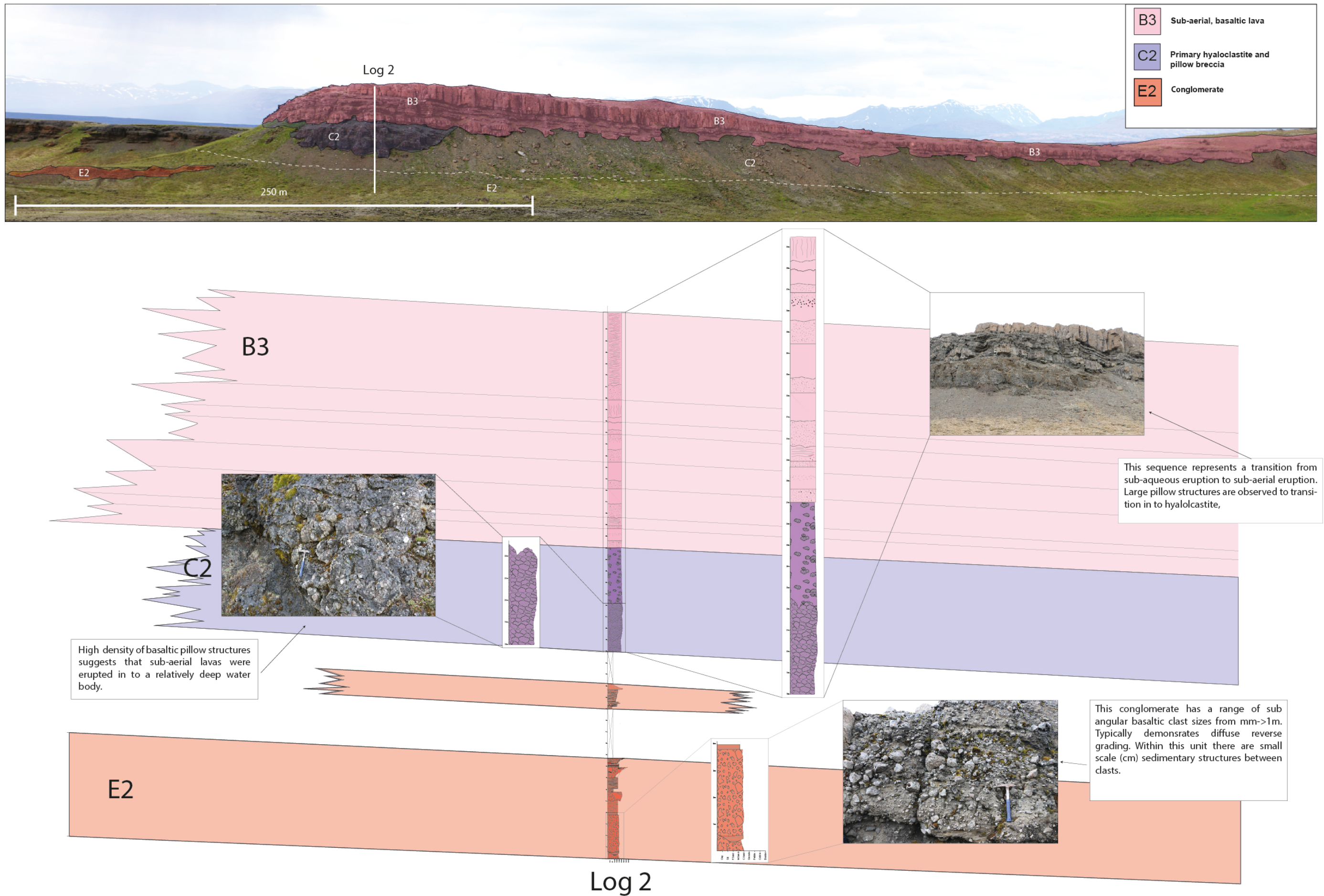


Figure 6-11 Panorama 4 documents the relationship between lithofacies E2, C2 and B3. Within the panorama, the change from a glacial dominated system to a volcanically dominated one is highlighted.

### 6.5.2 Interpretation of panorama 4

Panorama 4 documents the transition from glacial to sub-aqueous and then sub-aerial volcanism (Figure 6-11). The same sequence is observed at three other localities within the field area (chapter 10). The glacially derived conglomerates of E2 are most likely deposited during a glacial outburst event. Small sedimentary features such as cm scale cross-bedding are present indicating reworking by small fluvial channels. As the contact with C2 is not observed it is difficult to determine the relationship between the two lithofacies. However most likely the unit becomes much finer grained and sand rich towards the top. This would be the result of streams draining the retreating glacier, generating loose debris and water. It is probable the contact between the units is very irregular.

The presence of C2 indicates that sub-aerial lavas have interacted with a water body such as a lake. The thickness of C2 indicates that the water depth was relatively deep. The transition from high pillow density to low pillow density and increasing hyaloclastite suggests that the relative water depth was decreasing as a result of lavas entering and generating hyaloclastite, which filled it up. The water body formed most likely as a result of runoff from a glacier being trapped within the topography, which is very common in modern analogues found in Iceland.

The transition from C2 to B3 represents the change from sub-aqueous to sub-aerial volcanism. There is no lateral change from C2 to B3 indicating that the transport direction of the sub-aerial lavas was towards the observer. The sheet like nature of the lavas in B3 indicate that the lavas were erupted with a relatively continual supply of magma and the lack of sedimentary units between lavas suggests that the volcanism was continuous and dominant.

## 6.6 Sub-aerial lava, fluvial sandstone and conglomerate

A typical transition from sub-aerial lava in to fluvial sandstone and conglomerate within the HF. Panorama 5 depicts the relationships between each of these lithofacies.

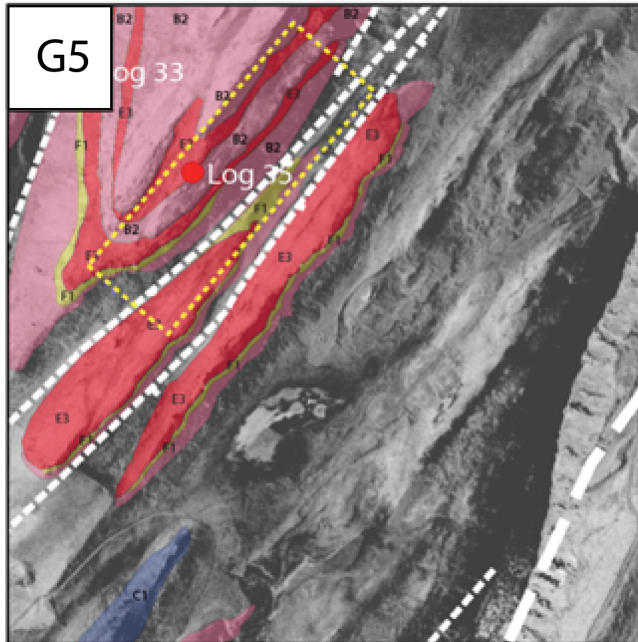


Figure 6-12 Location of panorama 5 Indicated by the dashed yellow line

### 6.6.1 Description of panorama 5

Panorama 5 is situated in grid square G5 (Figure 6-1, Figure 6-12). Four lithofacies are represented in this panorama; 'a' basalt lava with clinker top (B1), pāhoehoe basalt lava with columnar jointing (B2), stratified volcanoclastic sandstone (F1) and debris flow conglomerates (E3). Faulting within the sequence is easily identified by the repeating lithofacies (Figure 6-13).

At the base of the section 7m of lithofacies B1 is exposed. The overall thickness of this unit is not known because the base is not exposed. The upper 2.5 m is dominated by a well-developed rubbly top. This is not a consistent thickness along the lateral extent of this lava, and in some areas it is not present.

B1 grades in to F1, with a highly irregular contact. F1 is ~ 2-3 m thick and medium to coarse grained sand. The unit generally coarsens upwards before grading in to E3.

The contact between F1 and E3 is irregular, and locally F1 is reduced to a few tens of centimetres thick. E3 is 12 m thick and is composed of a series of alternating beds dominated by cobbles and boulders. These are predominantly basaltic in composition.

Between E3 and B2 there is 1-3 m of no exposure, therefore making it difficult to fully understand the nature of the contact. B2 is a ~12 m thick lava, with well-developed widely spaced, columnar jointing. Above this unit of B2 there is a ~4 m thick exposure of E3, the thickness of which varies along its length. Stratigraphically above this small unit of E3 another repeating sequence of B2 and E3 is present. The uppermost B2 unit is ~15 m thick and has an irregular contact with the unit of E3 underlying it. The whole sequence is capped by a laterally continuous, ~5 m thick unit of E3.

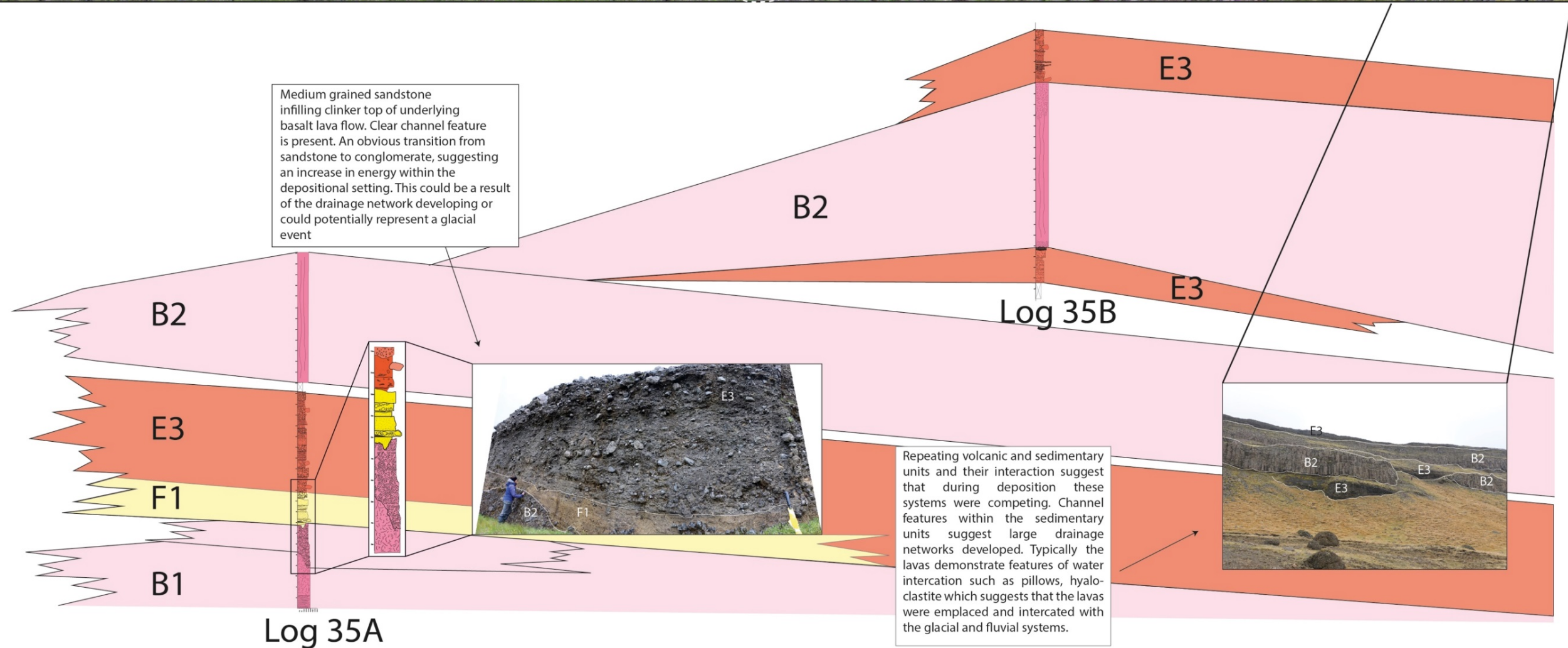
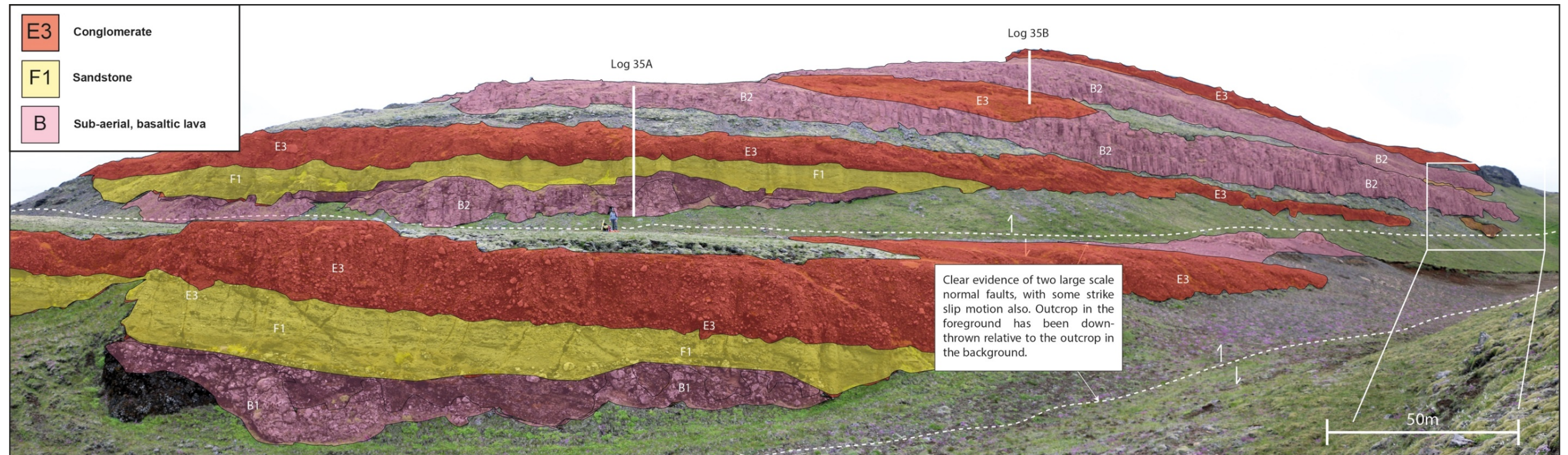


Figure 6-13 Panorama 5 documents the relationship between lithofacies B1, F1, E3 and B2. The panorama represents rapid changes between volcanically dominated systems and tectonically dominated systems

### 6.6.2 Interpretation of panorama 5

Panorama 5 records a very dynamic time in the HF, with volcanic, fluvial and tectonic systems interacting (Figure 6-13). The panorama can be divided into two main periods. Lithofacies B1 at the base of the panorama indicates that the volcanic system was highly active, with sudden increases in effusion rate generating rubbly tops to the lavas. As the magma was extruded, the lavas would have filled lows within the palaeo-topography.

The presence of F1 highlights that there was quiescence in the volcanic system allowing for the formation of a fluvial system. As the sedimentary rocks are predominantly coarse grained sandstone, this indicates that the fluvial system had the energy and ability to transport these larger grain sizes. The gradation from F1 into E3 represents a large increase in energy within the system. The debris flows are associated with heavy rainfall, loose eroded sediment and faulting in the area, generating steep gradients and acting as a trigger mechanism. The faulting could account for the apparent quiescence in volcanic activity by diverting lavas elsewhere in the HF as they fill lows within the palaeo-topography.

B2 represents an increase in volcanic activity, generating large lavas. The size of these lavas indicate that the system was very active, most likely dominating the environment. Along strike, B2 appears to have ponded in lows, which indicates that the volcanic system very quickly became active after faulting. The lows generated by faulting were most likely filled with thick accumulations of lava. The lack of an entablature in B2 suggests that fluvial systems did not interact with the cooling lavas, and were displaced and diverted during extrusion of lavas.

Above the first exposure of B2, there is another sequence of E3 and B2, with the whole sequence capped by E3. The repeating nature of the lithofacies, indicates that there has been continual tectonic activity in the HF. This has generated accommodation space for lavas to fill such as lithofacies B2. Tectonic activity also generates fault scarps, loose sediment and provides a potential trigger mechanism for deposition of lithofacies E3.

The faulting within the panorama is clearly evidenced by the repeating colours of individual lithofacies (Figure 6-13). Where the log positions are indicated, this is the footwall of the fault and the hanging wall is in the foreground.

## 6.7 Sub-aerial lava, sandstone/siltstone and hyaloclastite

A typical transition from sub-aerial lava in to sandstone/siltstone and then hyaloclastite within the HF. Panorama 6 depicts the relationships between each of these lithofacies.

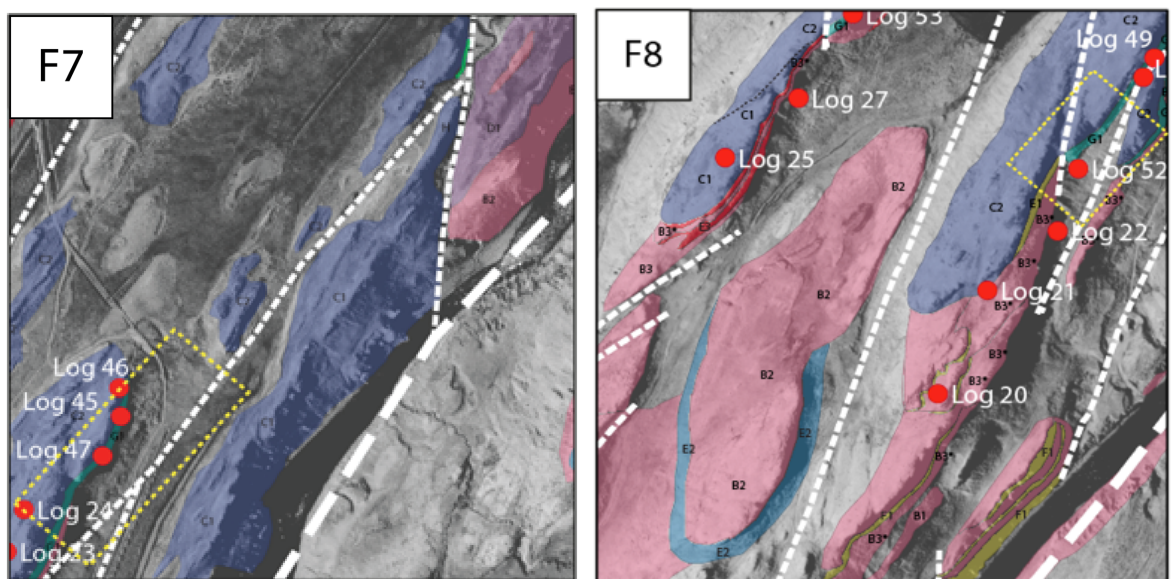


Figure 6-14 Location of panorama 6 Indicated by the dashed yellow line

### 6.7.1 Description of panorama 6

Panorama 6 is situated within grid squares F7 and F8 (Figure 6-1, Figure 6-14). Three main lithofacies are present; pāhoehoe basalt lava with large columnar jointing (B2), alternating siltstone and sandstone units (G1) and primary hyaloclastite and pillows (C1).

The lowest lithofacies exposed within the panorama is B2. The full thickness of B2 is unknown due to a lack of exposure. Log 50 captures the upper 1 m of the unit, but it is expected to have a full thickness of > 10 m. The unit has a very small, poorly developed rubbly top, which is only ~0.5 m thick. The unit is laterally continuous.

Overlying B2, lies a ~5.5 m thick unit of G1. This unit comprises siltstone beds up to ~0.5 m thick, which are punctuated by beds of sandstone up to ~1 m thick. Within the upper ~3 m of the unit, there are widespread sand injectites. These are up to 0.1 m wide and continue for ~3 m. Within the siltstone beds, 0.1 m thick horizons of white tuff are observed, which have some very small, mm scale cross bedding within them.

A unit of C1 caps the whole sequence. The gradation from G1 to C1 is irregular. The logged thickness of C1 is ~2 m, the unit is ~10 m thick and is composed of coarse grained hyaloclastite and patches of apparently coherent lava. It is laterally extensive. At the base of the unit there is interaction with the underlying sediment of G1. Small pillow like structures have developed, and are up to 150 mm in diameter.

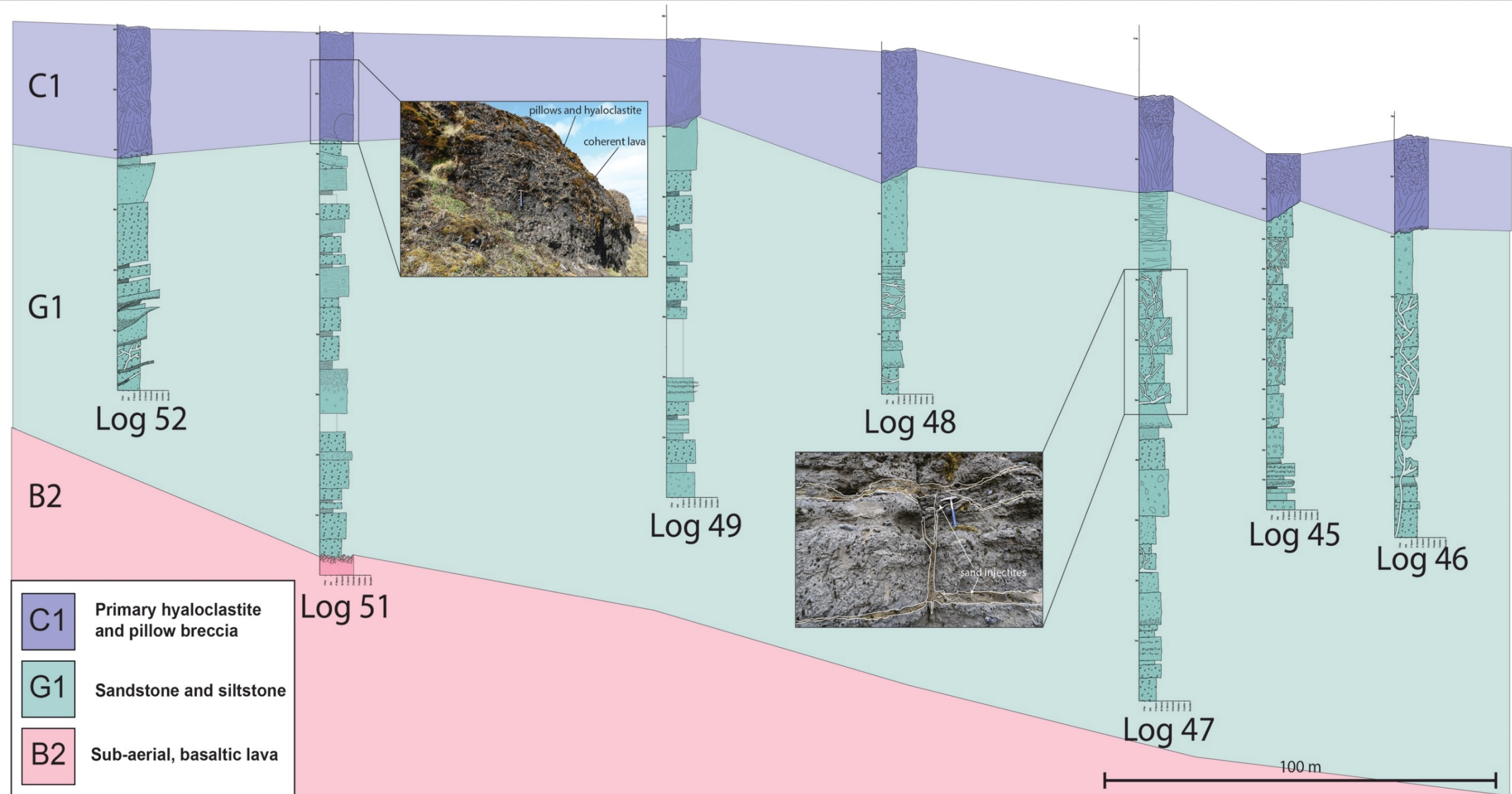
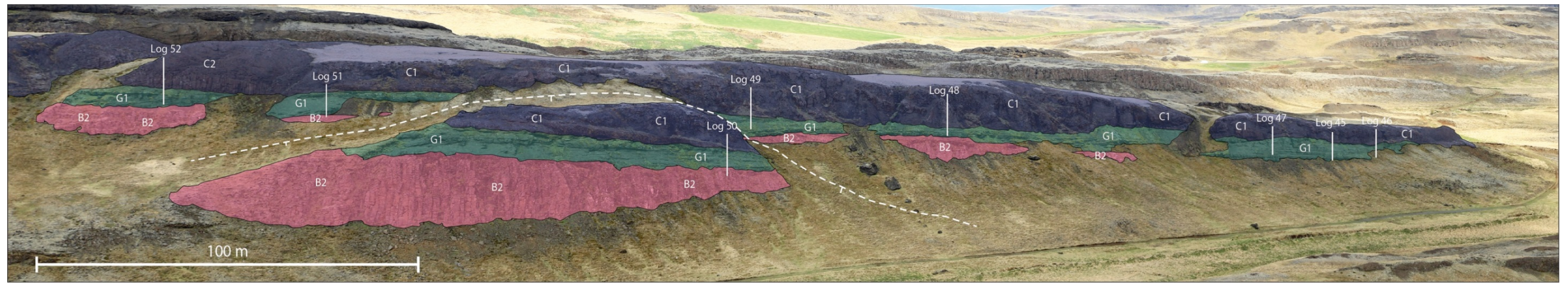


Figure 6-15 Panorama 6 documents the relationship between lithofacies B2, G1 and C1. It documents the development of a water body and the subsequent interaction with a return to the volcanic system.

### 6.7.2 Interpretation of panorama 6

B2 has well developed, thick columnar jointing, most likely the result of ponding and filling lows generated by tectonic activity. There is a lack of entablature to the lavas, indicating that they were not inundated by water whilst they were cooling. There was a time gap between the lavas cooling and the formation of a water body.

The formation of a water body was likely the result of the fluvial drainage network being diverted and filling in the low generated by earlier tectonic activity or as the result of melting glacial ice by volcanic heat (White and Riggs, 2001). The sedimentary units of G1 would have been deposited within a quiescent lake environment, as there are no obvious reworking structures present. The alternating siltstone and sandstone beds suggest cyclical input of sediment. The sandstone beds are thicker, which could be the result of spring input when glacial run off and snow melt is highest, and therefore able to carry coarser grained sediment. The presence of small dropstones suggests that there was a glacial interaction with this lake body. Small tuff horizons, preserved within the siltstone indicate that the environment was very quiescent as ash-fall would only be preserved in low energy conditions. Sand injectites are the result of a sudden trigger mechanism, which could have been tectonic activity or the eruption and subsequent loading of a lava on the water saturated sediments.

The unit is capped by C1, demonstrating that the volcanic system became active, producing lavas. These lavas were most likely erupted relatively close to the water body. They subsequently entered the water body producing hyaloclastite and pillow lavas. The pillow lavas are found in the deeper areas of the water body such as where log 48 is situated and hyaloclastite to the distal areas, such as where log 52 is situated (Figure 6-15).

## 6.8 Sub-aerial lava, conglomerates, hyaloclastite and fluvial sandstone

A typical sub-aerial lava dominated environment interacting with hyaloclastite, conglomerates and fluvial sediment within the HF. Panorama 7 depicts the relationships between each of these lithofacies.

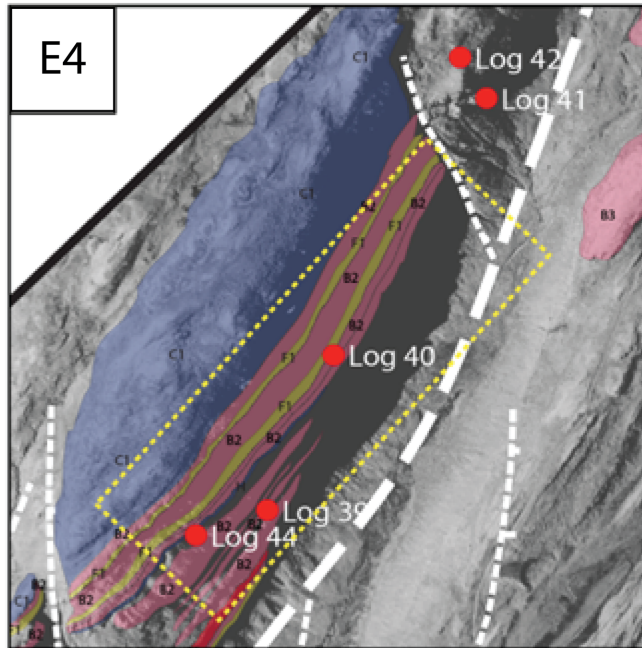


Figure 6-16 Location of panorama 7 Indicated by dashed yellow line

### 6.8.1 Description of panorama 7

Panorama 7 is situated within grid square F3 (Figure 6-1, Figure 6-16). Six lithofacies are present; stratified volcanoclastic sandstone (F1), pahoehoe basalt lava with large columnar jointing (B2), debris flow conglomerates (E3), pahoehoe basalt lava with poorly defined tops and bottoms (B3), primary hyaloclastite and pillows (C1) and pahoehoe lava with colonnade and entablature (B4) (Figure 6-17).

This panorama represents a series of lithofacies that are outside of the main graben of the HF, and therefore, the overall nature of the section is different to other panoramas as the units are generally laterally continuous.

The lowest exposed lithofacies is F1, which is a laterally discontinuous unit and is only ~0.5 m thick. Overlying F1, a laterally continuous unit of B2 is present. This is ~7 m thick with well developed large columnar jointing.

B2 has a very sharp, regular contact with the overlying unit of E3. The unit is ~9 m thick with large boulders of basalt present. These are up to 1.5 m in diameter, and are more dominant towards the top of the unit.

A small, discontinuous horizon of B3, ~3 m thick, directly overlies E3. The discontinuous nature of the unit, is most likely a function of exposure. A small ~1 m thick exposure of F1 is sandwiched, this is laterally discontinuous.

There is a sharp contact with the overlying B3 unit. This is an ~8 m thick lava with very well developed, large columnar jointing. The top of the unit is not observed due to a lack of exposure. There is a 5.5 m section of no exposure.

Above the area of no exposure there is a 5.5 m exposure of lithofacies B3. It is difficult to determine if this is part of the underlying lava flow or a separate one. Above this lava flow, there is ~6 m of no exposure.

A large B2 lava flow is exposed after the no exposure zone. This is a 19 m thick lava flow, with columnar jointing up to 2.5 m wide. The top of the flow is not observed but there is a ~4 m thick no exposure zone in which the top of the unit is most likely found.

After the zone of no exposure lies an outcrop of C1. This unit of C1 is relatively thin at ~2 m thick. There are very well developed pillows at the base up to 0.1 m in diameter.

C2 grades into a well developed unit of B1. B1 is ~12 m thick. The top of this unit has a 2-3 m thick hackly outer core, with a poorly developed rubbly top present. The rubbly top is ~1 m thick. This grades in to a ~11 m thick exposure of B2. This has well-developed, large columnar joints.

There is a sharp contact between B2 and F1. F1 is laterally continuous and ~5.5 m thick. It consists of a series of smaller beds, with well developed cross bedding and small normally graded beds present.

Overlying F1, there is a gradational change to B4 which is ~25 m thick. The unit has a well-developed colonnade and entablature. The entablature is ~9 m thick.

Overlying B4 there is a sharp contact with F1. The unit of F1 is smaller than the previous one at ~5 m thick. The unit is comprised of smaller beds, ~0.5 m thick.

The final lithofacies in log 39 is B2. This is an ~8 m thick exposure, with very well developed columnar jointing. The final lithofacies of the section, although not present in the log is a unit of C1. This thickens towards the right hand side of the panorama.

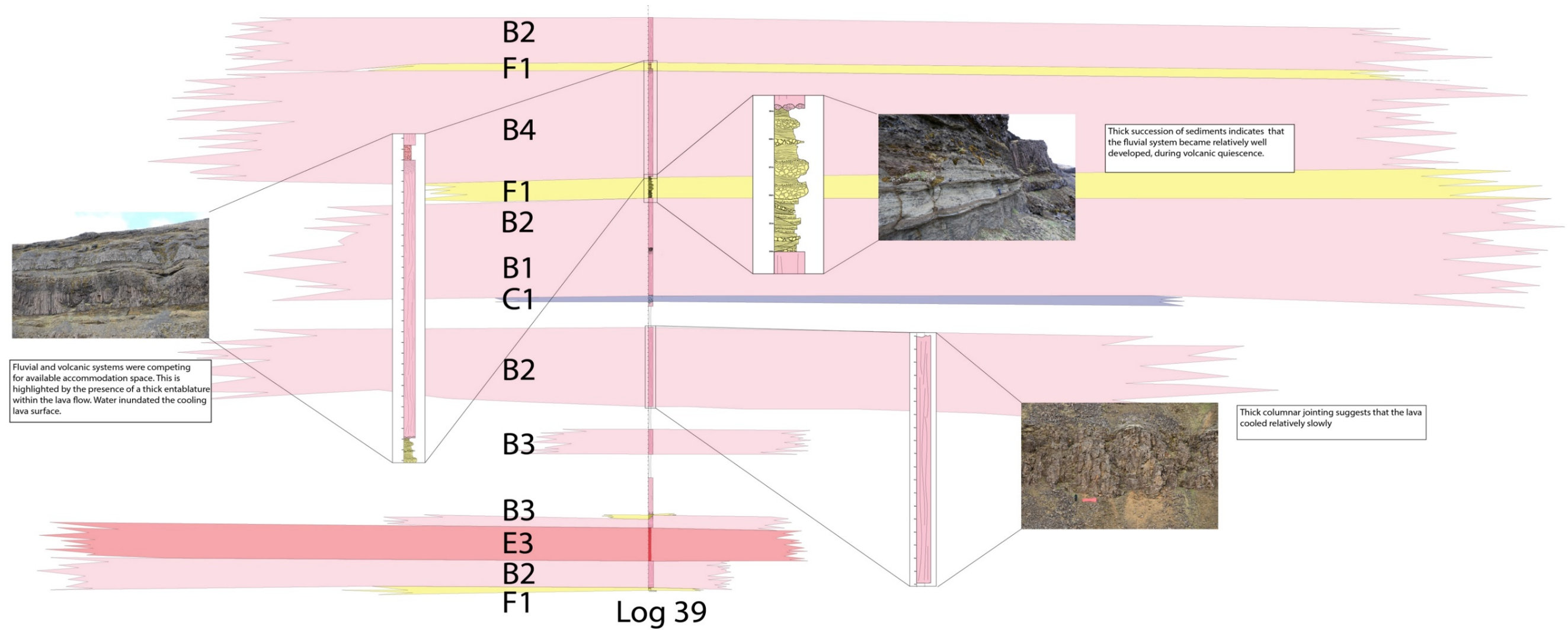
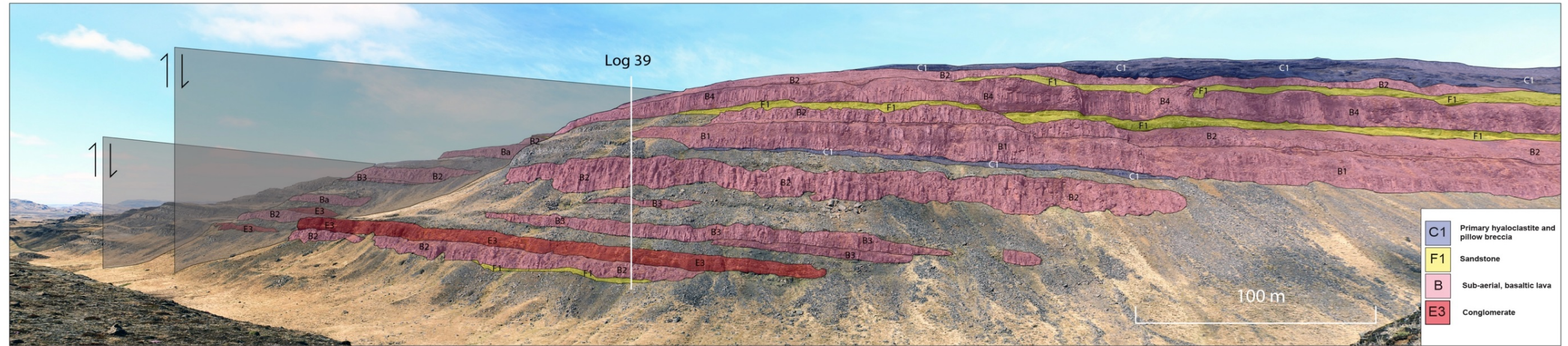


Figure 6-17 Details of panorama 7 Panorama 7 documents the relationship between lithofacies F1, B2, E3, B3, C1, F1 and B4. The panorama is situated outside of the main tectonic structure of the HF. The lithofacies are relatively laterally continuous

## 6.8.2 Interpretation of panorama 7

The whole panorama can be divided into three main sections, which highlight slightly differing environments, dominated by different systems.

The first five units, F1, B2, E3, F1, B3 represent a very dynamic environment with a lot of change. Initially there is a fluvial system depositing the small exposure of F1. There is a resurgence in volcanic activity which causes B2 to form. This lava would most likely have filled in the channel in which the fluvial system was deposited. This would have been a low in the palaeo land surface, allowing the lava to develop thick columnar jointing. Overlying the lava is a unit of debris flow conglomerate which has formed as the result of tectonic activity. The accommodation space generated by the tectonic activity was filled by a small lava. Overlying that is a very small, discontinuous sedimentary system, indicating that volcanic and fluvial systems were competing for accommodation space during this time.

The second section includes the lithofacies found within the middle of the panorama; B2, C1 and B2. These are the thickest lavas in the panorama and mapping area. The volcanic system was dominant at this point. The lack of interbeds between lavas, suggests that volcanic activity was almost continuous throughout this time. The lavas from the volcanic system would have diverted, altered and dammed the fluvial systems within the area. Lithofacies C1 highlights the fact that some water was present during the deposition of these units. This was probably the result of a dammed fluvial system having burst.

The third main section represents the upper part of the panorama (F1, B4, F1 and B2 and C1). The large deposits of F1 indicate that the fluvial system was very well developed. For the sedimentary system to be so well developed suggests that the volcanic system was relatively quiescent during this time. Alternatively the lavas could be following a different drainage network and we are only observing where the sediments were deposited. The B4 lithofacies indicates that the lava interacted with water whilst it was still hot, generating a large entablature. With F1 above this unit, this indicates that the B4 lava had occupied the underlying drainage network of F1, and ponded here before the fluvial system became active

again, interacting with the cooling lava. The capping C1 lithofacies indicates that the whole system was flooded, which could have been a result of faulting.

## 6.9 Sub-aerial lava, fluvial sandstone, conglomerate and ignimbrites

A typical transition from sub-aerial lava in to fluvial sediment, conglomerate and ignimbrites within the HF. Panorama 8 depicts the relationships between each of these lithofacies.

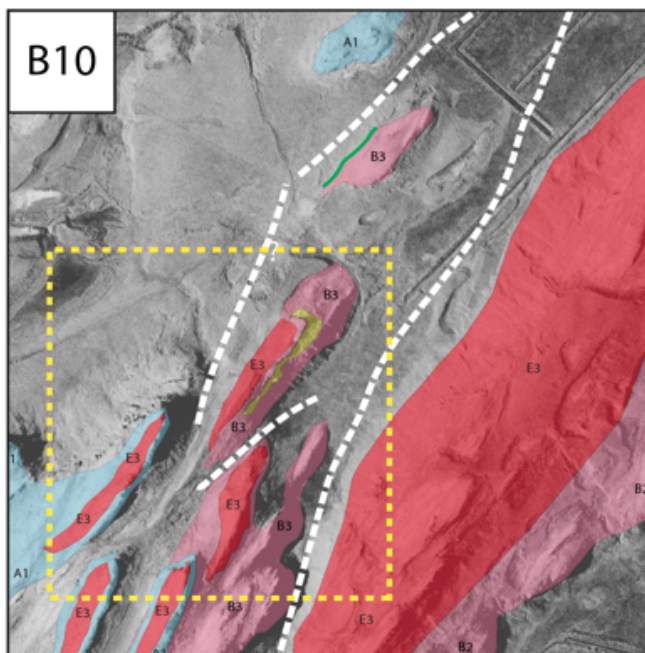


Figure 6-18 Location of panorama 8 indicated by the dashed yellow line

### 6.9.1 Description of panorama 8

Panorama 8 is situated within grid square B10 (Figure 6-1, Figure 6-18). Four lithofacies are present; 'a' basalt lava with clinker top (B1), stratified volcaniclastic sandstone (F1), mass flow derived conglomerate (E3) and lava-like ignimbrite (A1) (Figure 6-19).

The logs presented within panorama 10 are sketch logs. The lowest lithofacies observed in the panorama is B1. This is a laterally continuous unit, although exposure is limited. The top of the unit demonstrates a well-developed rubbly top.

There is no exposure above B1, which most likely hides the full thickness of lithofacies F1. This is a thin, laterally discontinuous unit. Lack of exposure most likely hides the rest of the unit as it is a lot softer than the surrounding volcanics.

Directly overlying the small exposure of F1 is a laterally discontinuous exposure of B1. This is relatively small and is not observed elsewhere in the panorama. The level of exposure is relatively poor.

A small area of no exposure is observed before a laterally continuous unit of E3 is found. Four main exposures of A1 have a sharp contact with the underlying E3 unit. The irregular outcrop pattern around log B highlights that the unit is thicker than the exposure suggests.

Lithofacies E3 caps the entire sequence above A1. All the exposures are disconnected, but these are likely part of the same event.

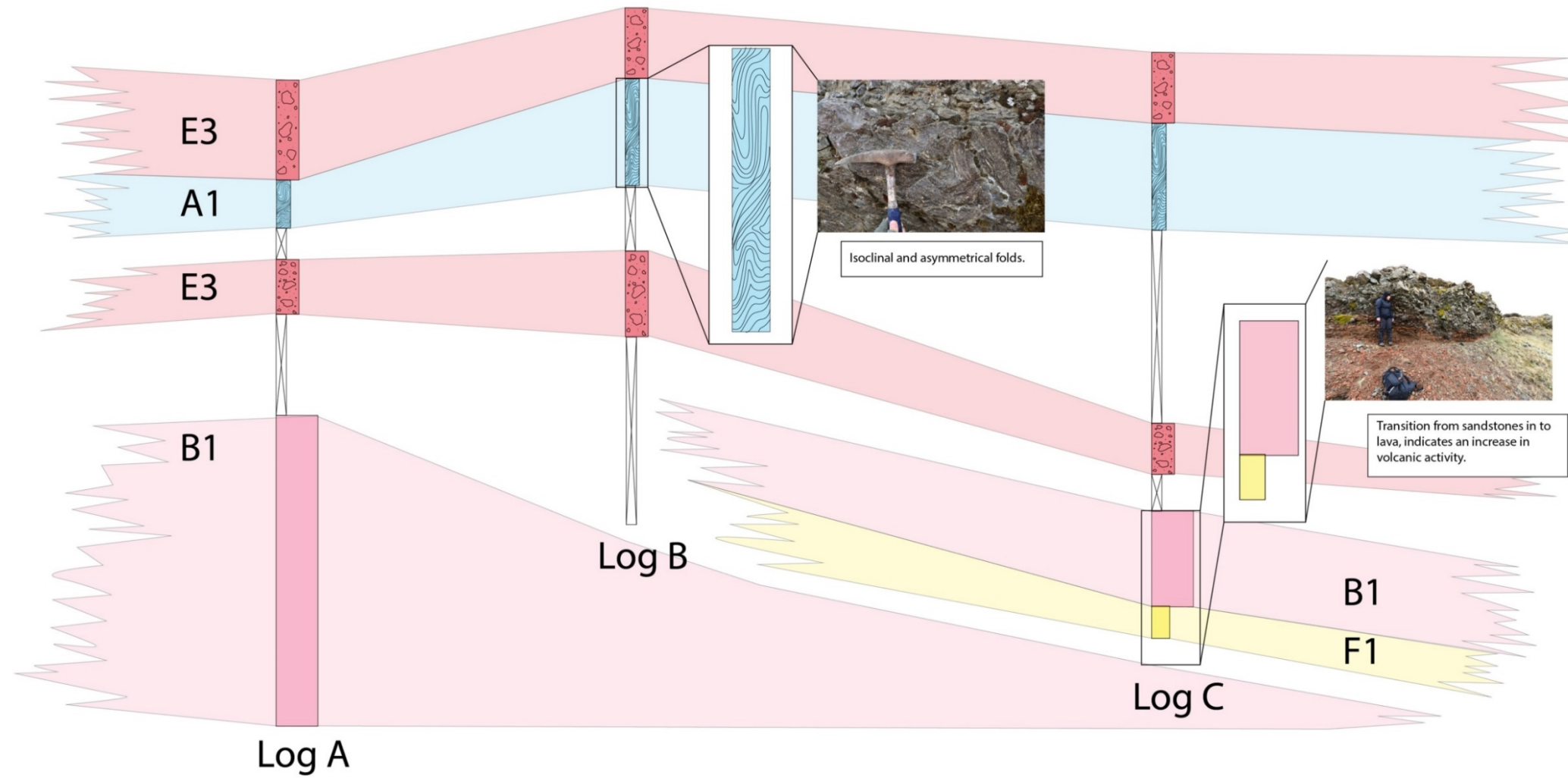
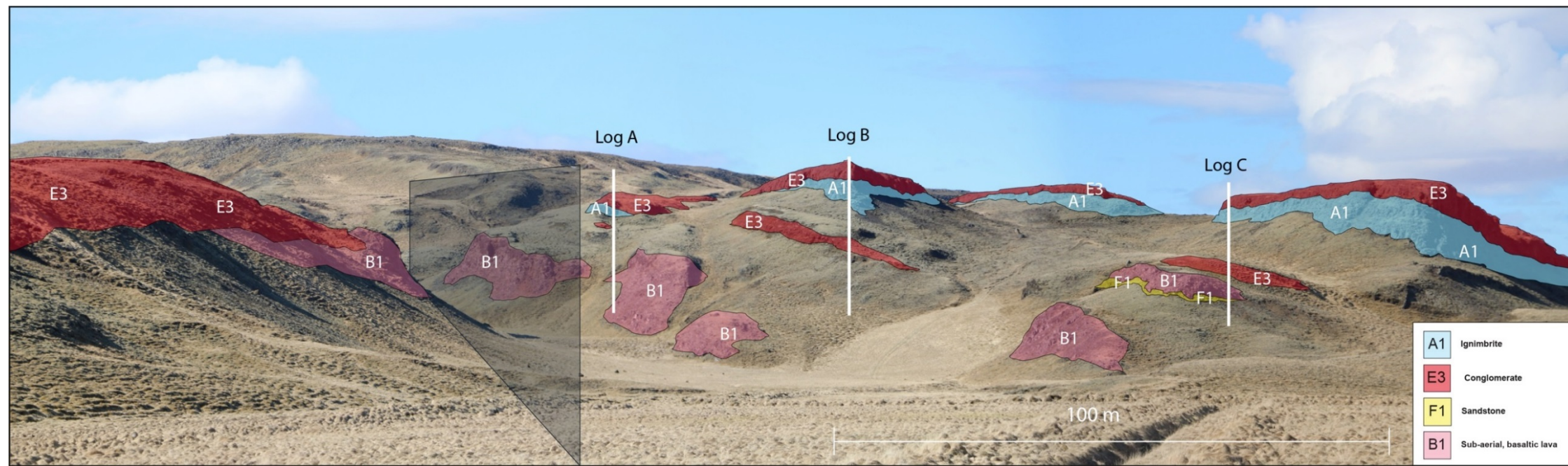


Figure 6-19 Details of panorama 8 Panorama 8 highlights the main relationship between lithofacies B1, E3 and A1. The panorama documents a very different style of volcanism to the rest of the HF

### 6.9.2 Interpretation of panorama 8

Panorama 8 highlights differing volcanic styles as well as active fluvial and tectonic systems. The large unit of B1 at the base of the panorama indicates that the volcanic system was particularly active. The rubbly top demonstrates that the eruption rate was not constant and instead waxed and waned.

As the volcanic system waned, it is highly likely that the fluvial system started to re-establish itself in the lows occupied by the lava. The lack of an entablature within the lava suggests that it had cooled before the fluvial system fully established.

The presence of the small discontinuous unit of B1 overlying F1 suggests that the volcanic system started to wax again, potentially diverting the course of the fluvial system to elsewhere in the HF.

The laterally continuous unit of E3 indicates high energy event(s) and it is likely that this material was preserved within a low in the environment.

Overlying E3 is A1. This represents a change in volcanic style from fissure fed lavas such as B1 to much more explosive, silicic volcanism. This indicates that the source area of this volcanic system could be different. A large explosive eruption generating a Plinian column would have deposited this unit in localised depressions left from previous tectonic and erosive activity.

The section being capped by a unit of E3 indicates that there was further tectonic activity generating the debris flow deposits. These would have again filled lows within the palaeo land surface. As the three bluffs are upstanding areas within today's landscape, it indicates that these are a lot less susceptible to weathering and erosion. It is also likely that late faulting has caused the units to become disconnected.

## 6.10 Conclusions

- Chapter 6 highlights example lithofacies successions within the HF. The examples presented are not an exhaustive list but are meant to highlight complicated interaction between different units.
- Within volcano sedimentary settings, common successions are often not genetically related, for example B1-4, E1-3 and F1. Within the HF these are frequently associated, however they are not genetically related, unlike B1-4 and C1 and C2 lithofacies.

## 7 Stora Laxa case study

### 7.1 Introduction

The focus of this chapter is a case study of the stratigraphy and environments of deposition on the west side of the Stora-Laxa river section (Figure 7-1). On the eastern side of the field area, the Stora-Laxa River flows from the NW to the SE (from the Icelandic Highlands to the Atlantic Ocean). The river exposes a cliff section approximately 5 km in length (Figure 7-1) and up to ~150 m in height. This is the largest continually exposed section in the field area and offers a unique opportunity to understand the stratigraphy and environments of deposition within the HF over a variety of scales.

This section was chosen as a case study to understand the palaeogeographies of the area because of the continuous exposure the section offers. It enables the lateral variability and heterogeneity in the palaeoenvironment to be clearly understood. Other areas in the HF, although fully exposed, do not provide the lateral extent of exposure in this section. This is predominantly due to the underlying structure of the HF at Flúðir.

A geology map of the field area has been provided with an enlarged section of the Stora-Laxa River section, detailing the location and relationship of each of the main panoramas within the chapter (Figure 7-1). The chapter details the main units and palaeoenvironments in each section and their relationships with other sections. This follows a SW to NE trend moving up the river and follows the stratigraphy from oldest to youngest.

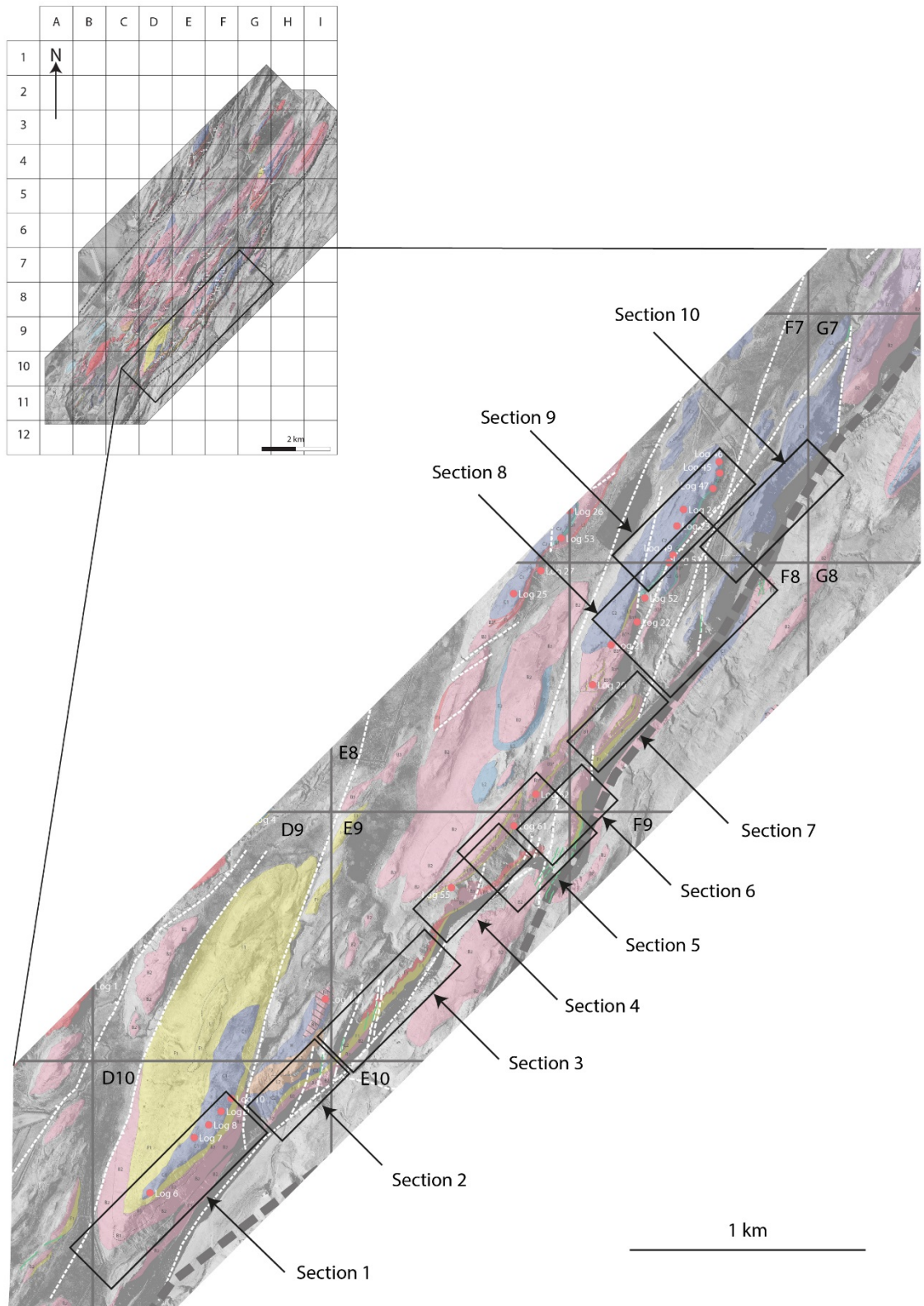


**Figure 7-1** Inset map of the Stora Laxa river section. This highlights the geographical position of each of the figures in the chapter and their relationships.

## 7.2 Field relationships and environments of deposition

### 7.2.1 Stora Laxa section 1

This section is the lowest in the stratigraphy and is most southerly within the Stora Laxa river section (Figure 7-1), it is situated within grid square D10. Figure 7-3 provides an un-interpreted image, followed by an interpreted image of the section.

Section 1 is dominated by two, large sub-aerial lava units. The lowermost lava is a B2 lithofacies lava, which is ~ 20 m thick. It has well developed columnar jointing and a distinctive pink colour. Directly overlying this lava is a thick, ~ 25 m B1 lithofacies lava, with a well-developed rubbly top. The presence of these thick lava units indicates that volcanic activity was waxing and likely dominated the environment at that time. There are numerous possibilities as to why the lavas are so thick in comparison with the rest of the field area. The average thickness of a lava within the field area is ~ 6.7 m, making these lavas some of the thickest individual units. The most probable reason for the thickness is that the lower lava filled a depression within the palaeo land surface, generated by faulting. There is a lack of entablature within the lava indicating that it did not have any contact with water. The lack of water is likely a result of lavas that are relatively proximal (within 1-10 km) altering the course of a pre-existing fluvial system or damming it.

The overlying B1 lithofacies lava has a very well developed rubbly top to it. This is a rubbly pāhoehoe lava, which formed as a result of an increase in effusion rate. This flux in flow overpowers the strength of the upper crust and as a result starts to generate a very broken, rubbly crust that gets carried along on the surface of the flow. At the base of the lava there is a relatively irregular contact with the underlying lava as small pockets of hyaloclastite are present (Figure 7-2). This indicates that there was a hiatus between the two lavas, enough for water to fill depressions in the surface of the lower lava. This could have been a relatively short time. The B1 lava has small well-developed columns at its base, quickly transitioning in to hackly jointing, indicating that whilst it was forming/during cooling, it interacted with water to produce the irregular joint pattern observed.

It is likely that the fluvial and volcanic system were competing for accommodation space at this time.

The rubbly top to the lava has been filled with volcanoclastic sandstone from the overlying F1 unit, indicating that there was a waning of volcanic activity and as a result, the fluvial system fully re-established, depositing sediment within and on top of the rubbly top of the lava as it flowed across. It would likely have eroded lava flows relatively close to produce the volcanoclastic sediments. The waning of volcanic activity in this area allowed the fluvial system to develop unhindered.

The section is capped by a unit of C1 primary hyaloclastite. This highlights that after a significant hiatus the volcanic system became active again. Sub-aerial lava would have interacted with the palaeotopography, filling lows. These lows are often occupied by fluvial systems, resulting in units like C1.

This section highlights the competition between fluvial and volcanic systems for available accommodation space. It appears that this creates a relatively layer-cake stratigraphy, however this is a result of the exposure. In 3D it is highly likely this isn't the case.

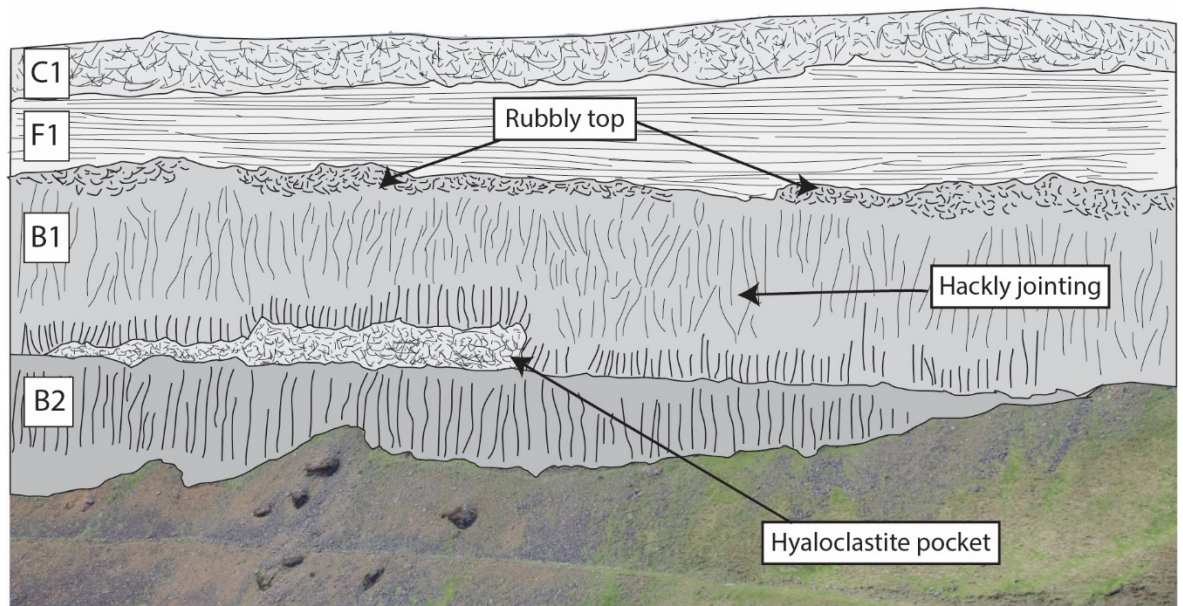


**Figure 7-2** Sketch illustration of the main units within the section and the key features of the B1 lava unit.



Figure 7-3 Panorama of section 1, the most southerly exposed section of the field area in the Stora Laxa River. The section is dominated by two large lava units before transitioning in to a more fluvial dominated system. The section appears to be layer cake, which is most likely a function of exposure and in the third dimension would not be the case

## 7.2.2 Stora Laxa section 2

Section 2 is situated NE of section one, on the west side of the Stora Laxa, predominantly found within grid square D10. Figure 7-4 demonstrates an un-interpreted image, followed by an interpreted image of the section.

The stratigraphy within section 2 is broadly the same as observed within section 1 (Figure 7-3) however as a result of faulting the units are lower within this section (~10-15 m) as they are on the hanging wall of the fault. Evidence of small scale faulting is much more apparent within this section. The apparent displacement between section 1 and 2 is smallest within the C1 unit. This could indicate that faulting was syn-depositional, with a thickening of hyaloclastite across the fault. C1 is a thicker unit in section 2 than in section 1 (Figure 7-3, Figure 7-4).

As in section 1, two sub-aerial lava units at the base dominate the stratigraphy before the development of a fluvial system deposited volcaniclastic sandstones and a waxing of the volcanic system, produced the hyaloclastites. Section 2 is capped by a unit of debris flow conglomerate (E2), unlike in section 1. The debris flow unit has a strong glacial, clast population, with rounded clasts and occasional striae, additionally the unit is characteristically grey. This debris flow conglomerate indicates that the units were deposited in a glacial proximal location. Continual advance and retreat of a glacier, generates a lot of loose material. The environment would have been very wet due to rainfall and fluvial systems, both of which there is abundant evidence for within the field area. Continual rainfall, in combination with steep slopes created by tectonic activity and loose, eroded glacial material would have the potential to generate a debris flow. This debris flow would have filled depressions within the palaeo land surface, as observed in this section. The unit is thickest in the middle and this thins to nothing either side (Figure 7-4), reflecting the palaeotopography.

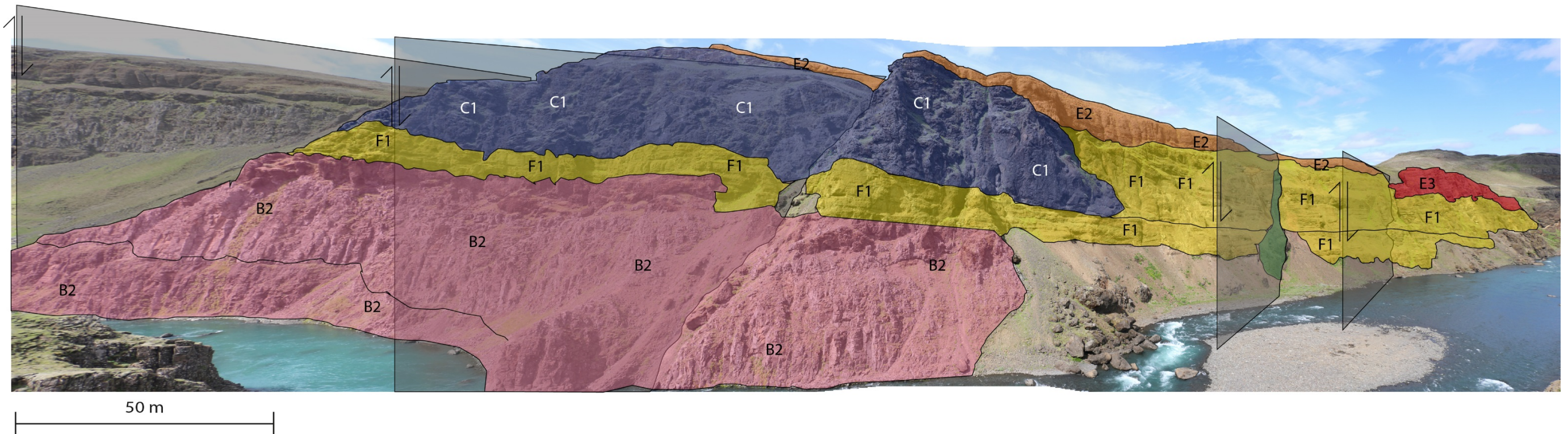
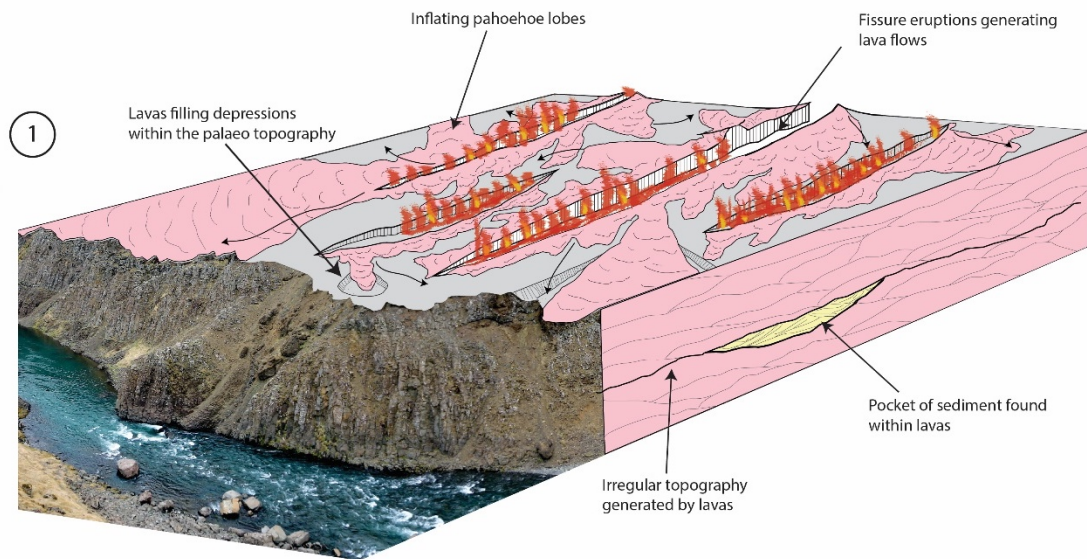


Figure 7-4 Panorama of section 2 which represents a complex interaction of volcanic and sedimentary units. The same stratigraphy as the previous panorama can be seen. They are offset by a large fault. Smaller scale faults affect this section.

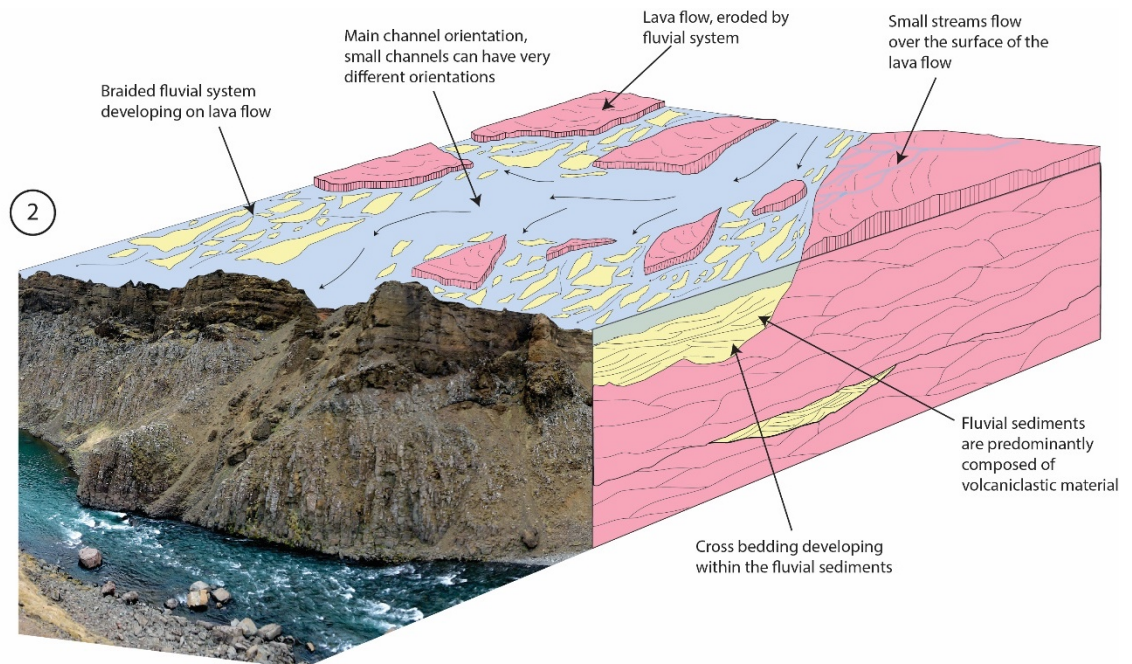
The stratigraphy in this section indicates that the palaeoenvironment was a wet, highly dynamic one with predominantly fluvial and volcanic systems competing for available accommodation space. In addition to lavas generating their own topography and fluvial systems occupying lows, tectonic activity played a dominant role in controlling deposition of these units.

### 7.2.2.1 3D models of depositional setting of section 1 and 2



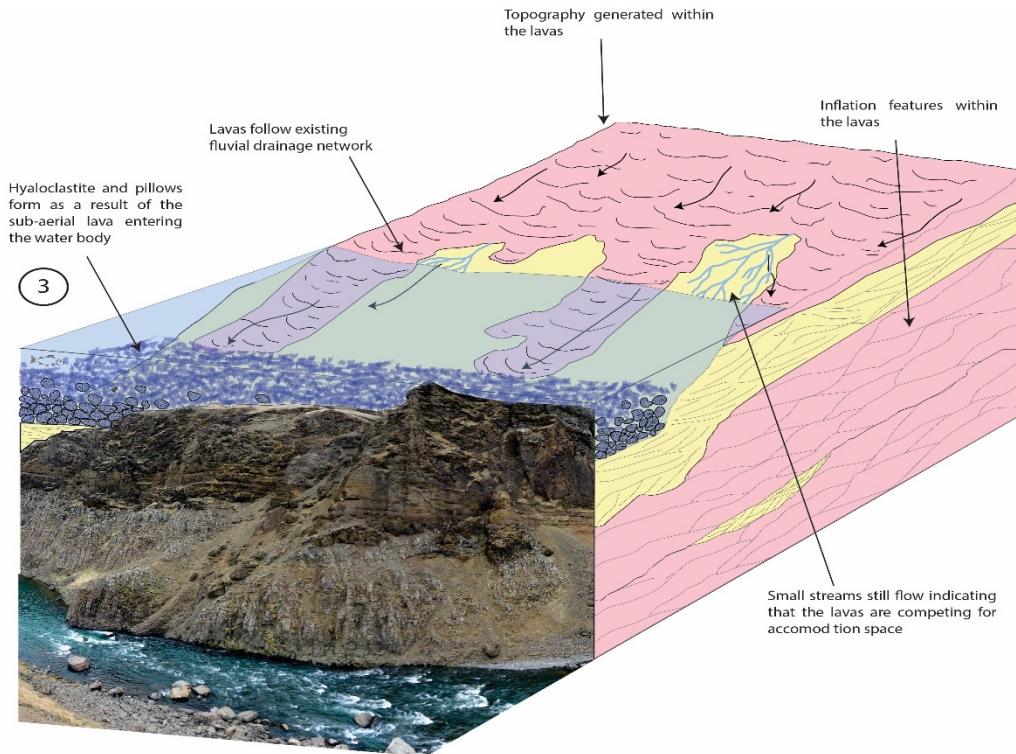
**Figure 7-5 Block diagram of fissure eruptions representing how the lavas in Figure 7-4 may have been extruded. The model uses a photo of the lavas within the Stora Laxa. The diagram is hypothetical and no scale or direction is implied.**

Figure 7-5 is a representation of how the lavas within section 1 and 2 formed. They would have initially been fed via fissure eruptions, no evidence of the fissures are preserved due to later lavas filling the lows within the topography and hiding the fissures. The lavas would have formed as inflated pahoehoe lobes that coalesced, creating sheets. The lavas would have filled any lows within the palaeotopography and in these depressions the lavas may have interacted with small bodies of water, forming hyaloclastite pockets (Figure 7-2). Through inflation of the lavas and the irregularity in the palaeo land surface, a significant amount of topography would have been generated.



**Figure 7-6 Block diagram of the development of a braided fluvial system. This represents how the system developed in Figure 7-4. The model uses a photo of lavas and sedimentary units from the Stora Laxa section. The diagram is hypothetical and no scale or direction is implied**

Figure 7-6 is a representation of the drainage system that developed when there was volcanic quiescence in sections 1 and 2. In volcano-sedimentary settings, it is common for fluvial and volcanic systems to interact and the HF is no different. Whilst volcanic activity was dominant, fluvial drainage networks would have still been active, potentially becoming dammed or diverted as a result of the lavas dominating the environment and as a result not depositing sediment in the area at that time. As the volcanic activity waned this allowed the fluvial system to fully re-establish. The fluvial system would have flowed around highs within the lava surface, eroding the lavas as it did so. Within the section there is evidence of large cross bedding within the sandstones, these would most likely have formed as a result of a braided system with channels flowing in a varied pattern.



**Figure 7-7 Block diagram of sub-aerial lavas entering a water body This generates pillows and primary hyaloclastite. This represents how the section in Figure 7-4 developed. The model is hypothetical and no scale or direction is implied**

Figure 7-7 is a representation of a water body that developed within the palaeo land surface. As there is evidence of syn-depositional faulting occurring in the area, it is likely that this caused a small graben or half graben in the landscape. With continued fluvial input and a lack of volcanic activity, this would have formed a standing body of water. As volcanism increased in activity, this resulted in an interaction of the two competing systems. Its highly likely that the lavas followed the drainage network of the fluvial system. As the sub-aerial lavas entered the standing body of water formed within the graben, this would have generated small pillow lavas and primary hyaloclastite. As lavas continued to flow, this would have generated more hyaloclastite, resulting in reworking of hyaloclastite as the slope became unstable and collapsed.

### 7.2.3 Stora Laxa section 3

Section 3 is situated NE of section two, on the west side of the Stora Laxa, predominantly found within grid square E9. Figure 7-9 provides an un-interpreted image, followed by an interpreted image of the section.

Volcaniclastic sedimentary units dominate section 3, although the stratigraphy featured in the previous two sections is found towards the left of the image, as this section has been photographed from a different angle to the previous two. Faults follow a roughly NE-SW trend and they appear to cut the entire stratigraphy in this section of the Stora Laxa (Figure 7-9).

This section demonstrates why the section needs to be observed in 3D to understand the palaeogeography of the section. The stratigraphy found within sections 1 and 2 (Figure 7-3, Figure 7-4) is also found within this section. As in the previous section, it is clear that a unit of C1 hyaloclastite has formed as a result of sub-aerial lava entering and interacting with water. This was most likely within a confined river valley or small water body. Overlying this unit of C1 hyaloclastite is an on-lapping unit of F1 sandstones which are very similar in nature to the underlying sedimentary units. Moving away laterally to the right, the two units of F1 are in contact and no C1 hyaloclastite is present (Figure 7-9). This indicates that when the sub-aerial lava entered the water, volcanic activity was potentially waning, resulting in the fluvial system not being completely suppressed by lava. The fluvial system would have continued to deposit sediment in to the water body, resulting in an onlapping relationship with the underlying C1 unit (Figure 7-8).

It is highly likely that the small body of water in which the hyaloclastites were deposited, formed at the edge of a large fluvial system. It is likely the fluvial system would have been a large sandur plain, type deposit (Figure 7-6). The area would have been glacially proximal (most likely proglacial) with an abundance of eroded sediment (volcaniclastic). In this type of setting it is possible for kettle holes to form and fill with water (Bennett and Glasser, 2013).

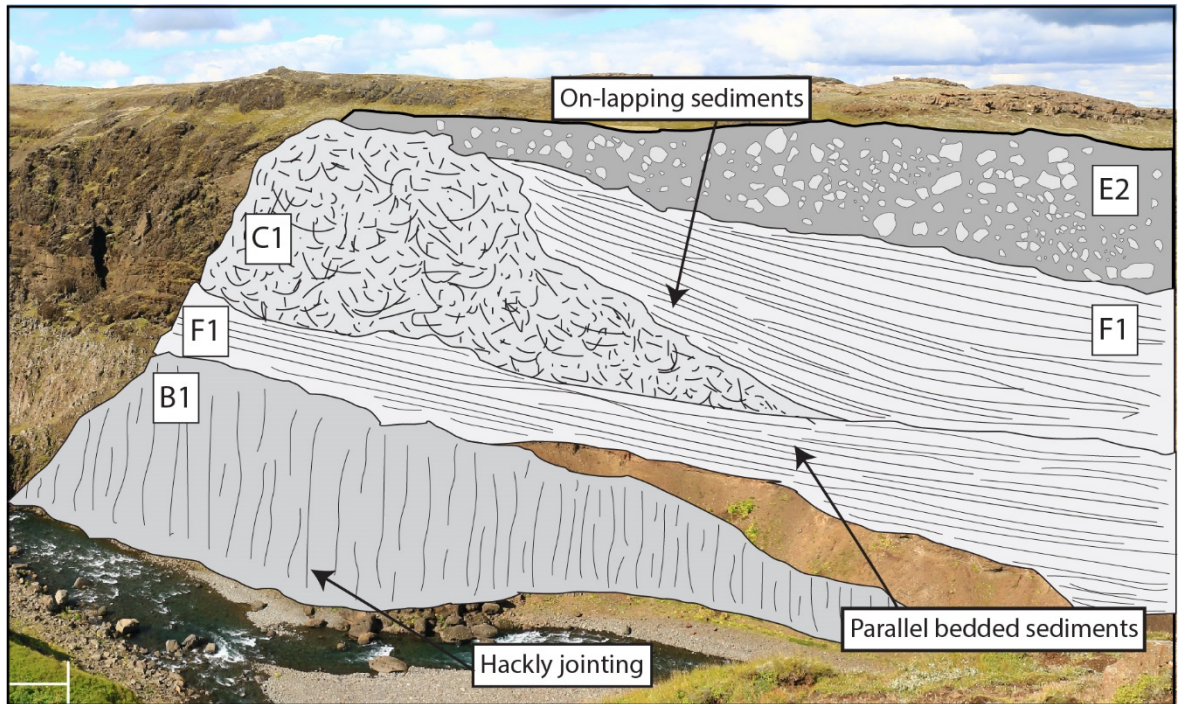


**Figure 7-8** Sketch illustration of section 3 Details of F1 sediment units, with F1 sandstones on-lapping C1 unit.

Overlying the F1 volcanoclastic unit is a unit of E2 debris flow conglomerates. E2 conglomerates have a strong glacial component to the clast population. This unit appears to fill a depression within the palaeotopography and onlaps the unit of C1 hyaloclastite and F1 sandstones (Figure 7-8). This debris flow conglomerate most likely formed as the result of a sudden, high energy jökulhlaup event (glacial outburst flood) draining the sandur plain and incorporating loose regolith. These events typically occur in proglacial environments and are often composed of boulder beds, normal to inversely graded cobble beds and deformed bedding (Maizels, 1997). They are a common occurrence in Iceland.

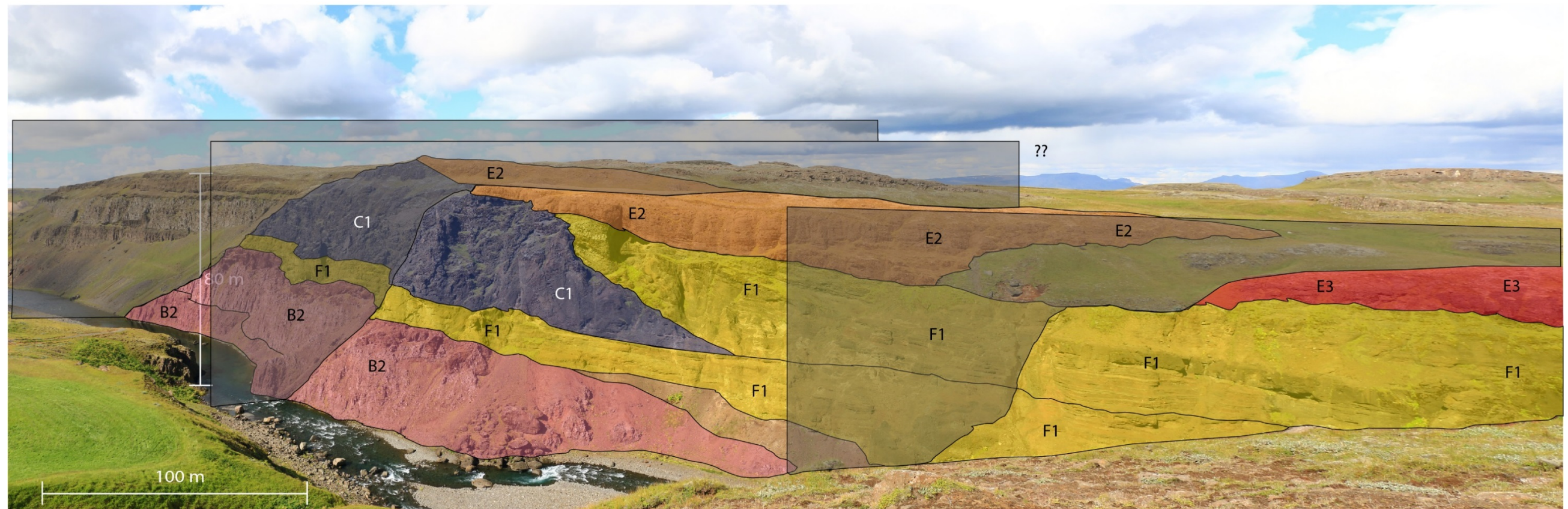


Figure 7-9 Panorama of section 3 Looking south towards the previous two panoramas (Figure 7-3, Figure 7-4). Moving north west up the river, the geology starts to become dominated by sedimentary systems, evidenced in this panorama. Fault is prevalent in the area, although it is difficult to determine how far the faults extend in to the interior of the field area

The sharp change in lithofacies from F1 to E2 (Figure 7-8, Figure 7-9) indicates that E2 was potentially deposited suddenly in a jökulhlaup event. This could have been triggered by geothermal heating, a sub-glacial eruptive event, breaching of an ice or moraine dam (Maizels, 1997). Discharge rates of jökulhlaups can suddenly become very high. A modern example in Baffin Island had a discharge of  $200\text{m}^3\text{ s}^{-1}$ , compared to the standard discharge rate of  $20\text{ m}^3\text{ s}^{-1}$  (Church, 1972), highlighting a 10x increase in flow. For large jökulhlaup events in Iceland it has been estimated that there is a 3-5 order of magnitude increase over the normal discharge rate of sandur plains (Maizels, 1997). This highlights how much energy these events have and indicates how such large clasts can become entrained within the deposits.

Section 3 represents that of a proglacial, braided fluvial system within a sandur plain setting that developed during quiescence in volcanic activity. This was a very dynamic environment, which would have been subjected to large jökulhlaup events, periodically depositing coarse conglomerate units. Evidence of the volcanic system having interacted with the sandur plain is evident in the form of hyaloclastite, although this interaction is small, suggesting that the main volcanic activity was distal or not very active, at the time.

## 7.2.4 Stora Laxa section 4

Section 4 is situated NE of section 3 on the west side of the Stora Laxa, found within grid square E9 (Figure 7-1). Figure 7-10 presents an un-interpreted panorama followed by an interpreted image of the section.

The lower half of section 4 is dominated by sedimentary units, whilst the upper half is dominated by volcanic units. The contrast between these general lithologies indicates that two very different systems have competed for accommodation space. In contrast to the previous sections (Figure 7-3, Figure 7-4, Figure 7-9) evidence of faulting is not very apparent, with only one small fault on the lower right of the section, observed (Figure 7-10).

The F1 sandstones within section 4 have a thickness of ~40 m, indicating that a large fluvial system was active and dominant for an extended period. The unit is predominantly composed of sand grade, basaltic volcanoclastic sedimentary units, with large scale (1 m) cross bedding present. The entire cliff on the left of the section (Figure 7-10) is composed of these sedimentary units. The bottom, centre-right of the section is dominated by F1 sandstones also, although these are part of a different system to those on the left of the section.

Between the two units of F1 in the bottom of the section is a large, angular unconformity which separates the whole section (Figure 7-10). This unconformity most likely resulted due to active faulting in the HF, evidenced most obviously within section 2 and 3 (Figure 7-4, Figure 7-9). Faulting would have displaced the F1 sandstones and created a low in which the fluvial system would have then occupied. This would have resulted in sediments being deposited within the new valley system (Figure 7-10).

As the volcanic system started to wax in activity, this produced lavas which would have followed the pre-existing drainage network created by the fluvial system. Lavas tend to follow existing low-lying areas within the landscape such as fluvial systems (Schofield and Jolley, 2013), there is evidence of this occurring within section 4 (Figure 7-11). Where these topographic lows are found, they typically have the thickest accumulations of sediment, but are also found to have the largest volume of lava units (Schofield and Jolley, 2013). As the lavas entered and

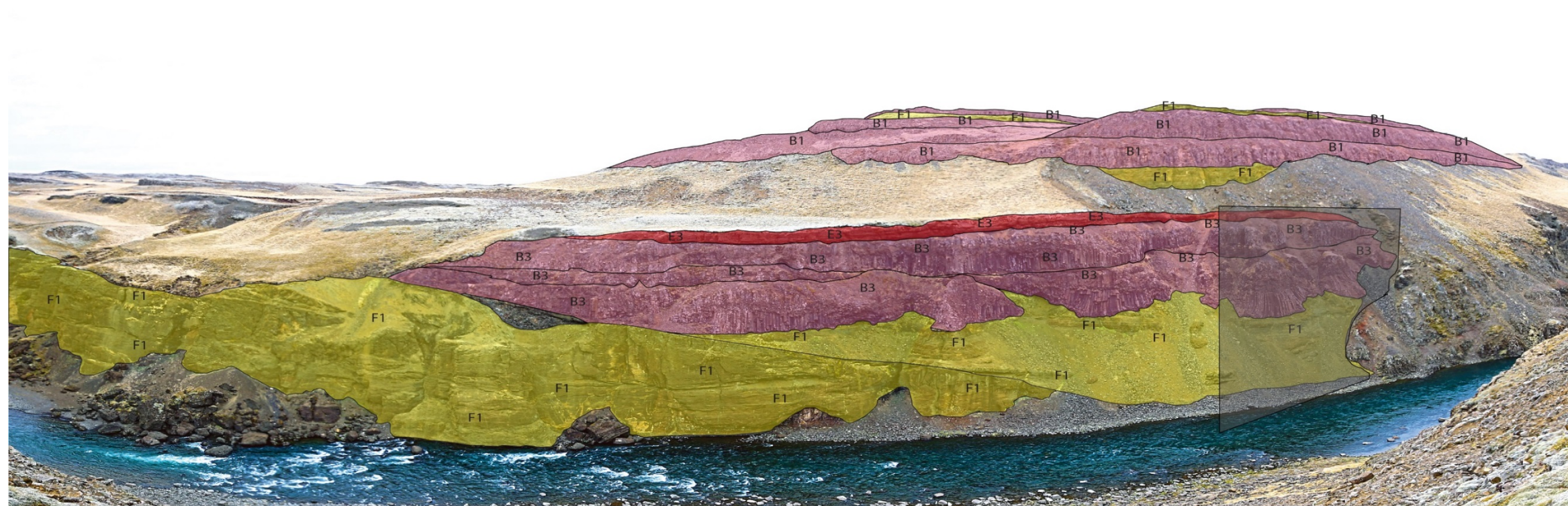


Figure 7-10 Panorama of section 4 This panorama represents two very dominant systems. The lower half of the stratigraphy is dominated by sandstones and the upper half is dominated by volcanic units. This competition for accommodation space is a recurring theme in the HF.

followed the existing drainage network, they filled lows in the system. Evidence for this is seen within the B3 lavas as the columns curve at their base where they have come in to contact with the cold country rock (Figure 7-11). As the lavas followed the drainage network, the fluvial system was still active and competing for the accommodation space. This is obvious from the entablature within each lava lobe seen within the section (Figure 7-11). The entablature would have formed as a result of water ingress from the active fluvial system, in to the upper surface of the cooling lava (Long and Wood, 1986; DeGraf and Aydin, 1987; DeGraf et al, 1989; Lyle and Preston, 1998). As each lobe has a colonnade and entablature it indicates that there was a small hiatus in time between each flow, otherwise they would have coalesced in to one large unit, whereas individual units can be observed (Figure 7-10, Figure 7-11). As there is a lack of sediment observed at this point in the stratigraphy of section 4, it is assumed that the fluvial system became inundated by the lavas as volcanism increased. This may have diverted the course of the fluvial system or dammed it, preventing sediments from being deposited.

Overlying the B3 lavas, is a capping unit of E3 debris flow conglomerate (Figure 7-10). This most likely formed as the result of regolith dominated slopes becoming unstable due to increased pore pressures, debris flows would have been generated (Innes, 1983). The debris flow would have travelled down the steep slopes of the palaeo valley causing it to be filled.

Above the unit of debris flow conglomerate is no exposure and then ~10 m of F1 sandstones (Figure 7-10). These F1 sandstones are very similar in nature to the underlying thick units of F1. This indicates that there was a significant period of quiescence in volcanism, allowing the fluvial system to re-establish in the valley it once occupied. The unit of E3 beneath these sedimentary units could be an indicator of the previously dammed (diverted?) fluvial system bursting the lava dam and re-establishing. The system was not as prevalent as before as there is a smaller thickness of sediment and capping these are thick B1 lavas.

The B3 lavas which are near the top of the section would have followed the already established fluvial system, dominating it. The lavas are thicker in this unit, indicating that volcanism was much more active and the effusion rates higher. These B1 lavas also have a rubbly top present which could have formed as the result of increased effusion rates.

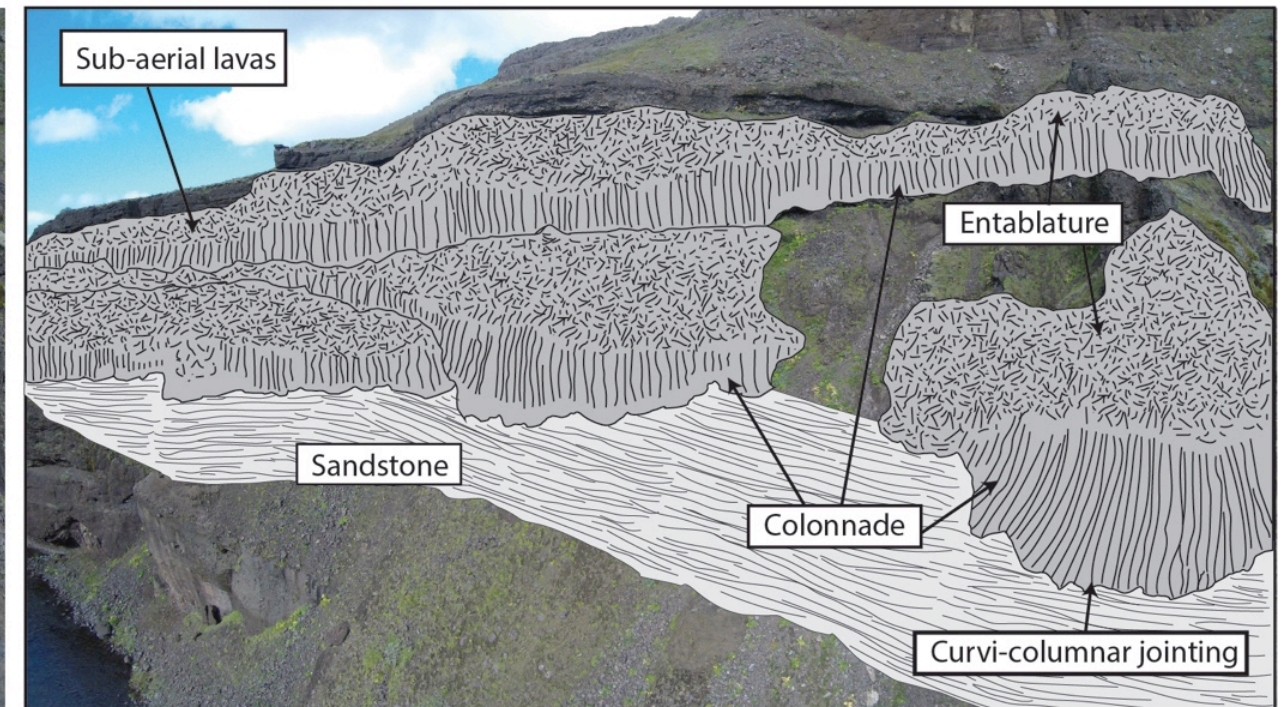
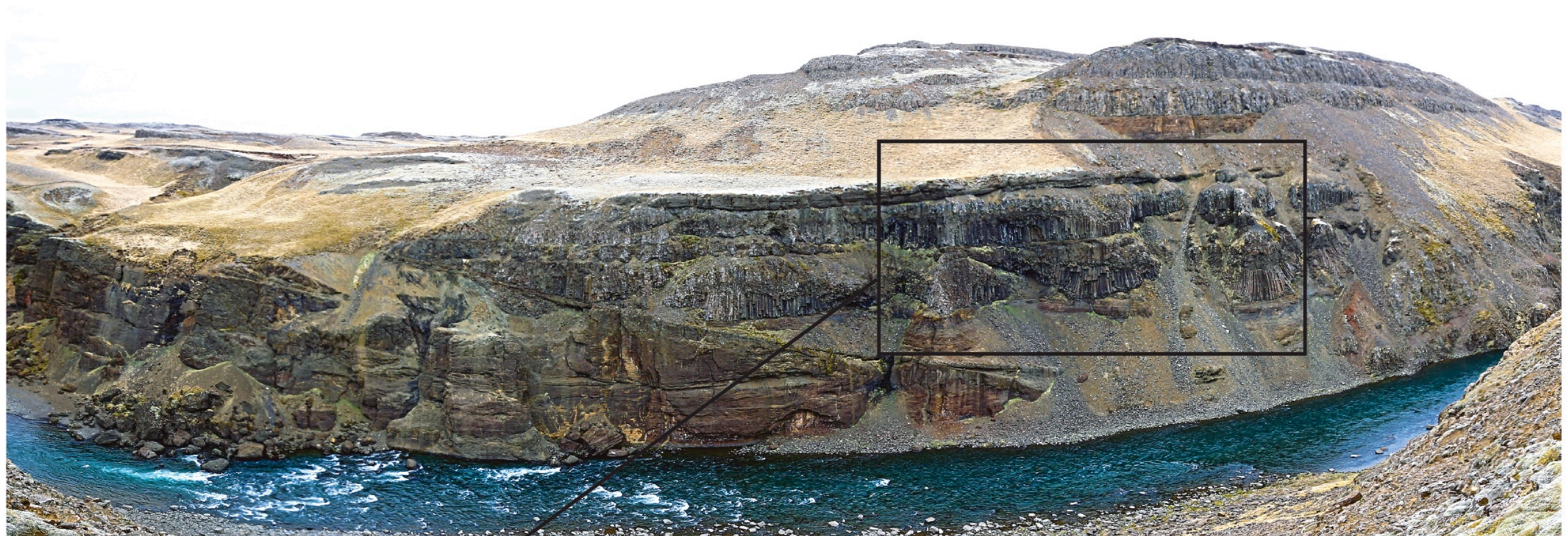


Figure 7-11 Details of sub-aerial lavas filling pre-existing topography. The lavas tend to have a lobate nature to them, they would have flowed towards the viewer. These lavas demonstrate curvicolumnar jointing in the colonnade of the lava, indicating that they filled some sort of low within the topography. They have very well developed entablatures indicating that they were inundated with water during cooling. This is most likely the result of the fluvial system trying to re-establish and compete for available accommodation space

At the top of section 4 there is a small unit of F1 sandstones, indicating the re-establishment of a fluvial system as volcanism wanes.

The cyclical nature of sediment units forming and being capped by volcanic units is a recurring theme in the Hreppar Formation and in similar types of lava dominated settings. It is highly likely that these fluvial sediments which form in large sandur plains would not be well preserved unless capped by an impermeable unit that is resistant to erosion. In this case the units are lavas which preserve the underlying sediments and hence give a potential bias in the rock record in comparison with other areas that do not have lavas preserving sediments.

Section 4 represents a palaeoenvironment which was initially dominated by a braided fluvial system before volcanism waxed and dominated the environment. This a repeating pattern of interbasaltic sand bodies developing. Section 4 creates a false sense of these systems being layer cake, but in reality they are very complex 3D systems.

#### 7.2.4.1 3D models of depositional setting of section 4

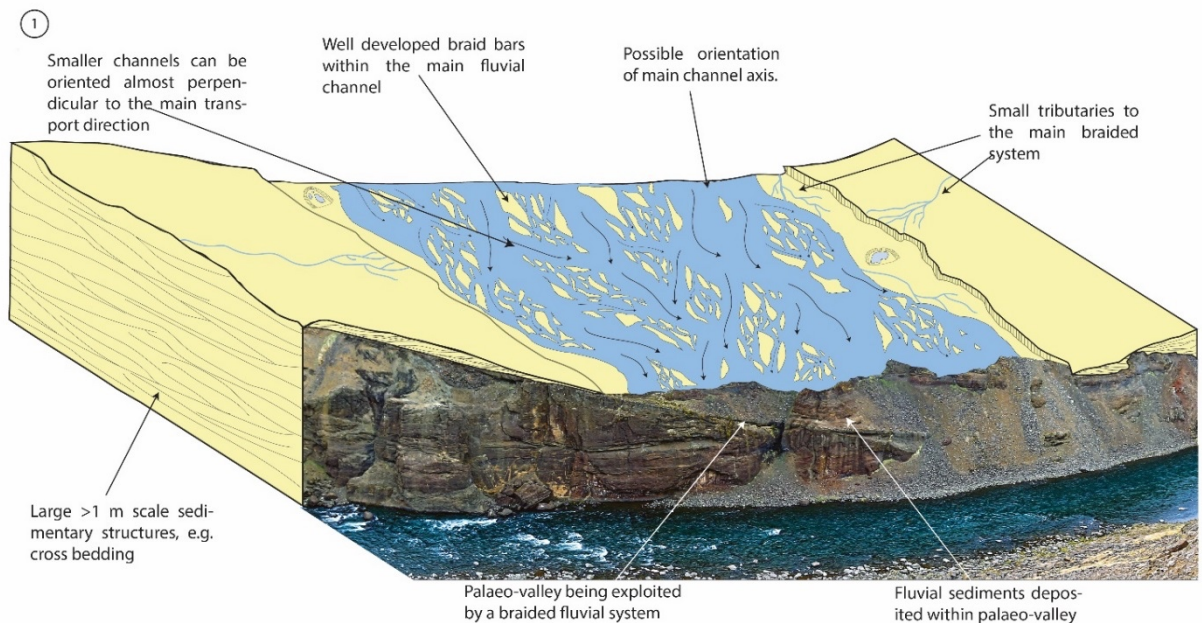


**Figure 7-12 Block diagram of a braided fluvial system** This represents how the sediments within the unconformity in Figure 7-10 were deposited. The model is hypothetical and no scale or direction is implied

Figure 7-12 is a representation of how the F1 unit above the angular unconformity in section 4 developed. The valley in which the fluvial system developed formed

most likely due to faulting within the area. At the time of faulting, volcanic activity was relatively quiescent, allowing the fluvial system to take advantage of the new low, formed as a result of faulting. It is highly likely that the braided fluvial system developed in a proglacial environment. In this setting there would have been an abundance of loose, eroded sediment from the glacier. The sediment would have been non cohesive, and as a result the river would have demonstrated low sinuosity and strong braiding (Bluck, 1974). As with modern braided fluvial systems, the lack of cohesion in the sediments allows the channels and bars to be very mobile. These would have changed from season to season based upon the fluctuation of discharge from snow melt and glaciers.

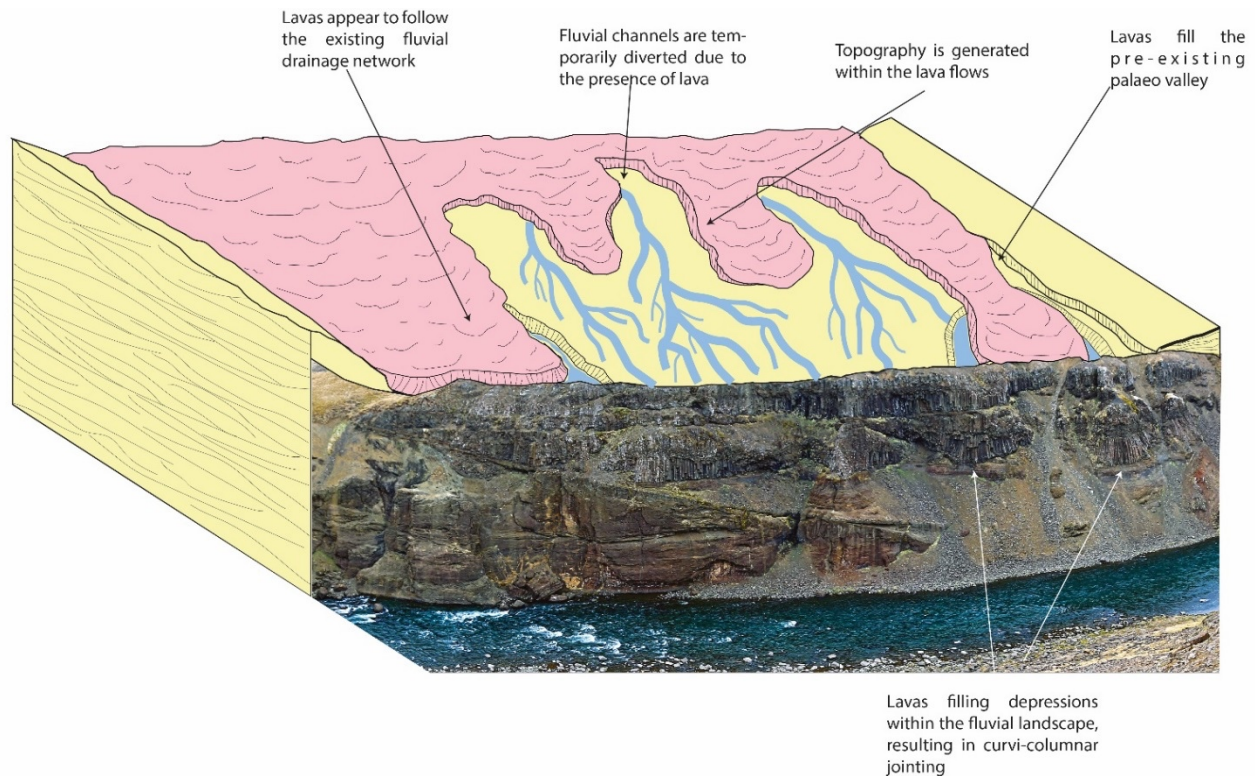


**Figure 7-13 Block diagram of sub-aerial lavas following a pre-existing drainage network. This represents the development of the lavas within Figure 7-10. The model is hypothetical and no scale or direction is implied**

Figure 7-13 represents how sub-aerial lavas followed the pre-existing drainage network and filled lows within the environment. The distribution of lava flows is typically controlled by the pre-existing surface topography, in this case, created by a combination of tectonic activity and surface drainage. The fluvial system would have been diverted or dammed as a result of the lavas infiltrating the system. Small fluvial channels would have still flowed before the lavas dominated

the environment. The fluvial system would have been contemporaneous with volcanism. This would have resulted in the presence of small sedimentary horizons between some of the lava lobes (Figure 7-10). Additionally this continued interaction with water from the fluvial system would have generated the large entablatures observed within each of the individual lava flows (Figure 7-11). No entablatures are observed in the lavas of the upper units in section 4 (Figure 7-10), this could be a result of the lavas having a higher effusion rate and therefore overwhelming the small fluvial system. This would result in no streams interacting with the slowly cooling lavas.

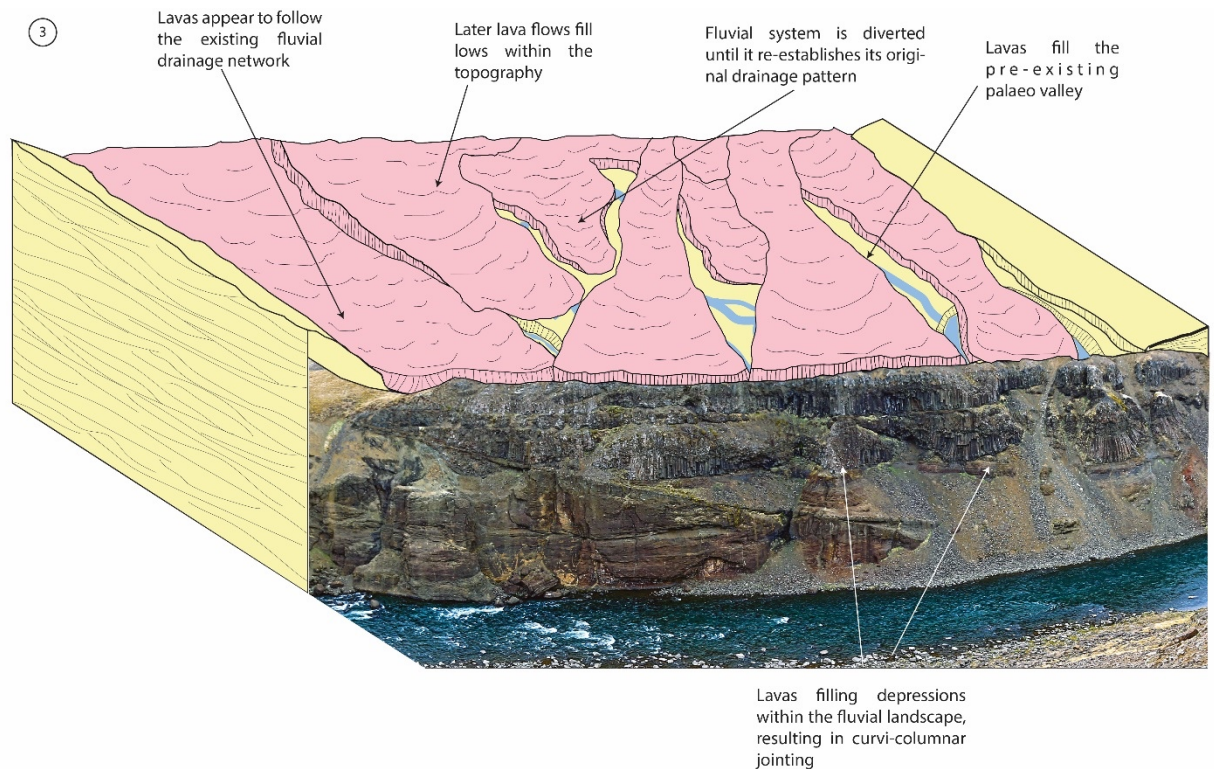


**Figure 7-14 Block diagram of continued extrusion of lava. This represents how the lavas filled lows within the palaeotopography (Figure 7-10) during waxing of volcanism in the area. The model is hypothetical and no scale or direction is implied**

The continued extrusion of lava in to the existing palaeovalley is highlighted in Figure 7-14. As volcanic activity increased, this would have led to the domination of the local environment, in this case, this fluvial system and valley in which it occupied. The lavas would have exploited topographic lows within the environment, resulting in curvi-columnar jointing observed within the basal colonnade of the lavas (Figure 7-11) as it cooled against valley sides. With continued extrusion of lavas, the lava flow field would have a much greater control on the development of topography within the area. As the lavas dominated the

palaeovalley the drainage system may have been diverted around the lavas or became dammed.

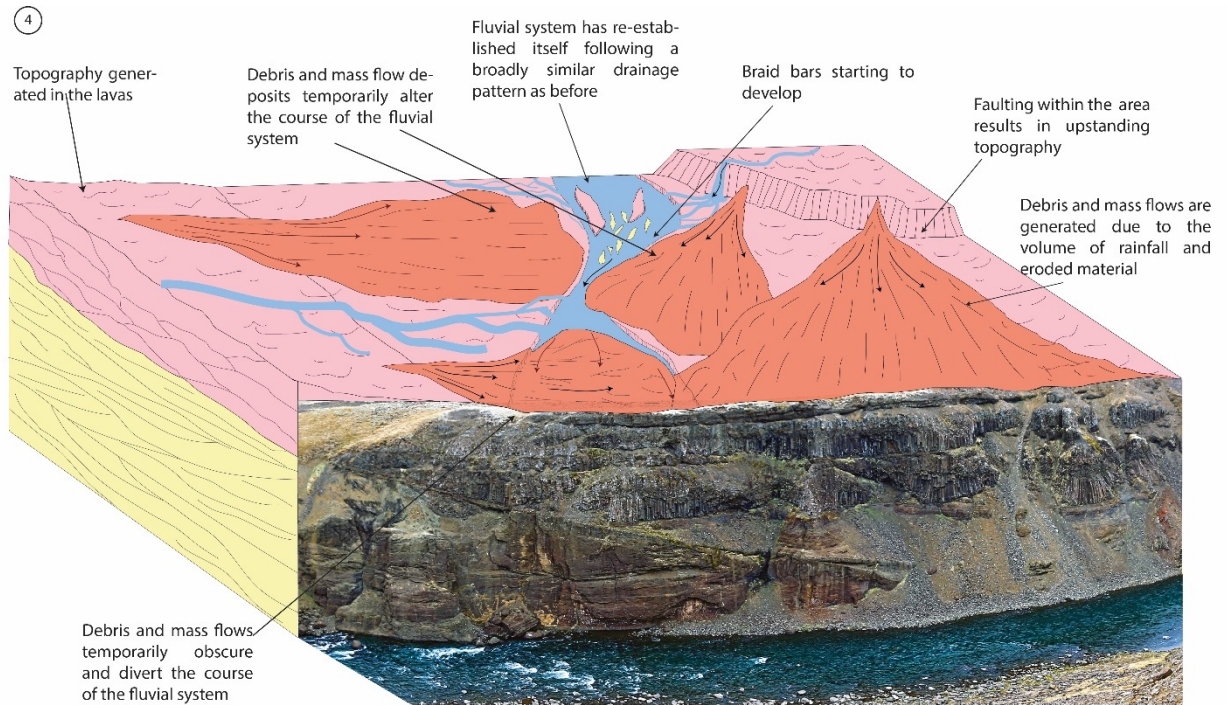


**Figure 7-15** Block diagram of the development of debris flow deposits This represents how the volcanically derived sediments in Figure 7-10 formed. The model is hypothetical and no scale or direction is implied.

The re-establishment of the fluvial system would have been controlled by the topography of the just formed, lava field. The drainage system would have preferentially re-established within topographic lows between lava flows initially, before occupying the wide topographic low, it previously occupied. It could potentially have re-established within a very short time period following the formation of the lavas (Ebinghaus et al, 2014). Re-occupation of fluvial systems is a common occurrence within basaltic systems (Ebinghaus et al, 2014). A thick unit of debris flow conglomerates overlies the basaltic lavas, indicating that they were deposited as the result of a high energy event. This could potentially have been the result of the original drainage system bursting the lava dam in which it was contained. The debris flow unit could also have formed as the result of an increase in relief in the area, and therefore energy (Williamson and Bell, 2012). This could have generated a large debris flow. Situated in a wet, tectonically active environment, there would likely have been numerous debris flows occur during

this time. The fluvial system would then have reoccupied the former fluvial pathway.

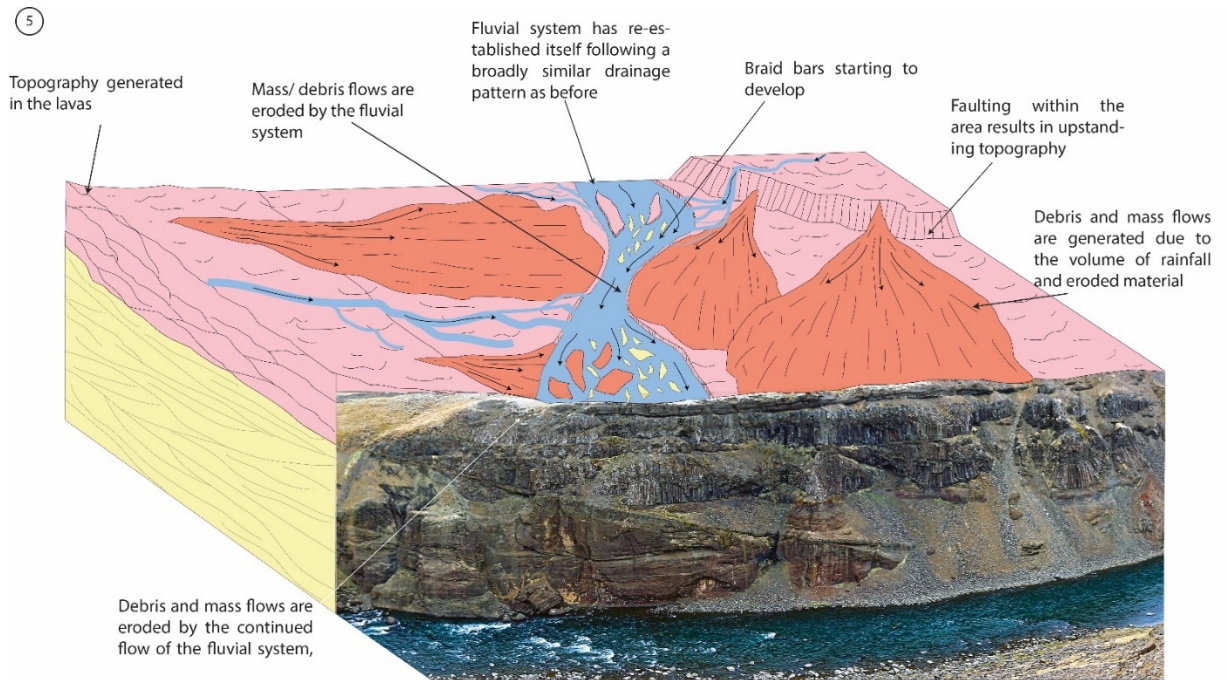


**Figure 7-16 Block diagram of the re-establishment of a fluvial system. This is an interpretation of how the fluvial system re-established itself within Figure 7-10. The model is hypothetical and no scale or direction is implied.**

Figure 7-16 highlights how the newly formed debris flows would likely become eroded by the growing fluvial system. The drainage system would have tried to fully re-establish itself in the pathway it previously occupied. This would have resulted in the erosion of the debris flow units and the deposition of more fluvial sediments.

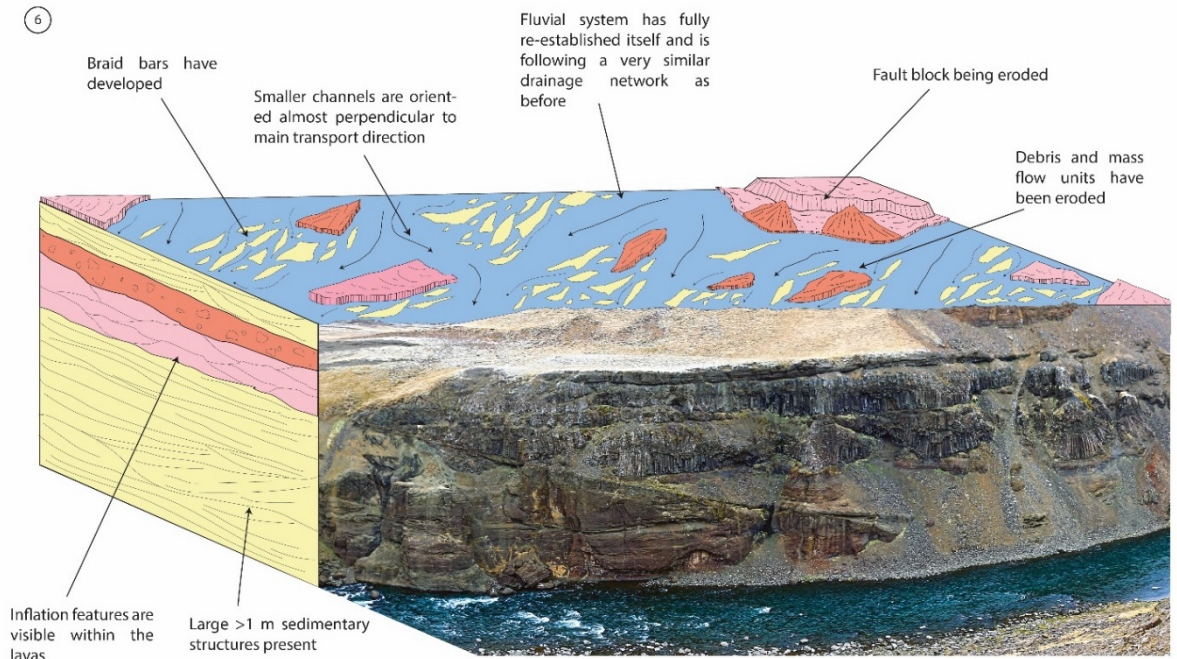


**Figure 7-17 Block diagram of a braided fluvial system with remnants of volcanic and sedimentary units. This represents how the system could of fully re-established itself after volcanic activity waned. The model is hypothetical and no scale or direction is implied.**

Figure 7-17 demonstrates how the fluvial system could have fully re-established after eroding debris flow conglomerates. This would have happened during volcanic quiescence, allowing the system to develop unhindered. The deposition of the underlying stratigraphy would have filled the previous valley, resulting in a less confined drainage network than previously existed. This would have allowed the fluvial system to develop a large braid plain, as seen in Figure 7-17. This braided fluvial system would have deposited similar sediments as before. This entire system may appear to be layer-cake in nature, however in reality the system is much more complex. This complexity arises from the interaction of fluvial and volcanic systems occupying the same depositional setting and competing for the same available accommodation space.

### 7.2.5 Stora Laxa section 5

Section 5 is situated NE of section 4 on the west side of the Stora Laxa, found predominantly within grid square E9 (Figure 7-1) and overlaps sections 3 and 5. Figure 7-19 presents an un-interpreted panorama followed by an interpreted image of the section.

The whole of section 5 is dominated by repeating units of sub-aerial lava and fluvial sediment (Figure 7-19). Abundant faulting is observed within the lower half of section 5, whereas this is not observed in the upper half. The stratigraphy observed within section 5 is very similar to that of section 4 (Figure 7-10) as they occupied very similar environments.

The lowest B3 lavas observed within the section are seen within section 4. These have been downthrown as a result of the fault observed within section 4 (Figure 7-10). These lavas would have followed the low areas within the palaeotopography which would have been the pre-existing drainage network that developed as a result of the braided fluvial system.

Overlying the B3 lavas of the lowest half of the section is a relatively thick unit (~10-20 m) of F1, volcanoclastic sandstones and conglomerates. This unit separates the lava flows of the lower and upper halves of section 5. This is a common occurrence within lava flow dominated areas as demonstrated by Vosgerau et al, 2015 in the Faroe Islands. This unit would have formed in a very similar setting to that of section 4, in a braided river plain (Figure 7-17). The fluvial system would have re-established itself during a volcanic hiatus and allowed for the erosion of the underlying B3 lava units as well as sub-aerial lavas in the local vicinity. This would have provided the material for the generation of these volcanoclastic sediments.

Stratigraphically above the F1 sedimentary units, lies a relatively thin (~5-10 m) capping unit of E3, debris flow conglomerate. This is associated with continued volcanic quiescence and a potential increase in relief (generated by faulting) combined with heavy rainfall, run-off and regolith. As regolith dominated slopes became unstable due to increased pore pressures, debris flows would have been generated (Innes, 1983). These debris flows could have travelled for km's and

would have filled lows within the palaeo-land surface, and in this case they would have come to rest in the valley in which the fluvial system resided.

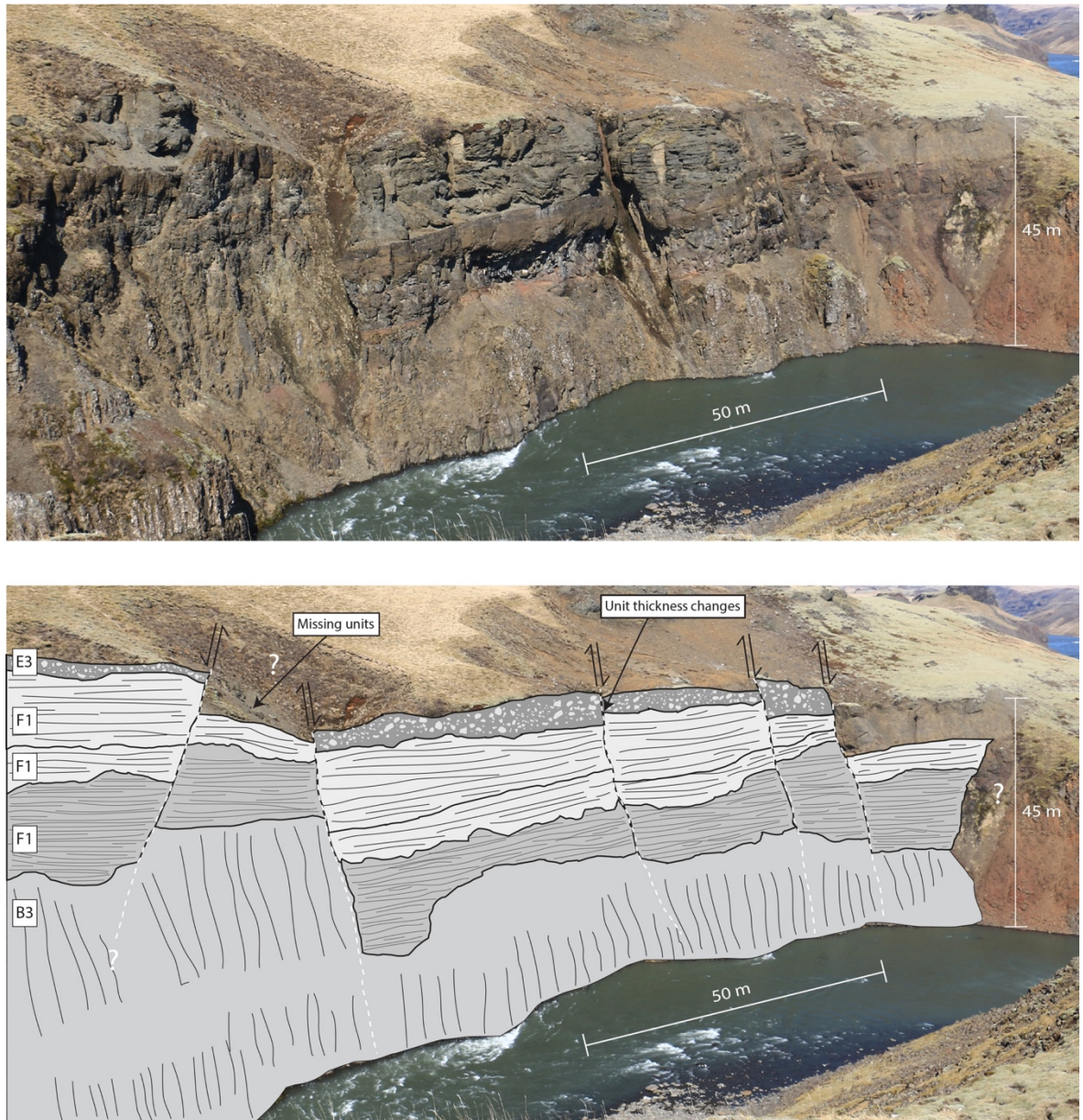


**Figure 7-18** Faulting within section 5. Evidence of small movement on the faults, this was evidently syn-depositional as there are significant thickness changes of units across the faults.

As in section 4, the unit overlying the E3 debris flow conglomerates is F1 fluvial sandstones (Figure 7-19). These are part of the same volcanoclastic sandstone observed in section 4 (Figure 7-10). This was evidently a large, laterally extensive, braided fluvial system, much like the sandur plains on the south coast of modern day Iceland (Figure 9-12). This would have developed during volcanic quiescence, however the time period in which these developed is smaller in comparison to the

F1 sandstones found at the bottom of section 4 (Figure 7-10) based upon their relative thicknesses.

Directly in contact with the F1 sandstones are two large units of B1, sub-aerial lavas. Individual lava flows are ~15-20 m thick and are laterally continuous. They represent an increase in volcanism in the area at that time. These lavas are some of the thickest in the field area and indicate that volcanism was very active during this time. The lavas have well developed clinker tops, indicating that they potentially formed as a result of much higher effusion rates at the source. The lavas do not have any well-defined entablature, indicating that they didn't interact with any large volumes of water. This is in contrast to the lavas seen within section 4 (Figure 7-10), where the lavas have well developed entablatures that formed as a result of interaction with the fluvial system. The contrast between these differing lavas indicates that the upper lavas in section 5 did not interact with the fluvial system which preceded them. This lack of interaction is most likely a result of the fluvial system being diverted by lava flows elsewhere. The lavas are also more laterally consistent in their thickness, indicating that the surface upon which they were erupted was relatively flat. This combined, with the fluvial sandstones underneath indicates there was a transition from a large braided plain to lavas occupying the same space.

Overlying the thick B1 lavas, there is a small inter-lava interval of F1, fluvial volcaniclastic sandstones which is ~ 5 m thick (Figure 7-19). These sandstones represent a pause in volcanism and the re-establishment of a small fluvial system.

The small fluvial unit is overlain by B1 lavas, indicating that the hiatus in volcanism was relatively short lived. The volcanic system would have used the same pathways as the fluvial system and would have dominated this environment.

As previously discussed, faulting plays a large role within section 5 (Figure 7-19). The faults demonstrate oblique movement (dip-slip and strike-slip) with relatively small displacement (~5 m) on each fault. These faults are part of the underlying structural control on the HF (Figure 7-1). The faults appear to only affect the lower half of the stratigraphy observed within section 5 (Figure 7-19), indicating that there were two main phases of deposition. The lower half of the section was significantly affected by syn-depositional faulting as there is obvious thickness

changes across faults (Figure 7-18). The upper stratigraphy is unaffected in this part of the HF, suggesting these units were deposited at a later, less tectonically active time.

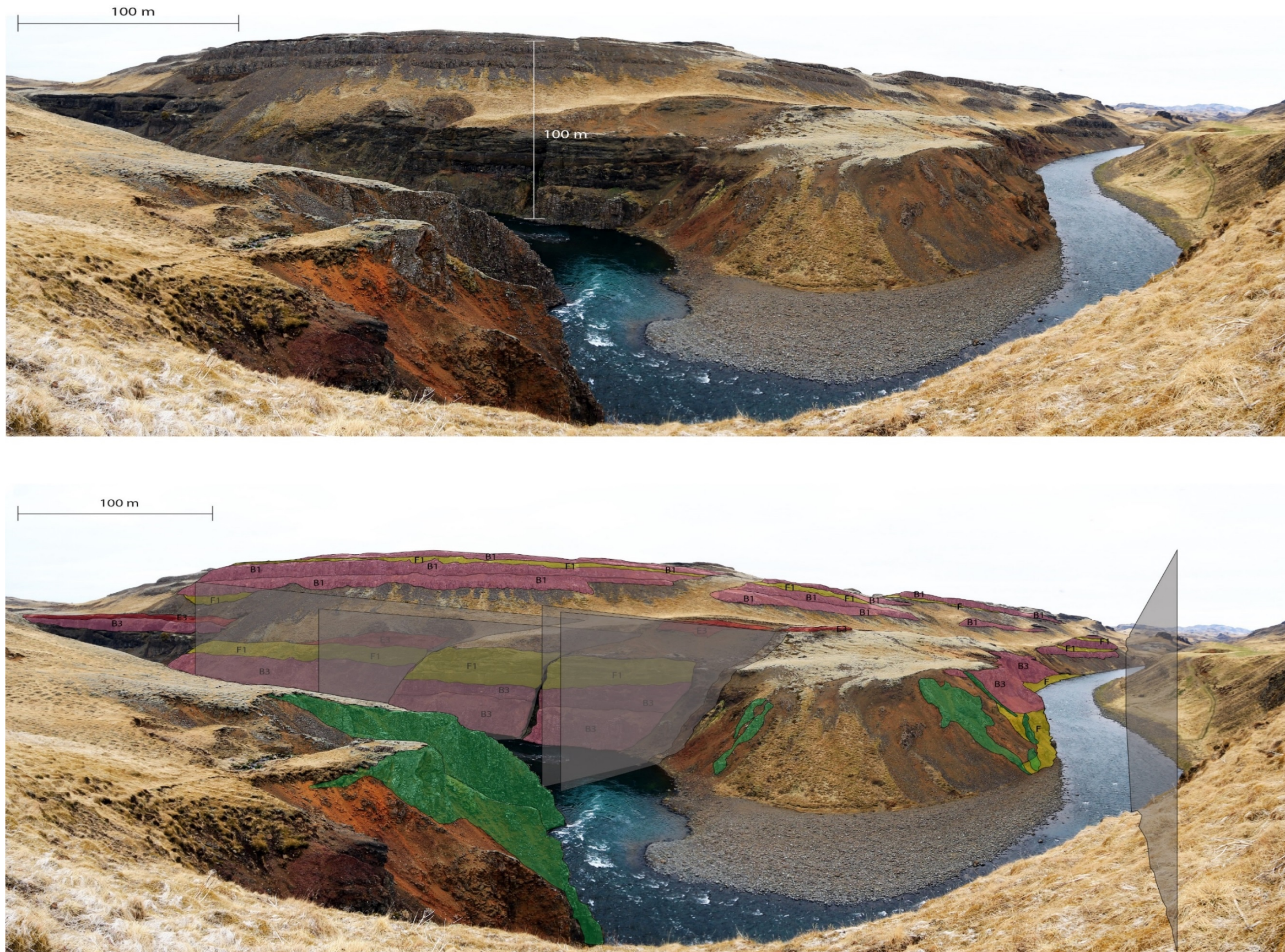


Figure 7-19 Panorama of section 5 This panorama highlights the nature of the faulting within the area and indicates that there was at least two stages of fault propagation. Taking advantage of the fault system is a series of dykes, which apparently compartmentalise the system

The meander bend within the Stora Laxa river in section 5 (Figure 7-19) is significant as this appears to be a concentrated area of fault development. Where there is obvious faulting, basaltic dykes appear to utilise this weakness within the stratigraphy. These dykes are common on the entire river section, and where there is no direct evidence of faulting, the presence of dykes suggests that there could be a fault present. The dykes are typically <1 m in width and demonstrate a similar trend to that of the faults of NE-SW. Dykes found outside the Stora Laxa river section, tend to demonstrate a similar trend.

The section records dramatic changes in environment. The bottom half of section 5 is dominated by long lived systems, where there was little change in the environment of deposition. However, when there was change, this was dramatic and would have become prolonged. This is in contrast with the upper half of the section which is dominated by rapid switches in environment. The fluvial and volcanic systems actively competed for accommodation space, with no one system dominating the environment for long periods (Figure 7-19).

## 7.2.6 Stora Laxa section 6

Section 6 is situated NE of section 5 on the west side of the Stora Laxa river. The section is found within grid square E9 and F8 (Figure 7-1). It overlaps section 5. Figure 7-20 presents an un-interpreted image of the section, followed by an interpretation of the section.

The section can be split in to two main halves. The lower half of the stratigraphy of section 6 is dominated by fluvial sandstones, whereas the top half is dominated by repeating units of fluvial sandstones and sub-aerial basaltic lavas. The upper half stratigraphy is predominantly the same as observed within sections 4 and 5 (Figure 7-10, Figure 7-19) whereas the bottom is completely different.

The unit found at the base of the section is a thick (~30-40 m) unit of F1 fluvial sandstones. This is one of the thickest units of F1 found within the field area. The section is observed at the bend in the Stora Laxa, within section 5 (Figure 7-19). The faulting separates the lower half of section 5 and 6 and the geology on the east side of the Stora Laxa at this locality is very different. This faulting indicates that the unit has undergone a different history, depositing primarily volcanoclastic sediments. The unit is bounded on its southern margin by dykes and the B3 lavas of section 5 (Figure 7-19, Figure 7-20). The presence of dykes and a sharp boundary with the lavas indicates that this is a faulted contact. It is highly likely that the B3 lavas formed and were then faulted. This faulting led to a large, low lying depression in which a fluvial system developed and deposited sediment. This would account for the sharp vertical contact with the lavas. The faulted lavas would also have acted as an area of upstanding topography which the fluvial system would have flowed around, actively eroding it. This highlights the complex topography generated by faulting and lava flows, where there was active deposition occurring alongside active erosion.

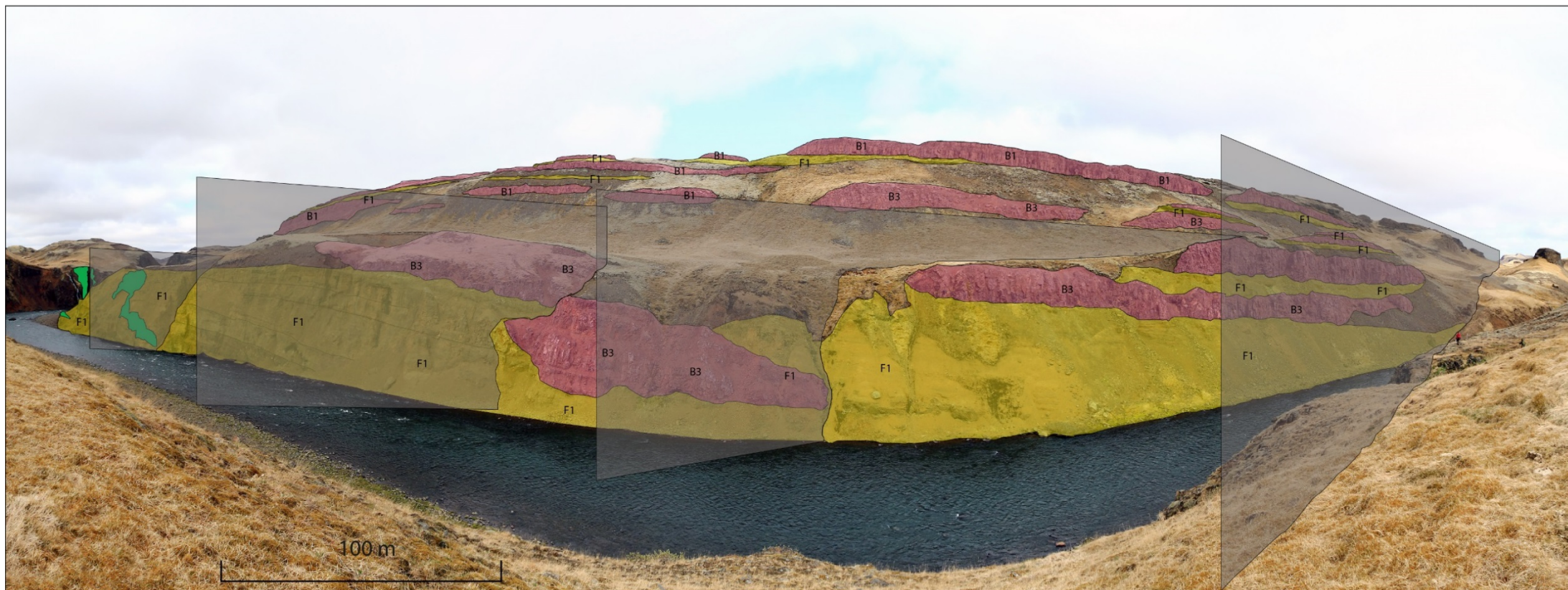


Figure 7-20 Panorama of section 6. This panorama represents the competition between fluvial and volcanic systems for available accommodation space. Notice the differences in faulting, with one set of faults cutting the entire stratigraphy, whereas the other one only cuts the lower stratigraphy

A small unit of B3 lavas overlies the large F1 fluvial sediment unit (Figure 7-20). The unit is laterally discontinuous due to later faulting. The unit represents an increase in volcanic activity within or proximal to the HF. The unit would have followed the drainage network generated by the fluvial system (Schofield and Jolley, 2013) and interacted with it. The fluvial system would have quickly become dominated by the lavas, causing the system to temporarily alter its course or become dammed. If it were not for the faulting observed in section 6 (Figure 7-20) it is likely that the B3 lava would demonstrate lateral continuity. This could indicate that the valley in which the sediments were deposited was relatively wide (~500 m) or the angle of view is from a longitudinal perspective of the valley. It is likely that it is the former, as the sedimentary structures within the sandstones indicate that palaeoflow was towards the reader (SE) (Figure 7-20).

The upper half of section 6 is composed of the stratigraphy observed within the upper halves of section 4 and 5 (Figure 7-10, Figure 7-19). This stratigraphy, composed of repeating units of F1 sandstones and B1/B3 lavas is laterally continuous over ~2-3 km. This is a large system where the underlying stratigraphy along these three sections is very different. (Figure 7-10, Figure 7-19, Figure 7-20). The difference indicates that the upper stratigraphy was deposited later in time, after the small basins (generated by the faulting within the area) had been filled with volcanic and sedimentary units. This would have generated a relatively flat plain upon which a large fluvial system formed during quiescence in volcanic activity. Waxing of volcanic activity led to the eruption of lavas on this large braided, fluvial plain. The upper stratigraphy of sections 4,5 and 6 indicates that this was a repeating process with the fluvial and volcanic systems competing on short time scales for available accommodation space. This would have rapidly developed the stratigraphy and would preferentially preserve the braided fluvial sediments in the rock record. Otherwise if the lavas were not enclosed by sub-aerial lavas, which are much more resistant to weathering, they would most likely not be as well preserved. The continual fight between these systems would have generated a complex palaeo land surface. Within section 6, there is evidence of large faults which cut the entire stratigraphy. These are much later than the ones lower within the stratigraphy (Figure 7-20) and these potentially re-use the pre-existing faults.

### 7.2.7 Stora Laxa section 7

Section 7 is situated NE of section 6 on the west side of the Stora Laxa river (Figure 7-1). The section is found within grid square F8. Figure 7-21 presents an uninterpreted image of the section, which is followed by an interpretation of the section.

Section 7 is dominated by the stratigraphy observed within the upper sections of 4, 5 and 6 (Figure 7-10, Figure 7-19, Figure 7-20). It is primarily composed of repeating units of F1 fluvial sandstones and B1 lavas. This repetition represents competition for accommodation space, within a wide braid plain. Unlike in the other sections, this stratigraphy is also found on the banks of the Stora Laxa river (Figure 7-21) as opposed to higher up in the cliff section. In the background of section 7, the stratigraphy is almost identical to that of the upper sections of 4, 5 and 6 (Figure 7-10, Figure 7-19, Figure 7-20).

This repetition in stratigraphy is most likely the result of rotational landslides, that have caused the upper stratigraphy to slip down to the Stora Laxa, therefore covering the in-situ geology from view. There are numerous examples of these rotational landslides within the HF, indicating it was/is a common feature of the area. These are a modern geological feature of the HF. This example is a ~150 m wide block, that has slipped from the top of the section 7 (Figure 7-21, Figure 7-22). These rotational landslides are a common feature of volcano-sedimentary systems. One of the most famous examples in the UK is the Quiraing in the Isle of Skye (Ballantyne, 1982).

The sequence of lavas at the top of the stratigraphy are much more numerous and thicker, than lower down in the stratigraphy (Figure 7-21). These igneous units are much stronger and less susceptible to weathering than the sedimentary units which they overlie. This has led to the breakdown of the underlying sedimentary units and the rotational landslide of the upper stratigraphy of section 7. This rotational landslide is most likely the result of a reduction in rock mass strength due to dilation or over-steepening or potentially the result of a build-up of hydrostatic pressure in cracks. Alternatively, this could be caused by a sudden event, such as an earthquake (Ballantyne, 1991). This rotational landslide in the HF likely resulted from a combination of these factors.

Evidence of large faults with the same orientation as the dykes in section 5 is present in the form of continuous, straight valleys up to 2 km in length (Figure 7-21). These are assumed to be part of the underlying tectonic structure of the HF.

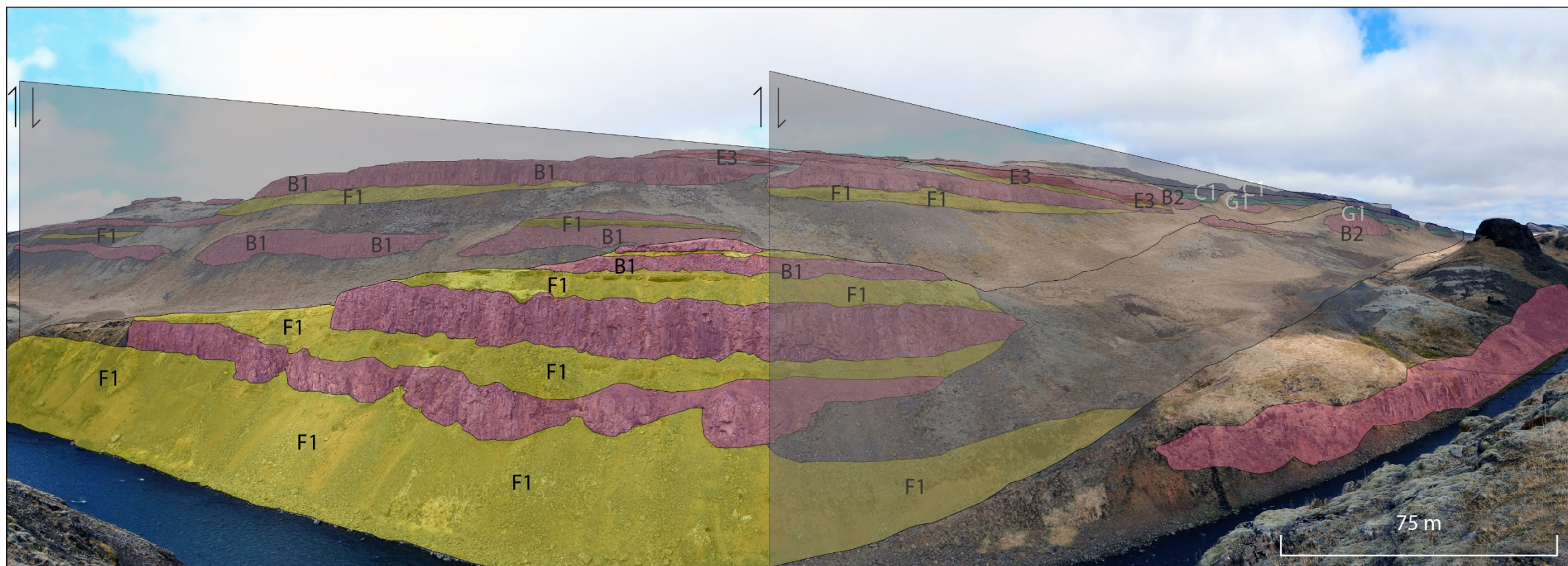
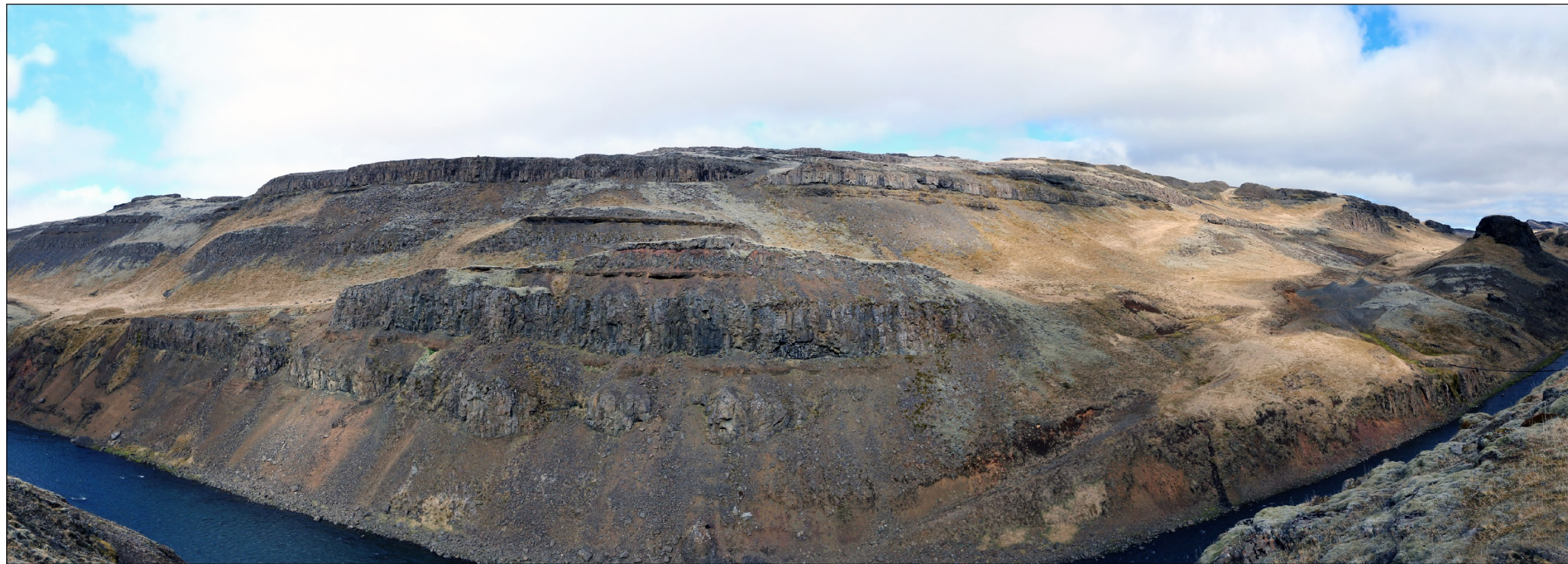
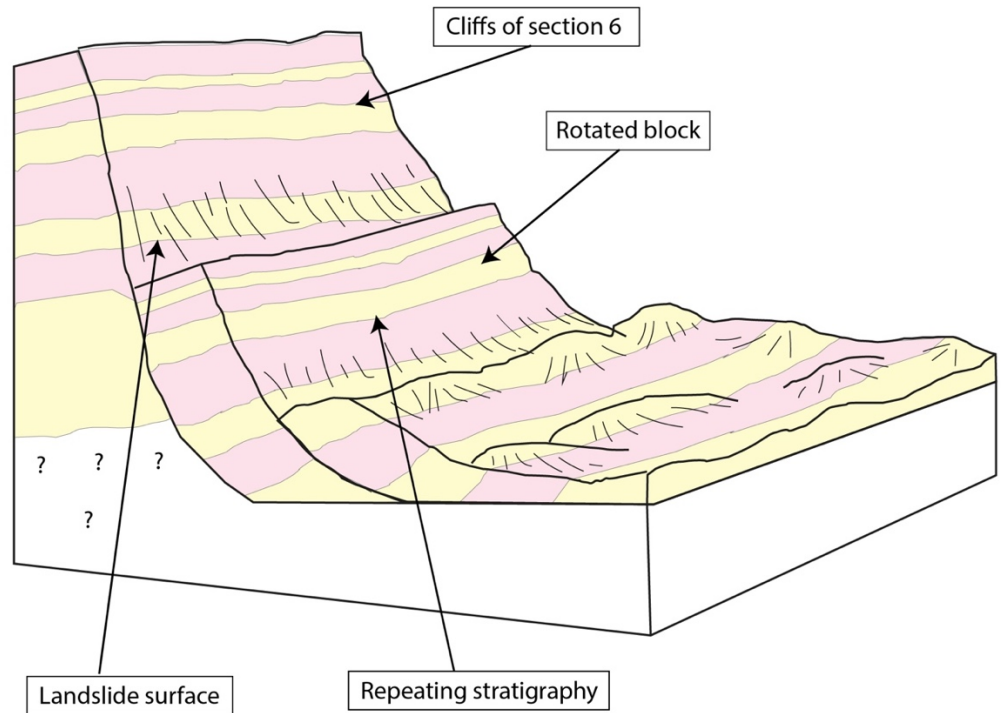
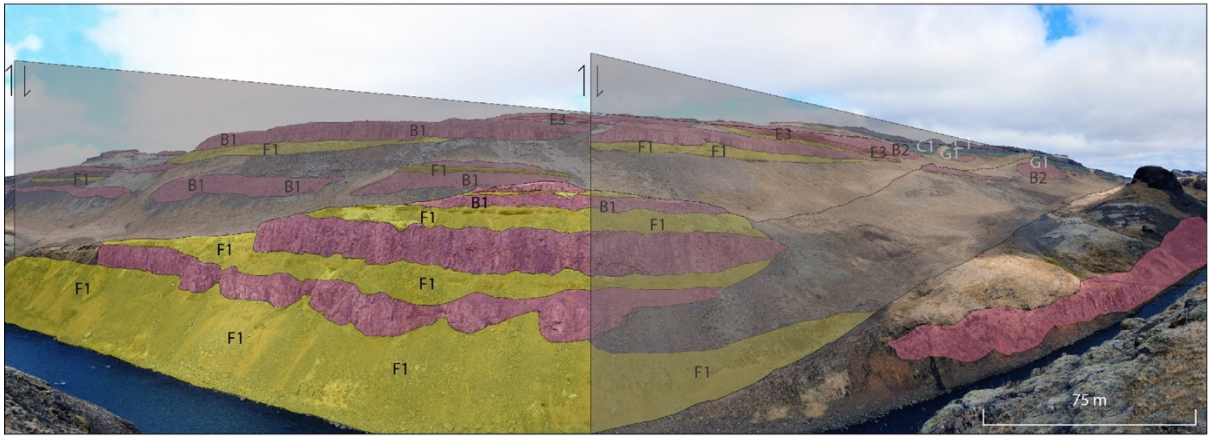


Figure 7-21 Panorama of section 7 The repeating nature of volcanic and sedimentary units is typical of these type settings. Faults cut the entire stratigraphy, indicating that they are more recent, or take utilise old fault systems (?)



**Figure 7-22 Rotational landslide.**

Rotational landslides are a common feature of the Hreppar Formation and volcano-sedimentary sequences in general.

.

.

## 7.2.8 Stora Laxa section 8

Section 8 is situated NE of section 7 on the west side of the Stora Laxa river (Figure 7-1). The section is found within grid squares F7 and F8. Figure 7-23 demonstrates an un-interpreted image of the section, which is followed by an interpretation of the section.

Section 8 focusses on the lower half of the stratigraphy and section 9 focusses on the upper stratigraphy (Figure 7-23, Figure 7-24) of this section of the Stora Laxa. Section 8 represents a transition from sedimentary units in to volcanic dominated units.

At the base of the section is a thick (~15-20 m) unit of E3 debris flow conglomerates. The E3 conglomerates were deposited as the result of a sudden high energy event. Before the event, there would have been a combination of factors that led to this unit forming, including: an increase in rainfall, where the ground likely became saturated; an abundance of regolith; and steep sided slopes. The trigger event was likely a sudden increase in pore pressures (Innes, 1983). The unit is laterally discontinuous, indicating that it filled a depression within the palaeo land surface. The unit would have formed during volcanic quiescence.

The E3 debris flow conglomerate is overlain by sub-aerial lava (Figure 7-23). The unit has not been given a lithofacies code, due to inaccessibility of the unit, however it is clearly a sub-aerial lava. The unit is laterally discontinuous, and has a very irregular thickness. This could be the result of exposure or this may reflect the palaeo land surface upon which the unit was extruded. It is highly likely that the morphology created by the debris flow conglomerates, was highly irregular. The unit indicates that volcanism was waning in the area of the HF.

To the left of the section, there is continuous exposure of the stratigraphy, unlike the centre left (Figure 7-23). Overlying the sub-aerial lava is a smaller unit of E3 debris flow conglomerate. This indicates that there has been a brief hiatus in volcanic activity and abundant rainfall. This indicates that the environment was saturated with water, there was an abundance of loose, eroded material and active faulting.

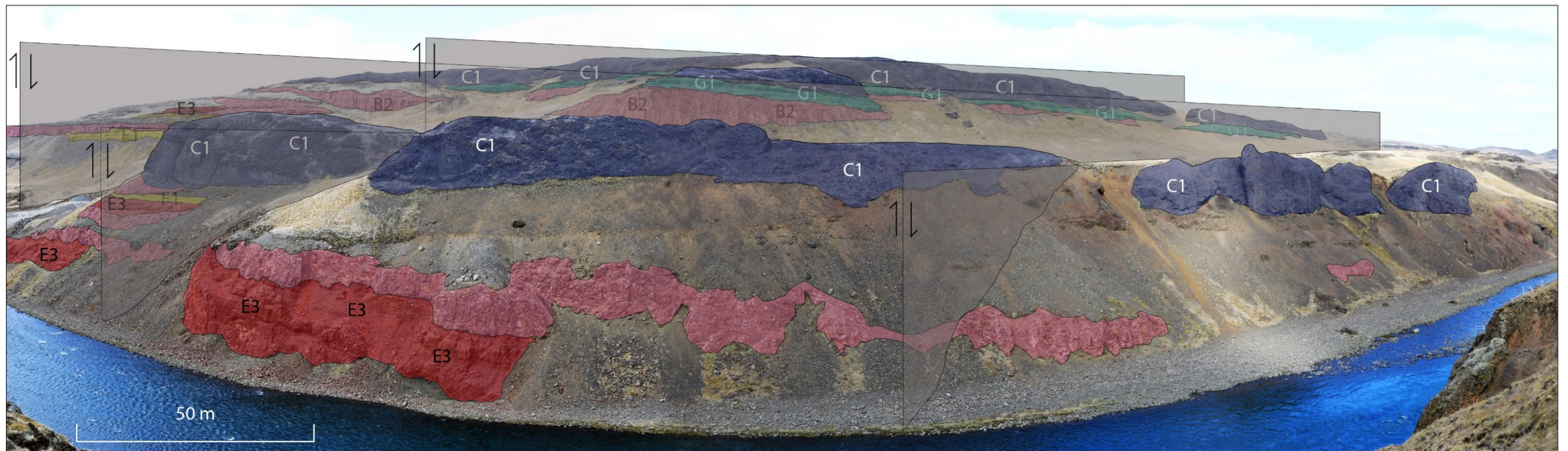
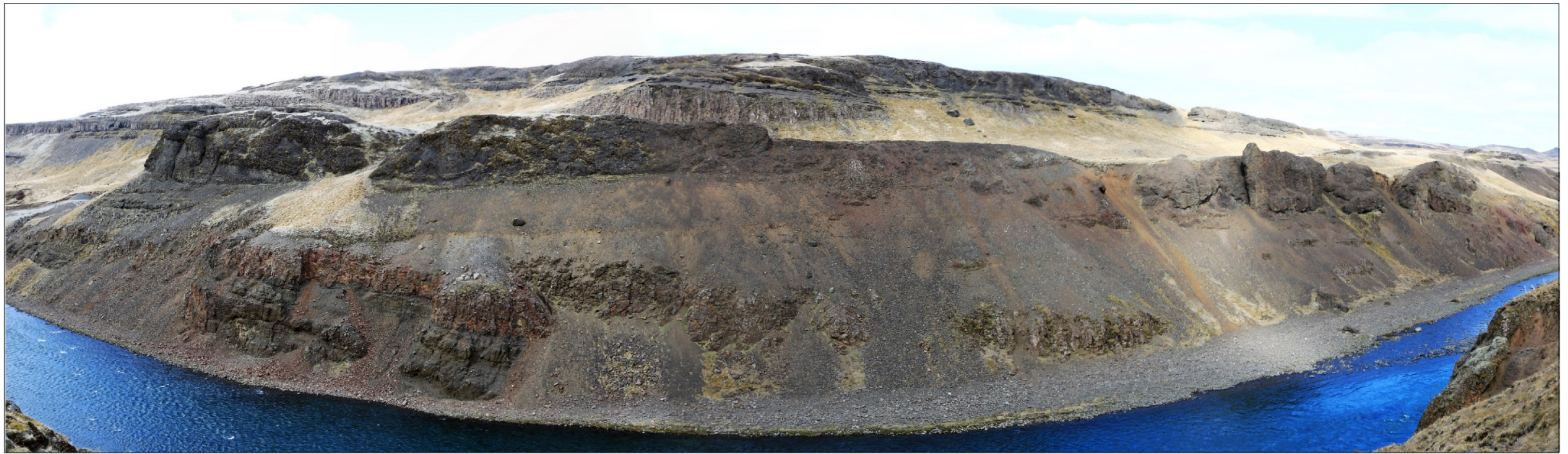


Figure 7-23 Panorama of section 8 Towards the north-west section of the Stora Laxa, the geology is dominated by volcanic units, potentially indicating that the fluvial system has been dammed or diverted

Overlying the E3 debris flow conglomerates is a thin (~5 m) unit of F1 sandstones. These fluvial sediments are likely related to the underlying conglomerate. They most likely represent the transition from debris flow to stream flow. The presence of these sediments suggests that volcanic activity was relatively quiescent, allowing the fluvial system to develop and deposit sediment.

A small exposure of <5 m of sub-aerial lava, overlies the F1 sandstones. This indicates that volcanic activity began to wax, with lavas following the low-lying areas in the palaeo landscape. This would have primarily been the fluvial drainage system. The sub-aerial lava quickly transitions in to a thick (>20 m) unit of C1 primary hyaloclastite. This indicates that the sub-aerial lava entered a water body and generated hyaloclastite. This contact between lava and hyaloclastite is only observed on the left of section 8 (Figure 7-23). The water body could have formed as a result of volcanic activity elsewhere in the HF. The lavas associated with the volcanic activity could have potentially dammed the small, fluvial system, generating a body of standing water in the area of section 8. The unit is relatively thick and indicates that volcanism was particularly active at this time.

## 7.2.9 Stora Laxa section 9

Section 9 is situated NE of section 8 on the west side of the Stora Laxa river (Figure 7-1). The section is found predominantly within grid square F7. Figure 7-24 presents an un-interpreted image of the section and underneath an interpretation of the section.

Section 9 is set back from the Stora Laxa river, by ~400 m, although is included within this chapter due to the significance of the stratigraphy. The section represents a simple transition from a volcanic dominated environment to a quiescent sedimentary environment and back to a volcanic dominated one.

The lowest unit in the stratigraphy is a thick B2 sub-aerial lava. This is laterally discontinuous due to exposure, although it is presumed it remains at the same stratigraphic level throughout the section (Figure 7-24). Where the unit is thickest in the section (centre-left) this is another rotational landslide, similar to section 7 (Figure 7-22). Where the block has rotated from the main section is highlighted by the white dashed line (Figure 7-24) indicating relatively minor displacement. The presence of the B2 lavas indicates that the volcanic system was very active at this time, dominating any fluvial systems present.

The B2 lavas are overlain by a laterally continuous unit of G1 lacustrine sedimentary rocks (Figure 7-24). The presence of these sedimentary units indicates that water became dammed within a low-lying area on the palaeo lava surface. The development of the water body was most likely a result of volcanic quiescence in the local vicinity of section 9. This would have allowed the fluvial system to re-establish itself. Volcanic activity distal to section 9, may have caused the fluvial system to become dammed. This would have resulted in a water body developing. The water body could also have formed in a proglacial environment, where the previously active volcanic system had caused the glacial outwash to become dammed. The dammed water body was a quiescent environment in which there was seasonal sediment input, resulting in cyclical deposits of sandstone and siltstone (Figure 7-25). Within the unit, thin tuffs are preserved, indicating that ash from relatively proximal eruptions settled on the water body and became preserved within the rock record, due to the quiescence of the environment.

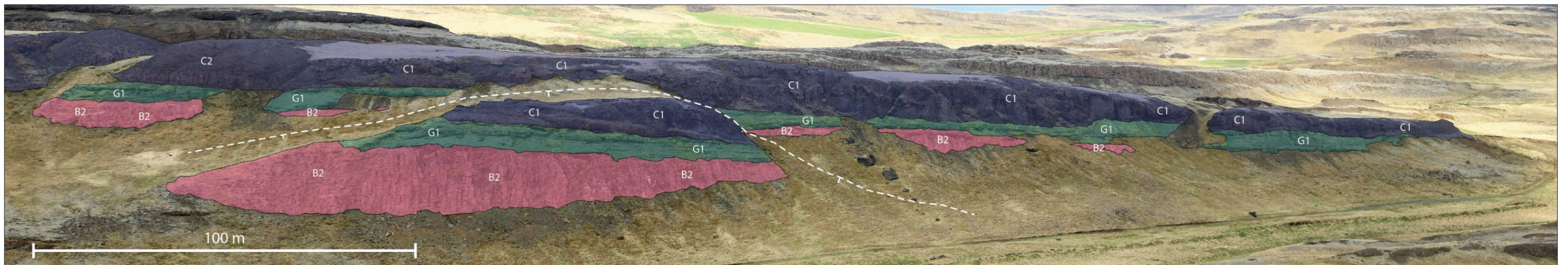


**Figure 7-24** Panorama of section 9 This section is slightly set back from the Stora Laxa, however it represents an important transition not observed elsewhere in the field area. The section documents the development of a small water body and the subsequent invasion by sub-aerial lavas to generate hyaloclastite and pillows.

A laterally continuous unit of C1 and C2 primary hyaloclastite caps the entire section (Figure 7-24). This unit indicates that volcanic activity within the local HF area became very active after a long period of quiescence. The unit is composed of areas of coherent sub-aerial lava entirely surrounded by hyaloclastite, but is predominantly hyaloclastite. This could be a result of the fluvial system which supplied the water body, interacting with the volcanic system producing the sub-aerial lavas. This would have generated pockets of hyaloclastite and sub-aerial lava in a complex unit. This volcanic activity was relatively sudden and was most likely the trigger event for sand injectites in the underlying lacustrine sediments (Figure 7-25).

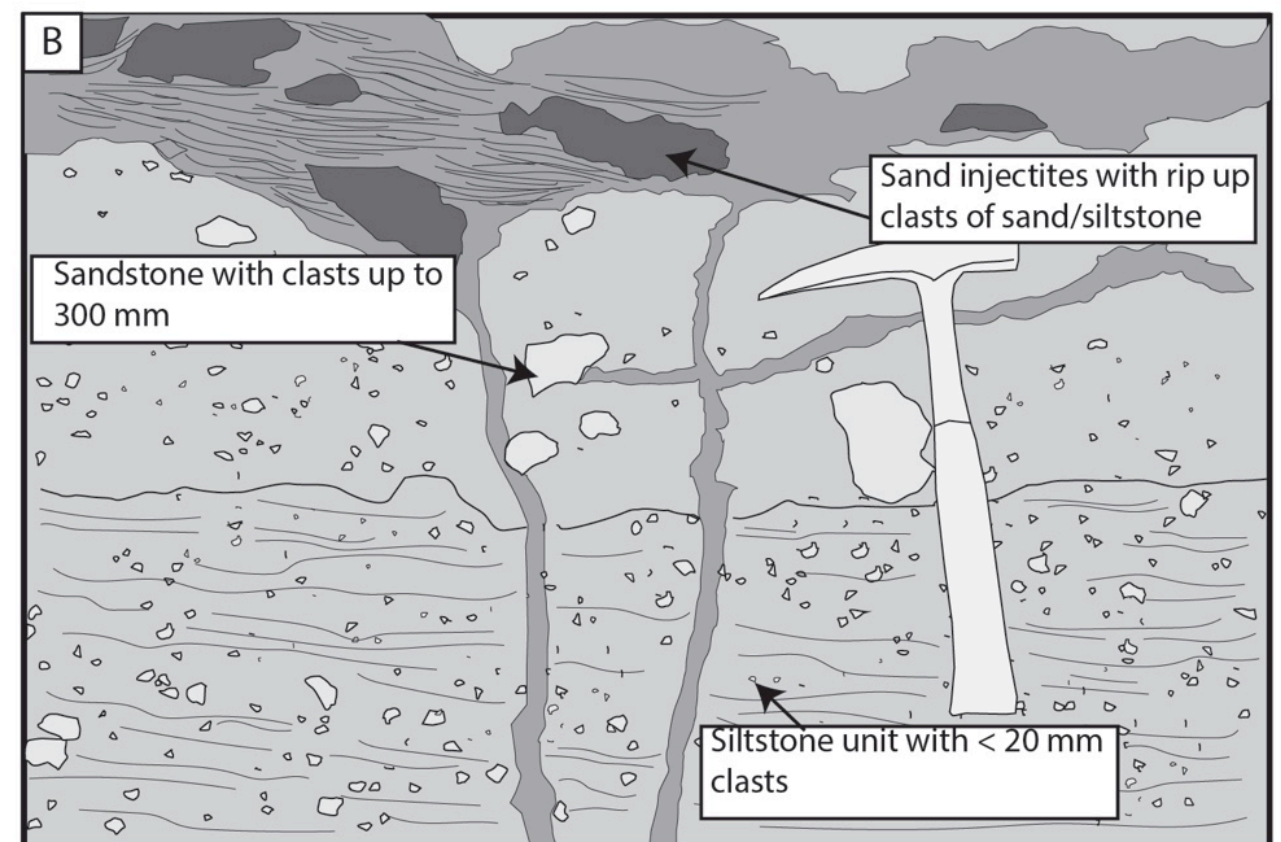
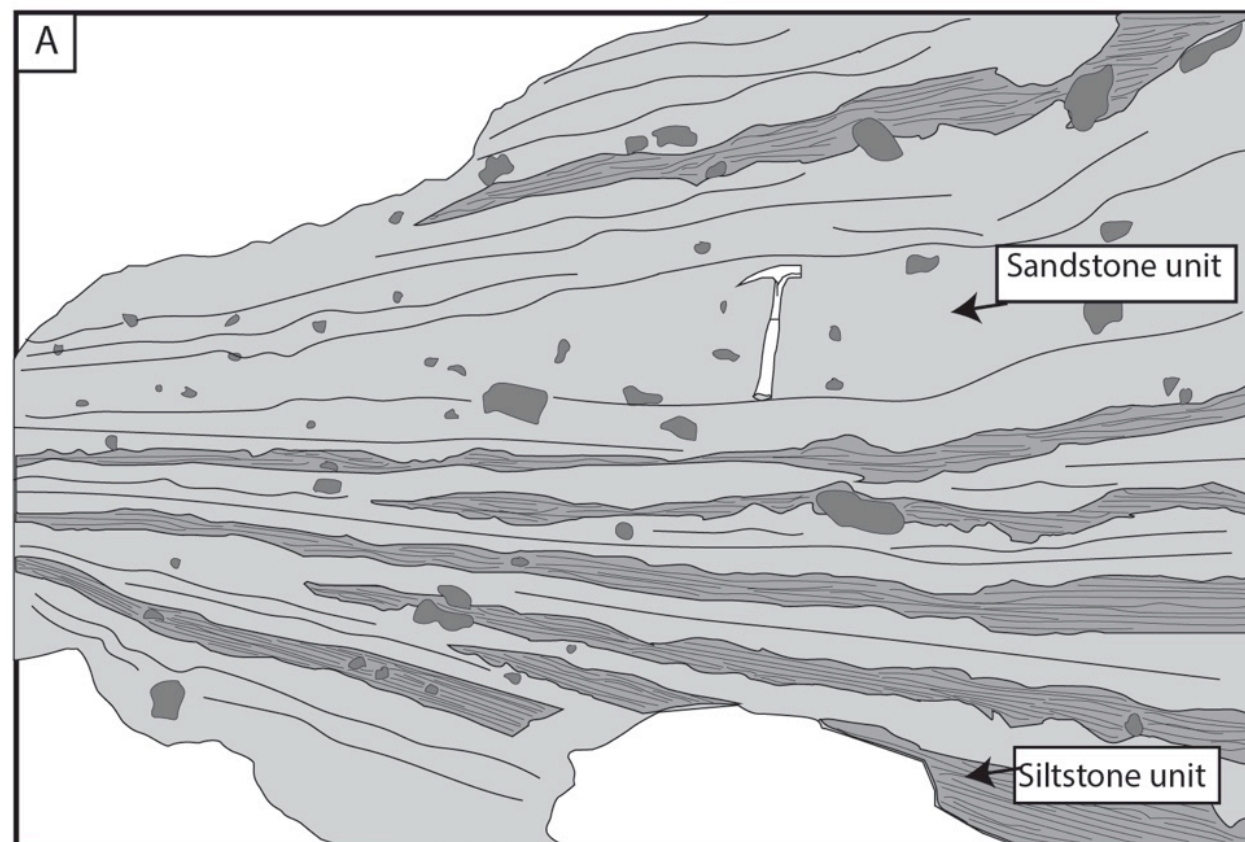
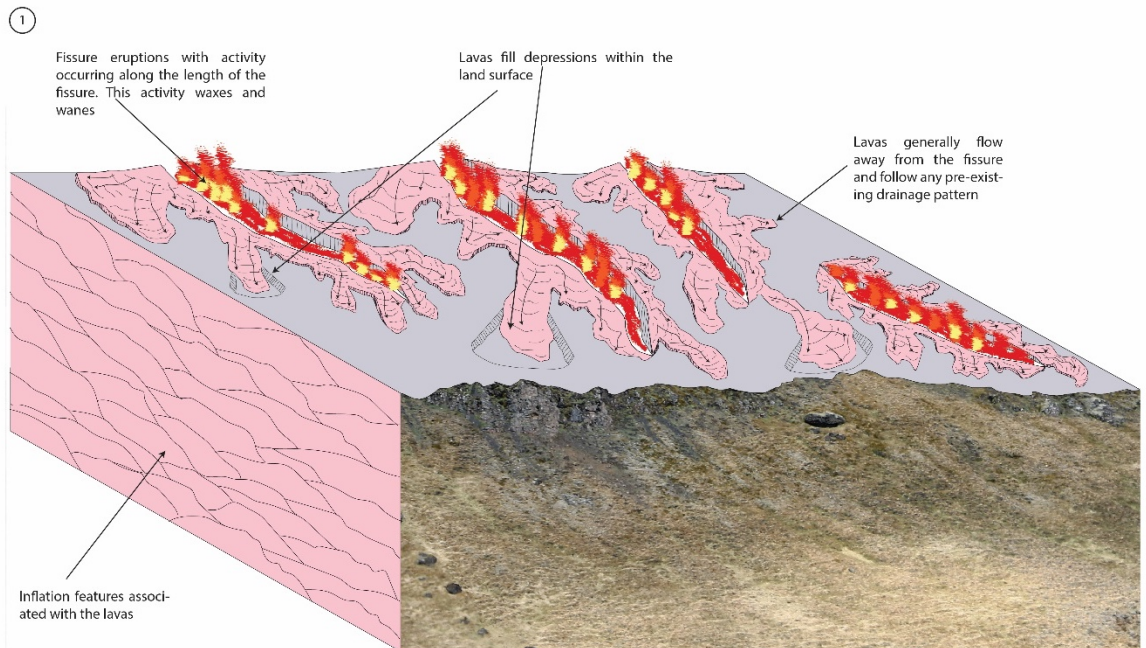


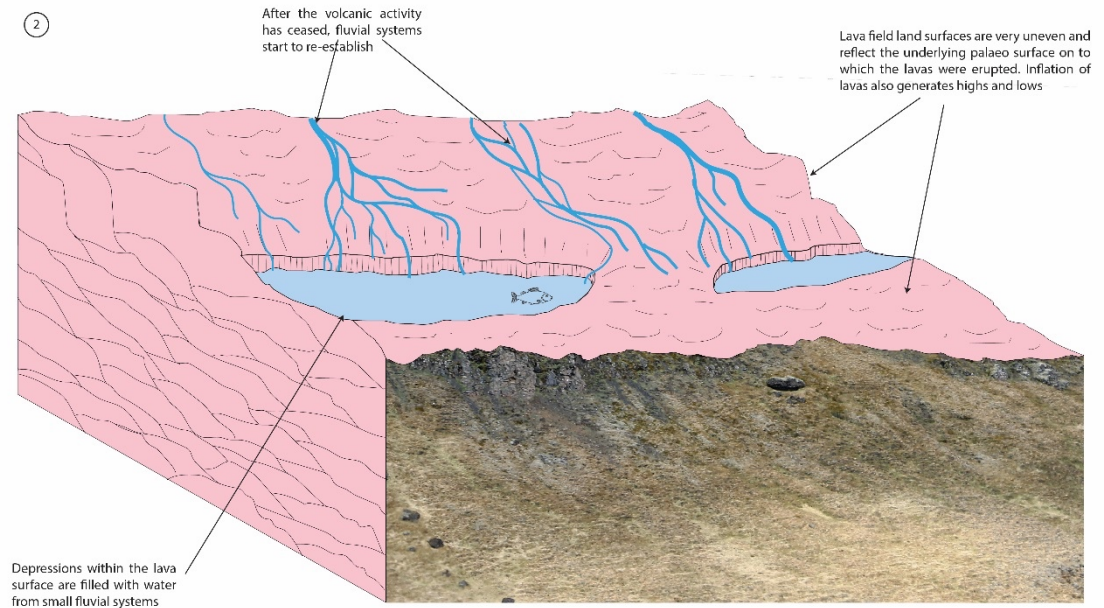
Figure 7-25 Details of the lacustrine unit featured in Figure 7 19. A) This image highlights cyclicality to the unit, with alternating siltstone and sandstone units. B) This image highlights the differences between the siltstone and sandstone units. Typically the larger clasts are found within the sandstone units, as these would have been transported when fluvial systems had more energy, during the summer months and when ice calved from the main glacier more readily. The siltstone units demonstrate a much smaller overall clast size, due to there being a general lack of sedimentary input during the winter months. Sand injectites cut the whole lacustrine unit, these would be associated with the emplacement of the overlying lava/hyaloclastite package (out of image).

### 7.2.9.1 3D models of depositional setting of section 9



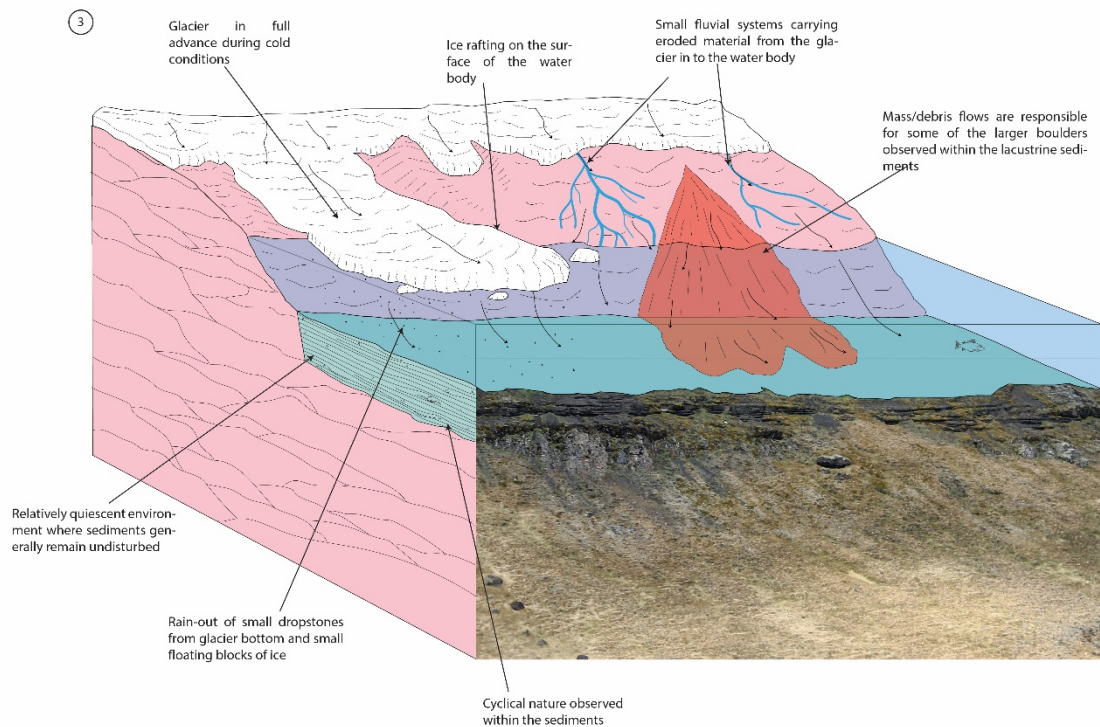
**Figure 7-26** Block diagram of the extrusion of sub-aerial lavas This model represents how the lavas in Figure 7-24 were extruded. The model is hypothetical and no scale or direction is implied.

Figure 7-26 is a representation of how the B2 lavas within section 9 developed. The B2 unit is thickest (~25 m) where there has been rotational landslides. It is assumed that this thickness is continuous along the length of the exposure ~0.5 km (Figure 7-24). The thickness of the unit indicates that the volcanic system was very active at this time. The lavas would have been produced through large fissure eruptions. These lavas would have preferentially flowed in to pre-existing lows within the palaeo-landscape, which were most likely caused by small fluvial systems. The volcanic activity would not have been constant at the fissures, instead it would have waxed and waned, resulting in areas receiving a greater thickness of lava than others.



**Figure 7-27 Block diagram of the development of small water bodies. The model represents how easily small water bodies develop within lava dominated settings. The model is hypothetical and no scale or direction is implied.**

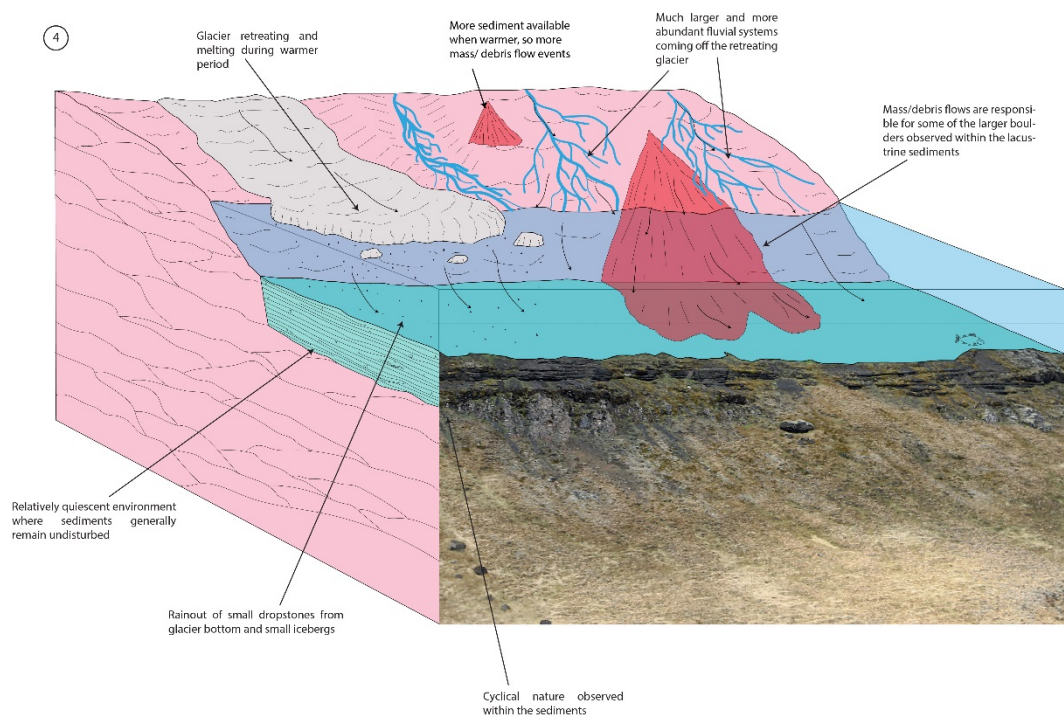
Figure 7-27 is a representation of how small water bodies developed within section 9 (Figure 7-24). After volcanic activity started to wane this would have allowed the re-establishment of pre-existing fluvial systems. It is highly likely that these systems could have been proglacial. The fluvial system, would have flowed over the surface of the newly formed lava field and developed within lows. These lows could have become filled with water from the fluvial system generating standing water bodies or they could also have formed as the result of volcanic activity close by, altering and damming the fluvial system. Small water bodies are a common feature of lava dominated systems, e.g. there are two small present day water bodies within the field area.



**Figure 7-28 Block diagram of coalesced water bodies.** These have coalesced to form a much larger water body. This model represents the winter environment. Various sediment input methods are highlighted- these could be fluvial, glacial or mass flow. Evidence of all three are found within the field. The model is hypothetical and no scale or direction is implied

Figure 7-28 is a representation of how the G1 unit within section 9 developed (Figure 7-24). With continued volcanic quiescence, this would have allowed the fluvial systems to continue to fill the lows within the lava field. These standing bodies of water would have coalesced, resulting in the formation of a much large standing body of water.

As it is likely that this standing water body formed in a proglacial environment, there would have been periodic advance and retreat of the glacier. This would have resulted in contact with the water body. The model (Figure 7-28) represents a winter input of sediment in to the standing body of water. During this time, there would have been much less run off, as snow and ice would have been actively accumulating, therefore the sedimentary load of those fluvial systems would have been considerably less. The sediments deposited within the water body at this time would have been finer grained and less than in spring/summer. Evidence of this cyclicity is present within the section (Figure 7-25). This continuous cyclicity indicates that the volcanic system was relatively quiescent.



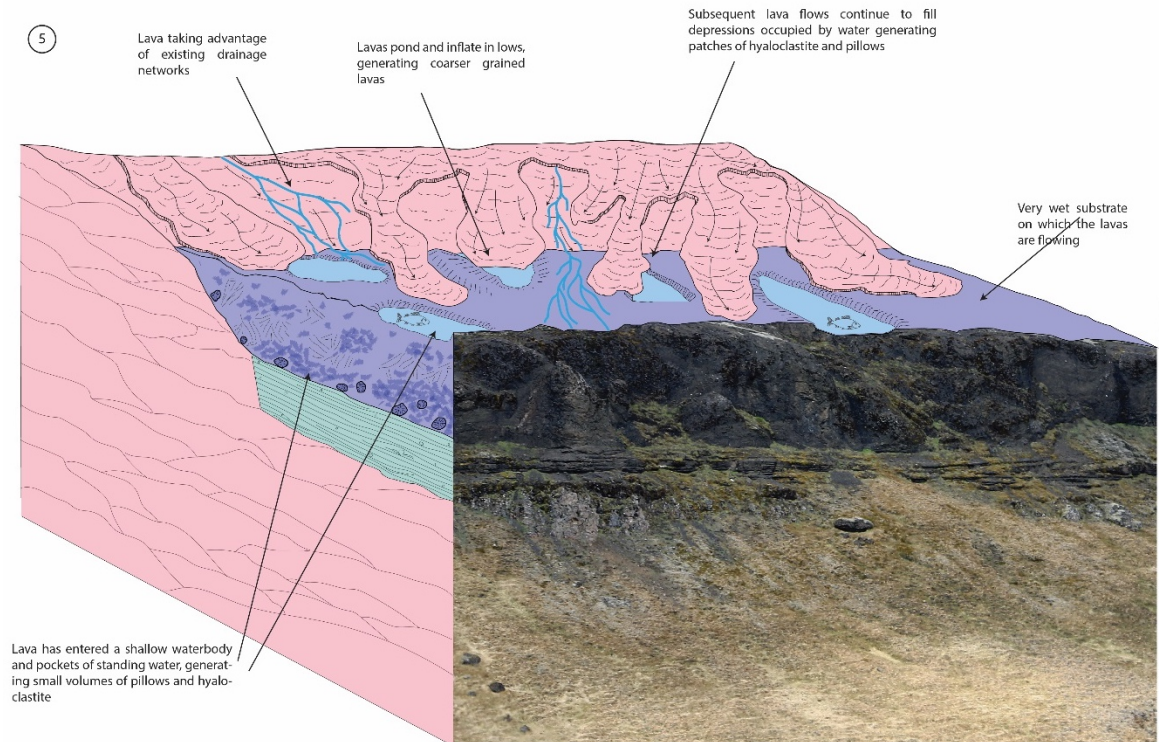
**Figure 7-29 Block diagram of coalesced water bodies. These have coalesced to form a much larger water body. This model represents the summer environment. Various sediment input methods are highlighted- these could be fluvial, glacial or mass flow. Evidence of all three are found within the field. The model is hypothetical and no scale or direction is implied**

Figure 7-29 is a representation of how the G1 unit continued to develop within a spring/summer setting. During spring/summer there would have been significantly more run off due to ice and snow melt. This would have led to the fluvial systems being able to carry greater sedimentary loads and would have resulted in coarser sediments being deposited within the standing water body. The volume of sediment would also have been much greater during this time (Figure 7-25). During these warmer periods of time, glacial ice would be much more likely to calve in to the water body. As a result of this, dropstones would be found within the sediments. These would have been originally incorporated in to the glacier as it scoured and plucked the land surface during advance of the glacier.

Large clasts found within the unit could potentially have been generated in a debris flow (Figure 7-25, Figure 7-29). Debris flows could have been generated during these warmer months due to increase in rainfall and availability of regolith.

Evidence of the water body being a relatively quiescent environment is present. Within the unit, there are small discontinuous units of tuff. These tuff units are

up to 40 mm thick in places and can be laterally continuous for up to 10 m. Preserving ash layers in the rock record is very difficult, as they are so easily eroded. This indicates that the units observed in section 9 were well protected.



**Figure 7-30 Block diagram of a lacustrine setting dominated by sub-aerial lavas This would produce hyaloclastite, pillows and various other products of lava-water-sediment interaction. This model represents how the units in Error! Reference source not found. may have formed. The model is hypothetical and no scale or direction is implied.**

Figure 7-30 is a representation of how the C1 unit in section 9 (Figure 7-24) developed. The transition from G1 to C1 indicates that the volcanic system became active within the local environment. Sub-aerial lavas would have followed the existing drainage network that supplied the water body, resulting in an interaction between the lavas and water. This would have generated primary hyaloclastite and pillow lavas, which we see evidence of in section 9. As the lavas continued to follow the pre-existing drainage network, this would have resulted in the water body being dominated by hyaloclastite, up to a point where only small pockets of water were left. During this continued extrusion of lava, the fluvial system would have continued to flow. Within the unit, there are areas that are dominated by hyaloclastite before quickly transitioning to sub-aerial lava. These areas of coherent sub-aerial lava have curvi-columnar jointing and large entablatures. This indicates that the fluvial system interacted with the lavas.

When the C1 unit formed, the weight of this unit on the underlying G1 sedimentary unit caused sand injectites to form (Figure 7-25). These injectites are relatively small, up to 60 mm in width, but continuous for >10 m. They cut the stratigraphy of the underlying G1 sedimentary unit, but do not breach the boundary with the C1 hyaloclastites.

### 7.2.10 Stora Laxa section 10

Section 10 is situated NE of section 9 on the west side of the Stora Laxa. The section is found within grid square F7 and G7.

Figure 7-31 presents an un-interpreted image of the section, followed by an interpretation of the section. Section 10 is dominated by C1 primary hyaloclastite and pillow fragments (

Figure 7-31). Within the centre left of section 10 (

Figure 7-31) there is a small exposure of stratigraphy. The lowest unit is sub-aerial lava, with an overlying unit of F1 fluvial sandstones. This exposure indicates that there was a hiatus in the volcanic activity to produce the small, laterally discontinuous unit of F1 sediment. Overlying the F1 sandstones is the large unit of C1 hyaloclastite which dominates the entire section. The transition from F1 sandstones into hyaloclastite indicates that during quiescence in the volcanic system a water body developed in the area. This water body most likely developed as a result of faulting, which would have generated accommodation space. This accommodation space would have been rapidly filled by the fluvial system, generating a water body in a small amount of time. As the volcanic system became active again, sub-aerial lavas would have entered the water body, generating primary hyaloclastite and pillow lavas. It appears that the low generated by faulting, has been a low for a prolonged period. The area today is a low, with small pockets of water developing within it. This indicates that there is a large structural control on the morphology and deposition in the area.

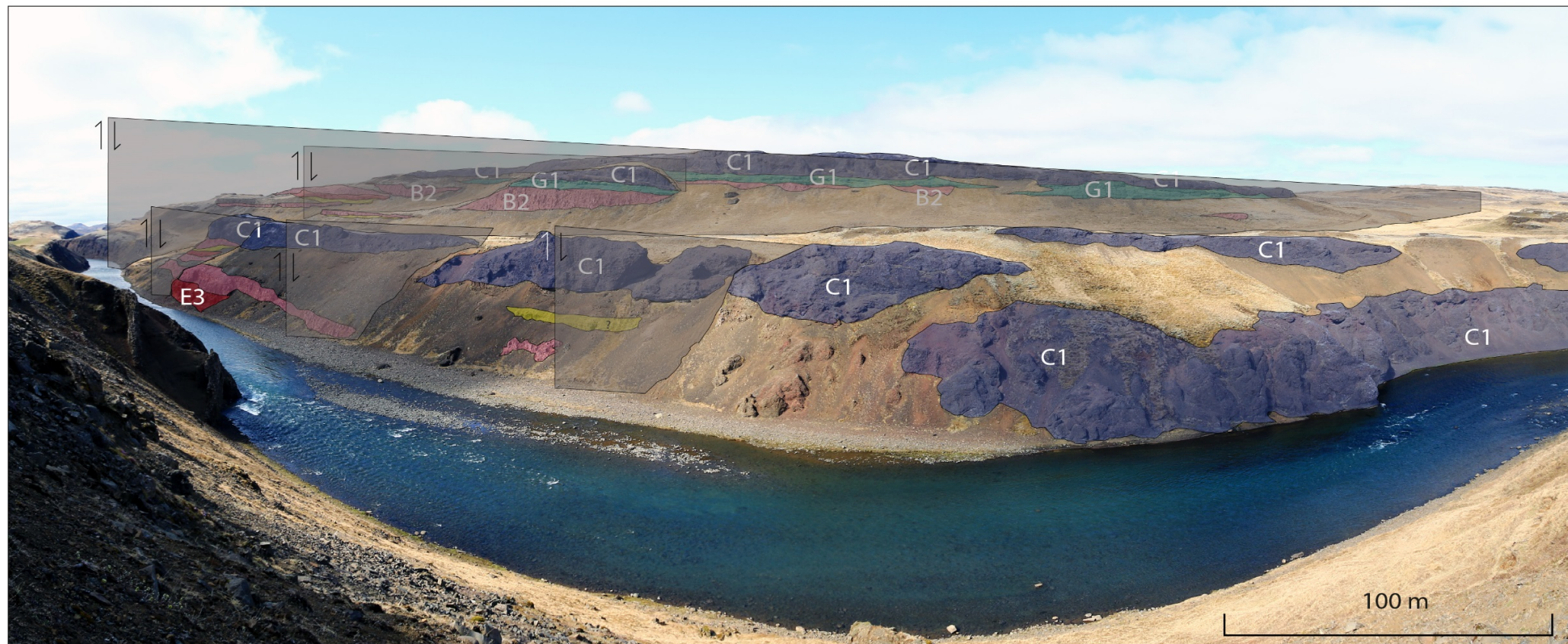


Figure 7-31 Panorama of section 10 This section of the Stora Laxa is dominated by hyaloclastite, indicating that there was a waxing of volcanic activity at the time, it also highlights the volume of water within the palaeo landscape.

### 7.3 Stora Laxa summary

The panoramas presented in this chapter highlight complex, lateral and vertical facies changes within a <2 km section from the HF. The section is dominated by repeating volcanic and sedimentary units and their complex interaction with the underlying tectonic structure (Figure 7-32). Moving upwards in the stratigraphy, individual units are generally thinner than lower in the stratigraphy (Figure 7-32). This could be due to numerous underlying factors in the HF. For instance, the larger volcanic units lower in the stratigraphy could be the result of sustained volcanic activity in the local area dominating the environments and suppressing the surrounding fluvial systems or could be the result of volcanic units ponding within accommodation space created by faulting. The volcanic and clastic units higher in the stratigraphy are thinner (Figure 7-32), this could be the result of short lived volcanic events punctuating fluvial deposition. A lack of available accommodation space in this area could also produce a similar pattern in the stratigraphy.

The uncertainty in these patterns highlights the need to understand the details within volcano sedimentary settings better as each scenario has very different implications, especially for hydrocarbon exploration. The Stora Laxa section can be interpreted as a typical representation of volcano sedimentary settings; however, other areas will be more or less complex than the HF and this needs to be taken in to account. Highlighting the detailed relationships between different lithofacies within the field is important as it provides answers to palaeogeographic questions. It is likely that these detailed relationships will not be observed in remote sensing, offshore data and highlights the need for field analogues to be used in conjunction with this data

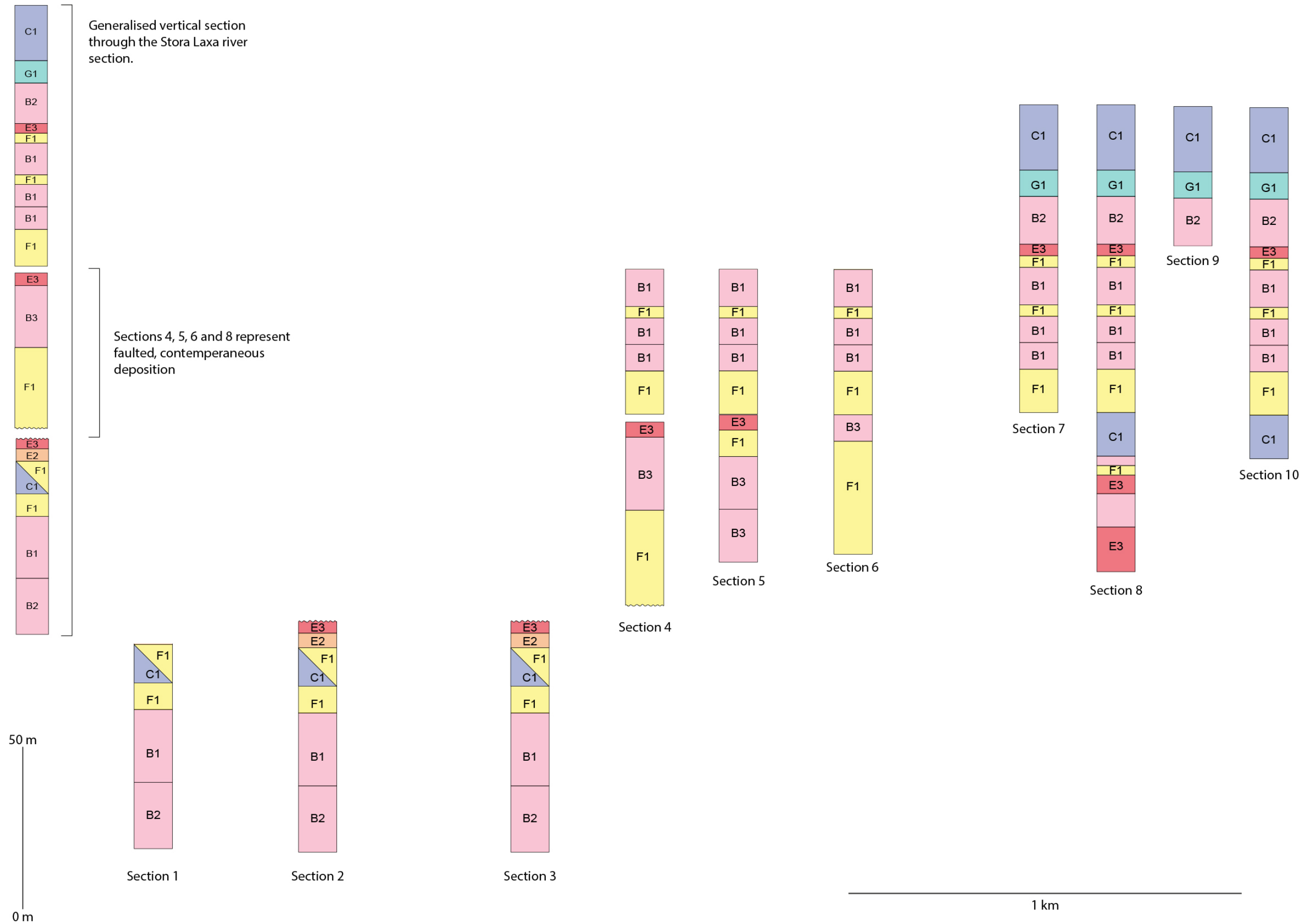


Figure 7-32 Generalised vertical section of the Stora Laxa river section. Central part of the stratigraphy is dominated by syn-depositional faulting, resulting in contemporaneous deposition of units. In the upper third of the stratigraphy, faulting is not as prevalent. The individual stratigraphic columns show the spatial relationship between different sections in the Stora Laxa river case study.

## 7.4 Conclusions

- The case study of the Stora Laxa presented within this chapter highlights the lateral and vertical facies changes within a <2 km section. The majority of the detail presented here would be below seismic resolution on offshore datasets. This highlights the need to analyse analogues to inform subsurface models.
- The section is characterised by repeating sequences; initially a volcanic sequence dominated before a mixed fluvial/glacial/lacustrine system developed. This sequence repeats in a similar manner, however it is complicated by faulting observed within the Stora Laxa river section.
- Repeating sequences of volcanic and sedimentary units are very common in volcano sedimentary settings. They appear to generate layer cake stratigraphy, however when examined closer, they are much more complicated and cannot be treated as simple layer cakes.

## 8 Integrated stratigraphic and structural model

### 8.1 Introduction

Iceland is situated in the North Atlantic Ocean, on the mid Atlantic Ridge between the Reykjanes Ridge and the Kolbeinsey Ridge. The North American Plate and Eurasian plate are separating across the Mid Atlantic Ridge at a rate of ~18 mm per year (full rate) at a trend of N105°E and 285°W (Thordarson and Höskuldsson, 2014). The eastern side of Iceland sits on the Eurasian plate, with the western side on the North American plate (Einarsson, 2008). The plate boundary zone is thought to be superimposed upon a large plume, with a deep mantle root (Einarsson, 1991), although this is debated by some authors (Lundin and Dóre, 2005; Ellis and Stoker, 2014). Onshore Iceland, the plate boundary zone is expressed by several volcanic zones. These are the West Volcanic Zone (WVZ), East Volcanic Zone (EVZ) and the Northern Volcanic Zone (NVZ) (Figure 8-1).

The plate boundaries are currently drifting westwards relative to the debated Icelandic hot spot, which, through time, is expected to result in an eastward ridge jump of the spreading zone (Einarsson, 1991). We are currently in the middle of a ridge jump, with both the WVZ and EVZ seeing active rifting. However, the EVZ is attempting to steadily replace the WVZ as it becomes extinct. The EVZ is currently propagating south (Einarsson 1991; Passerini et al, 1997) at the expense of the WVZ. These volcanic zones vary in their width from 20-50 km (Thordarson and Höskuldsson, 2014).

Accommodating the eastward movement of the NVZ and the EVZ relative to the Kolbeinsey ridge and Reykjanes Ridge are two major transform zones the Tjörnes Fracture Zone (TFZ) in the north of Iceland and the South Iceland Seismic Zone (SISZ) in the south of Iceland (Figure 8-1). These fracture zones probably accommodate a transfer of strain between rift segments, which results in a complex fracture network (Einarsson, 1991). The SISZ is ~15-20 km wide (N-S) and 70 km long (E-W) (Bergerat and Angelier, 2000; Einarsson, 1991).



The Hreppar Formation is situated between the WVZ and the EVZ, just north of the SISZ (Figure 8-1). This area is neither part of the North American Plate or the Eurasian Plate, instead it is separate plate, called the Hreppar Microplate (Clifton and Kattenhorn, 2006; Einarsson, 2008). This area is structurally complex due to the different motions of the WVZ, EVZ and SISZ. This tectonic complexity may contribute to the complicated geomorphology within the HF at Flúðir, with faults and intrusions having been preferentially eroded to form gullies. Those gullies separate a series of ~150 lozenge shaped elevated outcrops that range from 100 m to 1 km in length and are up to ~100 m in width, found within a ~16 km<sup>2</sup> area (Figure 8-2). The outcrops typically have a NE-SW trend, which is parallel to sets of faults and fractures observed within cliff sections. The purpose of this chapter is to describe the exposed structural framework of the HF. As a result of limited exposure within the area, the structural observations are discussed as a series of potential structural models that each fit the observed faults.

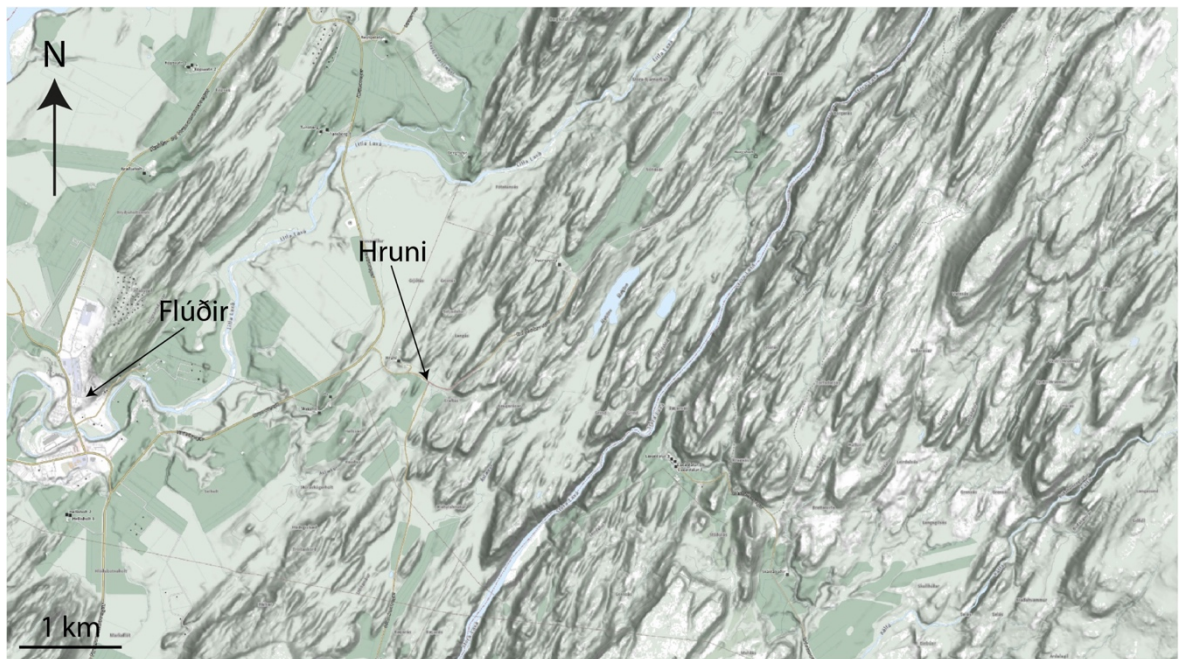


**Figure 8-2 Geomorphology of the Hreppar Formation with Flúðir and Hrúni marked. The HF is predominantly comprised of lozenge shaped outcrops that strike NE-SW.**

## 8.2 Evidence of tectonic setting in the HF

Chapter 7 demonstrates the lateral and vertical facies changes within the Stora Laxa river section, this also occurs in the rest of the HF as evidenced in the geological map (map insert). Deposition of units alone, cannot account for the outcrop pattern in the HF. Specifically, there is evidence for potential faulting occurring during and between depositional systems with offsets visible between units (Chapter 7). However, this evidence within the HF at Flúðir, is limited. This is primarily due to poor exposure within the centre of the field area. The geology and structure within grid squares such as F6, C10, C11, B11 and G6 (map insert) is very difficult to ascertain due to lack of exposure. Faulting relationships and the underlying structure in the HF have been inferred from stratigraphic relationships, topographic expression (i.e. orientation of gullies), aerial imagery, photogrammetry and direct fault evidence (where accessible). The best evidence for faulting within the HF is within the Stora Laxa river section (Chapter 7), here stratigraphic faulting relationships are relatively clear.

The most southern section within the Stora Laxa (Figure 8-3, Figure 8-4) (section 1 and 2, after the nomenclature of chapter 7) demonstrates clear evidence of faulted stratigraphy. The largest fault offsets the lavas at the base of the section, with an apparent displacement of ~10-15 m. Several other faults are observed within the same section, which show smaller apparent displacements (Figure 8-3, Figure 8-4). These faults although smaller, display the same strike of the largest fault. The stratigraphy demonstrates a stepping down relationship moving NE, as a result of the faulting. Dykes are commonly found within fault planes in the HF, indicating a component of extension and volume increase within the local area. The faults within section 1 all have approximately the same strike, which clusters around NNE (022.5°).

Further north along the Stora Laxa river, sections 3, 4, 5 and 6 (chapter 7) display a similar faulting pattern to that observed in sections 1 and 2 (Figure 8-3, Figure 8-4, Figure 8-5). In all cases, the faults accommodate a relative drop in the stratigraphy down towards the NE. The strike of the faults within sections 3 and 4 (Figure 8-5) strike approximately NNE (022.5°) however a few strike at ~010°. Dykes found within section 6 have a slightly different strike to the fault planes, these are oriented at ~030° (Figure 8-6).

There are two rivers in the HF at Flúðir, the Stora Laxa and the Litla Laxa, which lie to the east and west of the field area respectively (

Figure 8-7). The geology and geomorphology either side of these rivers contrasts sharply with the geology and geomorphology in between the rivers (Map insert).

The Stora Laxa and the area to the west of the Lita Laxa (

Figure 8-7) could demarcate large faults although no direct evidence of these faults has been found, only indirect evidence (stratigraphy and geomorphology).

The area between the two rivers is the main field area, which is dominated by lavas, hyaloclastite and sedimentary units. To the west of the area, west of the Litla Laxa, and to the east of the Stora Laxa (

Figure 8-7), these areas are dominated by lavas; only a few sedimentary units are found in both these areas (chapter 10). The difference in depositional histories may relate to a structural control on accommodation space within the area.

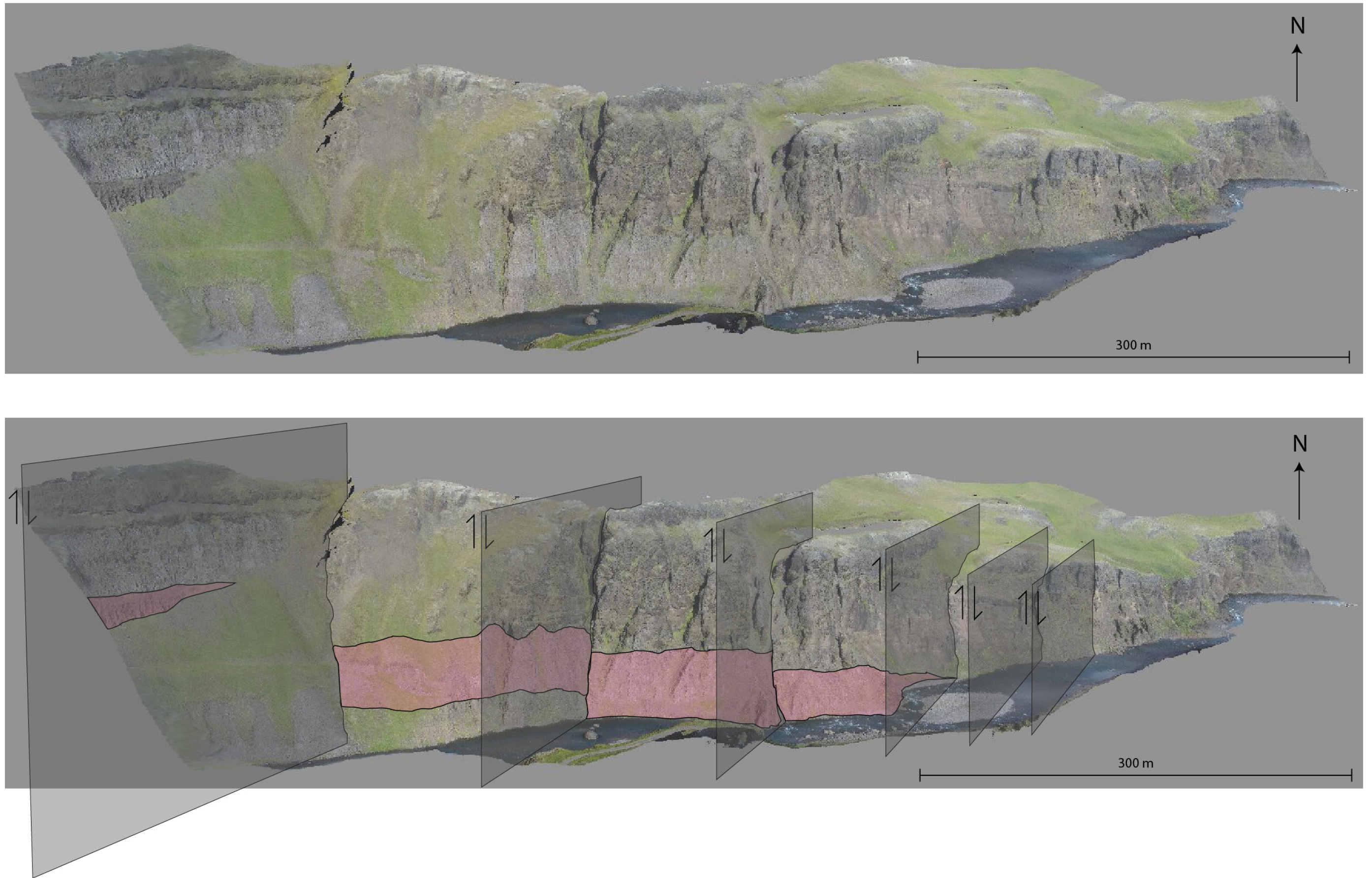


Figure 8-3 Uninterpreted photogrammetry model and interpreted model, highlighting the main faults within the Stora Laxa river section, and highlighting the orientation and relative displacements between units.

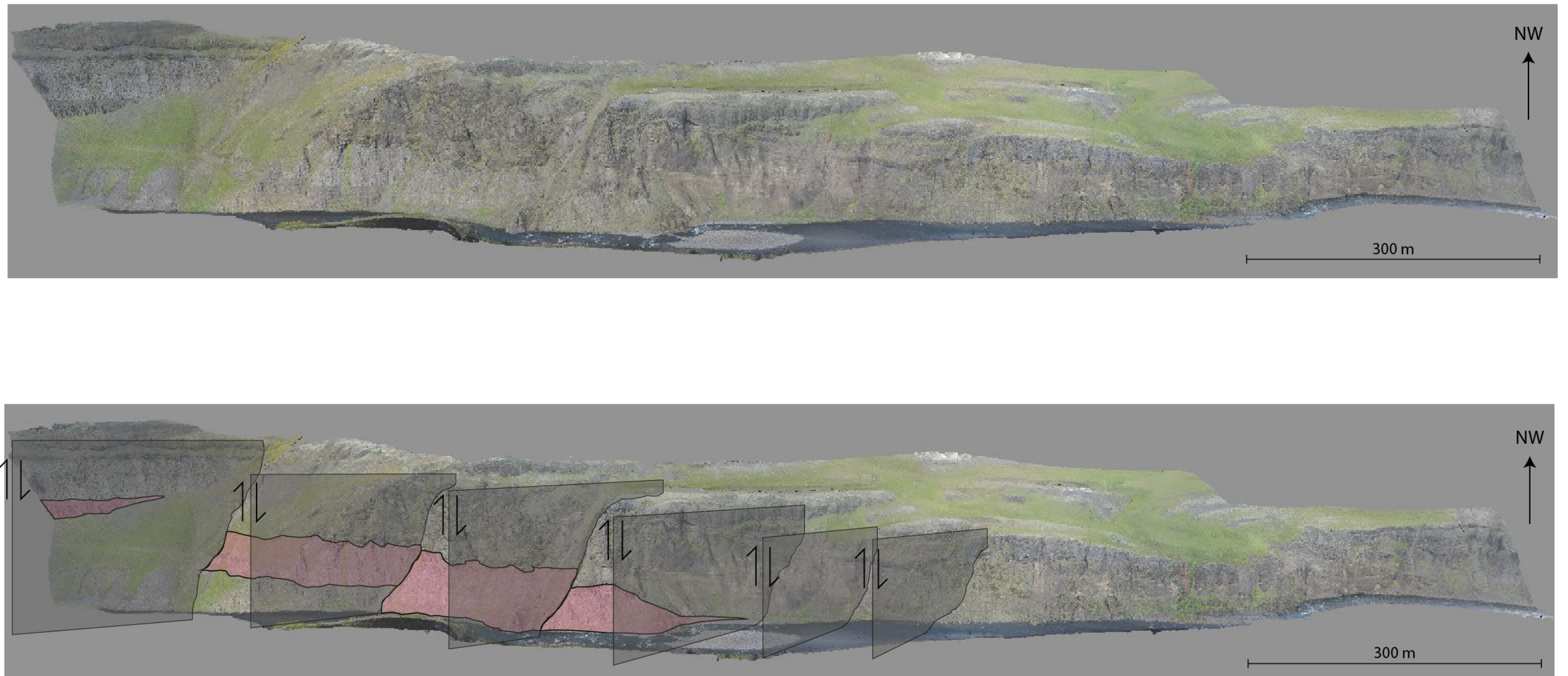


Figure 8-4 Uninterpreted photogrammetry model and interpreted model , highlighting the main faults within the Stora Laxa river section, and highlighting the orientation and relative displacements between units.

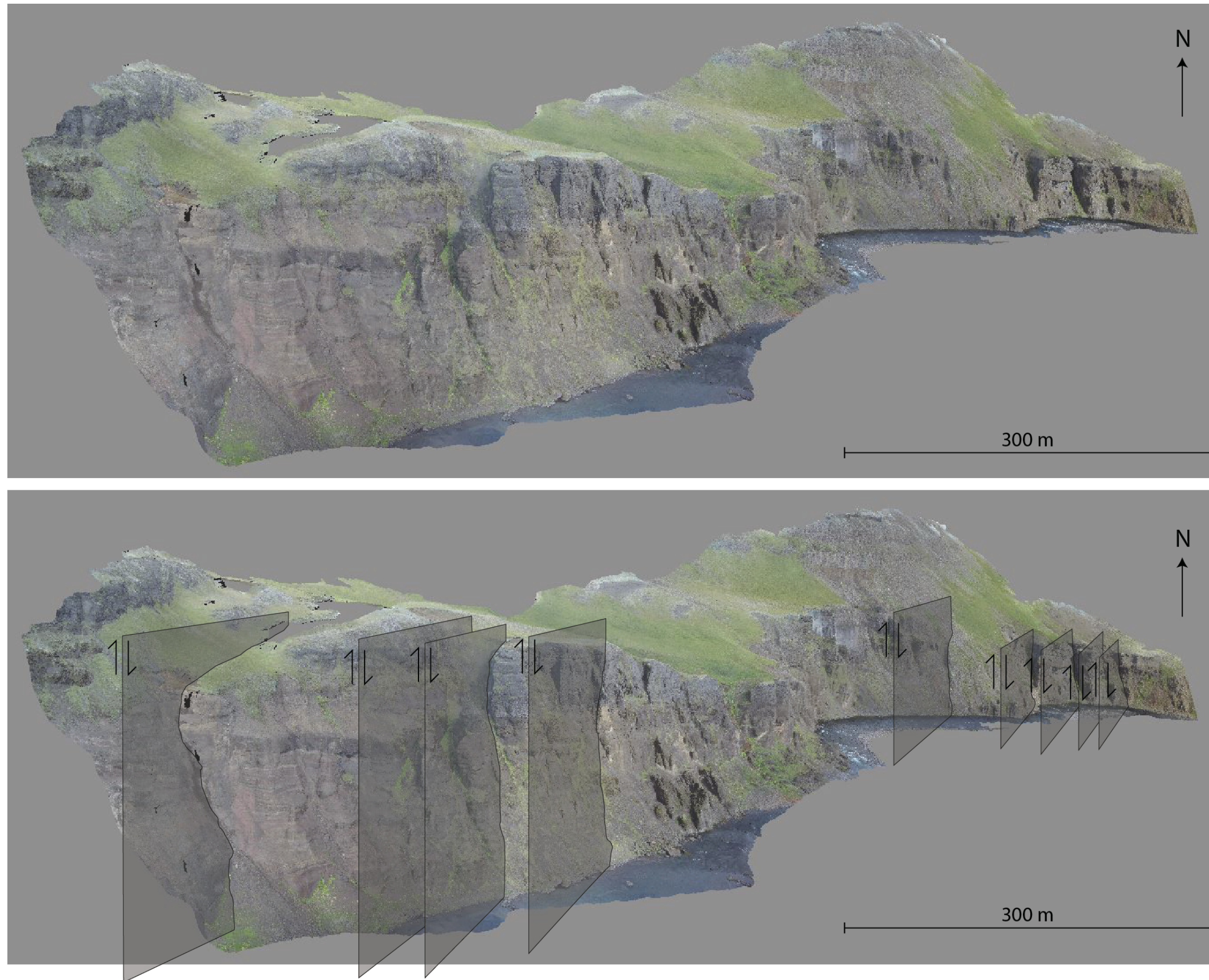


Figure 8-5 Uninterpreted photogrammetry model and interpreted model , highlighting the main faults within the Stora Laxa river section, and highlighting the orientation and relative displacements between units.

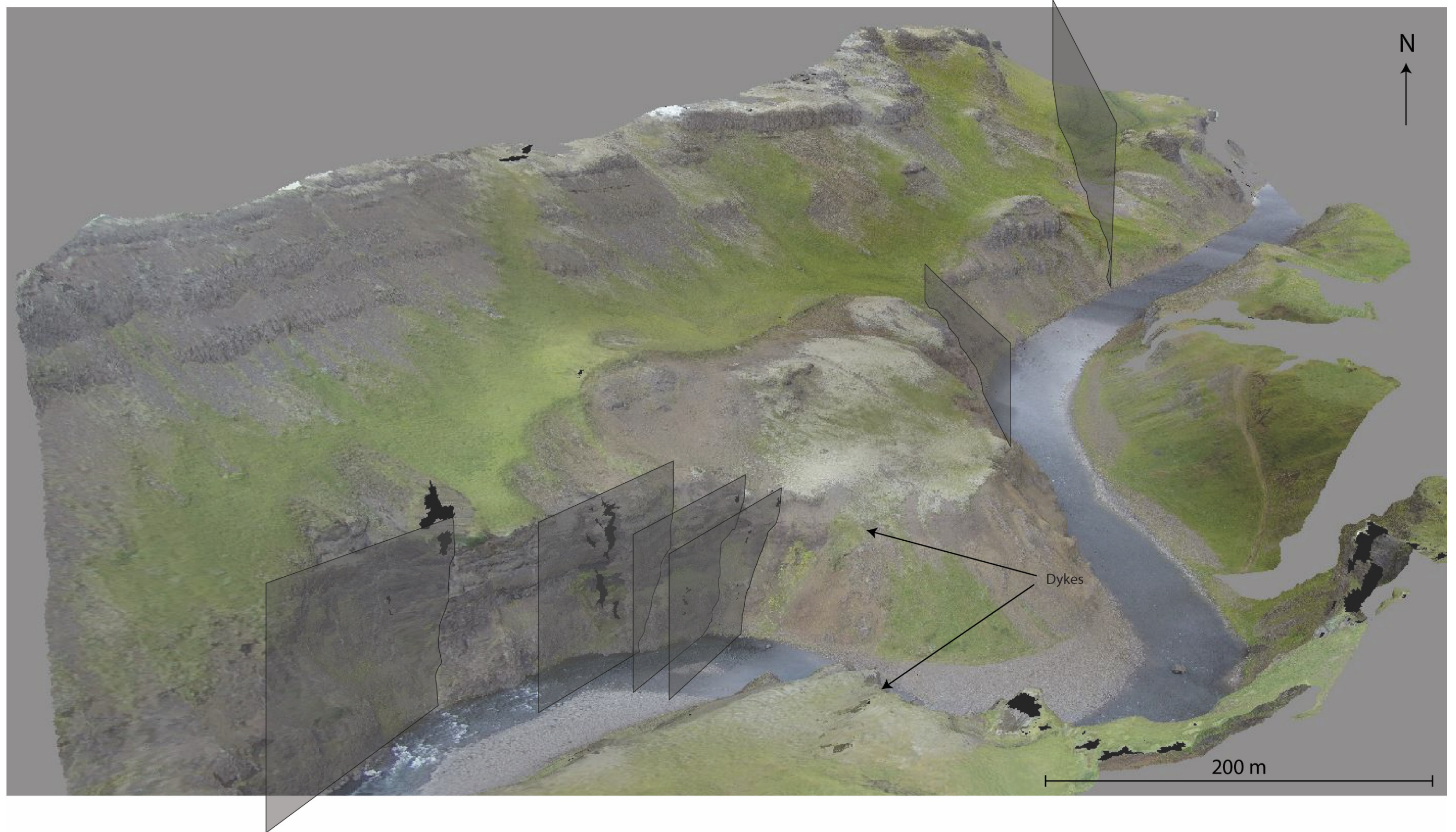


Figure 8-6 Photogrammetry model, highlighting the main faults within the Stora Laxa river section , and highlighting the orientation and relative displacements between units.

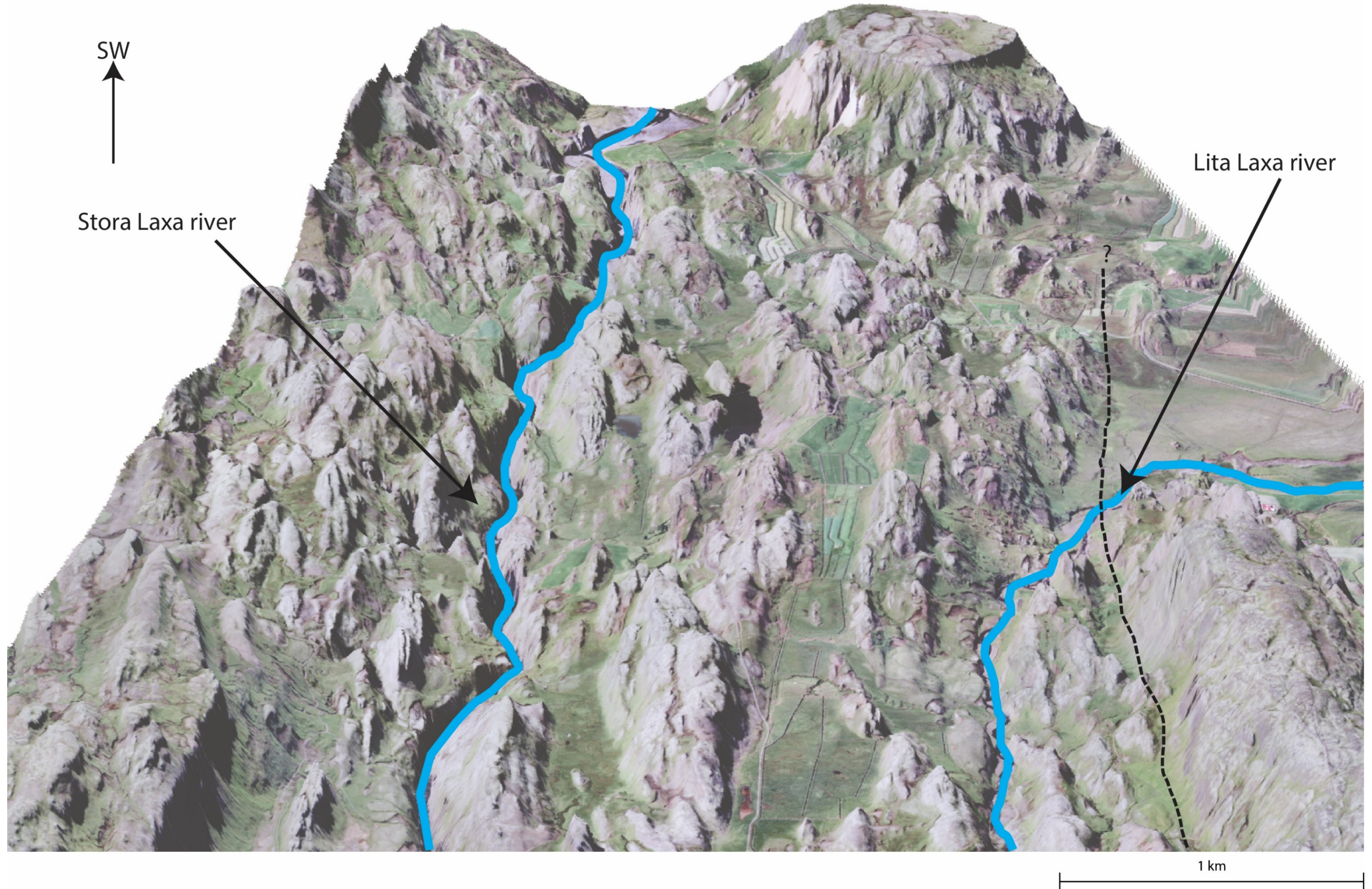


Figure 8-7 Looking SW in the HF at Flúðir with the main rivers (Stora Laxa and Lita Laxa) highlighted. The Stora Laxa potentially follows the same orientation of the hypothesized, underlying fault, whereas the Lita Laxa is to the east of the other large fault.

## 8.3 Cross sections of the Hreppar Formation

Cross sections of four key outcrops within the HF have been employed to highlight the relationships between different outcrops within the field area (Figure 8-8). These cross sections reveal different styles of faulting within the HF.

### 8.3.1 Cross section 1 (E7, F7, E8, F8)

Cross section 1 is situated within grid squares E7, F7, E8 and F8 (map insert)(Figure 8-8, Figure 8-9) and highlights the relationships between three main outcrops (A, B, C). The outcrops are distributed evenly over 1 km and are approximately 70-120 m in width and are all ~0.5 km in length. Based on the mapped units and the stratigraphy, outcrop A is unrelated to B and C. Outcrop A has a different depositional history to B and C. The subsurface stratigraphy of the three outcrops is unknown.

Outcrop A is dominated by B2 and B1 lavas, separated by a relatively thin interbed of E3 (Figure 8-9). The lack of water dominated lithofacies (hyaloclastite, pillows) indicates that these units were deposited within a relatively water free environment. Water may have formed later in this environment, indicated by the C1 hyaloclastites which cap the outcrop.

Outcrops B and C have a markedly different stratigraphy to that observed within outcrop A. B and C have the same stratigraphy, with thicknesses of each individual unit being relatively similar (Figure 8-9). In outcrop B more of the stratigraphy is observable, with a unit of E3 conglomerates at the base. In outcrops B and C, a large B2 lava is found at the base, which is overlain by a G1 sedimentary unit. The sequence is capped by a unit of C1 hyaloclastites. Outcrop C is described in detail in chapter 7.

As outcrops B and C show the exact same stratigraphy it is likely that they were connected prior to erosion (Figure 8-9). The outcrops are no longer connected as demonstrated by the projected dips of the units in outcrops B and C (Figure 8-9) which could indicate that faulting played a role.

This fault plane may have seen repeated movement, creating further separation between outcrops (Figure 8-9). Fluvial action and glaciation likely eroded the fault

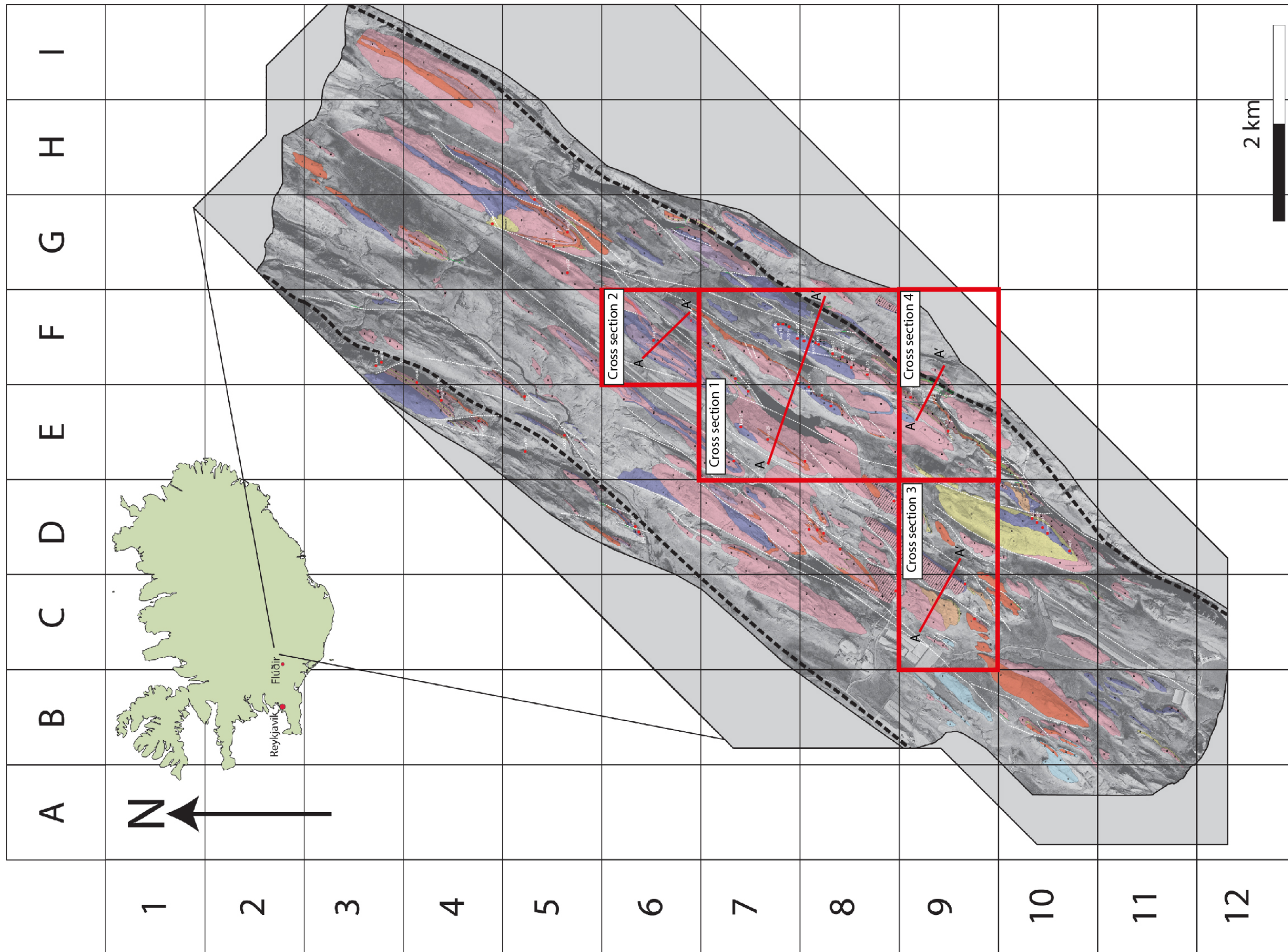


Figure 8-8 HF geological map with grid square location of cross sections. Cross sections are also highlighted with red line.

Cross section 1

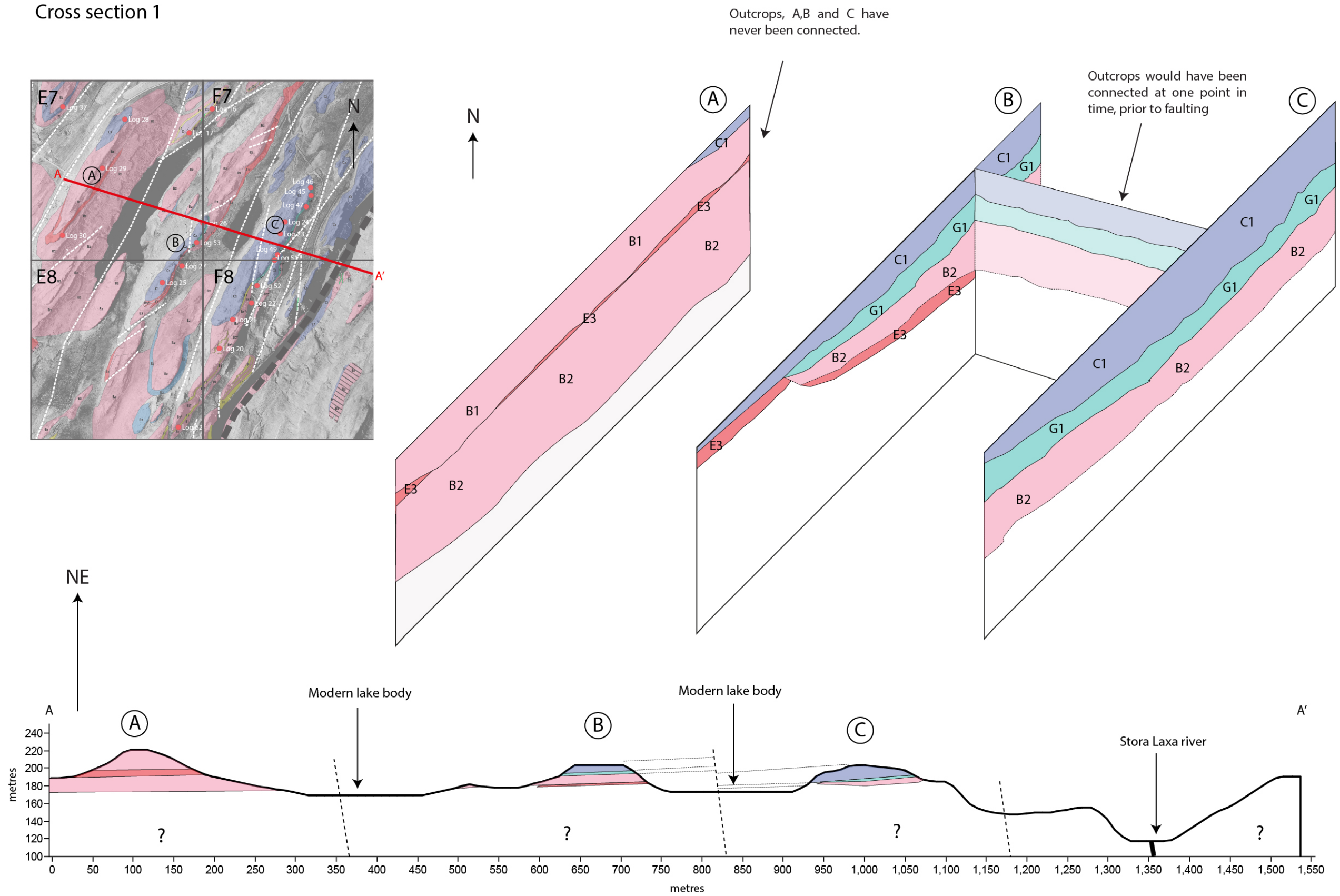


Figure 8-9 Faulted relationships between different outcrops. A is seemingly unrelated to B and C. B and C appear to have shared a similar depositional history, later separated via faulting.

plane further, separating outcrops B and C to their current positions. It is likely that outcrop A was never connected, this is most likely the result of earlier faulting.

It appears as if there is a general trend of units dropping down towards the east (Figure 8-3; Figure 8-4; Figure 8-5; Figure 8-6), potentially creating grabens or half grabens for the deposition of units. Continued faulting within the area is likely the biggest factor in the morphology observed in the HF today. Earlier faulting would have generated small horsts and grabens, resulting in areas where water bodies would have likely developed (outcrops B and C). There would also have been small grabens in which no water body developed (outcrop A).

### 8.3.2 Cross section 2 (F6)

Cross section 2 is situated within grid square F6 (map insert) (Figure 8-8) and highlights the relationship between two outcrops (D and E), whose facies were laterally continuous prior to erosion (Figure 8-10). The two outcrops are both ~70-80 m wide and ~0.3 km in length. Outcrops D and E both feature the same units that comprise the stratigraphy, however outcrop D demonstrates a repeat of the units in outcrop E (Figure 8-10).

The lowest unit within the stratigraphy in both outcrops, is a B3 lava which is overlain by C1 primary hyaloclastites and D1 re-worked hyaloclastites. This indicates that as there was continued volcanism in the area, the initial low in which the lavas formed became dominated by a water body. As lavas continued to enter this water body, this would have generated the primary and re-worked hyaloclastite observed within the two outcrops (Figure 8-10). As both outcrops have an identical stratigraphy and thicknesses of units, it is assumed that the water body covered the area represented by the two outcrops. However, outcrop A demonstrates a repeat of the previously mentioned units (Figure 8-10) which highlights that the initial water body could have moved more distally as hyaloclastite and re-worked hyaloclastite filled it.

Based on the observed downthrown sense across this fault set (Figure 8-10), it is inferred that outcrop E represents a downthrown block relative to outcrop A and as such, the lower units found in outcrop D should also be found below the exposure of outcrop E.

Cross section 2

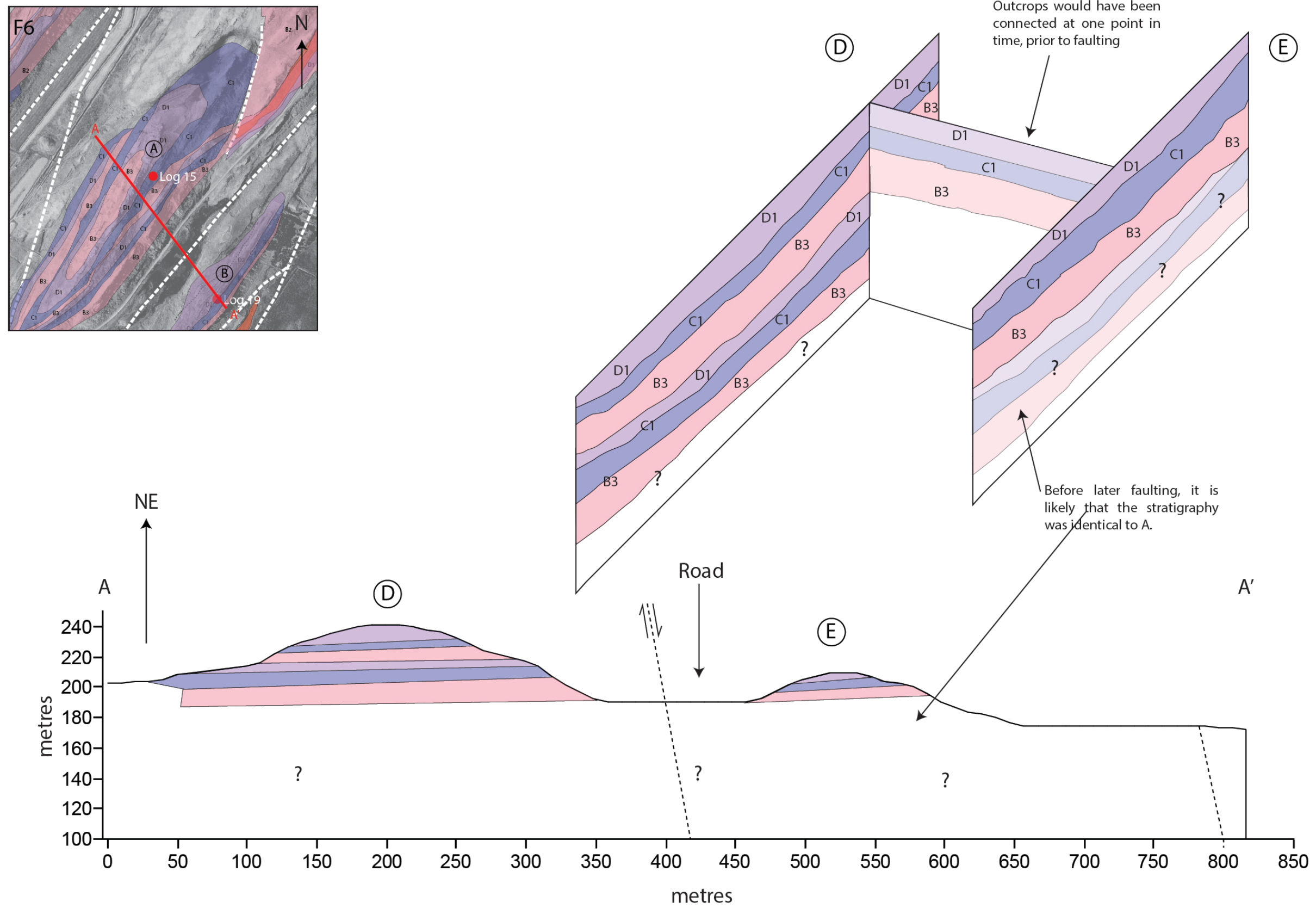


Figure 8-10 Faulted relationships of outcrops D and E. The outcrops have identical stratigraphy, indicating that they have seen the same depositional history. E is a smaller outcrop and does not demonstrate a repeat of the stratigraphy that is observed in outcrop D. It is likely this repeating stratigraphy is present, however is not exposed.

### 8.3.3 Cross section 3 (C9, D9)

Cross section 3 is situated within grid squares C9 and D9 (map insert, Figure 8-8 Figure 8-11). The cross section indicates the differences between two outcrops (F and G) that have markedly different geology. The outcrops have variable sizes; F is ~180 m wide by 245 m, G is ~150 m wide by 0.5 km long. The two outcrops appear to have had very different depositional histories.

Outcrop F is dominated by sub-aerial lavas and sedimentary units. The lowest unit exposed within outcrop F is a B1 lava, indicating that this was erupted sub-aerially. Overlying the B1 lava, is a ~12 m thick E3 debris flow conglomerate, suggesting that volcanic activity was waning and high levels of rainfall were occurring at the time of deposition. The transition from E3 conglomerate in to F1 sandstones indicates that there was a waning of energy and transition from debris flow processes to fluvial processes. The E3 unit grades in to E2 conglomerates, which have a glacial component to them, indicating that the area was glacial proximal. Outcrop F is capped by a B3 lava which highlights a return to volcanic activity.

In contrast to outcrop F, outcrop G has a significant sub-aqueous component to its geology. The lowest unit within the stratigraphy of outcrop G is an E2, glacially derived conglomerate (Figure 8-11). This unit transitions in to F1 sandstones, suggesting that a fluvial system rapidly developed. Overlying the fluvial sandstones is a unit of C1 primary hyaloclastite, indicating that the volcanic system started to wax and as a result lava entered a water body, generating primary hyaloclastite. This could indicate that the fluvial system became dammed and developed a water body in which the lava entered. At the top of the outcrop, lies a distinctive unit of B3 lava which has transitioned from the unit below. The transition indicates that the water body became dominated by lavas as volcanic activity waxed.

Without a fault between the outcrops, it would require unit C1 to laterally transition to F1 and E1. This is unlikely, given the thickness of unit C1 in outcrop G. It is possible that faulting would have generated a low which resulted in a water body forming in the area of outcrop G (Figure 8-11), whereas outcrop F remained on high ground. Again, this is consistent with the downthrown sense shown in the Stora Laxa section (Figure 8-3; Figure 8-4; Figure 8-5; Figure 8-6).

Cross section 3

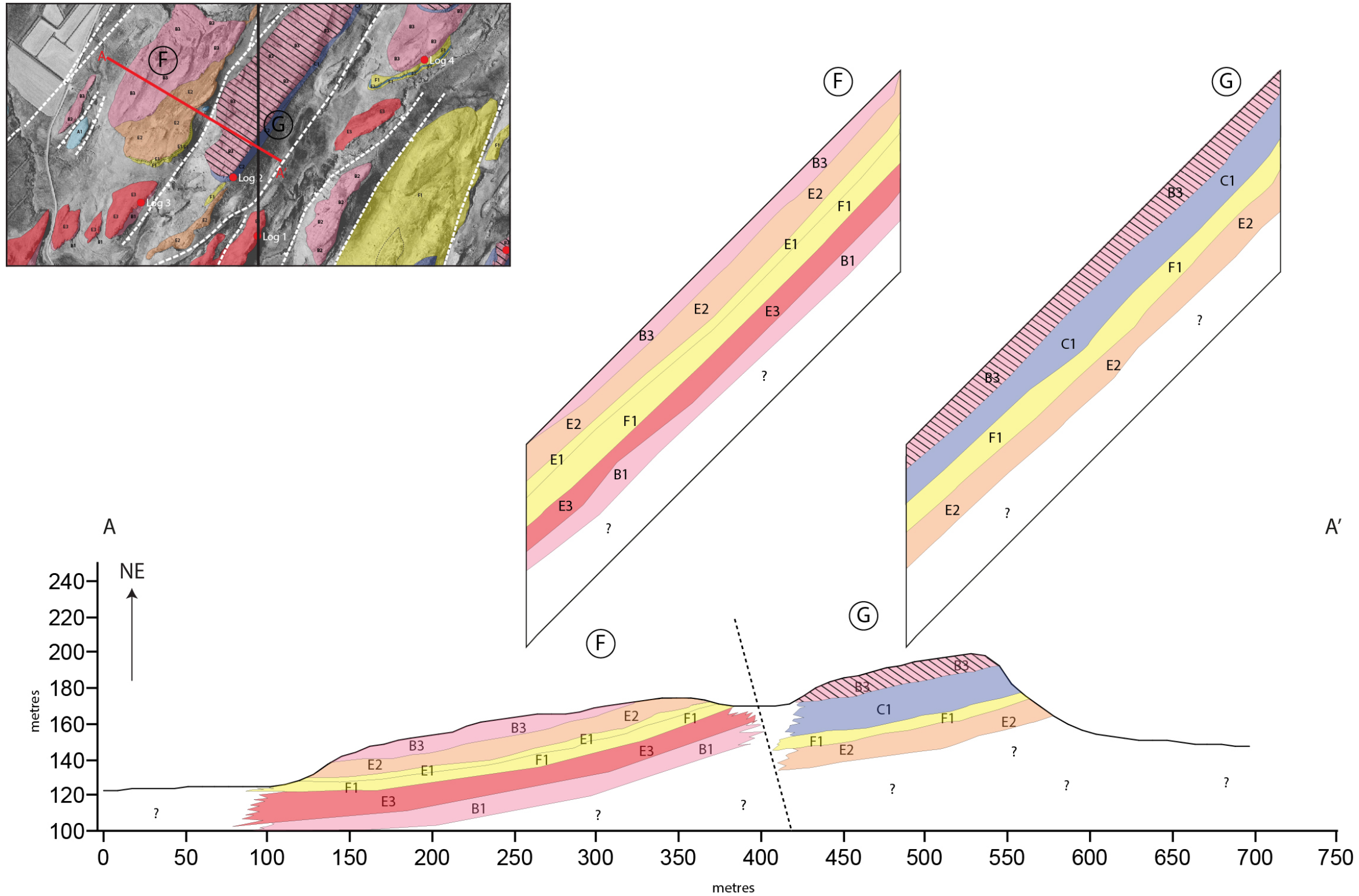


Figure 8-11 Faulted relationships between outcrops F and G. These two outcrops have seen markedly different depositional histories, with G demonstrating a strong sub-aqueous component. It is very likely that the two outcrops have a faulted relationship, explaining the different geology of each outcrop.

### 8.3.4 Cross section 4 (E9, F9)

Cross section 4 is situated within grid squares E9 and F9 (map insert, Figure 8-8, Figure 8-12) (chapter 7). The cross section lies on a NW-SE trend and spans a prominent bend in the Stora Laxa river. It highlights the differences in geology, either side of the river as mentioned previously, where a large fault is hypothesised to lie (

Figure 8-7). The west side of the Stora Laxa river, where outcrops H and I are situated, is dominated by lavas and sandstones/conglomerates, whereas the east side of the river where outcrop J is situated is dominated by sub-aerial lavas (Figure 8-12). The morphology either side of the river is also very different. The differences could be attributed to a combination of things such as; different lithologies, faulting (?) (Figure 8-7), erosion and glaciation.

Outcrop I and J are the lowest within the stratigraphy and their geology differs markedly. In outcrop I, the lower stratigraphy is dominated by B3 lavas, indicating the volcanic system was particularly active. Overlying the lavas are F1 sandstones and E3 conglomerates (Figure 8-12). The transition between these units indicates that volcanism began to wane and as a result, a fluvial system developed in area once dominated by volcanism. At this level in the stratigraphy, small scale faulting appears to be relatively common, with small displacements apparent (Figure 8-5, Figure 8-6, Figure 8-12), these small scale faults are not observed within the overlying stratigraphy, such as in outcrop H (Figure 8-6, Figure 8-12).

Outcrop J and the eastern side of the Stora Laxa, is dominated by sub-aerial lavas, relatively few sedimentary units are observed. Outcrop J is at the same stratigraphic level as I; in the absence of observed folds in the area, it is inferred that there is a fault separating the two outcrops (Figure 8-12).

Unconformably overlying outcrop I is outcrop H, which is defined by its repeating lavas and sandstones. The repeating units of F1 and B1 indicates that fluvial and volcanic systems competed for available accommodation space. The lack of a similar sequence on the eastern side of the river suggests that outcrop H and I experienced very different depositional histories to outcrop J (Figure 8-12). The small faults observed within outcrop I are not observed in outcrop J, suggesting

that they are bound by the fault marking the location of the river. Larger faults within the Stora Laxa section, cut the entire stratigraphy (Chapter 7, Figure 8-6) suggesting that they are much later faults.

The cross sections within the HF, highlight the variable deposition histories of some adjacent outcrops, with others having experienced the same depositional history and later faulting. The variable nature of these relationships indicates repeat faulting episodes that are regionally constrained to the HF and suggests that the observed faults are growth faults (Macdonald et al, 1996; Holland et al, 2006).

Cross section 4

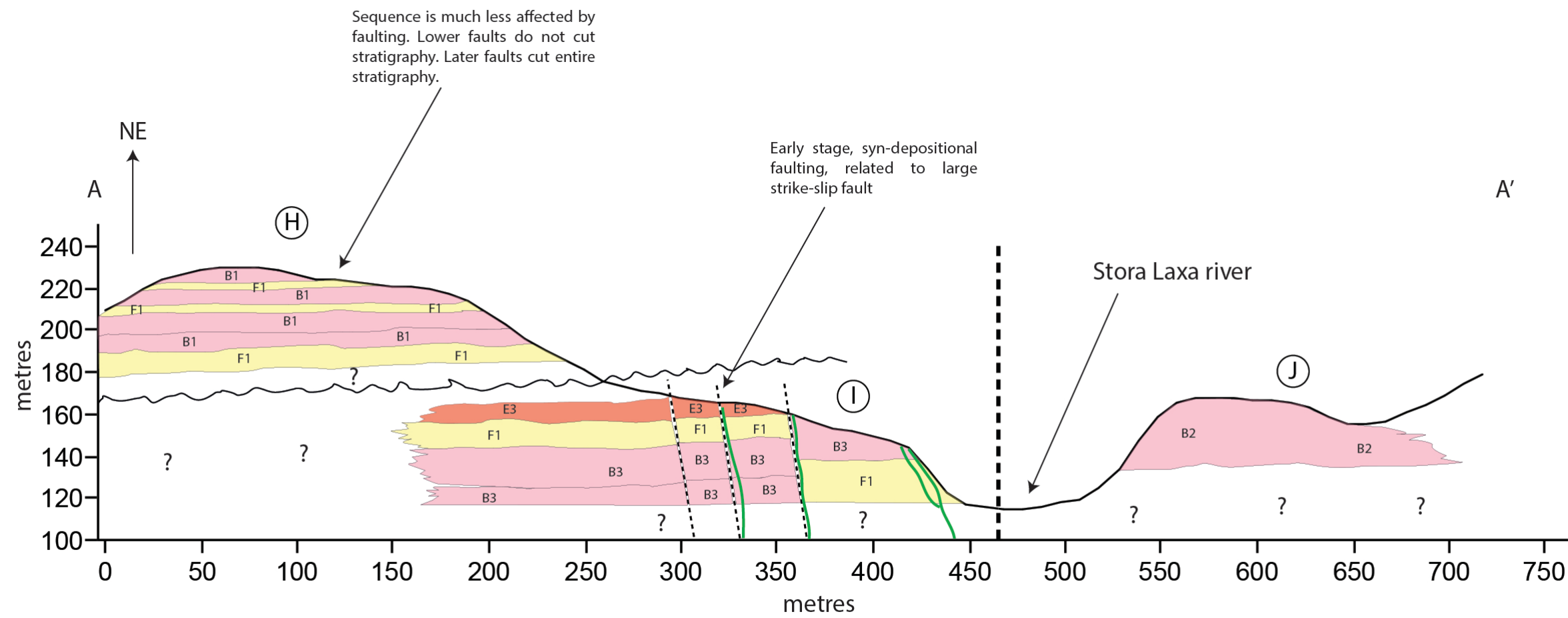
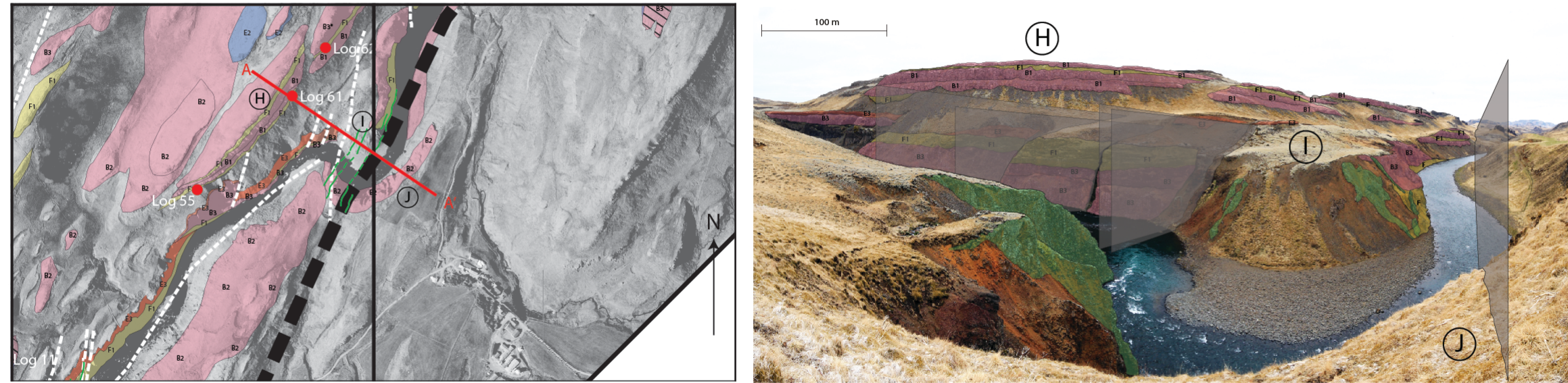


Figure 8-12 Complex faulted relationships in the Stora Laxa river. Outcrops I and J are separated by a hypothesized large fault, which bounds the HF at Flúðir. Outcrop I is dominated by lavas and sedimentary units, as well as numerous, small-scale faults. Outcrop J is dominated by lavas and apparently has no small scale faults, such as those observed in outcrop I. Outcrop H features a repeating series of lavas and sedimentary interbeds, that were deposited much later than outcrops I and J.

## 8.4 Tectonic evolution of the Hreppar Formation

Faulting of the Hreppar Formation has resulted in a piecemeal compilation of lozenge shaped outcrops dominated by volcanic, volcanoclastic, and sedimentary units. In most instances, these outcrops typically cannot be correlated, suggesting that these units were deposited in a series of small fault-bound basins or grabens, e.g. Figure 8-3, Figure 8-4, Figure 8-5, Figure 8-6.

Due to the lack of direct kinematic evidence for fault motions, several models are presented here that are consistent with the geometry and apparent offsets of these fault sets. A detailed structural interpretation is beyond the scope of this project, however, the importance of the tectonic structure in the HF is recognised as the main depositional control in the HF at Flúðir.

## 8.5 Koehn / Bubeck model

This model uses examples from the East African Rift System (EARS) (Koehn et al, 2008) and from Hawaii, Iceland and the North Atlantic (Bubeck et al, 2017) to understand the faulting pattern generated by overlapping rift segments and the resulting vertical axis rotation of crust (Figure 8-13, Figure 8-14). As mentioned previously, the HF occupies a region between the eastern and western rift zones of south Iceland, which demonstrate a right stepping geometry (Figure 8-1, Figure 8-13).

Segmented extensional systems dominated by normal faulting, can show complex fault patterns between bounding fault segments. The complex nature results from mechanical interaction between fault segments, in which competing elastic stress fields ahead of the fault tips may influence the propagation and geometry of first-order faults, and the development and distribution of second-order faults and fractures (Bubeck et al, 2017). The scale, distribution and motion of the second-order faults are a function of the first-order fault stepping direction (right, see Figure 8-13; left, see Figure 8-13) and the vertical axis rotation between fault segments, which accommodates variations in fault displacement (e.g. right stepping, anti-clockwise; left stepping, clockwise (Tentler and Acocella, 2010)).

Tentler and Acocella, (2010) demonstrated through scaled analogue modelling,

that as opposing rift segments propagate from underlap to overlap, fractures within the relay zone, may become increasingly oblique to the main rift structures. Bubeck et al (2017) demonstrated that if first order faults don't continue to propagate, but continue to accumulate opening displacement, the relay zone will be required to accommodate an increasing displacement gradient. Although new brittle structures are formed within the relay zone, Bubeck et al, (2017) highlighted a significant displacement shortfall in the relay zone: they inferred that the displacement gradient between the first-order faults is balanced by vertical axis rotation of the relay zone, and material thickening in the regional extension direction. To conserve volume, this rotation, and extension-direction-parallel material thickening, requires material thinning parallel to the rift axis. At the surface this thinning is accommodated by open-mode fractures that strike at a relatively high angle to the rift zone. In the subsurface this may be accommodated by normal faults, veins, and dykes (Bubeck et al, 2017).

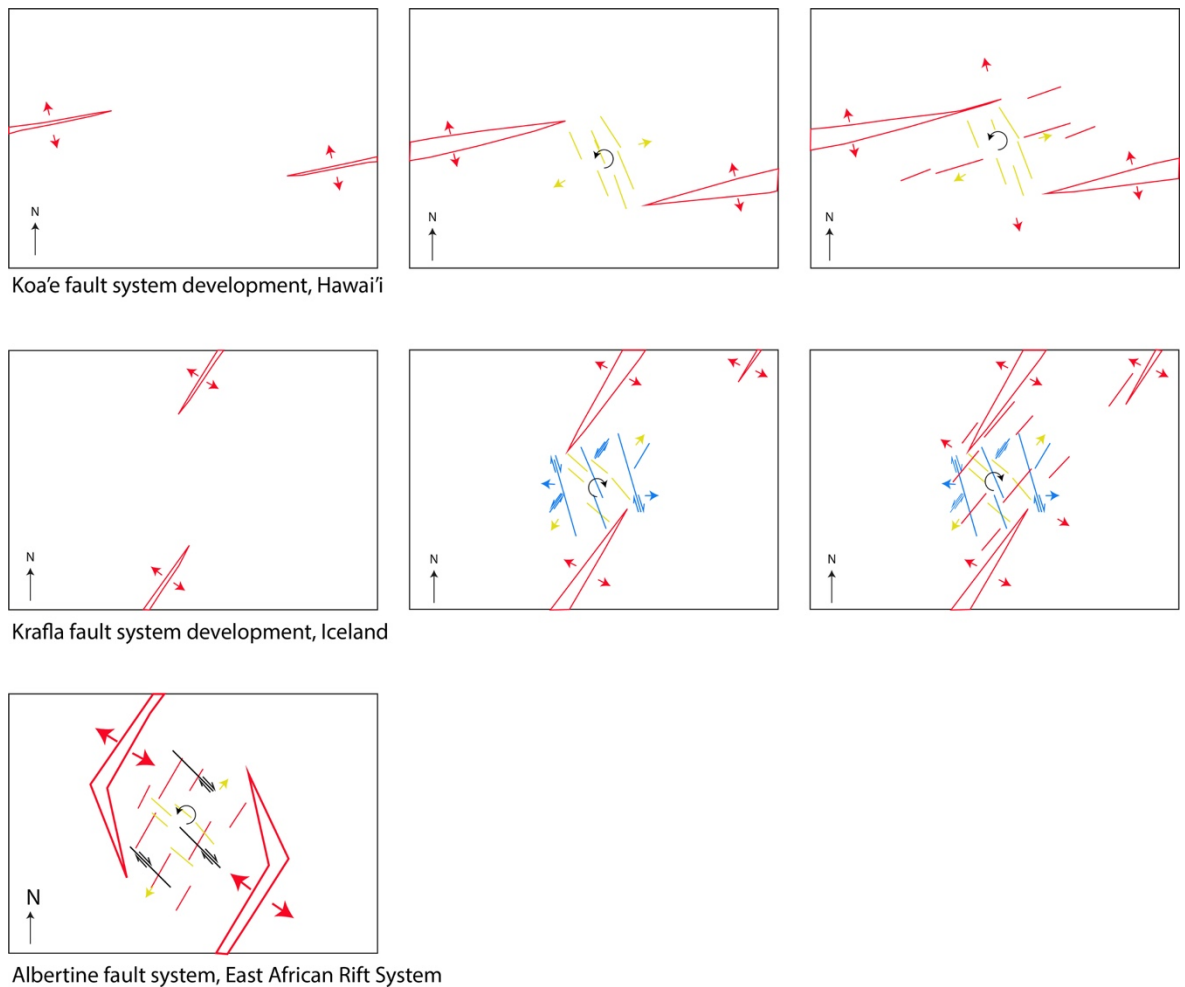


**Figure 8-13 Conceptual diagrams of the Koehn and Bubeck et al models. The main opening directions are highlighted by red arrows with the orientations generated as result, marked in red, yellow and dark red. Notice the similarity between all three localities.**

The examples presented in the Koehn and Bubeck models demonstrate very similar fault orientations and agree with analogue models of Tentler and Acocella, (2010). In Hawai'i Bubeck et al (2017) demonstrate two main fault directions; ENE-WSW (rift parallel) faulting which accommodates NNW-SSE extension and NW-SE (rift oblique) faulting which accommodates NE-SW extension (Figure 8-13).

In Iceland Bubeck et al (2017) demonstrate three main fault orientations; NNE-SSW (rift parallel) faulting which accommodates WNW-ESE extension, NW-SE (rift oblique) faulting which accommodates ENE-WSW extension and WNW-ESE (rift normal) which accommodates NNE-SSW extension (Figure 8-13).

In the EARS, Koehn et al (2008) demonstrated two main fault directions, these are similar to the Krafla model presented by Bubeck et al. The main orientations are; NNE-SSW (strike slip dominated) and ESE-WNW (normal dominated) with an additional minor set trending NW-SE (dextral strike slip and a normal component)(Figure 8-13).

The similarities between each of these faulting patterns indicates that the processes that produce them occur in numerous rift settings. According to Bubeck et al (2017) each of the areas have these in common;

- Segmented bounding faults
- Obliquely oriented fault structures that develop progressively and accommodate non-coaxial strains
- Rift zone parallel connecting faults

The Koehn/Bubeck model can be applied to the HF in southern Iceland. The Reykjanes Ridge propagates NE and its onshore expression is the WVZ; the opposing plate boundary zone is the EVZ which propagates SW (Figure 8-1). These overlapping rift segments are right-stepping, which would generate an anti-clockwise vertical rotation of the Hreppar Microplate (Einarsson, 2008) and a similar fault pattern to those described before (Figure 8-14). In this model, faults that strike parallel to the rift ( $33^{\circ}$ - $56^{\circ}$  and  $213^{\circ}$ - $236^{\circ}$ ) would accommodate regional WNW-ESE extension (Figure 8-15). Rift oblique striking faults with a strike of

between  $247.5^{\circ}$ - $292.5^{\circ}$  and  $067.5^{\circ}$ - $112.5^{\circ}$  would accommodate a shortening component along the rift axis and extension oblique to the regional extension direction (Figure 8-15). Faults that strike at a relatively high angle to the rift axis (those with a strike of between  $\sim 123^{\circ}$  -  $146^{\circ}$  and  $213^{\circ}$ - $236^{\circ}$ ) would accommodate extension parallel to the rift, and counteract the shortening caused by rift oblique structures (Figure 8-15).

When the modelled orientations are plotted on the HF map, there is a remarkable correlation between the model and orientations observed in the field (Figure 8-15). As with the model, the dominant faults within the area are rift parallel (red) which according to the model should be normal faults. Although field evidence for these faults is relatively poor, where normal faults are obviously present, they tend to have a strike of between  $33^{\circ}$ - $56^{\circ}$  and  $213^{\circ}$ - $236^{\circ}$ . In the HF where dykes are present these generally have a strike of between  $123^{\circ}$  -  $146^{\circ}$  and  $213^{\circ}$ - $236^{\circ}$  which fits with the modelled extensional fractures (yellow).

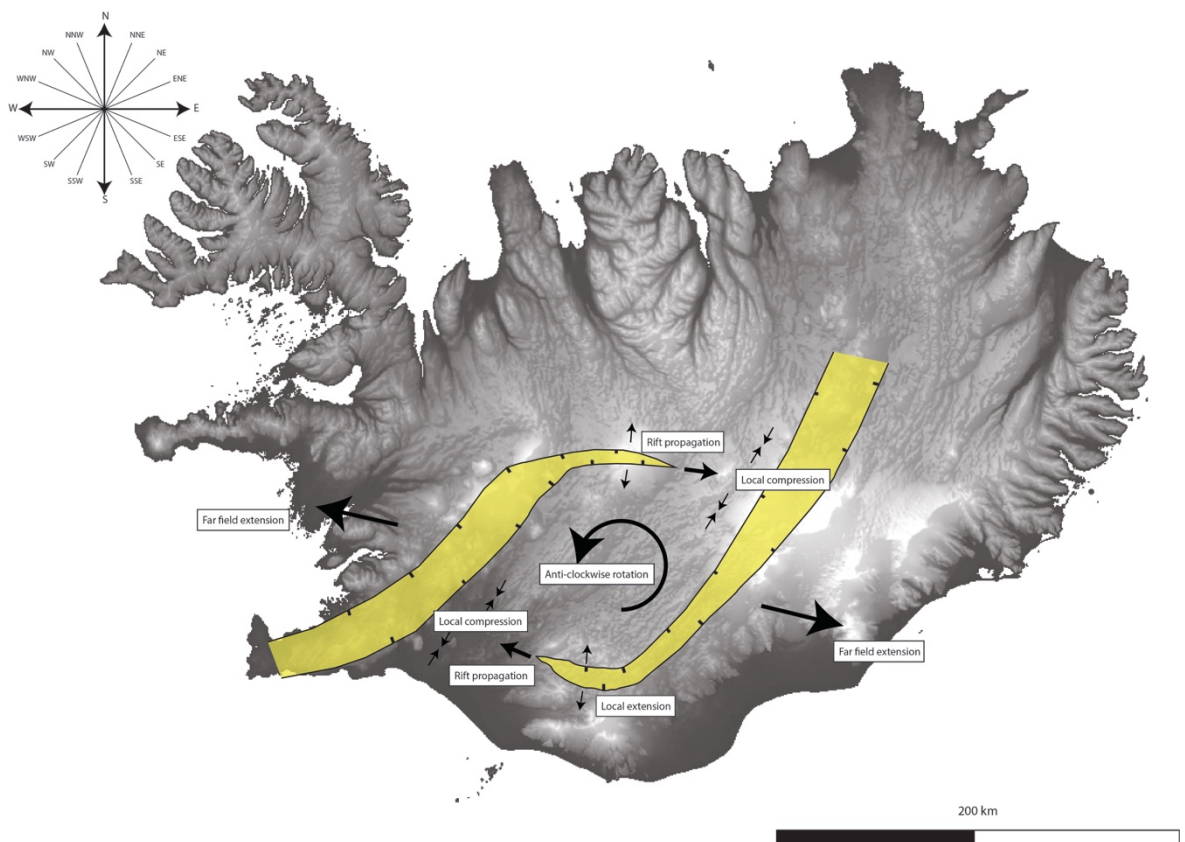


**Figure 8-14** Koehn 2008/ Bubeck et al model. The general direction of opening and closing in Iceland, creating an anti clockwise rotation in the Hreppar microplate. (After Koehn 2008).

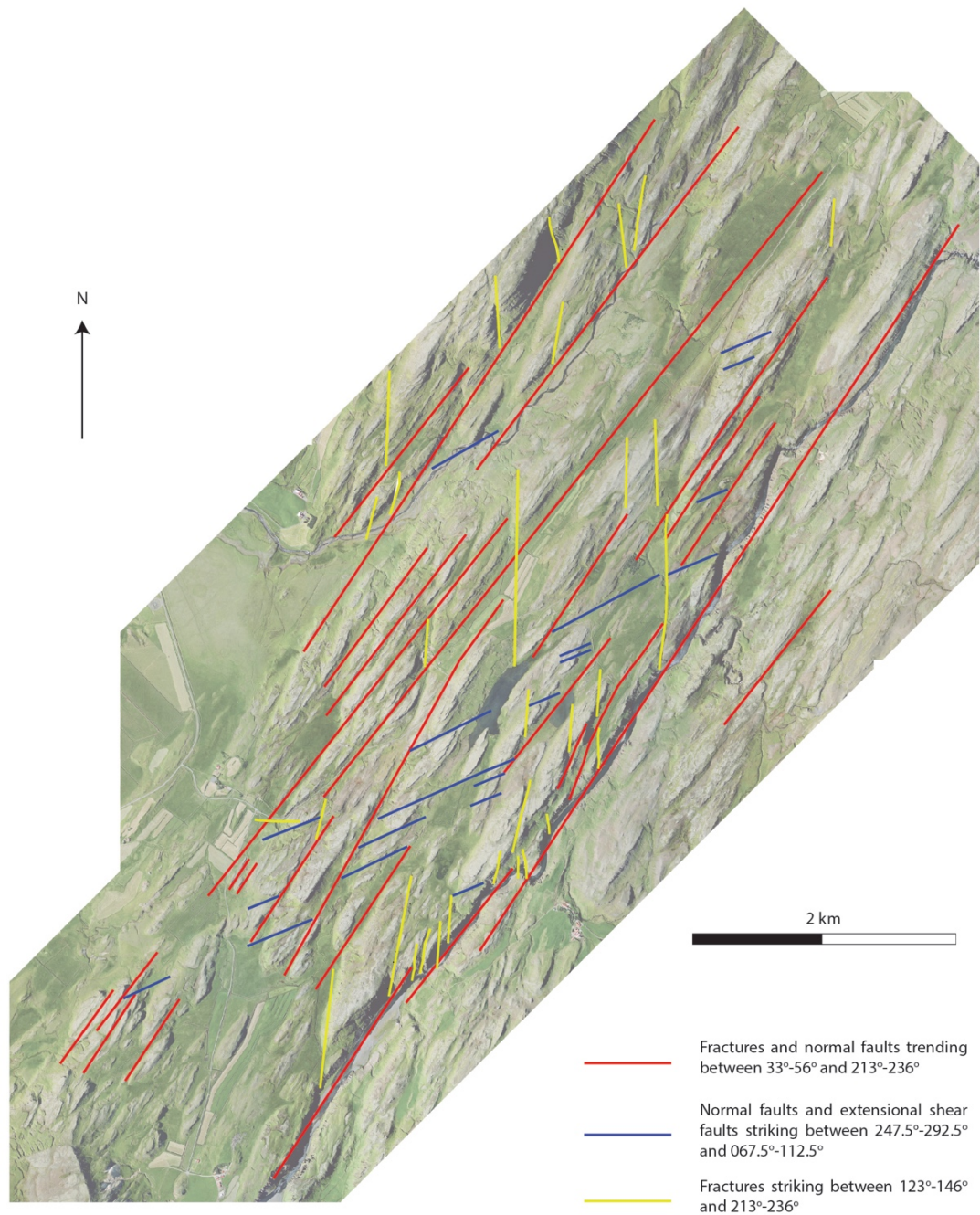


**Figure 8-15** Koehn 2008/ Bubeck et al model. Fractures and faults trending between  $33^{\circ}$ - $56^{\circ}$  and  $213^{\circ}$ - $236^{\circ}$  appear to be the dominant set when overlain the aerial image.

## 8.6 Passerini, 1997 model

Passerini et al, (1991, 1997) model suggests that a high occurrence of faults parallel and sub-parallel to rift axes in Iceland are strike slip. The presence of strike slip faults and normal faults is explained through varying stress fields and a combination of movements on the rift. Passerini et al used field examples from East Africa and Iceland (specifically around western, south central and south eastern Iceland) to try and explain the complex faulting patterns observed in these areas. The area they focus on in south central Iceland has a few localities which surround the HF at Flúðir to the east, south and west.

In these areas, Passerini et al (1997) recognise the lozenge shaped outcrops highlighted by faulting. They also state that the regional tectonic trend is between  $35^\circ$  and  $40^\circ$  E and the faults generally strike towards the NE ( $045^\circ$ ), with smaller faults striking ENE ( $067.5^\circ$ ) and N-S ( $000^\circ$ ). Strike slip faults are common in the area according to Passerini et al, who suggest they strike mainly NE. NNE striking faults accommodate right lateral strike slip motion, with ENE striking faults accommodating left lateral strike slip motion (Figure 8-16). These strike slip faults are produced through axial compression (Passerini et al, 1997).

The fault pattern that is observed in south central Iceland and the HF at Flúðir is formed as a result of two different stress regimes; rift parallel shear and rift parallel compression (Passerini et al, 1997). The axial compression according to Passerini et al (1997) created conjugate sets of right lateral (NNE) and left lateral (ENE) strike slip faults. Passerini et al (1997) explain that axial shear can form as the result of differences in directions of extension on rift segments and as a result of lateral displacement between the major lithospheric plates. Axial compression could have resulted from imbalances between lithospheric spreading and mantle upwelling, although this hasn't been proven in Iceland, or could have been generated as the result of rift-oblique transform shear.

Passerini et al (1997) state that the data they have presented is not enough to actually determine in what order the faults formed, but note that strike slip and oblique slip faults alternated. This is unlike the model presented by Koehn/ Bubeck et al, as in their model all fault orientations can occur at once, whereas the Passerini model suggests that a switching of stress regimes needs to occur.

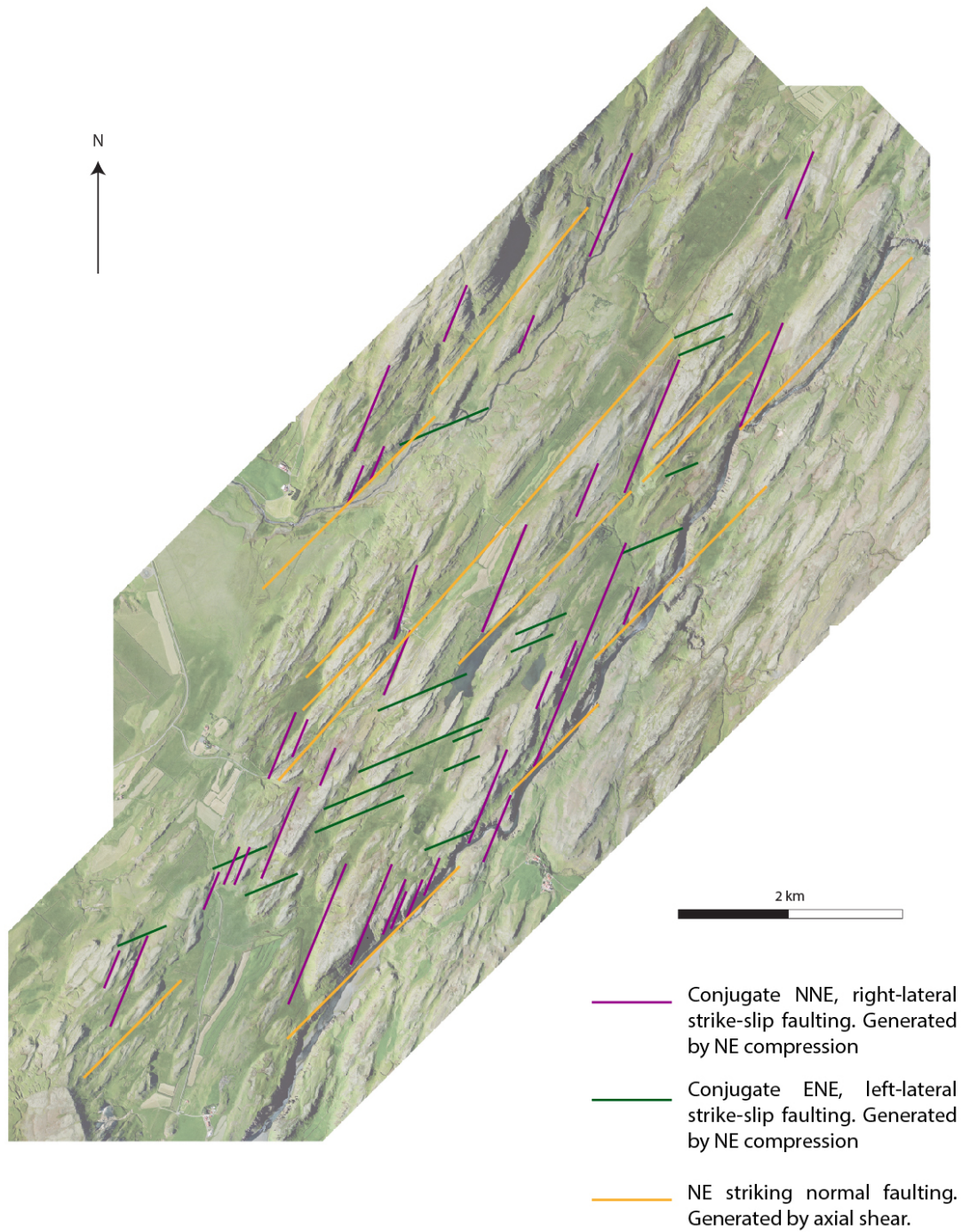


**Figure 8-16** Passerini et al 1991, 1997 model. When the model is applied to the aerial image in the HF, the fault orientations do not match as well as in the Koehn 2008/ Bubeck et al model.

## 8.7 Clifton and Kattenhorn, 2006 model

Clifton and Kattenhorn, (2006) focused on the Reykjanes Peninsula, an onshore expression of the Mid Atlantic Ridge. They use this area to understand the faulting pattern generated within the peninsula. The faulting pattern within the peninsula is very similar to that observed in the HF and the model can be applied here.

The Reykjanes Peninsula plate boundary zone is oblique ( $\sim 30^\circ$ ) to the direction of rifting, and as a result accommodates left lateral shear and extensional strain (Clifton and Kattenhorn, 2006). This is very similar to the SISZ, which is an E-W striking transform boundary system that accommodates left lateral shear. The area to the north of the SISZ (Hreppar Formation) is moving towards the west with the North American plate, whereas the area to the south of the SISZ is moving towards the east with the Eurasian plate (Sigmundsson et al, 1995) (Figure 8-1). As a result of this left lateral motion on the SISZ, the N-S striking faults accommodate this left-lateral motion through right-lateral bookshelf faulting (Sigmundsson et al, 1995; Clifton and Kattenhorn, 2006). Sigmundsson et al, (1995) conclude that there has been a left lateral transform motion throughout historical times.

Clifton and Kattenhorn (2006) modelled left lateral transform zones, using a clay model. In their experiments, 3 main sets of faults were produced (Figure 8-17): (1) rift perpendicular right lateral oblique slip faults; (2) rift subparallel left lateral oblique slip faults; and (3) normal faults striking at  $20^\circ$  to the main trend of the rift. However, Clifton and Kattenhorn, (2006) acknowledge that their models do not account for other factors such as proximity to volcanic centres, occurrence of magmatic activity and the associated variability in the stress and strain fields, change in orientation of the rift orientation, reactivation of old structures and the development of fractures, hence these orientations and types of faults may underestimate the complexity within the Reykjanes Peninsula and in other natural systems, such as the HF.

Within the Reykjanes Peninsula Clifton and Kattenhorn, (2006) state that the orientation of the volcanic fissure swarms is a result of oblique motion at the plate boundary on the 10's of km scale, however they note that on a smaller scale the fractures within the fissure swarms are highly variable. Associating a single strain

direction with these fractures is very difficult. This is probably the case also for the HF, where no one strain direction has generated the outcrop pattern, but a series of different strains.

According to Clifton and Kattenhorn, (2006) fractures that strike between  $000^{\circ}$  and  $020^{\circ}$  are primarily right lateral strike slip faults (Figure 8-17) and are considered active and are predominantly where the major earthquakes in Iceland occur. These faults typically have a faint surface manifestation and are mainly highlighted by smaller en echelon NE striking fractures. NE striking fractures are a common occurrence in the HF and could be the result of these right lateral, strike slip faults.

Models for infinitesimal displacement predict that a principal extensional strain direction oriented half way between the displacement vector and the normal to the plate boundary. When this model is applied to the Reykjanes peninsula (a left lateral transform zone striking E-W), this creates extensional strain oriented  $45^{\circ}$  clockwise. This in turn would produce right-lateral movement along N-S strike slip faults and would produce normal faults, striking NE. Clifton and Kattenhorn, (2006) have proven this modelled theory to be accurate.

According to Clifton and Kattenhorn, (2006) when the extensional component of the absolute plate motion is accommodated during magmatic periods, the principal extensional shear direction becomes oriented  $60^{\circ}$  to the zone of spreading. This would result in normal to right lateral oblique slip movement on NE to ENE striking faults. Therefore, this would most likely occur during periods of volcanic activity.

Clifton and Kattenhorn, (2006) suggest that strike slip faulting is dominant during periods of volcanic quiescence, whereas normal faulting dominates during periods of volcanic activity. They note however that all fault types will be active to a certain extent during volcanic activity and quiescence, depending on the relative orientations of the principal strain and fracture strike at any point in time. They cite examples where individual faults show variable slip histories. This is again applicable to the HF.

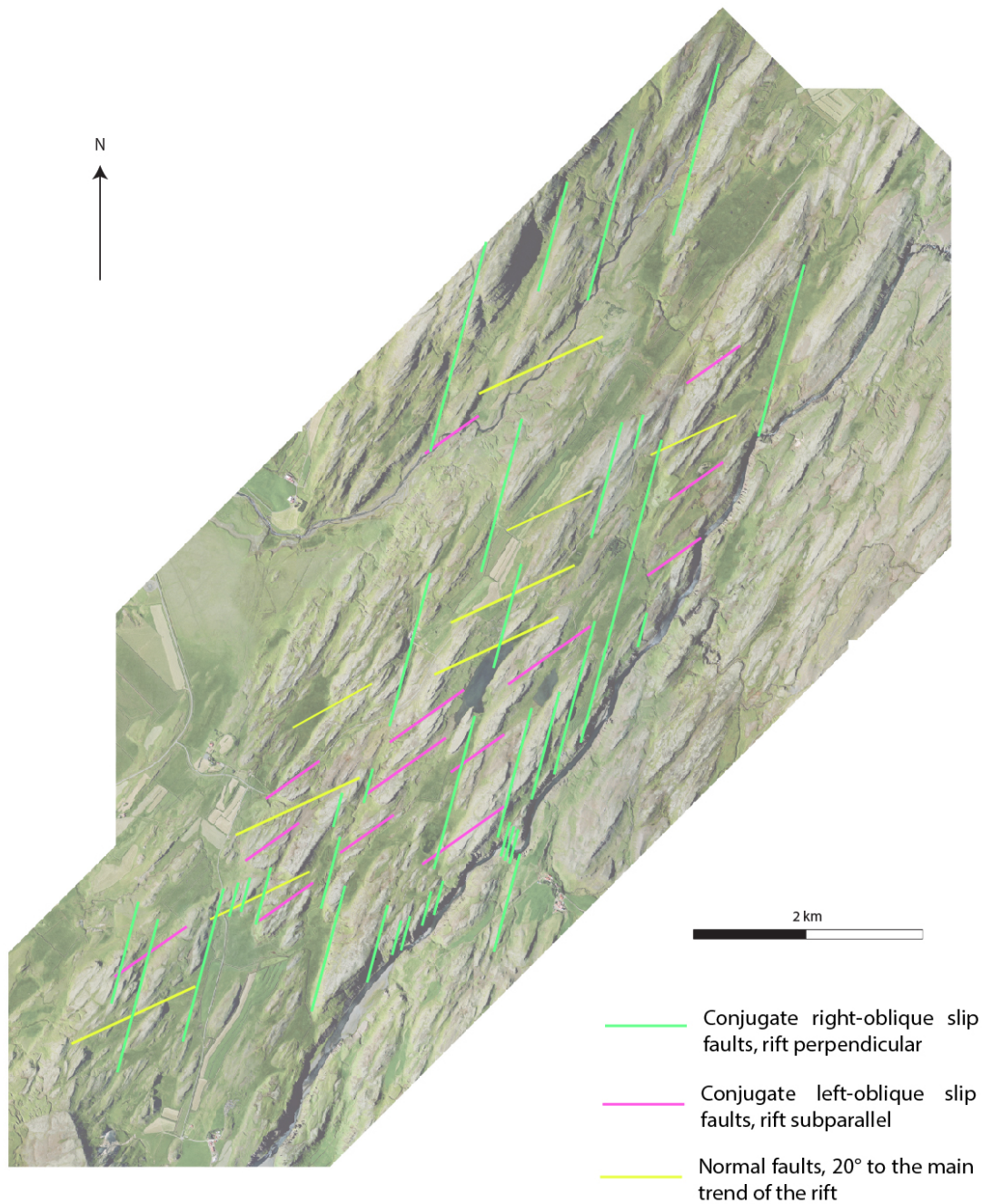


**Figure 8-17** Clifton and Kattenhorn modelled faults and fractures applied to the HF. The dominant fault set appears to be rift perpendicular, right-oblique slip faults.

## 8.8 Tectonic summary of the Hreppar Formation

Each of the models presented predict fault and fracture sets that are similar to those observed in the HF (Figure 8-18). The main differences between the models and observed fault and fracture sets concern the timing and kinematics of individual fault sets. Based on the geometries and in the absence of kinematics (due to lack of good exposure), each of the models could be applied to the HF. Based on the evidence presented here, the favoured model is the Koehn/Bubeck model as this has been demonstrated to fit the data and outcrop pattern best, however, further work needs to be done to confirm this is the most accurate representation of the underlying structure within the HF.

Regardless of the model, it is clear that the area is structurally complex, with multiple, potentially simultaneous, fault sets formed throughout the depositional history of the area. The individual models become important when considering the juxtaposition of individual units, and specifically for prediction of the subsurface, and the magnitudes of displacement required to achieve the observed apparent displacements.

Local effects within the HF such as topography and volcanic centres which would alter near-field stress perturbations and will affect the far field stress state (Stephens et al, 2017; Muirhead et al, 2017), the stress distribution and depth, differing lithological units, differences in mechanical properties of units, pre-existing structures and directional variations in material properties, could all play a role in the underlying structure of the HF (cf, Holland et al, 2006; Walker et al, 2012; Bubeck et al, in review). Within the HF, different lithological units are found in the centre of the area compared with the margins (map insert, e.g. Figure 8-12) these also typically have varying thicknesses, which could affect fluid flow due to the differing material properties (Walker et al, 2013). Thickness and depositional history variations across the study area suggest that the fault sets represent growth faults, and these buried structures may have been reactivated multiple times. Understanding the structural framework of a volcano sedimentary setting is key to predicting where different units may occur. In an offshore hydrocarbon setting this is particularly important as it will aid location of potential reservoir, source, trapping mechanism and allow fluid flow to be determined.

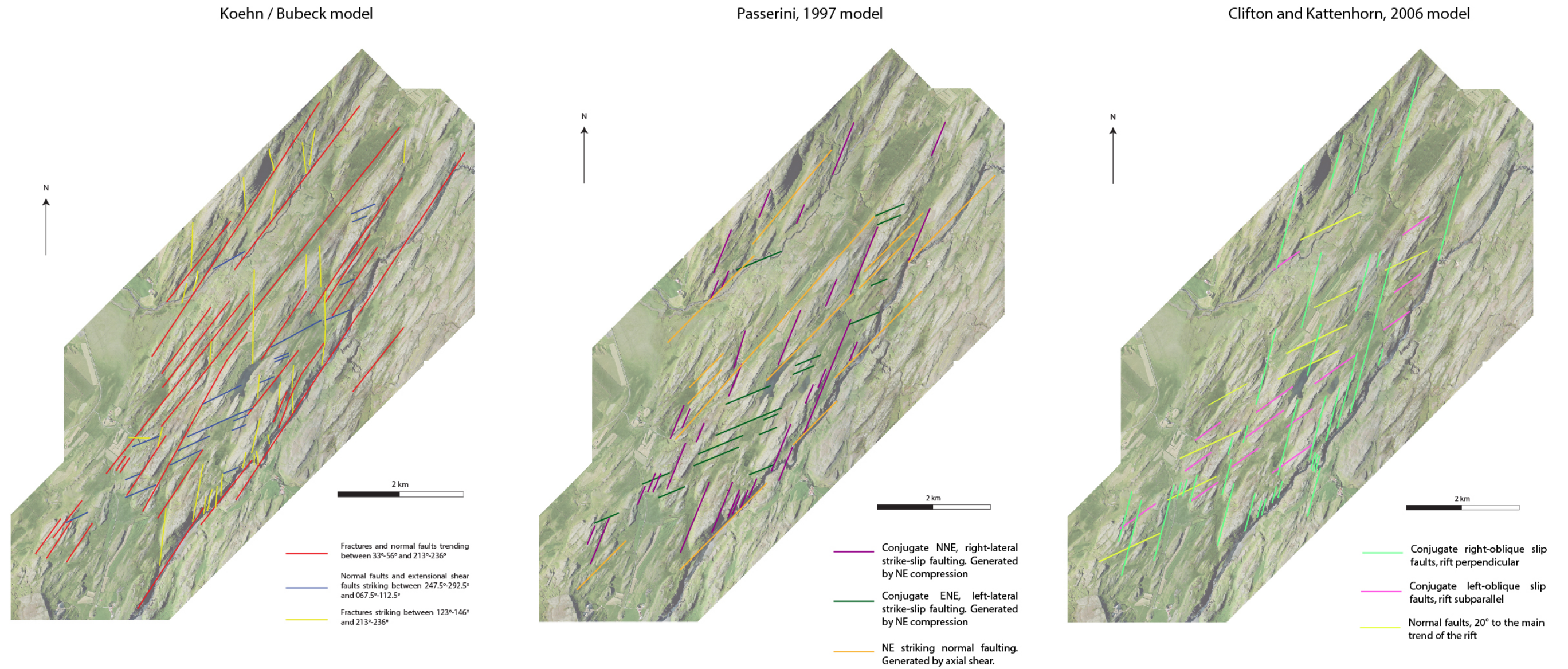


**Figure 8-18 Summarised models of Koehn/Bubeck, Passerini and Clifton and Kattenhorn.** This is a side by side comparison of the different models that have been applied to the HF. Each of the models fits the data within the HF, further work would be required to accurately determine which model is most appropriate.

## 8.9 Conclusions

- The HF is situated between the Eurasian and North American Plates on its own microplate called the Hreppar Microplate. This has resulted in a structurally complex evolution of HF.
- Within the HF field area there is a lack of direct evidence for faulting, however there is abundant indirect evidence as demonstrated here.
- Three models have been presented to understand the underlying structure within the HF. Each model has valid arguments and all three could be applied to the HF based on the evidence observed within the field.
- The favoured model is the Koehn/Bubeck model as this fits the presented data best, however, further work would be required to fully understand the structural history of this complicated area of Iceland.

## 9 Discussion

### 9.1 Introduction

This project has combined a variety of field and lab based techniques to demonstrate that the interaction between volcanic and sedimentary systems in volcanic margin settings produces complex lithofacies architectures. These settings are well known; however, detailed studies are rare. The research presented here on the HF highlights the need to better understand the interaction of these systems in order to successfully explore for hydrocarbons in lava dominated settings. This chapter focusses on the general conclusions of the project and also makes suggestions for future work.

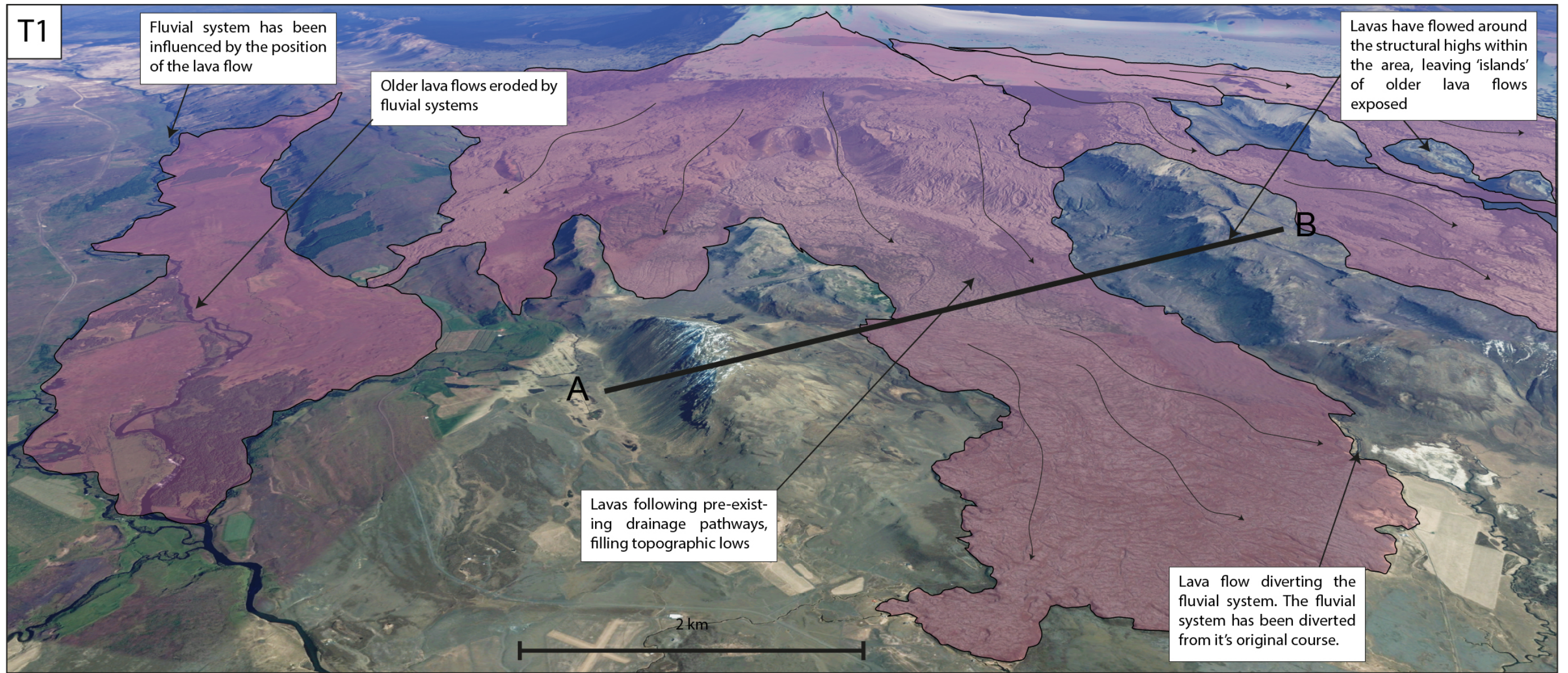
### 9.2 Volcano-sedimentary settings away from the HF

Volcano-sedimentary settings occur all over the world and within these settings various products of the interaction between these systems are found. This final chapter uses examples from Iceland and Ethiopia to highlight how common and complex the lithofacies architectures of these systems are and to compare and contrast with the HF. The HF may actually be more predictable than other volcano-sedimentary settings if the underlying structure can be accurately determined. Where there are no structural controls in other areas, these may be more problematic to predict.

#### 9.2.1 Höfðasandur, Iceland

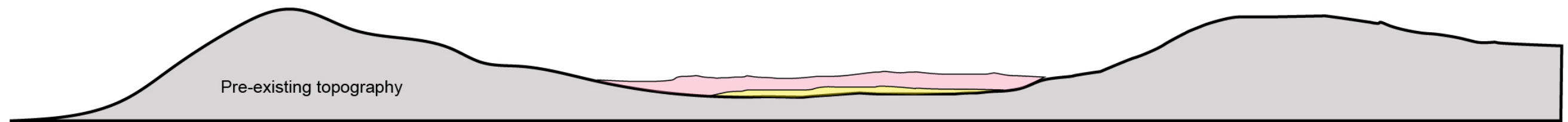
The first area is Höfðasandur, 25 km SE of Flúðir. This area has been chosen to highlight how different systems can interact and produce complex lava fields. A series of three images (Figure 9-1, T1, T2, T3), which hypothesize how the lava field around the village of Höfðasandur may develop with time and interact and influence the surrounding geology.

The first figure, T1, (Figure 9-1) is the present day aerial imagery of the area with only the most recent lava flows highlighted in pink as these are easy to identify due to the lack of vegetation cover on the lavas. Below the aerial image is a cross section through the area, demonstrating how this 2D view point changes with the



A

B



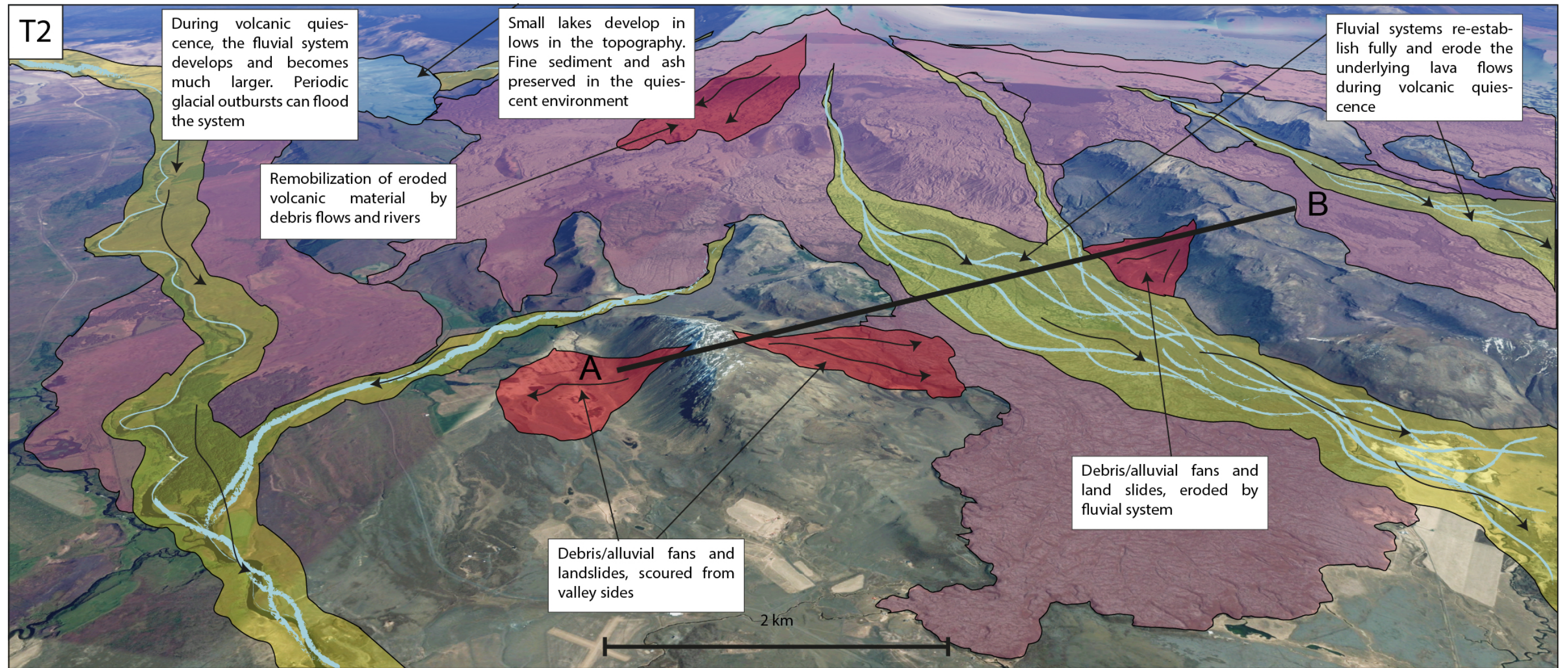
Lavas
  Fluvial sandstones and conglomerates

Figure 9-1 Lava field development around Höfðasandur. Note the lava flows following pre-existing drainage pathways and avoiding the structural highs. The lava on the left hand side of the image has started to be eroded by a small fluvial system that has re-established itself after it was blocked by the lavas. In the cross section from A-B it is hypothesized that a small fluvial system existed before the lavas were emplaced.

interaction of different systems. It also provides a useful comparison with areas in the HF at Flúðir (chapter 7). The lavas tend to follow pre-existing topographic lows such as fluvial systems as these offer a low resistance pathway for the lavas to follow. With continued extrusion of lava, these pathways will fill over time. In following the pre-existing drainage pathways, the lavas have avoided contact with any of the structural highs in the area, which can lead to islands of older geology, surrounded by younger lava flows (Figure 9-1).

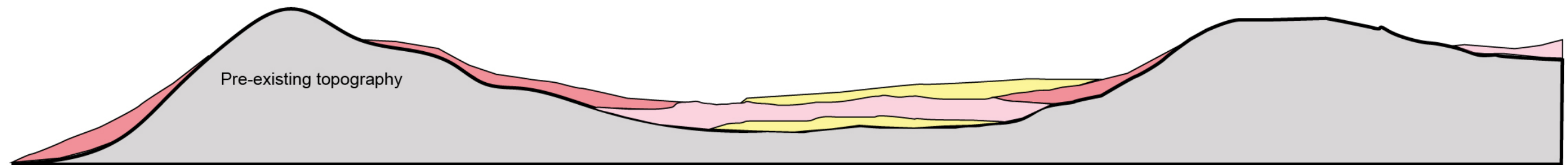
The second image in the development of the lava field (Figure 9-2) highlights how the area could evolve during quiescence in the volcanic system. The quiescence in the volcanic system allows the fluvial systems to re-establish. They could re-establish in the same location in which they previously occupied or they may re-establish in a different location due to lavas altering their course. In the HF at Flúðir there is evidence for both of these, Schofield and Jolley (2013) and Ebinghaus et al (2014) document the same processes occurring in the FSB and Columbia River, respectively. Within Figure 9-2, examples of both are present. With continued volcanic quiescence, the fluvial systems will start to erode the lavas that occupy the previous drainage systems, generating volcanoclastic sediments. These are very common in volcanic dominated settings, with an abundance of these occurring in the HF. In addition to fluvial sediments, these environments can produce debris/mass flow, glacial and lacustrine sediments to name a few. All of these are very common in present day Iceland and lithified examples are present in the HF at Flúðir. In Figure 9-2 examples of where these sediments may occur are highlighted.

The cross section in in T2 (Figure 9-2) indicates how laterally extensive different units can be and how the lithofacies architecture may develop with time. This is the result of just one volcanic and one volcanic quiescent period.



A

B



Lavas
  Mass flow conglomerates
  Fluvial sandstones and conglomerates

Figure 9-2 Continued lava field development around Höfðasandur. With volcanic quiescence, fluvial systems re-establish in valleys and low lying areas. This leads to the deposition of volcanoclastic sediment. The cross section highlights how complex volcano-sedimentary settings can be with laterally continuous and discontinuous units.

In T3 (Figure 9-3), there is hypothesized volcanic activity in the area around Höfðasandur. This volcanic activity temporarily dominates the environment. Where fluvial systems were, lavas take advantage of these low lying areas and quickly dominate the fluvial system. Lavas will also divert the course of other fluvial systems, potentially resulting in water bodies developing in confined areas (Figure 9-3).

The cross section (Figure 9-3) presents a simplification of how complex the architectures can be within a very small area with the contacts likely to be much more heterogeneous.

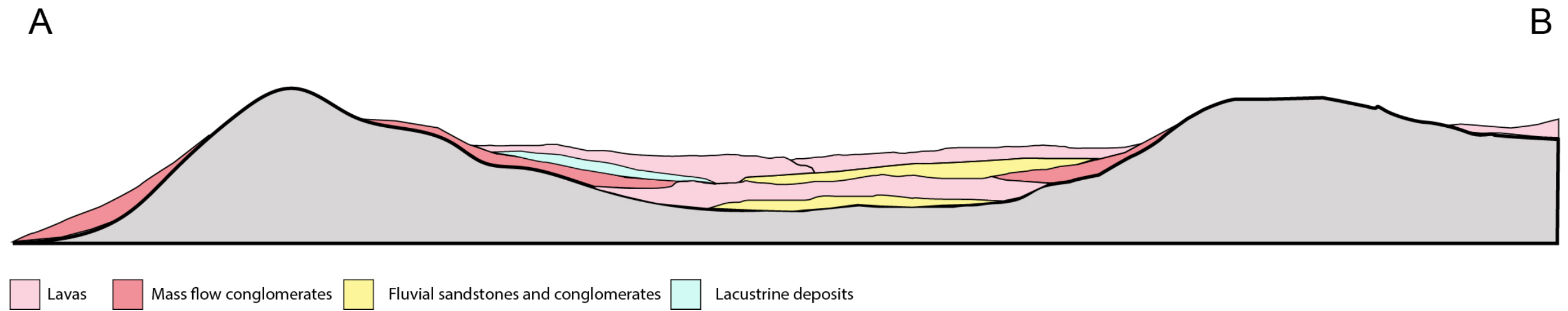
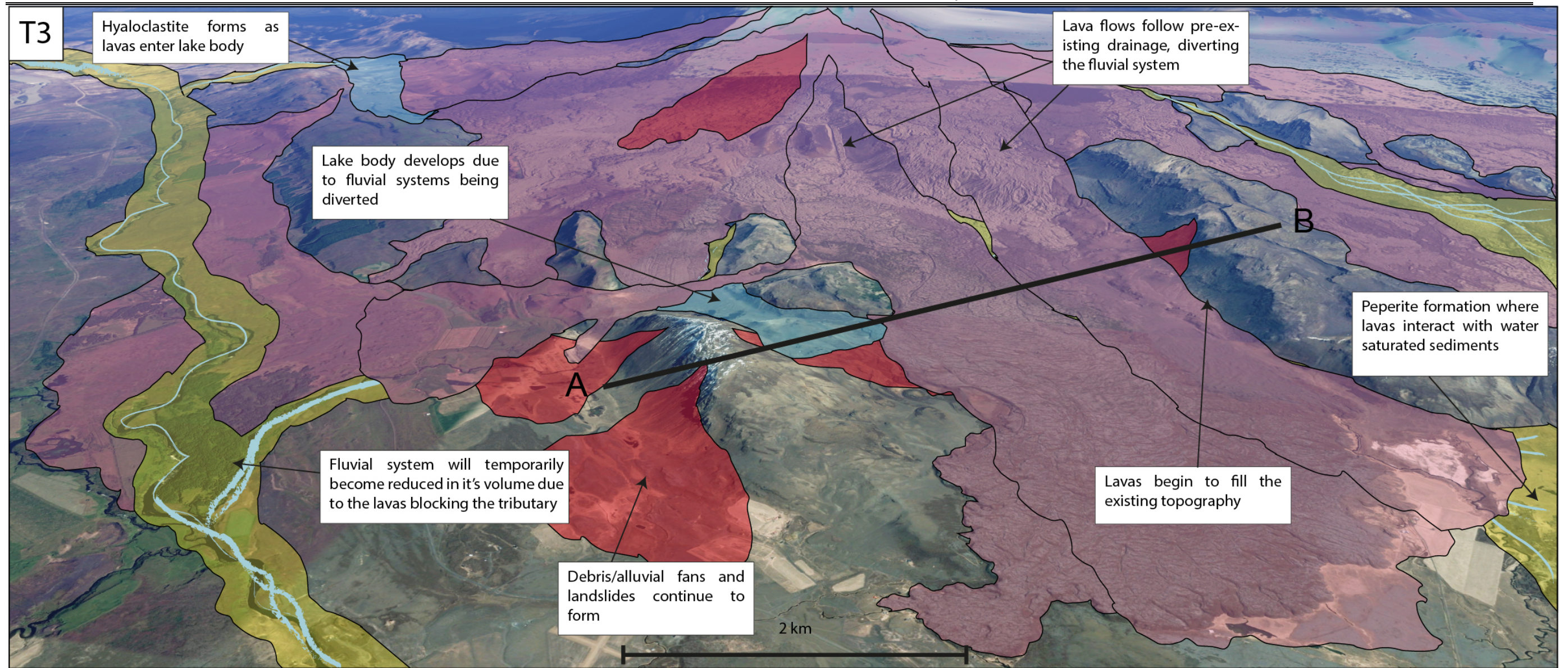


**Figure 9-3** Final stages of lava field development around Höfðasandur. With reactivation of the volcanic system, lavas follow fluvial drainage pathways and interact with wet sediment. The lavas will block and alter the course of the fluvial systems, potentially resulting in the formation of new water bodies.

### 9.2.2 Blue Nile and Afar region, Ethiopia

This series of figures highlights characteristics of lava fields in Ethiopia and demonstrates how these have developed in a very similar way to those described previously. The first figure (Figure 9-4) highlights field examples from Ethiopia and then a series of figures, T1-T3 (Figure 9-5, Figure 9-6, Figure 9-7) displays a hypothetical lava field development in the Afar Region. The purpose of this is to highlight how volcano sedimentary settings develop in a very similar way regardless of their geography.

Figure 9-4 highlights some examples of how lava and sediments interact. In A, lava has been extruded from within a valley and has travelled down this valley following the pre-existing drainage pathway. The fluvial system was completely dominated by the lava, which filled the entire valley. After the volcanic activity had ceased, the Blue Nile fluvial system became re-established and began to erode in to the valley where the lava is situated, widening the valley from its original state. The valley lavas are much younger than the surrounding flood basalt, plateau lavas. The lava within the valley, therefore records the width of the palaeo valley. In this situation, a lava has followed the pre-existing drainage pathway and after volcanic activity has ceased the fluvial system has re-established in broadly the same location. This is very similar to areas in the HF at Flúðir and numerous examples are observed in the FSB (Rosebank), Columbia River and British Palaeogene igneous province (BPIP), (see Passey and Bell, 2007; Williamson and Bell, 2012; Schofield and Jolley, 2013; Ebinghaus et al, 2014; and references therein).

Images B and C (Figure 9-4) highlight the contact between underlying mudstones and thick basaltic lava. In both images the contacts are highly irregular and demonstrate lavas filling low lying areas within the palaeotopography.

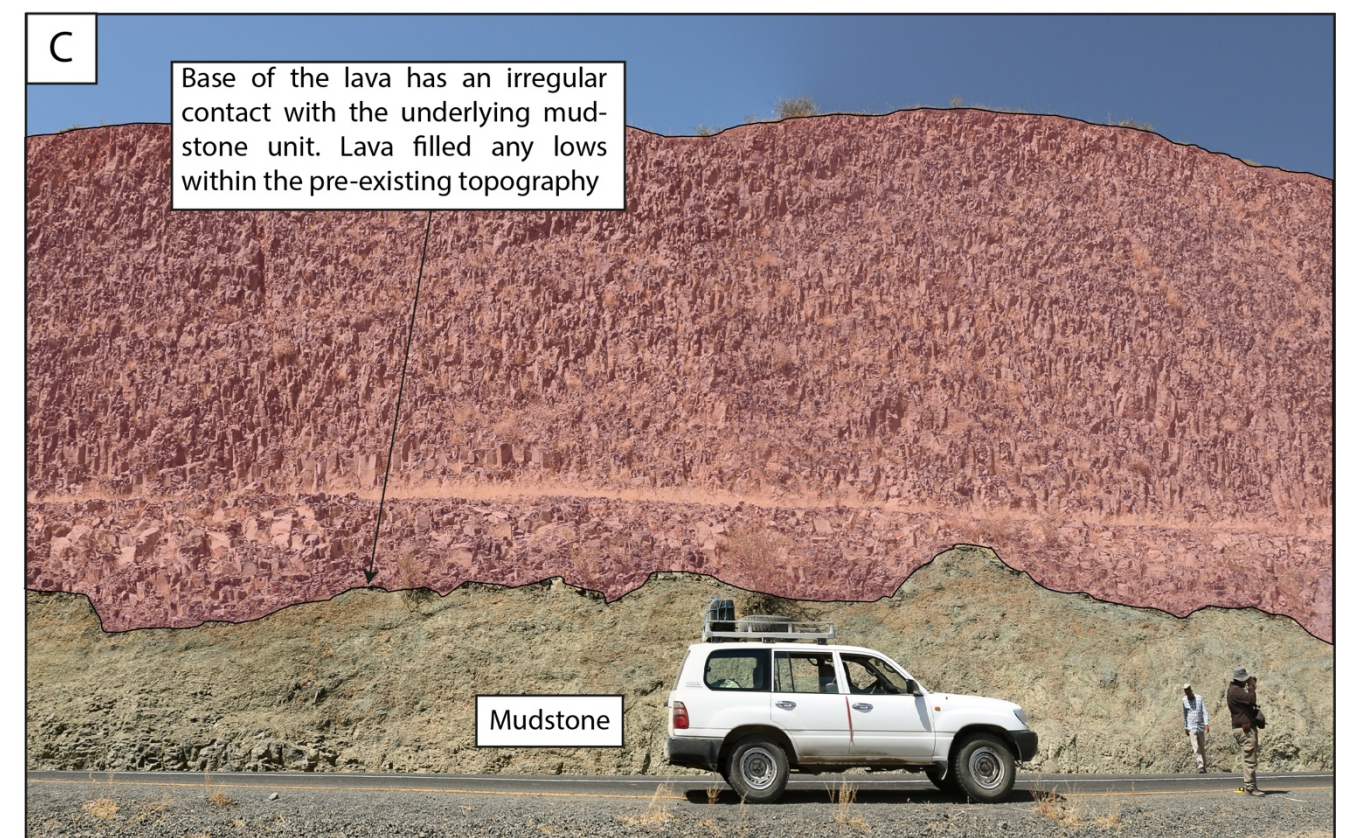
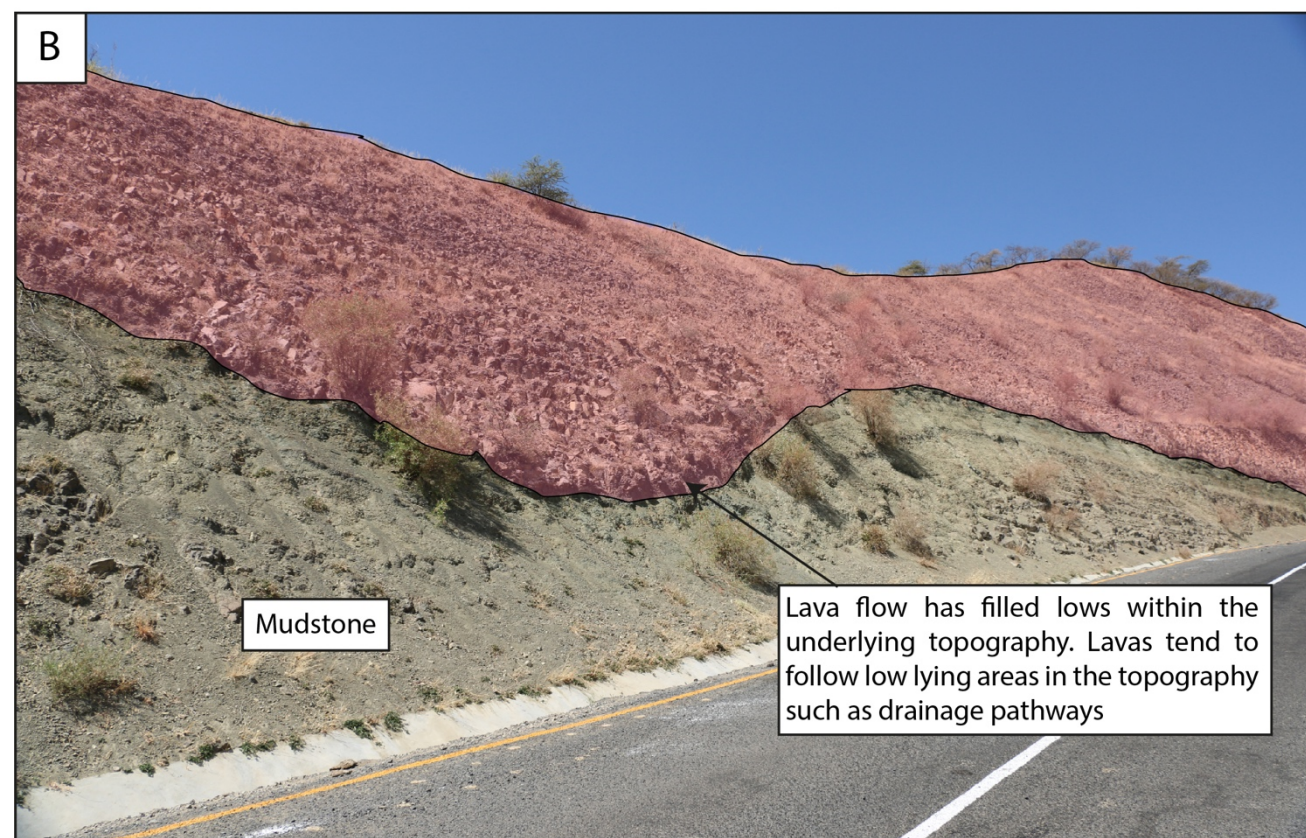
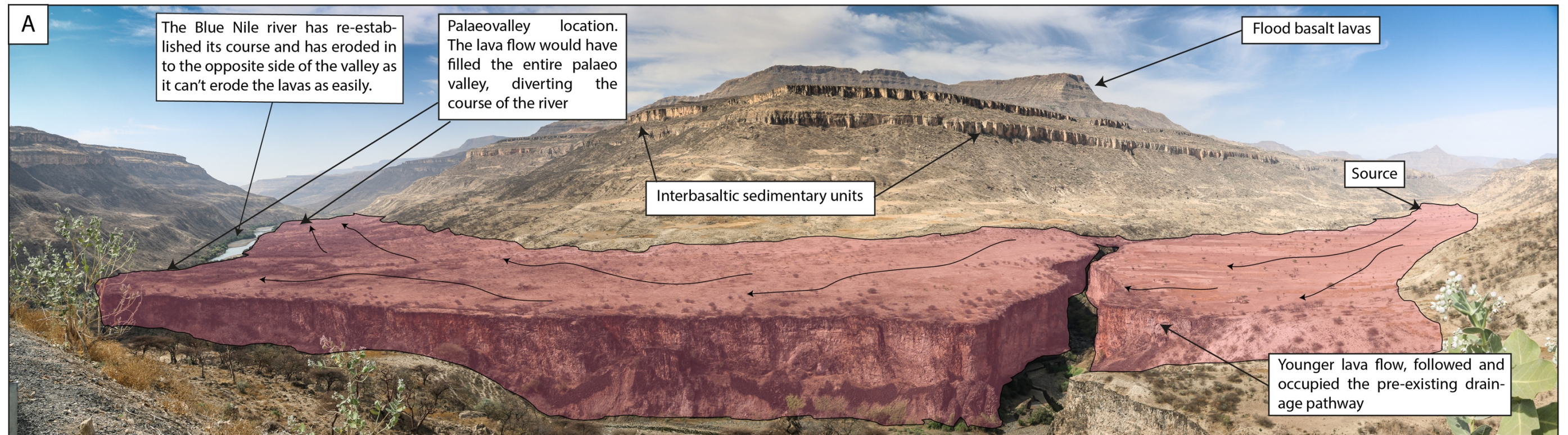


Figure 9-4 Lava field development in Ethiopia. A) Younger lavas have occupied a fluvial drainage pathway, completely dominating the fluvial system and causing it to erode in to the valley side. This demonstrates how lavas and fluvial systems can interact. B+C) Contact between lava flow and underlying mudstone. The lava has filled all the lows within the palaeo topography resulting in an irregular contact between the two different units. This very common in volcano-sedimentary settings.

The 3 figures from the Afar Region T1, T2 and T3 (Figure 9-5, Figure 9-6, Figure 9-7) represent how the volcanic and sedimentary systems may evolve with time. In T1 (Figure 9-5) the most recent lavas are highlighted in pink (these are obvious to pick out as they are very dark in comparison to the surrounding geology, implying they are relatively young) with their obvious travel directions. The lavas have originated from shield volcanoes such as Erta Ale (Figure 9-5) and have followed dried up stream/river beds (the pre-existing fluvial drainage pathways). The lavas have also preferentially flowed to the lowest points in the topography. This is where the ephemeral lake is (Figure 9-5) situated and there could be evidence of lavas having interacted with it previously, generating hyaloclastite. As well as seeking the topographical lows, the lavas have avoided the structural highs in the area, such as other shield volcanoes. This occurs in the HF at Flúðir and the example from the area around Höfðasandur demonstrates the same phenomenon. The scale is relatively large, with one lava flow  $>15 \text{ km}^2$  in width, which is bigger than observed in the HF at Flúðir, but nonetheless the lavas have behaved in the same manner.

In T1 the cross section (Figure 9-5) is relatively simple, with only lava flows highlighted. As the area hypothetically sees more volcanic activity, this becomes more complex.

T2 (Figure 9-6) demonstrates how the area could potentially evolve with continued volcanic activity and ephemeral fluvial systems. Whilst the Afar region of Ethiopia is very dry, there is evidence of ephemeral fluvial systems, most likely occurring during the rainy season. With continued volcanic activity in the area, lavas would continue to seek out the low-lying areas in the environment-such as the valleys created by ephemeral fluvial systems. The lavas would continue to avoid the structural highs and fill in the basinal lows. With time, the ephemeral lake body could grow in size, occupying lows in the topography. This would likely result in lavas interacting with the water body, generating peperite, hyaloclastite and re-worked hyaloclastite (Figure 9-6). Additionally, ephemeral fluvial systems could quickly deposit sediment within the valley in which the lavas occupy. In the future the lavas could interact with the unconsolidated sediment, resulting in a complex interface between the two different units.

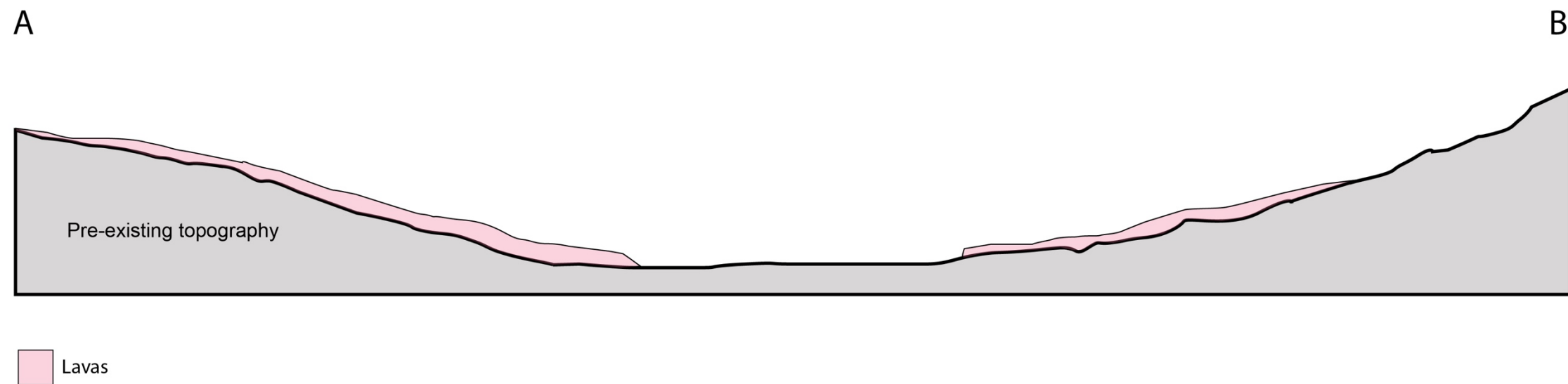
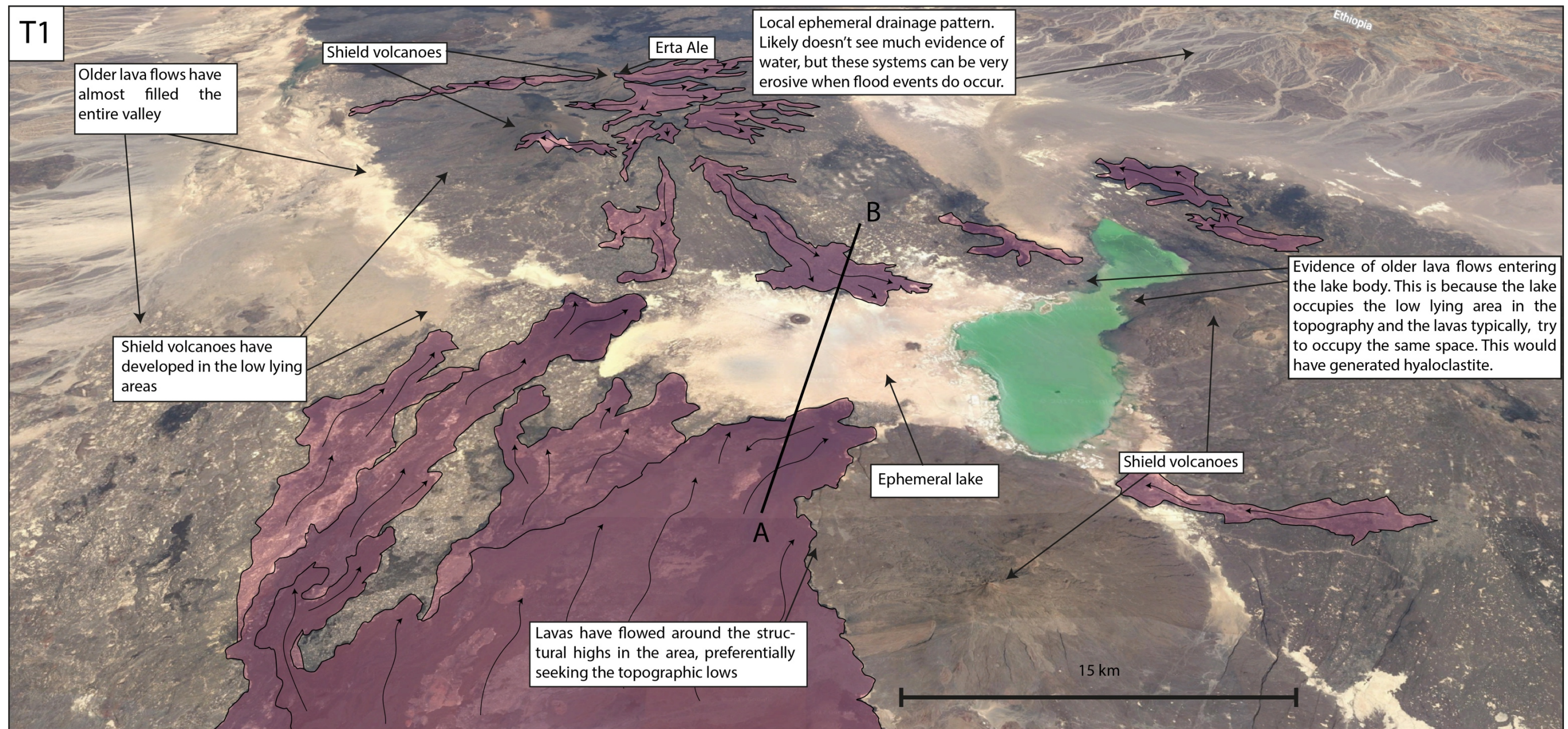
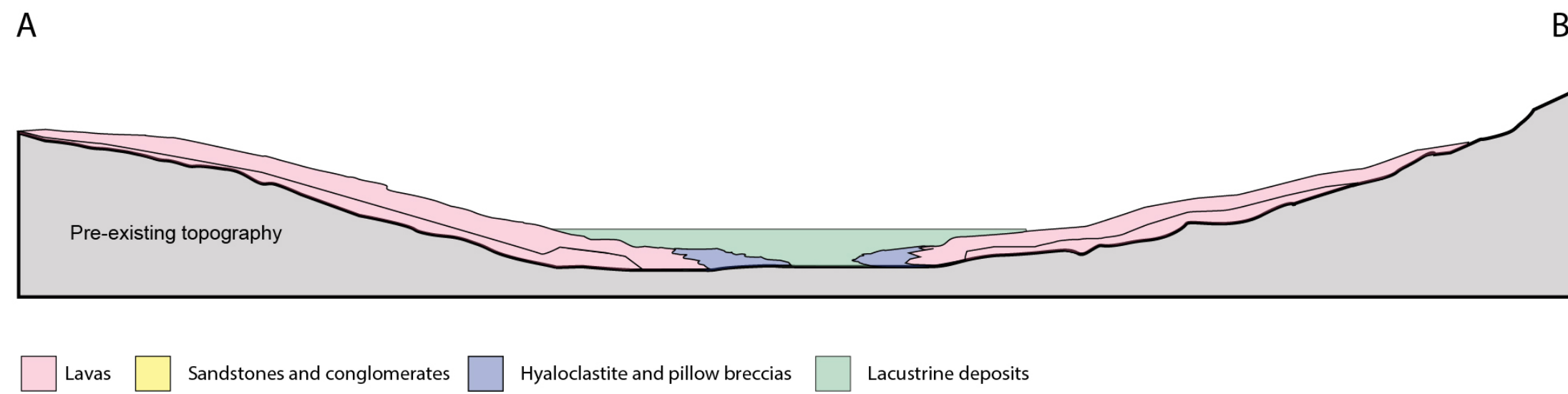
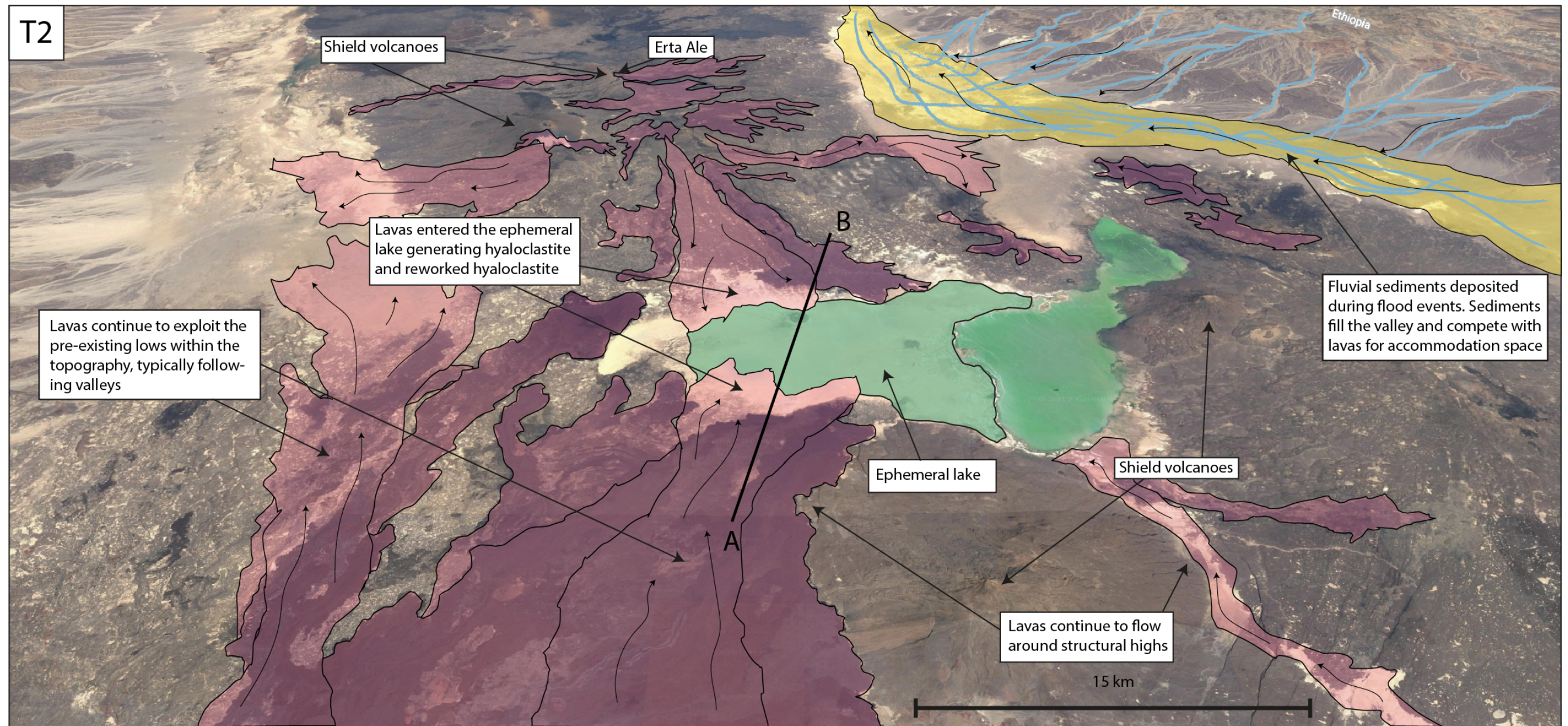


Figure 9-5 Lava field development of the Afar region, Ethiopia. Lavas follow pre-existing drainage pathways and flow towards the low lying areas in the region.



**Figure 9-6 Continued lava field development of the Afar region, Ethiopia. With continued volcanic activity, lavas would dominate the valleys in which previous lavas had flowed. Lavas would continue to seek out lows within the topography, which could result in lavas entering and interacting with water bodies- producing hyaloclastite. Ephemeral fluvial systems, develop during the rainy season, leading to the deposition of sediment.**

The cross section in T2 (Figure 9-6), highlights how hyaloclastite could develop with the continued input of lava in to a water body. It would likely prograde from the hinterland to the foreland as the lava enters the water body, progressively becoming more brecciated as it enters the water, resulting in a hyaloclastite pile. Away from the pile, loose brecciated pieces would become reworked by undercurrents in the waterbody.

T3 (Figure 9-7) represents how the system could further develop during volcanic quiescence. With no volcanic input altering the system, there is time for the sedimentary system to fully develop. During a prolonged period of drought in the area, the ephemeral lake could reduce to its original size, which would leave a large depression in the landscape. With sudden flood events occurring during rainy seasons, building up over time, ephemeral streams would take advantage of valleys, which lavas have exploited. This exploitation of valleys would lead to the erosion of the lavas over time, resulting in volcaniclastic sediments being deposited within the low-lying areas, such as the evaporated ephemeral lake. In addition to volcaniclastic sediments there could also be an abundance of siliciclastic sediments that are incorporated in to the deposits of the ephemeral streams. Modern examples of fluvial systems reworking volcanic units and depositing them within a lacustrine body are common in Iceland and the HF at Flúðir.

The cross section in T3 (Figure 9-7) demonstrates how the fluvial sediments could be deposited within the basin. It is likely that there would be mingling of sediments and lithified lava/hyaloclastite. After lithification of the sediments also, this could lead to complex breccias, evidence of which we see in the HF at Flúðir.

Many volcano-sedimentary settings around the world display similar architectures and detailed geological features such as those observed in the HF at Flúðir and those hypothesized to occur in the area around Höfðasandur. Passey and Bell, (2007); Williamson and Bell (2012); Schofield and Jolley (2013) and Ebinghaus et al (2014) and references therein, all describe how these systems can develop in similar settings. Detailed studies such as those of Brown and Bell (2006, 2007), Watton (2013) and Rawcliffe (2015) and references therein, demonstrate the

---

detailed geological features of these systems. Whilst small scale features may differ between different areas, the overall architectures remain similar.

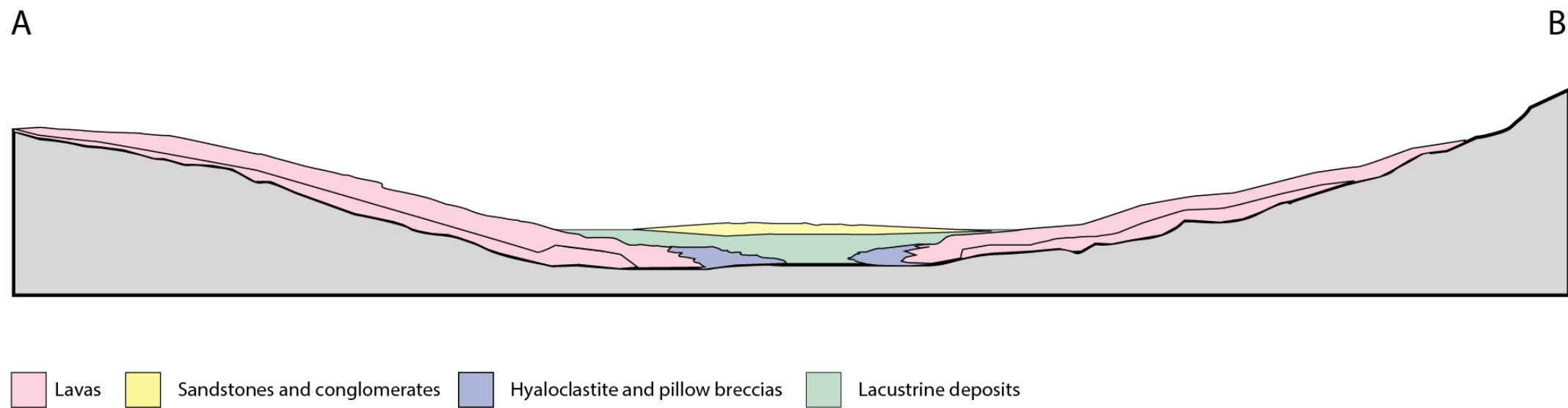
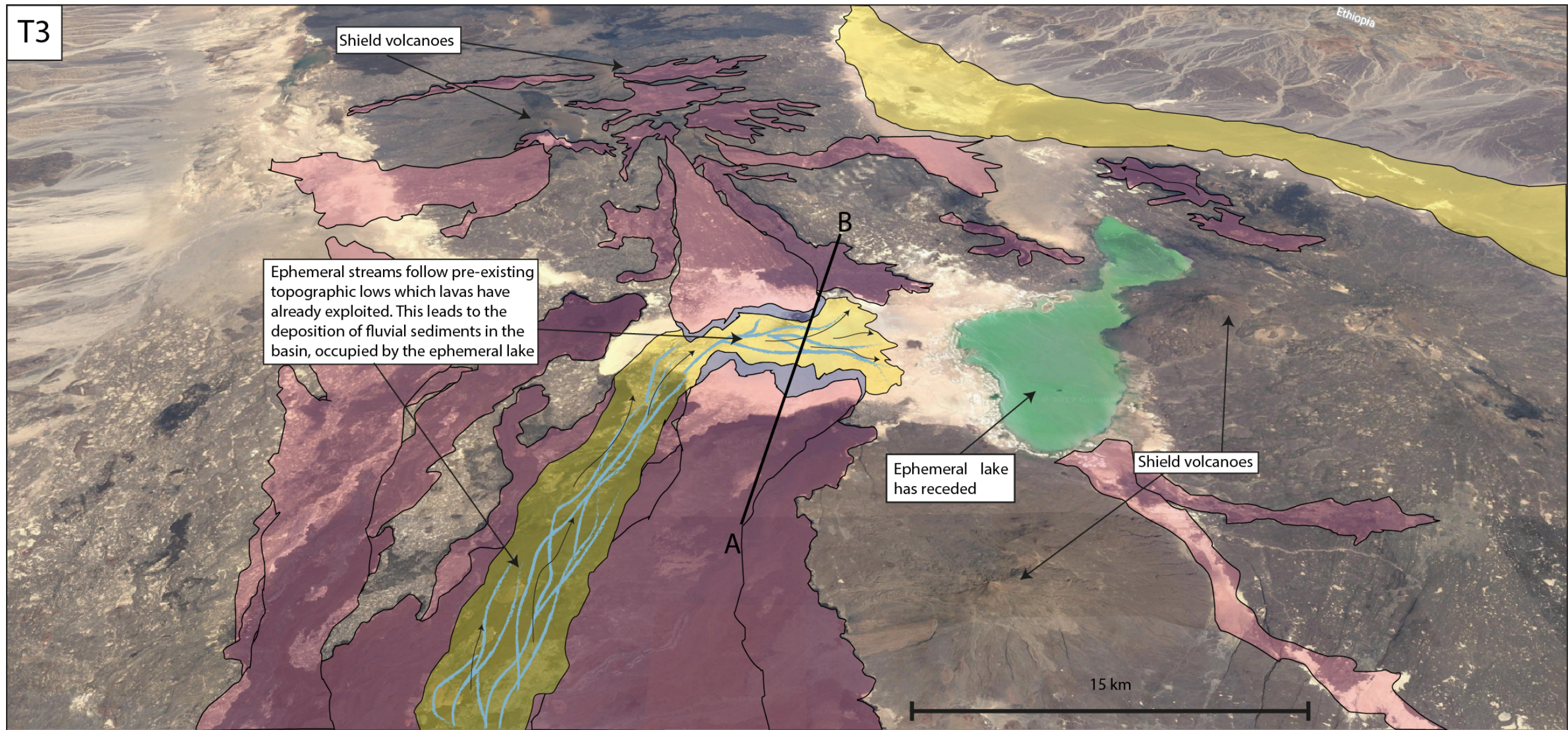


**Figure 9-7** Final stages of lava field development in the Afar region. During volcanic quiescence, fluvial systems can re-establish, often taking advantage of old drainage pathways. This leads to the development of inter basaltic sedimentary units. With lithification and burial, these could potentially become reservoir units for hydrocarbons if the conditions are correct.

## 9.3 Modern analogues; Iceland

The sections within the Stora Laxa river section (chapter 7) and from the rest of the HF can be compared with modern examples from around Iceland to better understand the differing palaeo-environments of the area. The Hreppar Formation is Plio-Pleistocene (3.3-0.7 Ma) in age and therefore relatively young in geological terms. Plio-Pleistocene processes are broadly comparable with modern day processes, and these can therefore be used to support palaeo-environment interpretations.

### 9.3.1 Proglacial lakes

There are numerous glaciers in modern day Iceland and throughout its geological past they have been an important feature. This has led to much research in to glacial processes and deposits within Iceland. The glacial processes and deposits are a very different type of geology and are largely beyond the scope of this project, however there are some aspects that are useful to understand.

Proglacial lakes are a very common occurrence in Iceland. These glacial lakes typically form as a result of melting of stagnant glacial ice, beneath the proglacial surface. The meltwater can be dammed as the result of moraines blocking the drainage or if it drains in to a natural basin (Bennett and Glasser, 2013; Carrivick and Tweed, 2013). As part of this project three proglacial lakes have been examined (Figure 9-8): the Sólheimajökull glacier mouth (part of the Mýrdalsjökull ice cap); Norðujökull and Suðurjökull glacier mouth (part of the Langjökull ice cap); and the Breiðamerkurjökull glacier mouth (part of the largest ice cap in Iceland, Vatnajökull). All of these glaciers have a proglacial lake at their mouths.

This proglacial lake setting was a feature common to the HF during its development as there is direct evidence of glacially derived lakes (Figure 7-24). These settings are complex, with numerous processes occurring at once. Proximity to the ice is the primary control on sedimentation within proglacial lakes (Carrivick and Tweed, 2013). All of the proglacial lakes that have been observed have fluvial inputs in addition to glacial (Figure 9-8). The sediment content within these fluvial inputs is a key controlling factor on sedimentation within

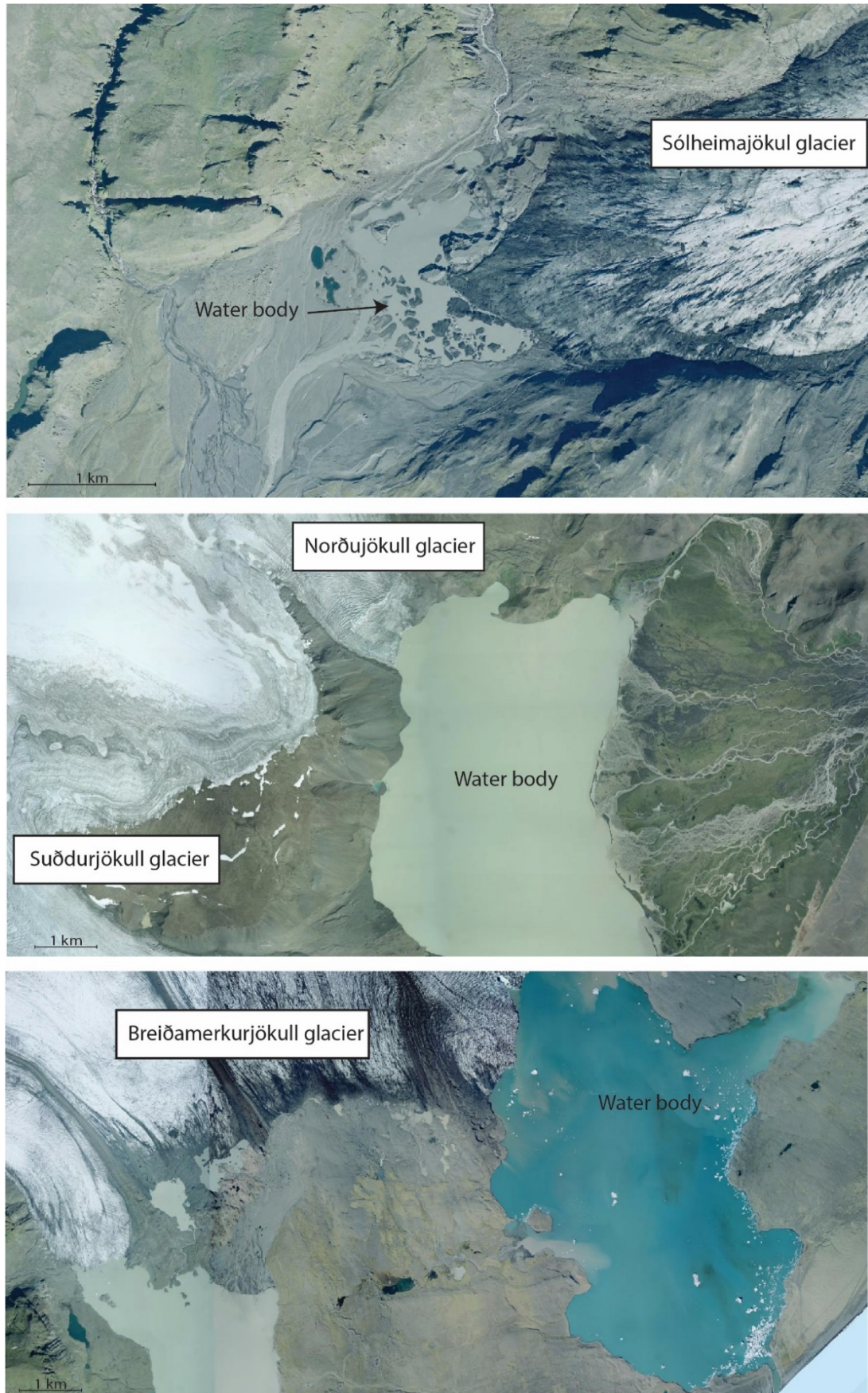


**Figure 9-8** Aerial images of examples of lake bodies developing at the front of glaciers in Iceland. These are a common occurrence in today's lava dominated environment and it is likely they were in the rock record

proglacial lakes (Carrivick and Tweed, 2013). Calving icebergs also play a role in the sedimentation involved in proglacial lakes, depositing rain out material and dropstones. All of these processes can be observed within the Sólheimajökull glacier mouth (Figure 9-9). These sedimentary controls lead to the development of cyclical deposits based on season (Figure 7-28, Figure 7-29), especially in locations such as Iceland, where winters are harsh. Winter inputs typically have less sediment concentration, leading to the deposition of thinner, finer grained units, which is in contrast to spring/summer deposits that have a much higher sediment concentration. This is typically a result of warming temperatures leading to snow melt and rainfall.

Figure 9-10 is a photogrammetry model of the Sólheimajökull glacier mouth with a hypothetical lava flow interacting with this proglacial setting. This hypothetical situation of lavas entering confined valleys and interacting with proglacial lakes is very similar to what would have occurred during development of the HF (e.g. in section 9) (Figure 7-24). The lava would typically follow the pre-existing drainage network and would likely dominate this environment. The interaction of the lava with the proglacial lake would generate primary hyaloclastite and pillow lavas, much like in section 9. In addition to the pillow lavas and hyaloclastite, the lava would potentially dam the fluvial system, as they occupy the same space. Over time this could lead to a sudden jökulhlaup. If the fluvial system was not dammed it could be diverted by the presence of the lavas. The introduction of lavas in to the system would also result in the sediments being preferentially preserved in the rock record.



Figure 9-9 Aerial panorama of the mouth of the Sólheimajökull glacier. The setting is analogous to certain areas within the HF. It is a very dynamic environment with various sources of sediment input

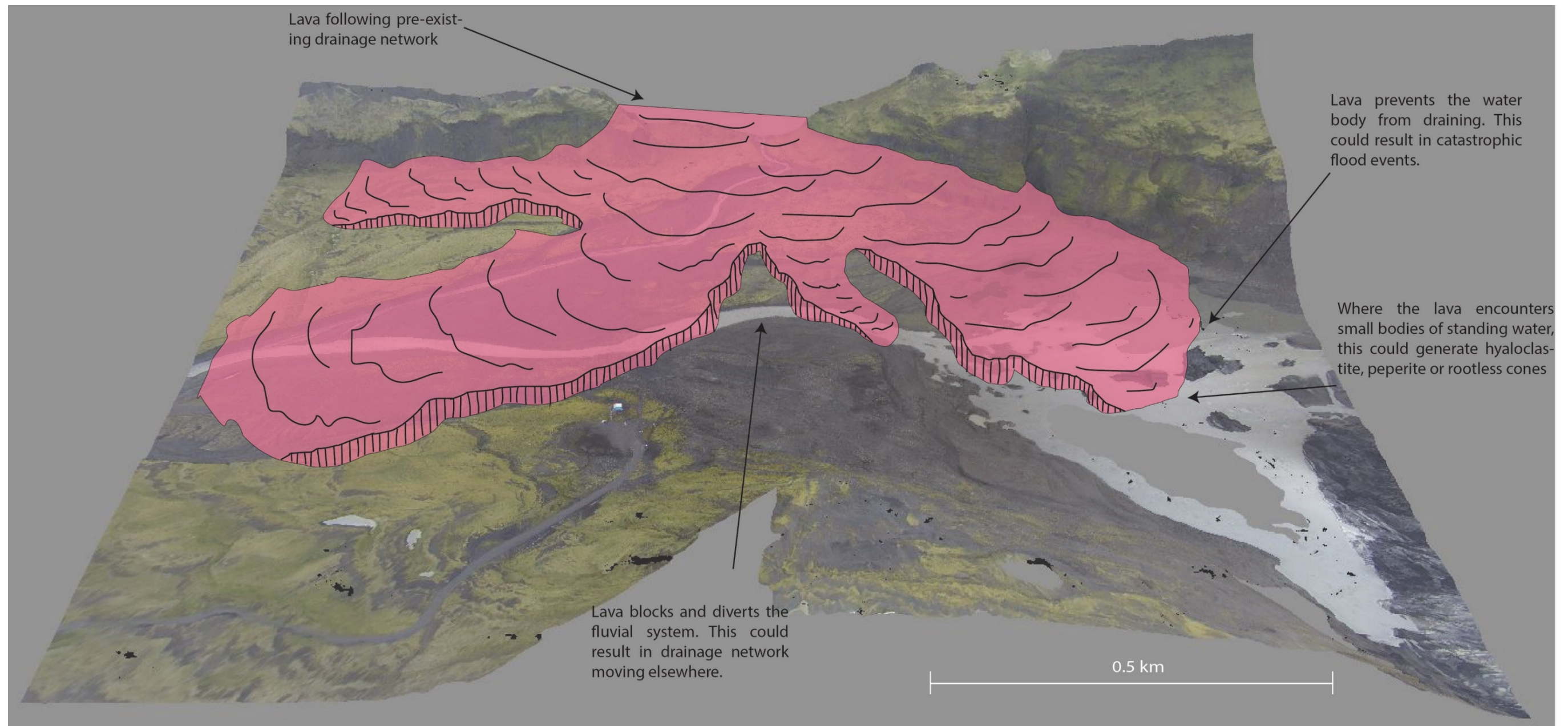


Figure 9-10 Photogrammetry model of the Sólheimajökull glacier mouth, with a hypothetical lava flow interacting with it. This scenario is very similar to the Hreppar Formation, where lavas would have entered confined valleys and interact with standing bodies of water and fluvial systems in a glacier proximal environment.

### 9.3.2 Braided fluvial systems

Braided fluvial systems are a common occurrence in Iceland (Bluck, 1974), and typically form sandur plains which are large sedimentary deposits deposited by proglacial meltwater (Zielinski and Van Loon, 2003).

Braided fluvial systems were a common feature of sediment deposition in the HF as evidenced in sections 1-7. Braided rivers typically form as a result of having a coarse-grained bed load. The sediment is non-cohesive, resulting in the river banks being easily eroded and channels being very mobile (Collinson, 1996), with the lack of vegetation in Icelandic systems, contributing significantly to the mobility of the sediment. Braiding also occurs as a result of a downstream reduction in gradient (Collinson, 1996).

Two braided fluvial systems have been studied as analogues for sections 1-7 within the Stora Laxa river (Figure 7-1). These are the Markarfljót and Hvítá rivers (Figure 9-11, Figure 9-12) and both demonstrate braiding. These rivers are proglacial braided systems and their sedimentary loads fluctuate, based upon season. Typically, in winter, the discharge is significantly less, due to the systems being frozen in areas and a lack of snow melt. Spring is when discharge rates are highest and as a result, the river has a much greater capacity to carry coarser grained sediments (Lunt et al, 2004). Suspended sediment is deposited on the surface of the emergent bar, filling in pore space of the gravel framework. This flux in discharge results in alternating layers of matrix filled and openwork gravel within the bar (Collinson, 1996).

These systems can be very large. The Markarfljót has an active channel belt which is up to 1 km in width at its widest point. The channel belt system has been altered by man to prevent flooding on farm land (Figure 9-11), without this intervention the channels would dominate and seasonally flood fields. Examples of abandoned channels and bars are present within Figure 9-11. If the system was left naturally, it would likely be considerably wider as the surrounding land is flat and expansive which would allow the system to spread out (Lunt et al, 2004 use a river in Alaska that is 2.4 km for their study). Within the main channel axis there is a general transport direction, however numerous smaller channels flow almost perpendicular to this direction (Figure 9-11, Figure 9-12). Palaeoflow data from

the HF (cross bedding and imbrication) show evidence of smaller channels having different flow directions to that of the main transport direction of the fluvial system (chapter 6). The variability of measurements of palaeoflow direction reflects the braided nature of the fluvial deposits. Whilst there is an overall general direction of transport the palaeoflow indicators highlight the variability within. The variability of measurements also indicates why such large averaged values are required to determine the overall palaeoflow direction of braided fluvial systems.

Braided fluvial systems like the Markarfljót and Hvítá rivers would have competed for accommodation space with volcanic systems, in the HF. The two systems would have occupied lows within the palaeotopography. This resulted in the complex repeating units of sandstones and conglomerates, with lavas and hyaloclastites observed today (Stora Laxa sections 1-10).

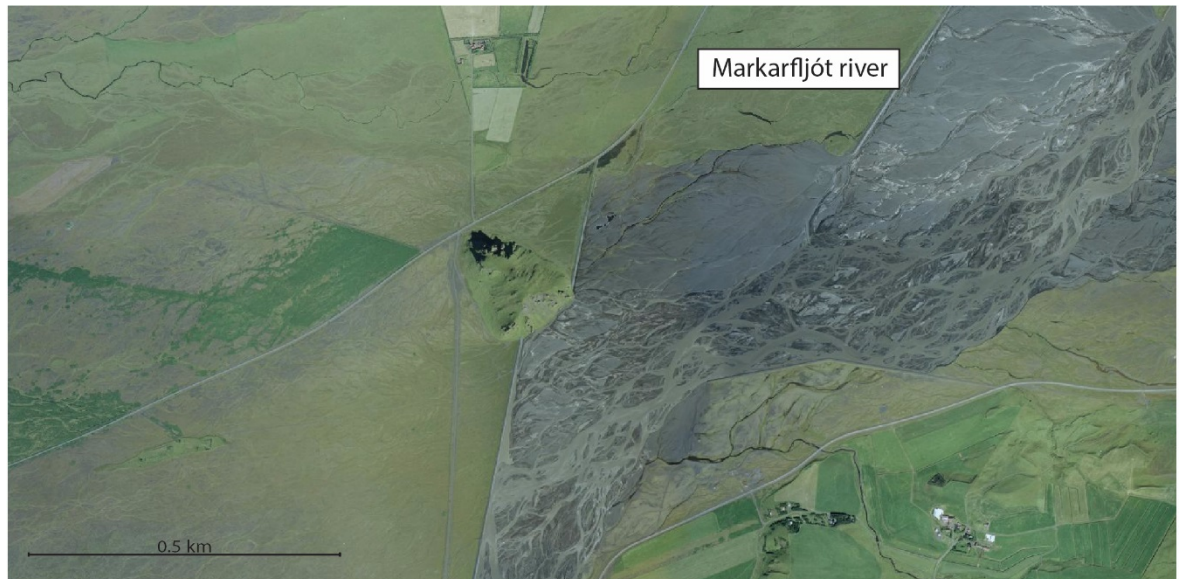


**Figure 9-11** Two examples of braided river systems in Iceland. In both examples here, they drain lake bodies associated with glaciers.

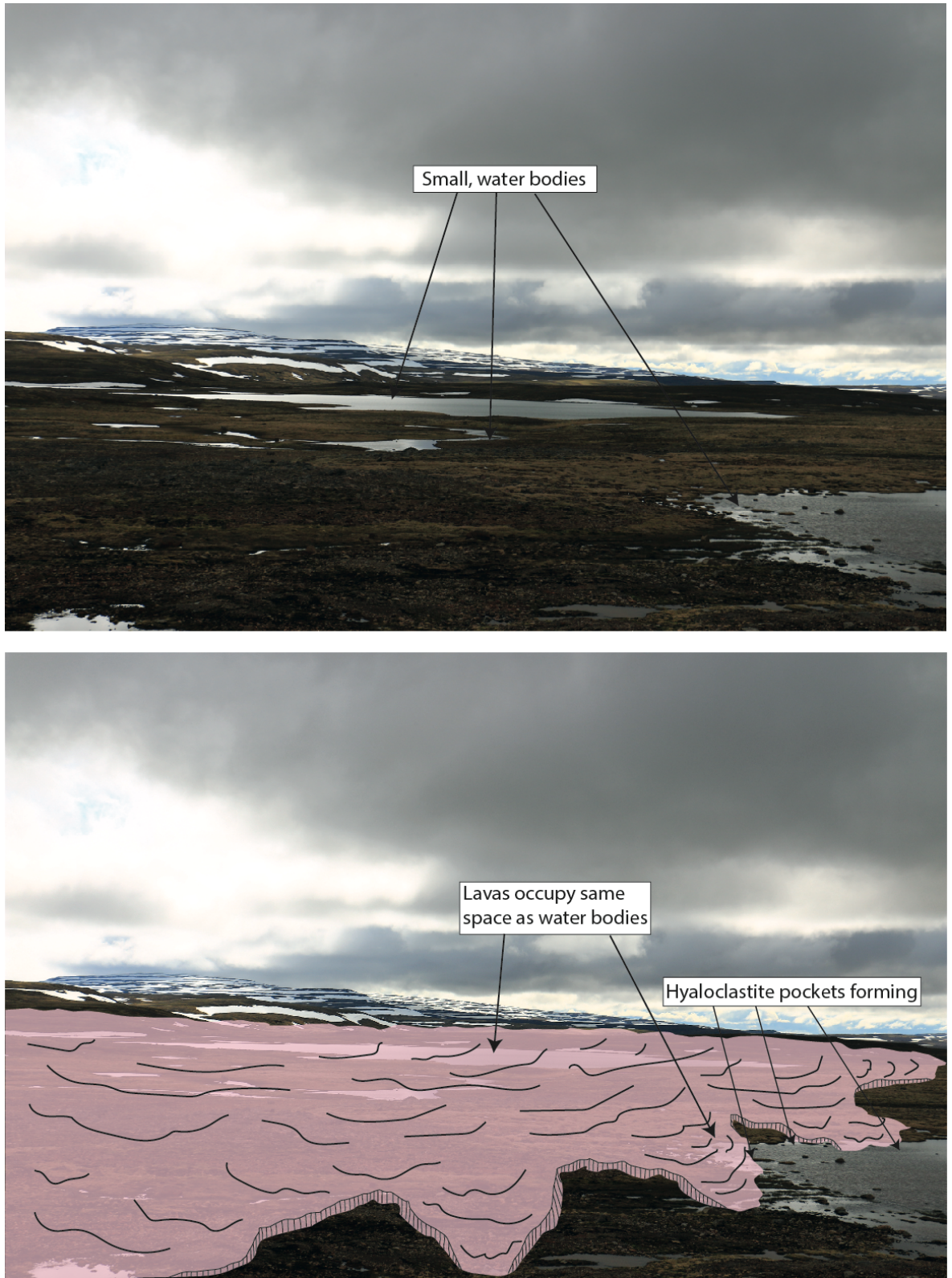


Figure 9-12 Overview images of braided river systems in Iceland. These can be very large and transport large volumes of sediment. They typically have an overall transport direction however smaller channels within the system can appear to flow perpendicular to the general direction of transport. Evidence of braid plains are observed within the HF

### 9.3.3 Lava extrusion in the Hreppar Formation

The modern-day landscape in the HF and in other areas in Iceland are similar to the landscape of that in the Plio-Pleistocene, with recent lava flows, braided fluvial systems and glaciers, all within close proximity. These environments are typically very wet with an abundance of small standing water bodies (Figure 9-13) that develop within the lows in the environment.

When volcanic systems were active and dominating the local environment, the extruded lavas would have preferentially flowed in to the low-lying areas interacting with fluvial systems and standing bodies of water (this is why hyaloclastite is often found at the base of the lava units). In Figure 9-13 and Figure 9-14 two examples of modern Icelandic environments have been used to highlight how lava may have travelled through these landscapes. Notice in Figure 9-13 the lava appears to prograde in to the standing water body, potentially this could generate prograding hyaloclastite foresets. In Figure 9-14 notice lavas hypothetically flow round high ground within the HF, preserving fluvial systems that likely would not be preserved and creating complex stratigraphical relationships between different units.



**Figure 9-13** Modern day landscape in the Westfjords of Iceland. These are dominated by areas of large topography as well as low plains that are water logged. The Hreppar Formation at Flúðir would have had been a very similar setting. If a sub-aerial lava flow was to encounter this, a whole range of different lithofacies would be generated. We see evidence of this within the Hreppar Formation.



Figure 9-14 Looking NW in the Hreppar Formation to the Icelandic Highlands. The current geomorphology is a series of valleys and long lozenge shaped outcrops. If a lava were to flow across this landscape it would typically follow the pre-existing drainage network and occupy the low lying areas.

## 9.4 Spatial distribution of lithofacies in the HF

The location of units within the HF is highly variable (Figure 9-15), primarily due to the underlying tectonic structure within the area, controlling deposition. Here, quantitative data (Figure 9-15, Figure 9-16, Figure 9-17, Figure 9-18, Figure 9-19) is presented to determine any clear relationships within the HF. As discussed throughout this thesis, the HF is a structurally complex area, which tends to bias any observable trends within the HF. The data presented here is a tentative step towards understanding spatial changes in lithofacies distribution within a volcano-sedimentary setting. This is something that few previous studies have addressed even within fluvial sedimentology (Owen et al, 2015). The techniques used here are similar to Owen et al, 2015, who focus on characterising facies variations within the Salt Wash Member of the Morrison Formation, SW USA.

### 9.4.1 Normalised log data

Figure 9-15 demonstrates the spatial distribution of lithofacies within the HF. The values are normalised percentages, based on logged data. The logs have been conducted in areas where exposure is near 100% and in order to attempt correlation between outcrops. The criteria for the logs to be used in Figure 9-15 was; logs have to have >3 different lithofacies present and >10m thick. Logs used to look at a specific feature (e.g. correlation of lacustrine units), have been discarded to avoid a bias in the data. As a result, Figure 9-15 clearly highlights areas which are dominated by specific lithofacies. The central area of the HF (Figure 9-15) is dominated by hyaloclastite and lacustrine facies, indicating that this area has been dominated by water bodies. The southern area of the HF (Figure 9-15) is not dominated by a specific lithofacies, instead there is clearly mixed lithofacies present, highlighting the dominance of the underlying structural control. The NW area of the HF is dominated by sub-aerial lavas, with relatively small volumes of sediment. This could reflect the structure within the HF, where the NW of the area is governed by a different tectonic structure than that of the central area of the HF.

### 9.4.2 Actual log data

Figure 9-16 presents the non-normalised log data, to highlight where strata is thickest within the HF and to identify relationships between different lithofacies. The thickest strata are found within the NW of the field area, which corresponds with where the highest percentage of lavas are found (Figure 9-15). The thinnest strata is found in the central area of the HF. The amount of exposure within the HF is primarily controlled by the underlying tectonic structure (chapter 8).

In the majority of logs within the HF, fluvial sandstones, glacial and mass flow conglomerates as well as fluvial conglomerates are almost always overlain by volcanic units (lavas or hyaloclastite) (Figure 9-16). Where these sedimentary units are found at the top of logs and not overlain by other units, they are typically thinner. This potentially indicates that sandstones found within volcano-sedimentary settings are better preserved in the rock record, due to the encapsulating nature, rapid emplacement and difficulty in erosion of volcanic units. This could provide an opportunity for hydrocarbon exploration within a seemingly unprospective basin, provided there is evidence of volcanic units capping sedimentary ones.

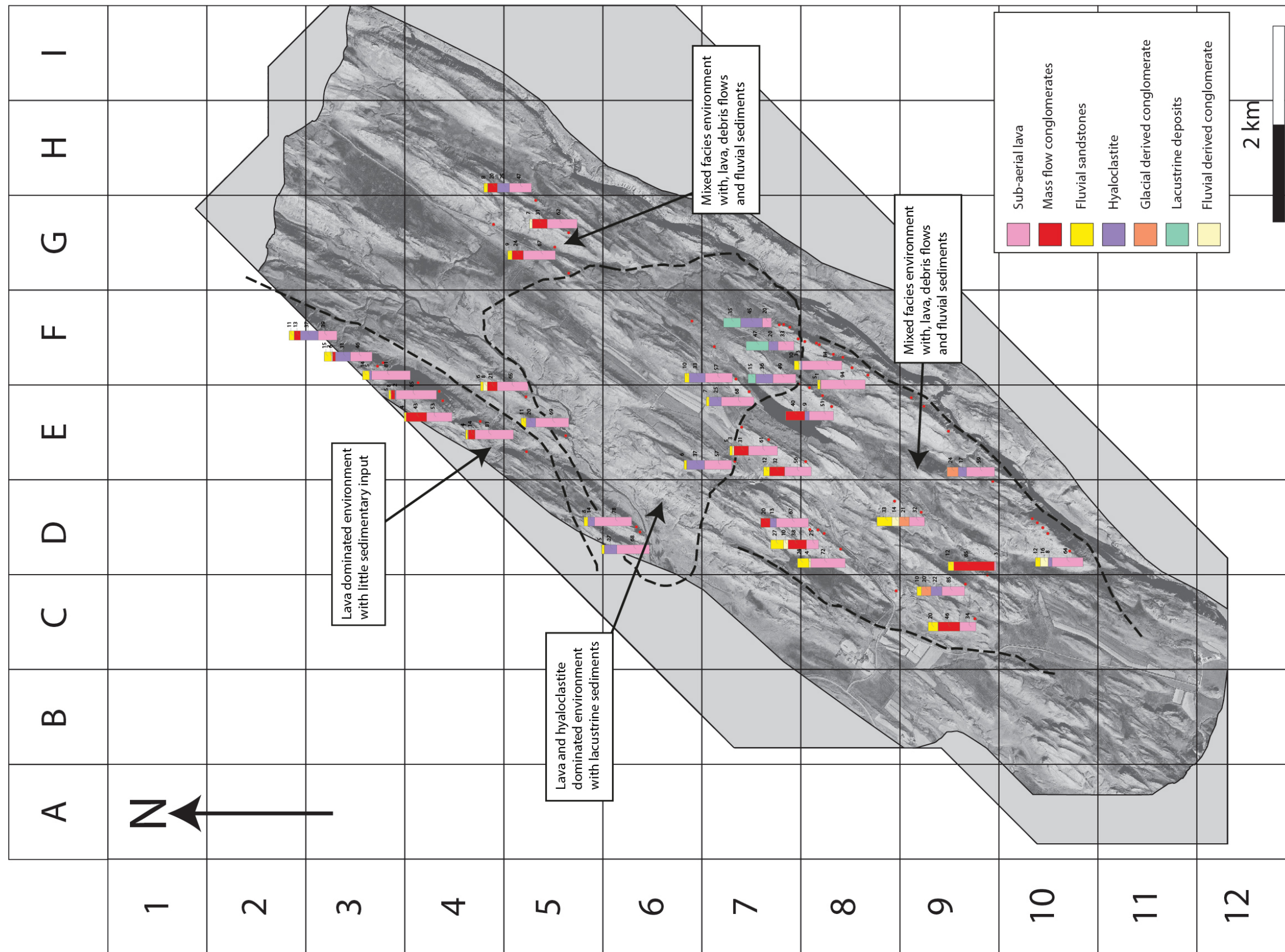


Figure 9-15 Hreppar Formation area map with normalised percentages of units in each log locality. The figure clearly demonstrates areas of the map which are dominated by specific units. The east and west sides of the area are dominated by lavas. The central and southern areas are much more heavily influenced by sedimentary units, with the central area dominated by lacustrine sedimentary units and the southern area dominated by mass flow and fluvial conglomerates.

### 9.4.3 Lavas and fluvial sediment thickness

Figure 9-17 specifically focusses on the thickness of lavas and fluvial sandstones within the HF and identifies where the thickest of each of these logged lithofacies are found. As demonstrated in Figure 9-15, Figure 9-16 the thickest lava accumulations are found in the NW of the field area, however, thick accumulations of lavas are also found throughout the HF, with no real observable pattern present. Within the Stora Laxa river section, there is a large thickness of lavas present, however these are not logged due to their inaccessible nature and therefore do not feature within Figure 9-17. The average logged thickness of a lava within the HF is 2-4 m, with the majority of lavas (94.6%) below 20 m (Figure 9-20).

In contrast to the total lava thicknesses, the logged fluvial sandstones are relatively evenly spread throughout the HF. As is the case for the lavas, the thickest accumulations of fluvial sandstones are found within the Stora Laxa river section, however these also do not feature within Figure 9-17 due to accessibility issues. The average thickness of sandstone units within the HF is <1m (Figure 9-21). This could represent the rate of accumulation of sediment within the HF, with fluvial systems deposition occurring over a greater period of time in comparison with lava units. It could also reflect the frequency of volcanic activity. If volcanic activity occurred frequently, this could prevent a fluvial system from fully developing. The average thickness of sandstones in the HF would be considerably thicker than 1 m if the Stora Laxa sedimentary units had been logged. Mass flow conglomerates are evenly distributed throughout the field area (Figure 9-16) and the average thickness of these units is ~6-8 m, indicating there was an abundance of loose regolith in the HF at this time.

Figure 9-18 highlights the palaeoflow directions of the logged fluvial sandstones within the HF. These are primarily based on imbrication of clasts and cross bedding directions. The general palaeoflow direction is from the NE-SW, which appears to fit with the structural grain of the area. The current sediment transport direction in the HF is from the NE-SW, indicating that it has remained relatively constant. To the north of the field area, lies the Icelandic highlands and to the south, the Atlantic Ocean, naturally the sediment transport direction will be north to south. The two most northerly outcrops that display palaeoflow data (Figure 9-18) within

the HF, demonstrate a linear trend within the rose diagrams, which is uncharacteristic of a braided fluvial system. The reason for this is most likely due to the limited palaeoflow data available at these outcrops. The four other sites within the HF that display good palaeoflow indicators (Figure 9-18) are more characteristic of braided fluvial systems and show a wide spread of flow directions centred around the general NE-SW trend.

Figure 9-19 highlights the average fluvial sediment grain size from the logged data within the HF. This was calculated by converting grain size to mm. The average was then calculated and weighted according to the thickness of the unit within each log, so a fair comparison could be conducted. Throughout the HF there is significant variation in grain size, often with the coarsest sedimentary units adjacent to the finest grained sedimentary units. There is a weak, observable trend within the grain size data which indicates that the coarsest sedimentary units are found in the north of the HF and the finest in the SE. However, various data points go against this trend (Figure 9-19). In order to achieve a more in depth analysis of grain size trends within the HF, significantly more data would need to be collected.

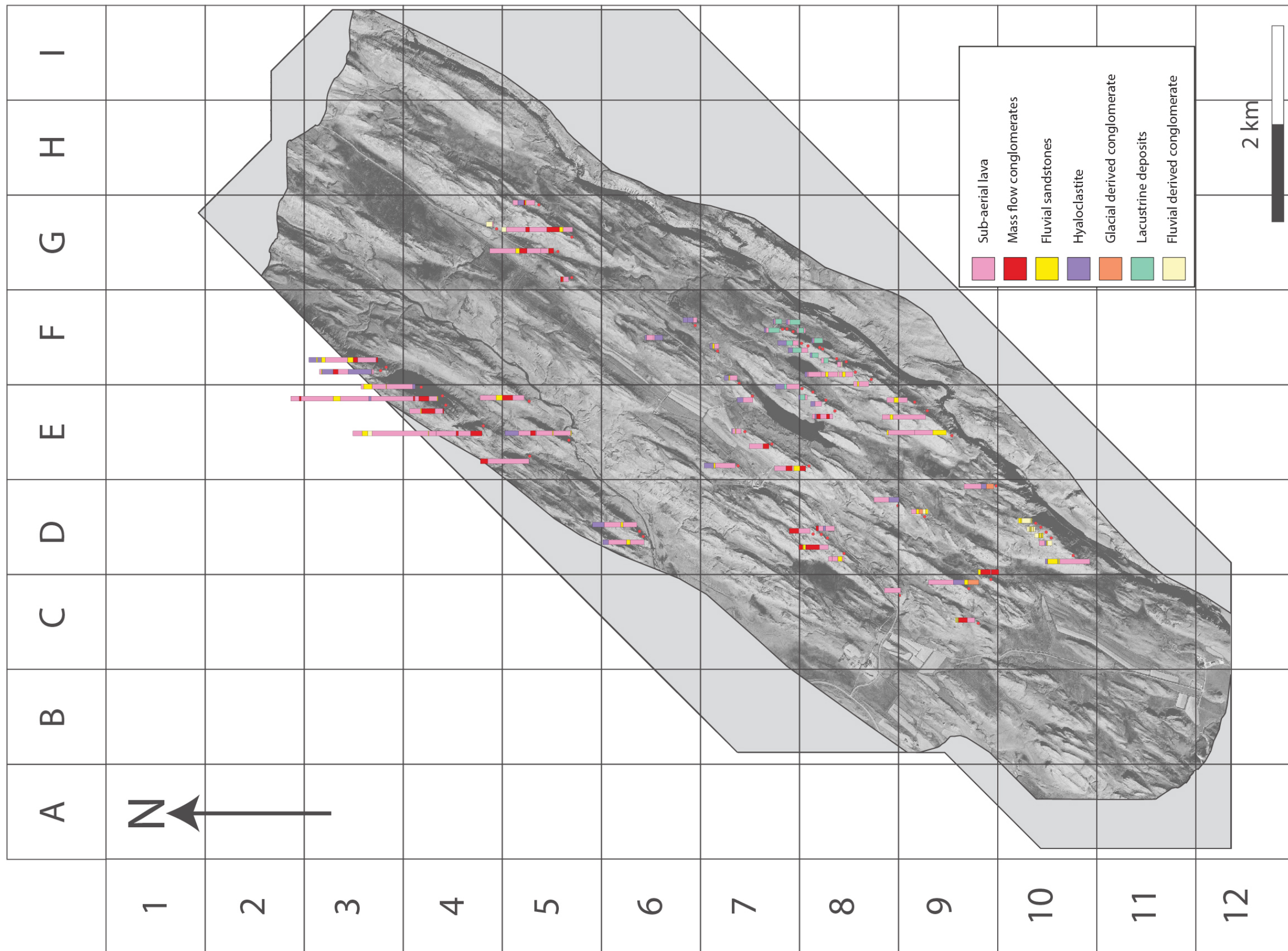


Figure 9-16 Non-normalised log data from the HF. The logs have been scaled to reflect their actual thicknesses and all, no exposure, within each log has been removed. Logs are thickest in the NW of the field area, where exposure is greatest.

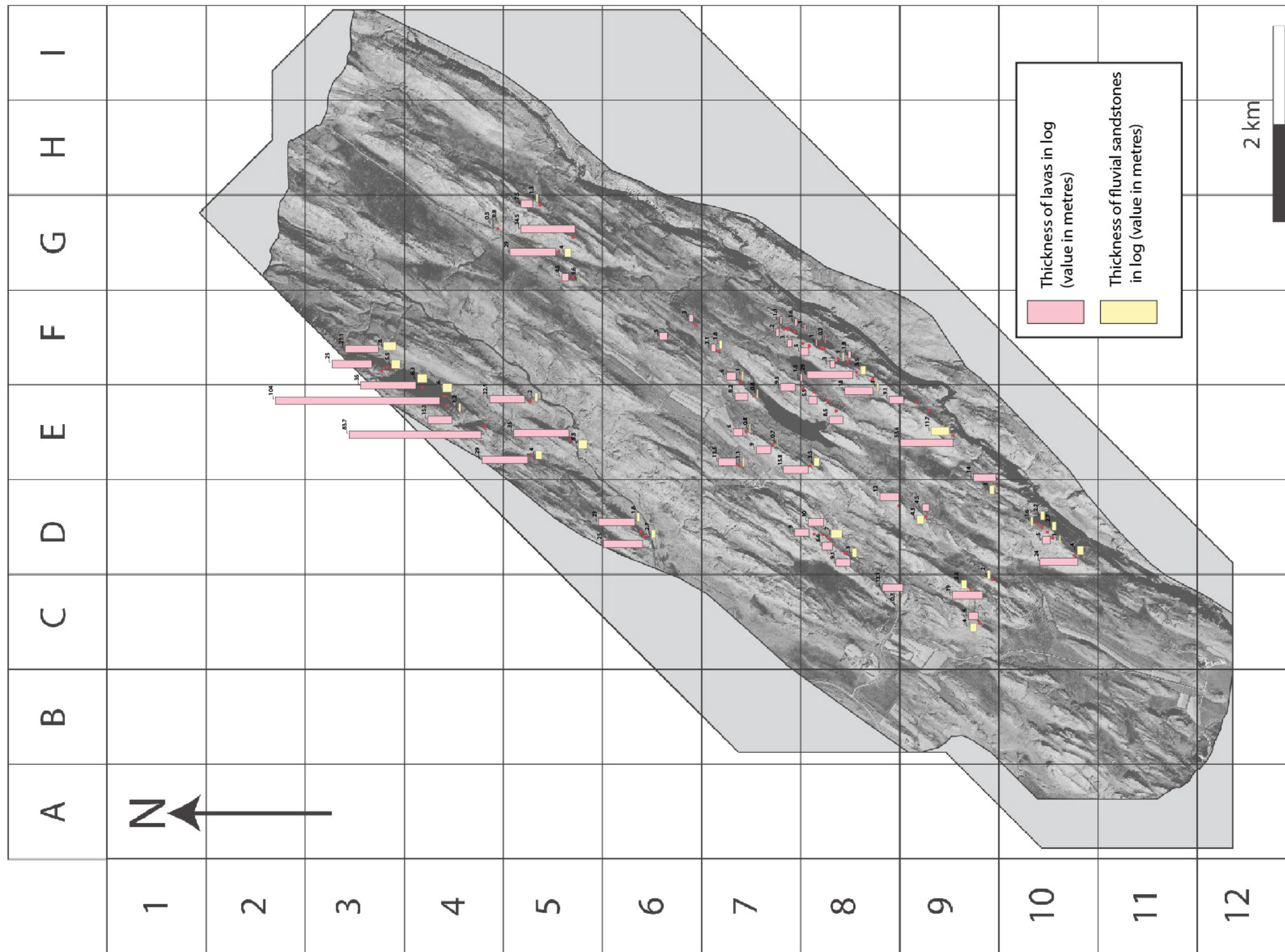
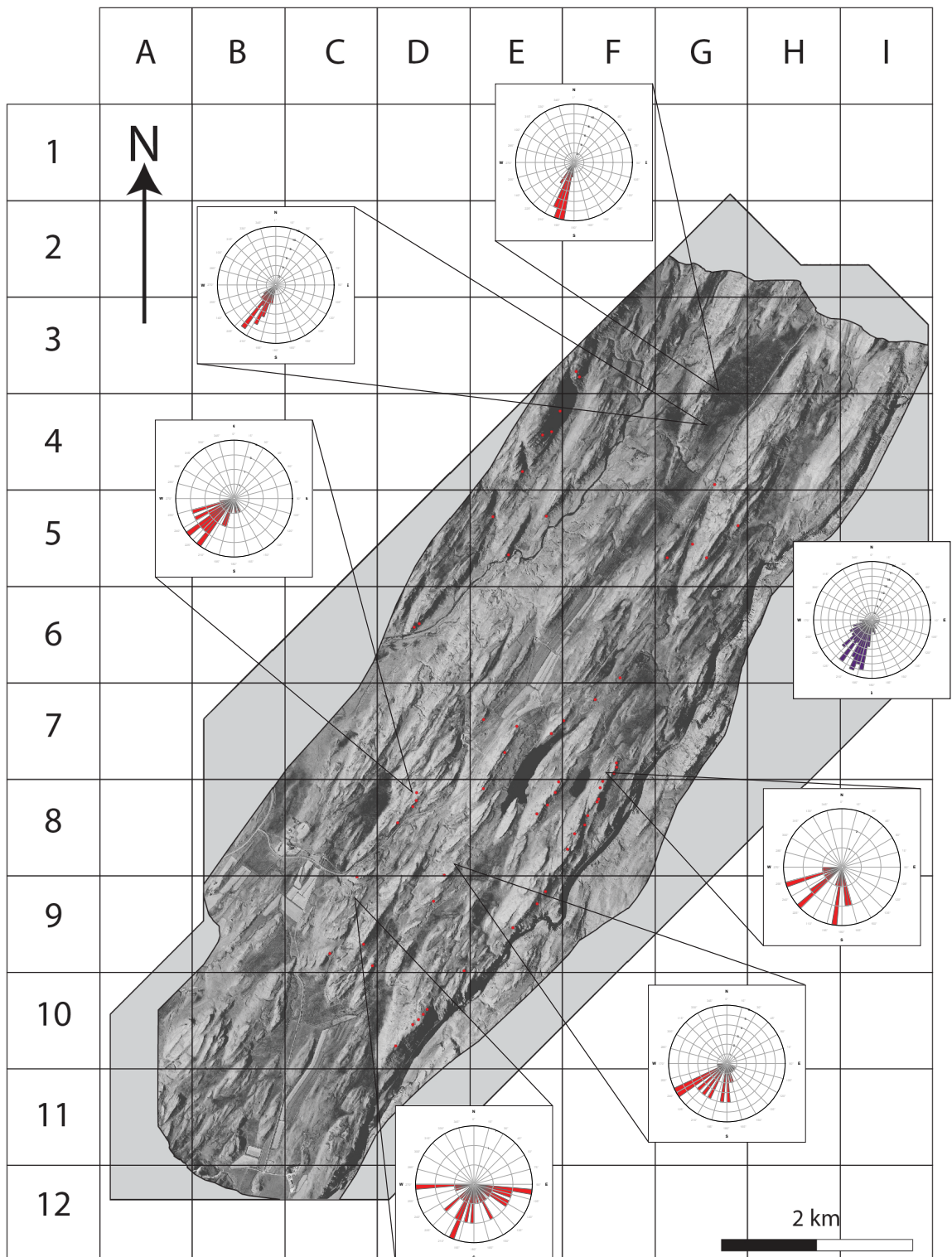
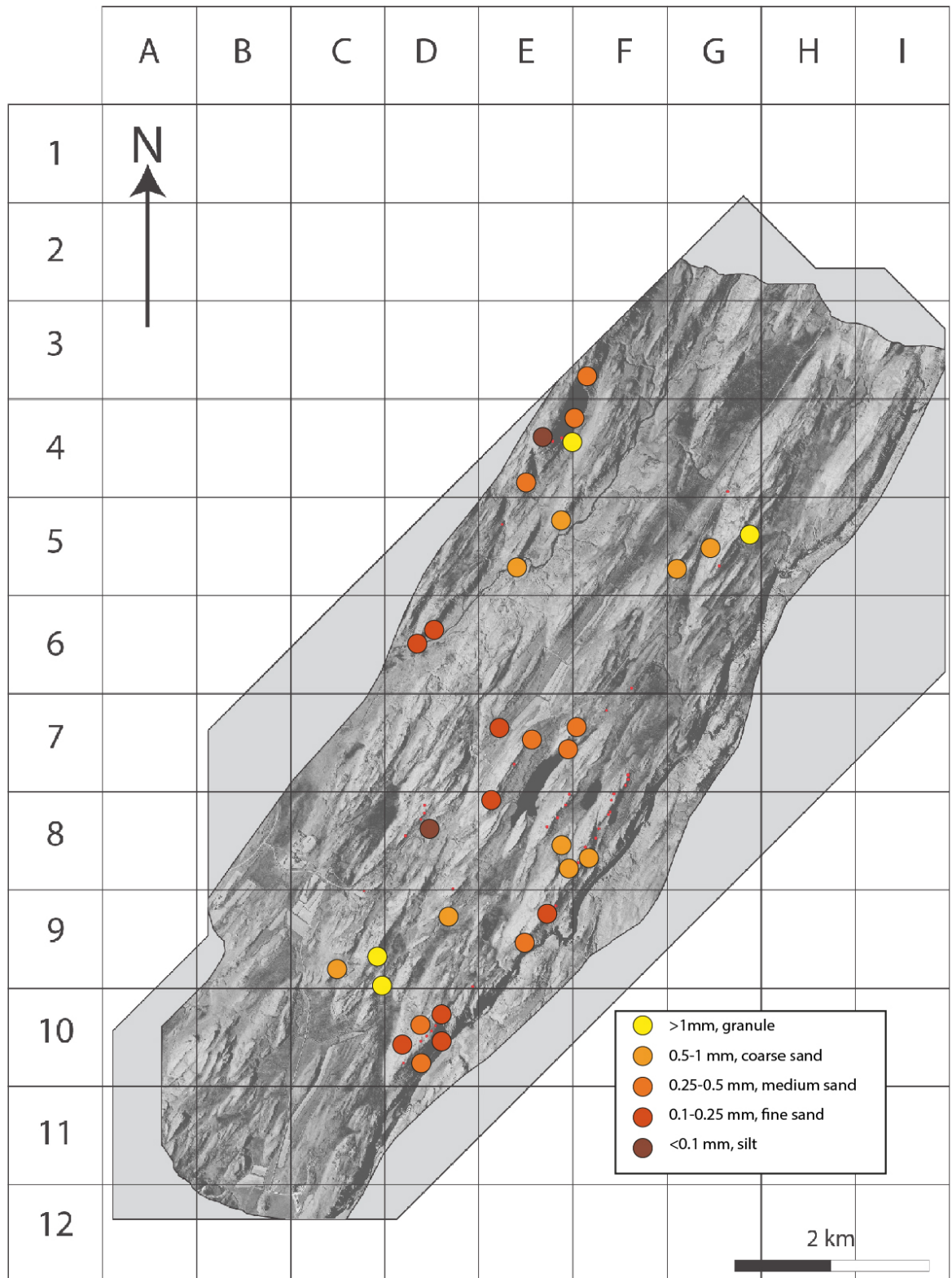


Figure 9-17 Thickness of sub-aerial lavas and fluvial sandstones. Lavas dominate the HF. Lavas are thickest in the NW of the field area, however this is likely due to a function of available exposure. The thickness of sediment throughout the HF is highly variable and this figure only accounts for logged lavas and sandstones. Localities within the Stora Laxa river section are dominated by fluvial sandstones, however these are completely inaccessible so do not feature. The thickness of lavas and sandstones is controlled by the underlying tectonic structure with the HF.



**Figure 9-18 Palaeoflow directions from the HF. The six rose diagrams coloured red represent the palaeoflow directions from the fluvial sandstones within the HF. These palaeoflow directions are primarily from cross bedding and imbrication of clasts. They demonstrate that the palaeoflow direction is generally from the NE to the SW, much like the current sediment transport direction. In the south of the area, the palaeoflow directions are much more variable and likely represent a braided fluvial system. The purple rose diagram represents the collated palaeoflow directions.**



**Figure 9-19 Average fluvial sediment grain size. All the logged fluvial sandstone grainsizes within the HF have been averaged to determine if there are any observable trends in grainsize. There is no observable pattern of grain size distribution within the HF. Notice, coarse sedimentary units are often found adjacent to fine grained sedimentary units. Controlling this grain size distribution is most likely, the underlying tectonic structure of the HF.**

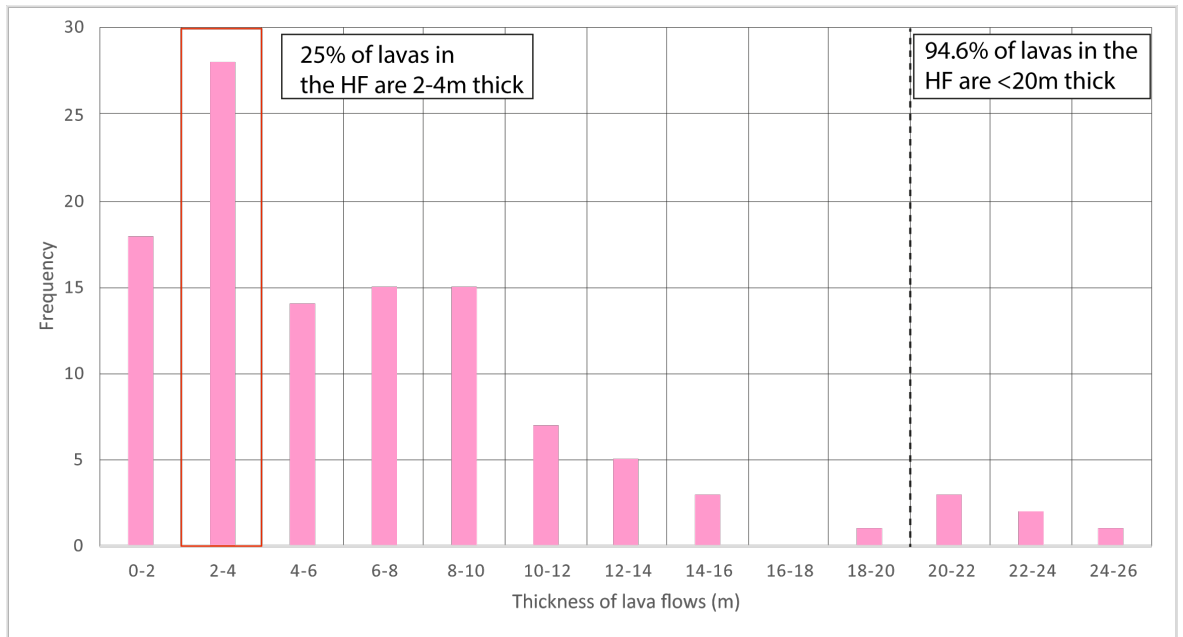


**Figure 9-20 Thickness of lava flows within the HF.** The most common thickness of lava flows in the HF is between 2-4 m. The majority (94.6%) of lavas within the HF are below 20 m thickness, roughly seismic resolution. Highlighting how little detail would be observed if the HF was in the subsurface.

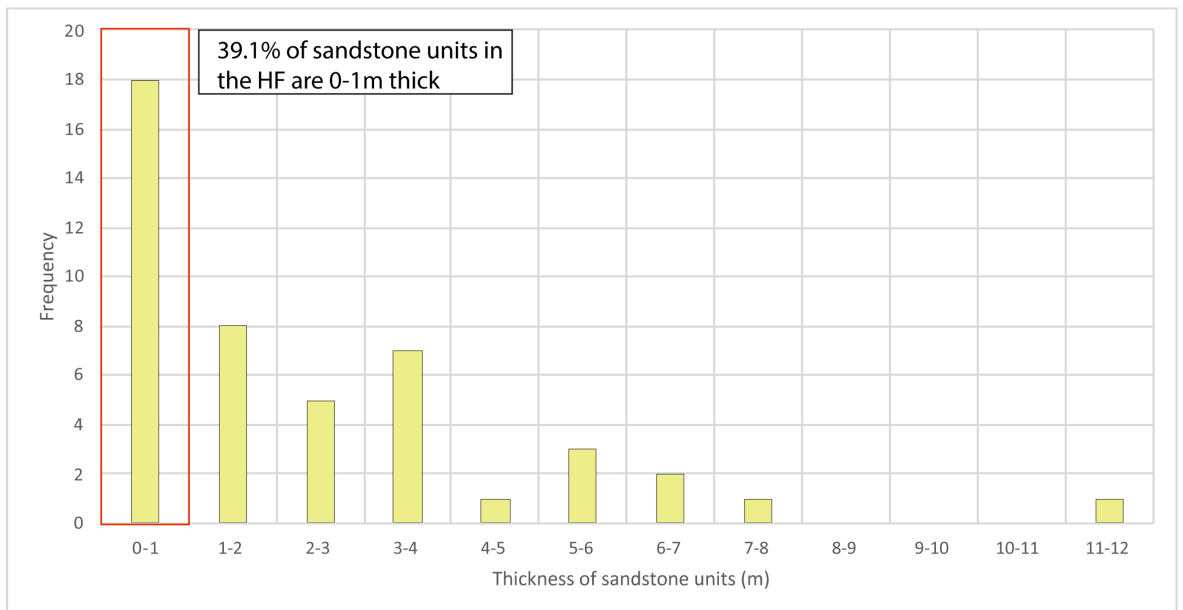


**Figure 9-21 Thickness of sandstone units within the HF.** The majority of sandstone units within the HF are <1 m thick, however, much thicker units >10 m observed within the Stora Laxa (Chapter 7) are not included in this dataset due to inaccessibility issues.

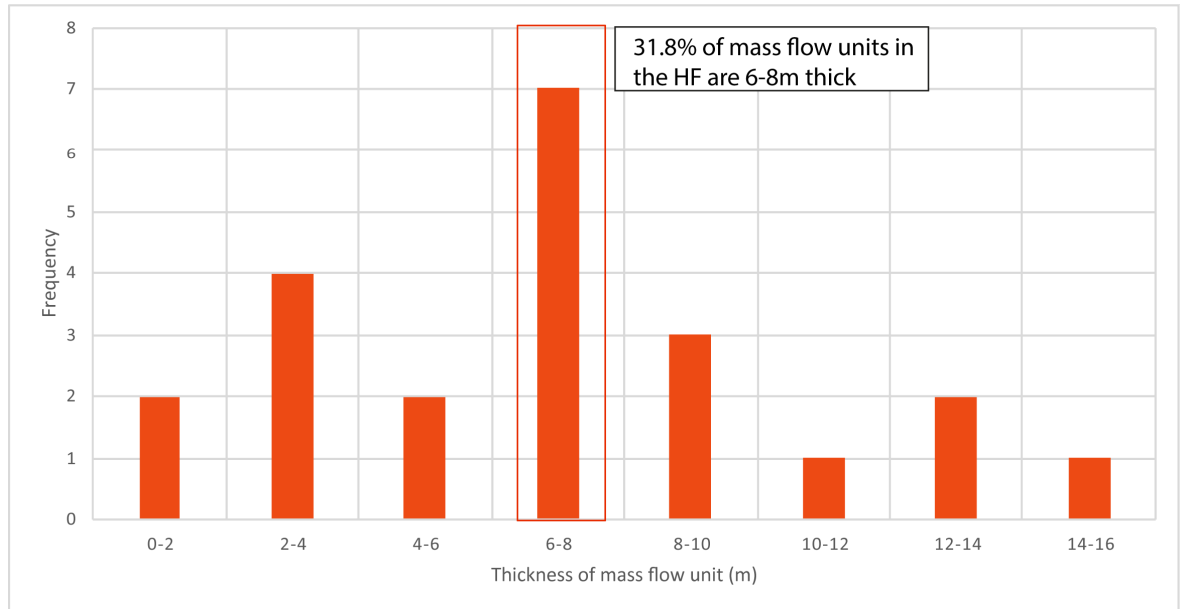


**Figure 9-22 Thickness of mass flows units within the HF. Mass flow units are relatively evenly distributed throughout the HF, the average thickness is 6-8 m.**

## 9.5 HF model

In order to develop our understanding of how the HF may have developed with time, a 3D model of the area has been created which honours all of the lithofacies spatial data (Figure 9-24). The model highlights the structural controls on the HF at Flúðir and attempts to explain the spatial relationship between different lithofacies. The central area of the HF, is dominated by mixed lithofacies deposited in small grabens. Adjacent grabens see deposition of different lithofacies, making correlation between outcrops very difficult. Fluvial outcrops are widespread throughout the HF and indicate that a braided fluvial system was almost always present. Laterally discontinuous lavas are common in the central HF area and form as the result of following pre-existing fluvial drainage networks. To the east and west of the central HF area, laterally continuous lavas and small volumes of sediment are present, this is in contrast to the central HF area. The lithofacies in these areas are seemingly much less affected by small scale faulting such as that of the central HF area and are thought to represent wide plateaus that are elevated compared with the central HF area.

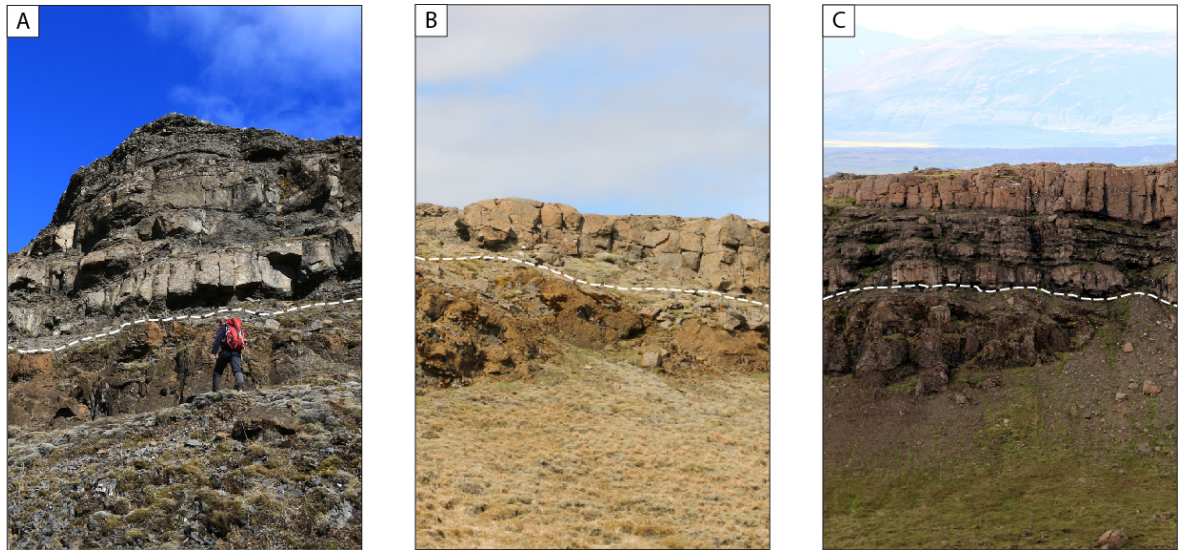


**Figure 9-23 Distinctive B3 lava unit. In three of the four localities of the unit, there is a transition from hyaloclastite and pillow lavas in to sub-aerial lava. This transition is indicated by the dashed white line in each of the images.**

The repeating sequence of units in (Figure 9-23) indicate that within the central area of the HF model (Figure 9-24) it would have been dominated by a large water body, before lavas interacted with it, generating hyaloclastite and pillow lavas before transitioning in to sub-aerial lavas as volcanic activity waxed, filling the central HF area. The outcrops are widely spread within the HF and span significant, present geomorphic features (Stora Laxa river, numerous valleys and hills), indicating that there have been large volumes of erosion in the area. As all outcrops of the sampled B3 unit transition from primary hyaloclastite in to the sub-aerial B3 lava, it indicates that a water body developed in the HF area. Lacustrine facies such as G1 and those that indicate water such as C1, C2, D1 and D2 suggest that the depth of the water bodies within the HF could have been up to 16m.

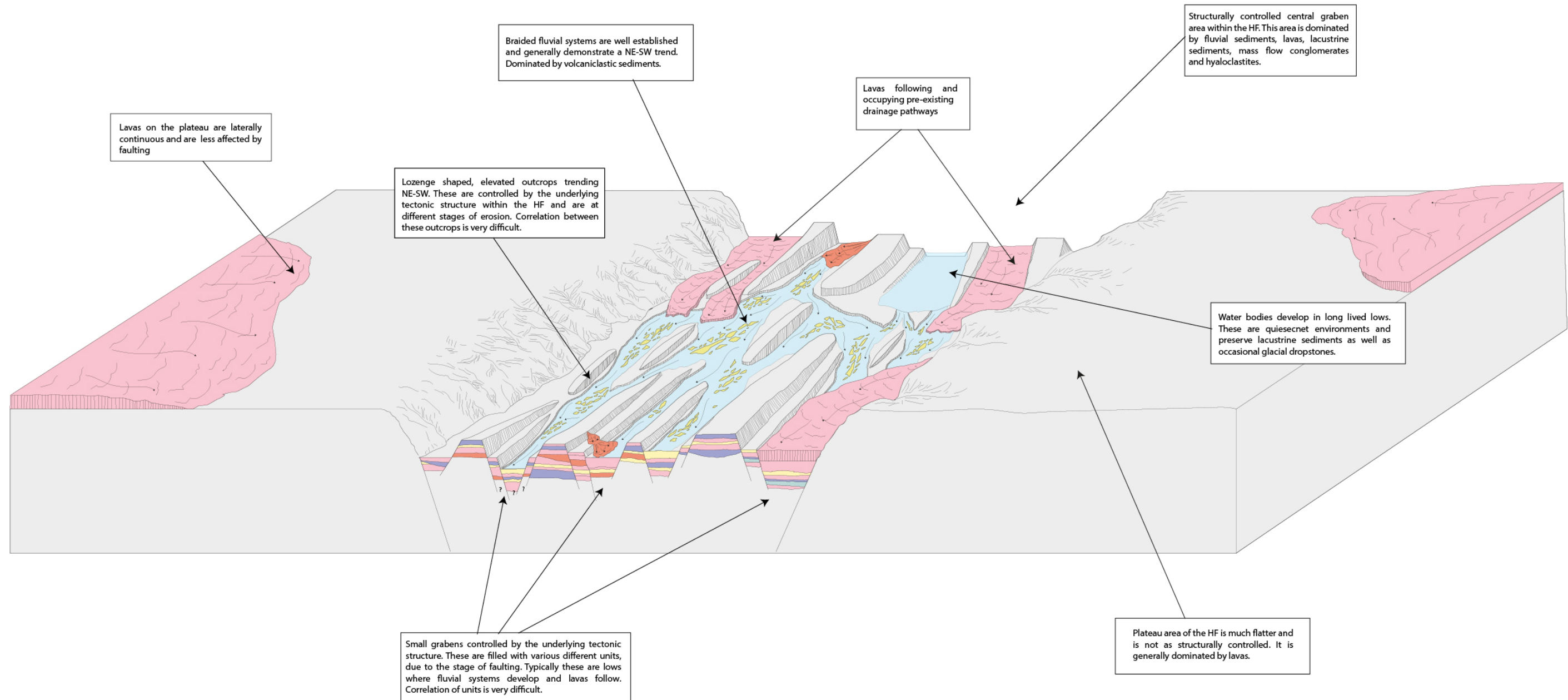


**Figure 9-24 Conceptual development of the HF at Flúðir.** The model presented here is not to scale and is a representation of how the HF may have developed with time. The central region of the HF is dominated by mixed units of fluvial sandstones, mass flow conglomerates, lavas and hyaloclastites. Deposition within the central area of the HF is primarily controlled by the underlying tectonic structure. This has resulted in a series of small, un-correlatable fault bounded grabens. Fluvial systems are common and represent the background sedimentation processes within the HF. When volcanic activity is waxing, lavas tend to follow the pre-established fluvial drainage networks. The plateau areas either side of the main HF are dominated by lavas and other volcanic units, these are typically laterally extensive and correlatable.

## 9.6 Hydrocarbon implications

Commercially viable accumulations of hydrocarbons can be found within and around igneous rocks (Schutter, 2003; Farooqui et al, 2009; Ellis and Stoker, 2014; Jerram, 2015; Millet et al, 2016) all around the world (Figure 9-25). Traditionally hydrocarbon exploration and production companies avoided volcanic rocks because of the various challenges involved with these types of rocks (Holford et al, 2013). As large volumes of hydrocarbons become more difficult to discover in 'easy' to explore basins, exploration has started to focus on more challenging areas, such as those basins associated with continental break up and therefore, intrusive and extrusive, igneous rocks (e.g. along the Atlantic Margin, The Faroe-Shetland Basin (FSB), North West Shelf of Australia). Volcanic rocks found within sedimentary basins are common because of the regularity with which volcanism has occurred in these areas at one time or another (Farooqui et al, 2009). Volcanic rocks can affect every aspect of petroleum systems: producing source rocks, creating migration pathways, traps, reservoirs, seals and maturation (Farooqui et al, 2009). Volcanics can therefore have positive and negative impacts on hydrocarbon systems (Jerram, 2015). Typically, hydrocarbon accumulations associated with igneous rocks are small in nature (between 1-10 million barrels) (Schutter, 2003). However, large accumulations have been discovered and are producing (Jatibarang, Indonesia; 1.2 billion barrels of oil and 2.7 TCF gas, Kudu, Namibia; 3 TCF gas) (Schutter, 2003).

Volcanic rocks are incredibly diverse due to their differing chemistries and emplacement mechanisms as well as where they are emplaced. The most common type of volcanic margins are those associated with rift settings (Jerram, 2015). It is speculated that there is >7 billion barrels of oil equivalent (BBOE) yet to be found on the UKCS Atlantic Margin alone (Gray, 2013) with some significant discoveries including Cambo, Clair, Rosebank and Schielhalion (Muirhead et al, 2017). Exploration for hydrocarbons within these volcanic dominated basins has resulted in a variety of academic projects being funded, as the target areas are still relatively poorly understood and need to be focussed on to enable the discovery and exploitation of hydrocarbons that may be present. Volcanic dominated areas present numerous challenges to exploration, including imaging, drilling, heterogeneity and connectivity issues that will be discussed in this chapter.

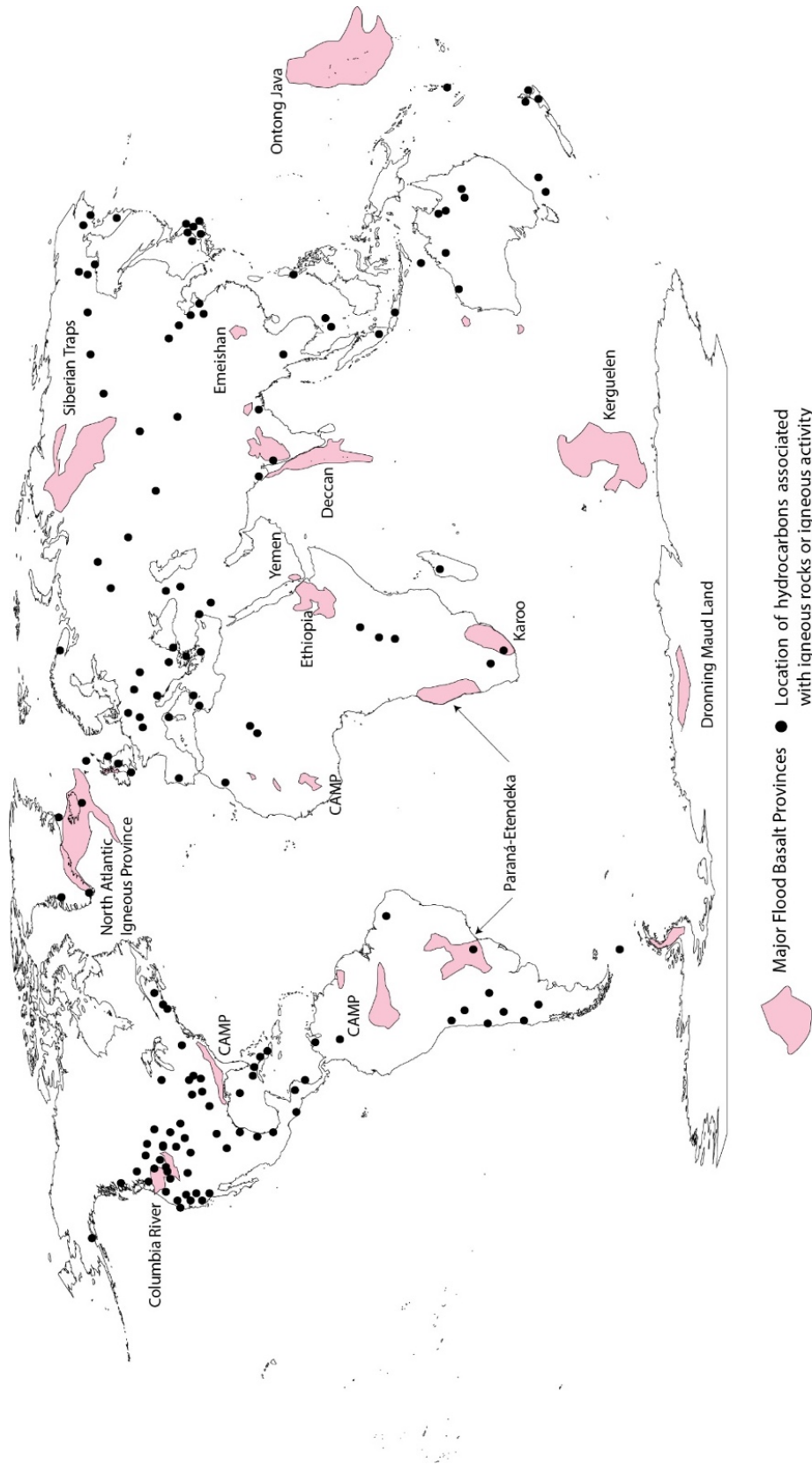


**Figure 9-25** Map of the world, indicating large igneous provinces in red and black dots signify the presence of hydrocarbons associated with igneous rocks (after Jerram and Widdowson, 2005; Nelson, 2010; Bryan and Ferrari, 2013; Wright, 2013).

### 9.6.1 General issues surrounding hydrocarbon exploration in volcanics

As briefly mentioned, igneous rocks have associated complexities which may be encountered during hydrocarbon exploration. These complexities can both be positive and negative. For example, magma is very hot and when emplaced as a sill could push immature kerogens in to the oil window and generate hydrocarbons at shallow levels (Perregaard and Schiener, 1979; Jerram, 2015). There are commercial accumulations of hydrocarbons found to have been produced as a result of this phenomenon in the Nequen Basin, Argentina (Monreal et al, 2009). This could lead to the future exploration for hydrocarbons in immature basins that have been affected by intrusions (Muirhead et al, 2017). The effect of intrusions may also cause over maturation of the source rock, leading hydrocarbons to be driven off (Schofield et al, 2015). Lava extrusion rates in volcanically dominated basins are typically very high, which could lead to the rapid burial of sedimentary units, pushing them in to the oil window, generating hydrocarbons.

### 9.6.2 Sub basalt imaging

When exploring for hydrocarbons offshore, this typically involves using remote sensing data, such as seismic surveys to image broad scale features within a basin or even image an entire basin and identify any potential opportunities for further exploration. The problem with doing this in an area dominated by extrusive and intrusive igneous rocks, such as the FSB (Figure 9-26), is that the coverage of igneous material is extensive. The igneous material results in high-velocity layers within the basin (Woodburn et al, 2014). The high velocity units (lavas, sills etc) are incredibly heterogeneous and typically occur at different stratigraphic levels within the basin (the result of cyclicity in volcanic activity). Often the units have highly irregular architectures compared with the surrounding sedimentary units (Jerram, 2015). All of these elements combine, which typically results in poor quality seismic imaging of underlying sedimentary units and potential hydrocarbons. Low frequencies are typically used to penetrate through the high velocity volcanic layers, however these usually provide lower resolution images (Woodburn et al, 2014) making it difficult to understand the nature of the sub-volcanic geology. Higher frequencies generally provide better resolution; however, they cannot penetrate deep in to the stratigraphy (Gallagher and

Dromgoole, 2007), making it a compromise between depth of investigation and resolution of image.

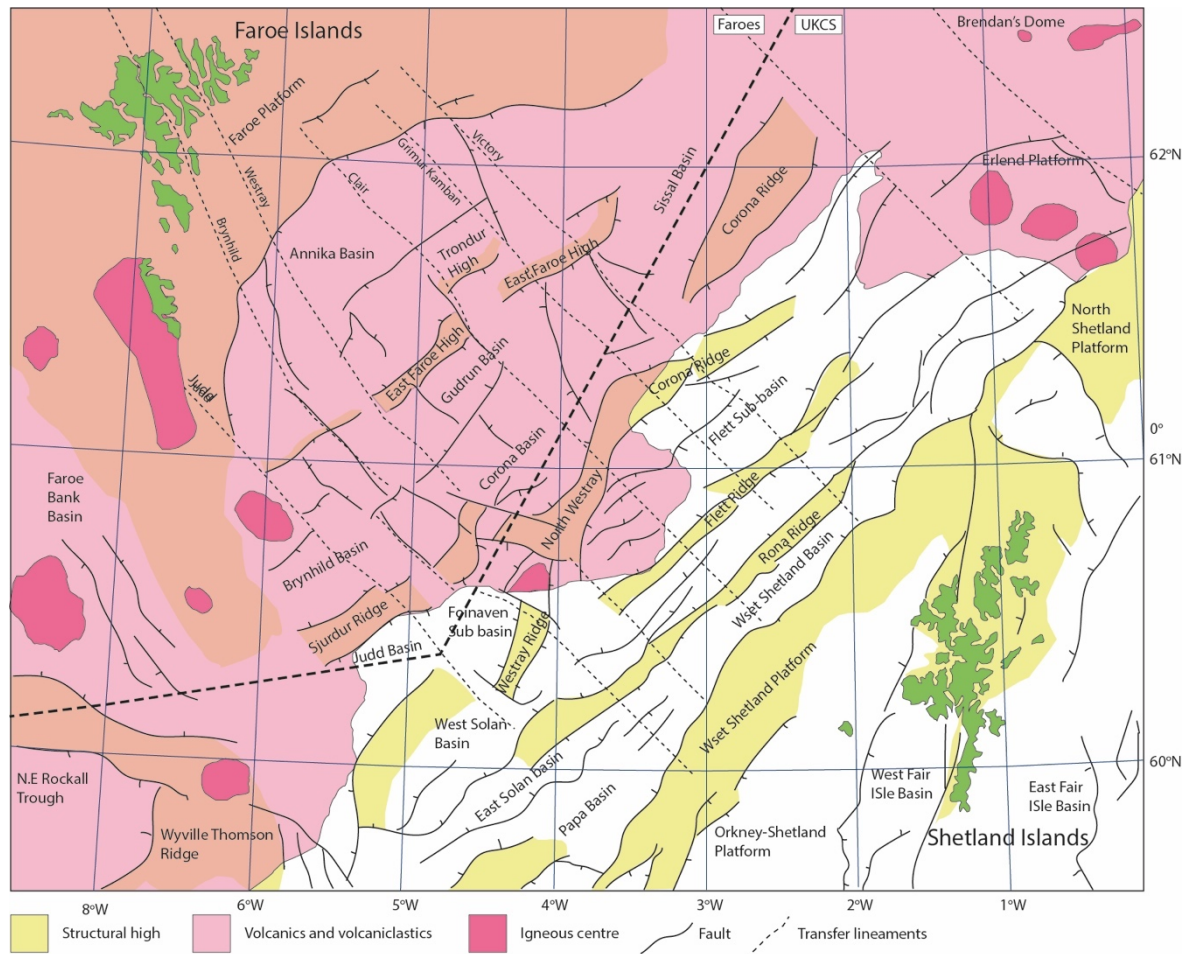


**Figure 9-26** Volcanic and volcanoclastic cover in the FSB. The coverage is extensive within the basin and presents numerous challenges to hydrocarbon exploration (after Moy and Imber, 2009).

In order to obtain higher resolution seismic data in volcanic dominated areas, reprocessing of original data can generate much higher resolution images of the geology beneath the basalt cover (Figure 9-27). This reprocessing typically focusses on boosting the lower frequencies, removing multiples at all stages and reducing high frequency noise (Gallagher and Dromgoole, 2007; Woodburn et al, 2014). As well as reprocessing previously acquired data, improvements can be made to acquiring new data beneath the volcanic cover. This may include improving the position and recording of the seismic source at specific depths within the water, types of source fired, and the types and positions of the receivers used (Jerram 2015).

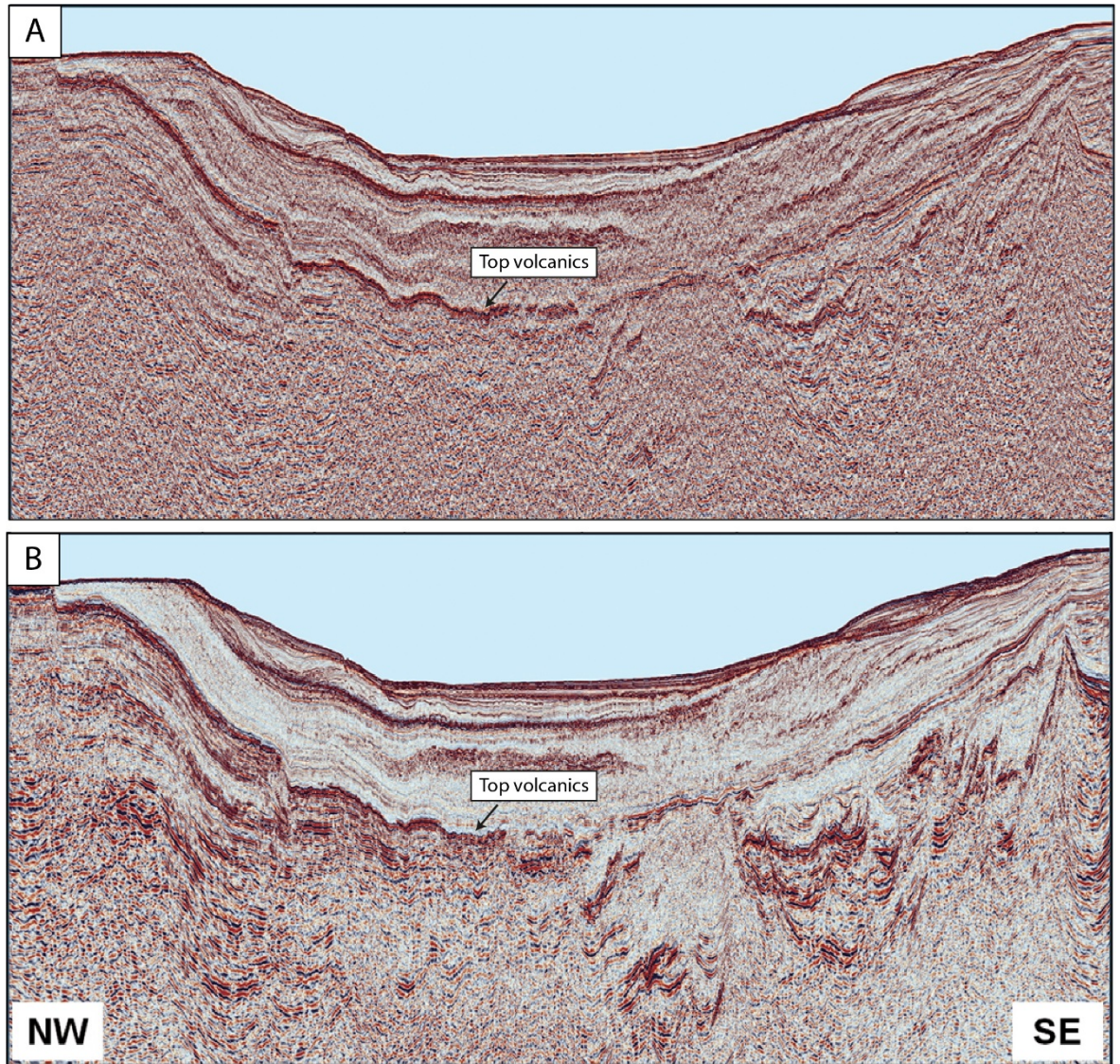


**Figure 9-27** Seismic images across the Faroe-Shetland Basin. a) Represents the original image and b) represents the reprocessed image. Notice in B the much higher resolution beneath the basalt cover, however this it is still difficult to determine features (after Woodburn et al, 2014).

Typically, where discoveries have been made in the FSB, they have a thinner accumulation of volcanics than elsewhere in the basin; however, even these areas are still challenging to image. To understand the geology of areas that have thicker accumulations of volcanic units, it relies on combining all available data to fully understand the area. In general this should include correlation of wells, extrapolation of units within wells, core data calibrated with petrophysical data and seismic, and the correlation of seismic data with analogues. Analogue data is key to understanding volcanically dominated areas, as analogues provide access to mm-km scale, often 3D, geological data sets. Studying an analogue will be significantly cheaper than acquiring more offshore data and can often provide more information. This is why areas such as the HF are key as they provide almost

100% exposure to volcano-sedimentary settings and inform models of sub-surface exploration targets.

To better understand how a lava dominated environment like the HF may look in the subsurface, it is important to model it. As part of this project synthetic seismic images of a section in the Stora Laxa river (map insert) were created using Ikon's RokDoc programme and with the help of Niall Mark (University of Aberdeen) to determine what could be resolved at various frequencies. The results of modelling the cliff section are found within Figure 9-28 and Figure 9-29 where the frequencies become progressively lower. The cliff section is a relatively simple model, but effectively conveys what can and can't be seen in the subsurface.

For simplicity, the lavas were given a P wave velocity of 4.6 Km/s and an S wave velocity of 3.0 km/s (Bourbié et al, 1987; Nelson et al, 2009). These figures are based on the section predominantly comprising of compound lava flows, where the ratio of crust to core is much higher than in simple lava flows. Velocities for the crust are lower than the core (Nelson et al, 2009). The sedimentary units were given a P wave velocity of 2.56 km/s and an S wave velocity of 1.130 km/s (Bourbié et al, 1987; Kassab and Weller, 2015). The model therefore only dealt with two lithologies; basalts and sandstones. In reality there would be significantly more heterogeneity within the section, some volcanic units would have lower velocities and others, higher. In reality the sedimentary units within the section are all volcanoclastic, however the model doesn't take this in to account and instead has been modelled as if the sandstones were all clean quartz arenites. This has been done so that there was a clear contrast between different units and the effect the volcanic rocks have on the resolution of the images is clear. The model also does not incorporate fluids that may be present within the units, (e.g. water or hydrocarbons) which would affect the velocities in the model. A more complex model would incorporate more lithologies and more complex architectures of units as well as accounting for different fluid types. If volcanoclastic units had been incorporated in to the model there would likely have been a lower contrast between units, making the seismic image much poorer.

The section was chosen to be modelled as there is a good division between volcanic and sedimentary units, all hard kicks in the model are red. 100 Hz was the initial frequency used, and at this high frequency, individual units are clearly

observed within the model (Figure 9-28). In the FSB, typical frequencies used in seismic imaging are between 10-45 Hz (Loizou et al, 2008). 100 Hz, as modelled here, would not be achievable offshore, however this is the frequency at which individual units became observable (Figure 9-28). At 40 Hz, individual units start to become unresolvable, which is more akin to offshore data. The detailed architecture between the two different frequencies has been lost but the overall geometries of the units are still present (Figure 9-28).

When frequencies at the lower end of the scale (10, 15, 25 Hz) are used, much of the detail in the section is lost (Figure 9-29). At 25 Hz the sedimentary units between the two main lava packages are just resolvable (Figure 9-29). At 15 and 10 Hz, all the detail is lost within the section, and this is much more representative of the quality of data achievable in volcanically dominated basins such as the FSB. In order for analogue data, such as that obtained from the HF, to be used in aiding seismic interpretation, more complex models need to be created. Creating more complex models will give a more representative view of what these sequences look like in the subsurface and this data can be directly compared with offshore exploration data sets to make this a valuable exploration tool.

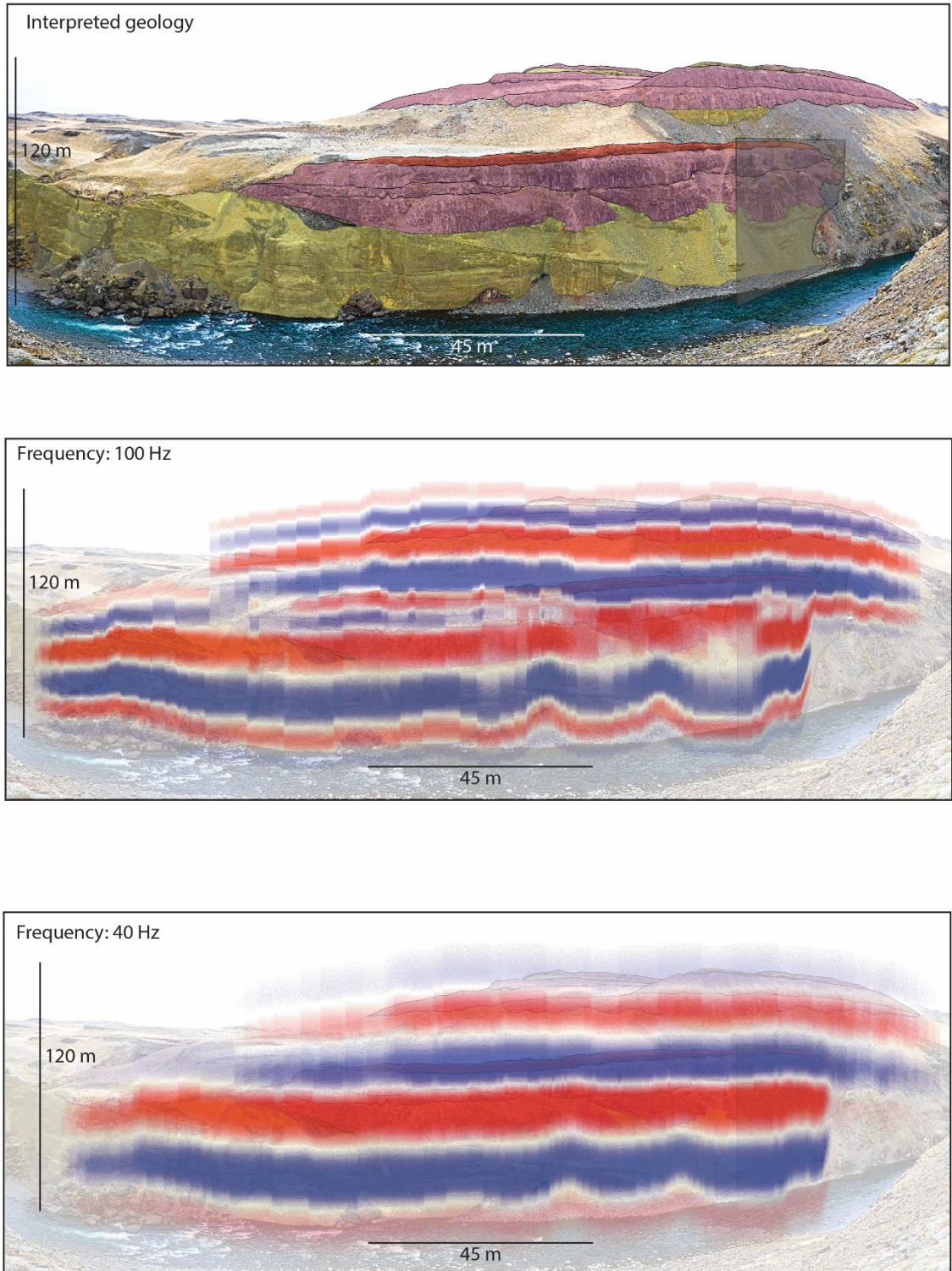


**Figure 9-28 Synthetic seismic images** of a section from the Stora Laxa River, Iceland. First image is an interpreted image of the section. The section has been modelled using two lithologies, sandstone and basalt lava. The first model is a 100Hz model of the section, all units are identifiable. The second image is a 40Hz model of the section, the detail is starting to become lost.

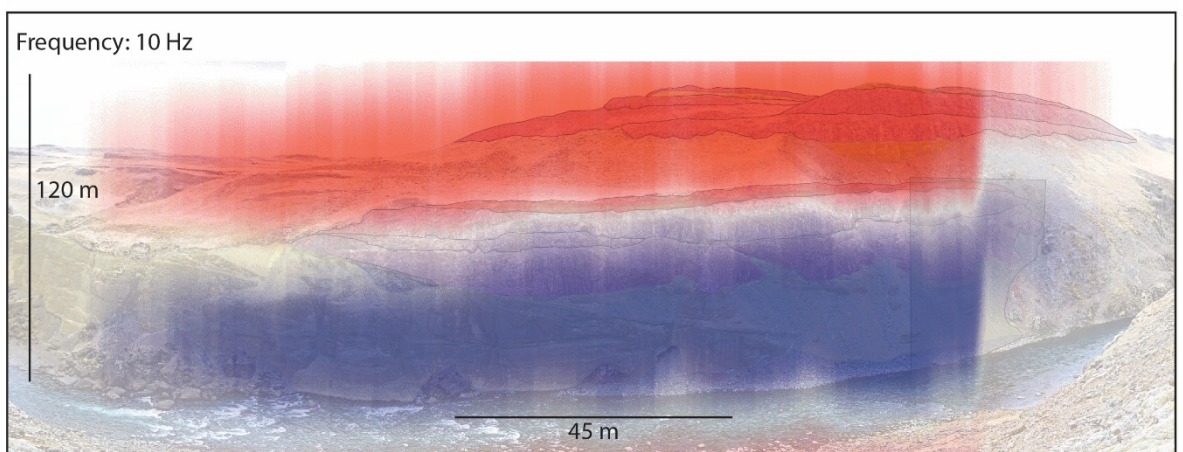
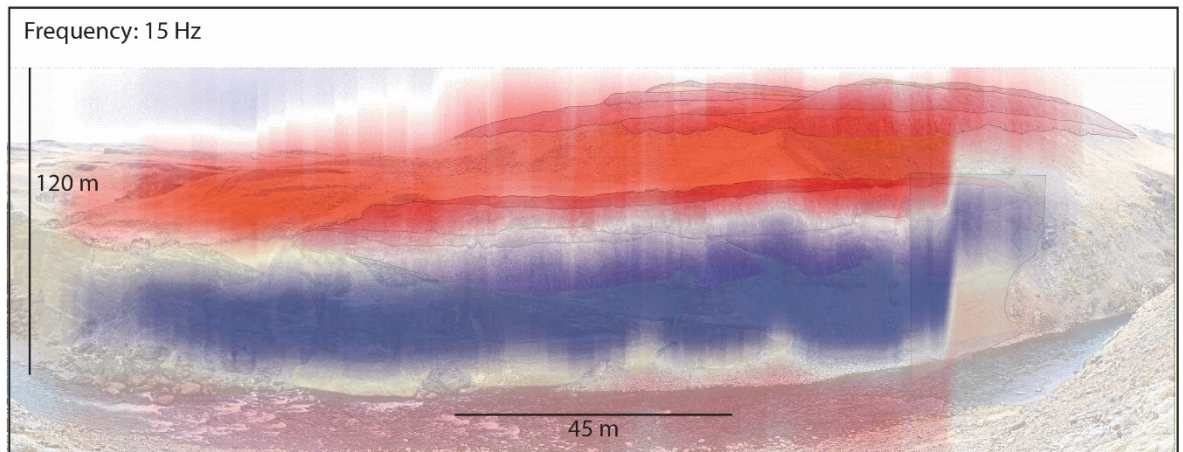
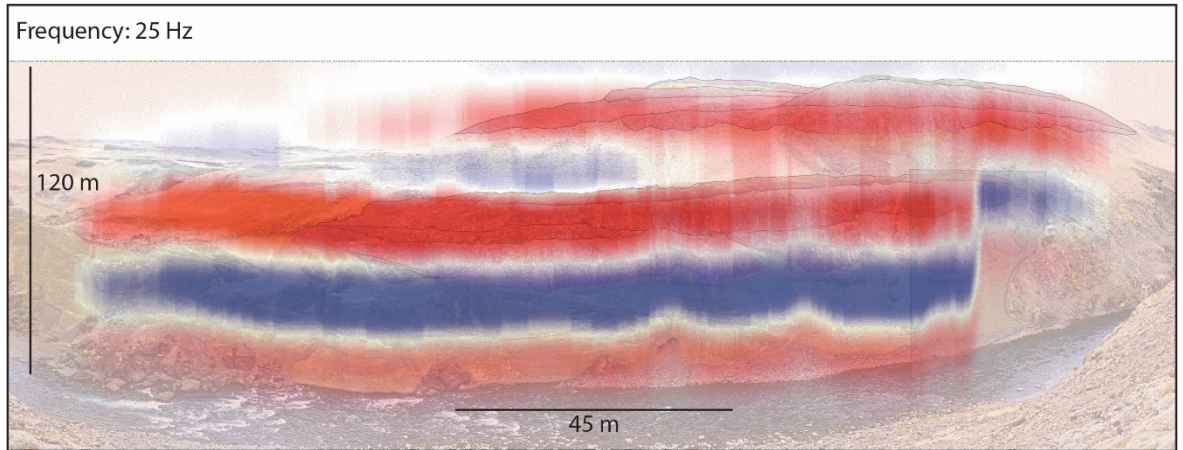


**Figure 9-29 Synthetic seismic images of a section from the Stora Laxa River, Iceland. The first image is a model run at 25Hz, with some detail within the section still resolvable. The second image is the model of the section at 15Hz, this is they typical frequency in areas like the FSB. All detail within the section has been lost. The final image is the model ran at 10Hz, as with the previous model, all detail has been lost for the section.**

### 9.6.3 Drilling through volcanics (basalt)

After a prospective accumulation of hydrocarbons have been identified in the subsurface, these are typically drilled to understand more about the geology before a production plan is implemented. In volcanic dominated areas, this can present numerous challenges due to the nature of the volcanic rocks, which are typically; hard, thick, extensive and also have interbedded soft sedimentary rocks in between units. Going to an analogue such as the HF and analysing specific details will aid the production of inter basaltic hydrocarbons.

There are numerous examples from around the world, where basalts have been drilled for commercial gain (e.g. water aquifers, geothermal energy and hydrocarbons; Millet et al, 2016). Arguably in the offshore setting, drilling through basalts to access hydrocarbons is more challenging due to the increased depth of penetration and added complexity of drilling fluids and safety measures required. Furthermore, it is also much more expensive as any issues could increase down time in drilling (Millet et al, 2016).

The rate of penetration (ROP) in volcanic dominated settings is typically low in comparison with sedimentary units (e.g. ~10 metres per hour for volcanics compared to > 20 metres per hour in sedimentary units; (Millet et al, 2016) which is typically due to the hardness of volcanic rocks. This difference in speed of drilling to reach specific targets adds significant costs on to the drilling campaign, making it potentially more expensive to drill volcanic rocks. Within volcanic sequences, there is significant heterogeneity as evidenced in the HF (see chapter 7). Heterogeneity significantly affects the ROP. When drilling through a thick, sub-aerial lava flow the ROP will be relatively slow in comparison with a volcanoclastic unit, such as a hyaloclastite. Predicting where individual units may occur is difficult on remote sensing data, however using facies models from areas like the HF such as those in chapter 7 will aid the process, additionally the ROPs could help to indicate which facies the well has penetrated.

When drilling a prospect that may involve volcanic rocks, other factors that may affect drilling also have to be considered. This includes factors such as a loss of drilling fluids which can cause a range of issues. Drilling fluids are costly, and there may be a loss of time (which can be very costly offshore), an increased risk

of blowouts, side tracks and well abandonment (Millet et al, 2016). In volcanic sequences a loss of fluids can be a result of highly permeable and porous units as well as fractures, which can be induced by the drilling process itself. Volcanic rocks can make it very challenging to predict where fluid losses may occur as they are so heterogeneous, both internally and system wide (Single and Jerram, 2004).

Within volcanic dominated systems, clay minerals have to be considered when drilling (especially swelling clays such as kaolinite, illite, chlorite, vermiculite and smectite) as these lithologies can cause significant issues such as sticking to the drill bit, reducing the ROP, and a reduction in the hole diameter which could lead to a loss of the bottom hole assembly (Millet et al, 2016). Clay rich units are very common in volcanic dominated sequences such as in volcanic interbeds, altered hyaloclastite, altered lavas, volcanic ash and soils (Passey, 2004). These are all commonly found within the HF. Studying the effects of these types of clays on drilling could be undertaken in the HF as it provides excellent exposure.

Millet et al (2016) identify the instability of volcanic sequences as being a major concern when drilling in these types of environments. They identify weaker units in volcanic sequences such as hyaloclastite and clay-rich, volcanoclastic and heavily fractured intervals, which are soft, poorly consolidated and prone to wash out (Figure 9-30), as particularly vulnerable. Where softer intervals are present and eroded by drilling fluids etc, this could lead to the collapse of blocks of harder coherent material such as basalt lava or intrusions in to the hole or could lead to the formation of ledges, which could pose risks for wireline tools and the bottom hole assembly (Millet et al, 2016).

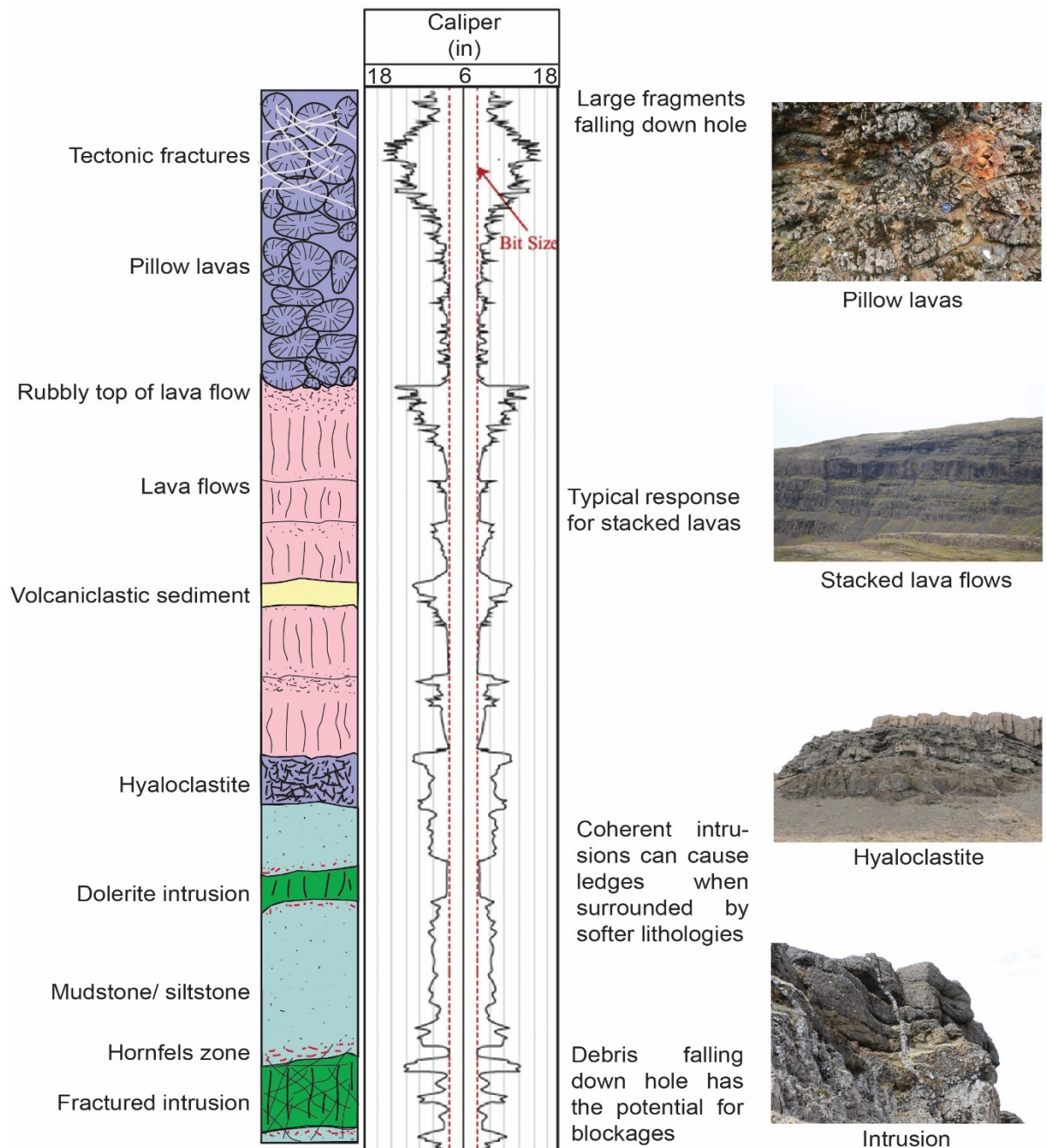


**Figure 9-30** Caliper log responses of various volcanic facies. Implications of each of the main lithologies on drilling, with explanation and image of each key lithofacies after Millet et al, 2016. The images used to highlight the main lithofacies are field examples from the HF.

### 9.6.4 Connectivity in volcanic dominated environments

Within volcanically dominated basins often intrusions have supplied significant volumes of extrusive lavas (Senger et al, 2017). Intrusions can significantly affect a basin in terms of compartmentalisation, creating barriers and baffles to flow as well as creating migration pathways for hydrocarbons (Holford et al, 2013; Rateau et al, 2013; Senger et al, 2015, 2017; Schofield et al, 2015). Generally intrusions

have a lack of permeability due to mineralisation and as a result are barriers to flow (Rateau et al, 2013; Senger et al, 2017) however, if the intrusion is fractured it may provide a pathway for fluid migration (Rateau et al, 2013; Senger et al, 2017) (Figure 9-31).

In the HF, the volume of intrusions is limited, however they are still present (Figure 9-31). The main control on connectivity between units in the HF is the underlying tectonic structure (chapter 8). The area is very heavily faulted (chapter 8) which most likely creates barriers and baffles to fluid flow within the area. If the HF was to be considered in an offshore setting, the biggest concern for the system would be the connectivity between potential reservoir intervals due to faulting and intrusions within the area. In reality this would most likely lead to compartmentalisation of the system making it challenging to produce from, if hydrocarbons were present. In hydrocarbon systems affected by volcanics, compartmentalisation is something that has to be considered at all stages of hydrocarbon exploration, to maximise recovery.

Again, if the HF was considered in an offshore setting where the sedimentary units were “clean”, faulting could create potential traps and fluid flow pathways for hydrocarbons if there was a viable source rock and charge (Figure 9-31, Figure 9-32). Producing an offshore field like this would be difficult as each compartment may not be in pressure communication with the next, potentially increasing costs to recover the in place hydrocarbons. Compartmentalisation can also occur from deposition of sediments. For example, within the FSB, lavas were predominantly erupted in to a sub-aerial environment from fissures, resulting in vertically and laterally overlapping sequences of lavas with interbedded sediments deposited during hiatuses (Naylor et al, 1999). This is very similar to the process of deposition of lavas and sandstones in the HF. This type of deposition resulted in potential intra basaltic reservoir units isolated within volcanic facies, naturally compartmentalising the system. Faulting in this situation may enhance the field (Figure 9-31, Figure 9-32).

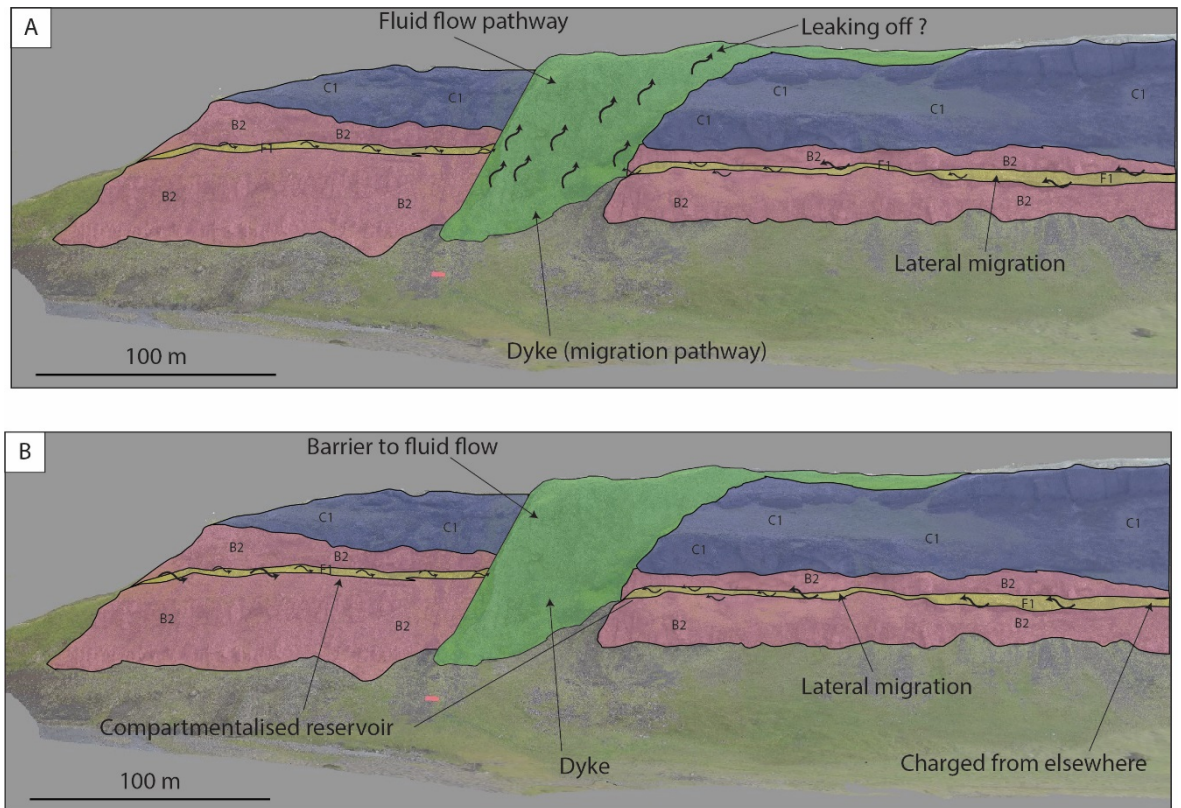


**Figure 9-31 Large dyke within the HF compartmentalising the system. If this outcrop was to be considered in the subsurface, then fluids may use the dyke as a migration pathway or it may be a barrier to flow. In A, the dyke has been hypothesized to be fractured and permeable, acting as a conduit to fluid flow. This could potentially lead to hydrocarbons leaking off from the reservoir, but it could also lead to hydrocarbons migrating in to reservoirs higher in the stratigraphy. In B, the dyke has been hypothesized to be mineralised and impermeable to fluid flow. This would result in the reservoir being compartmentalised.**

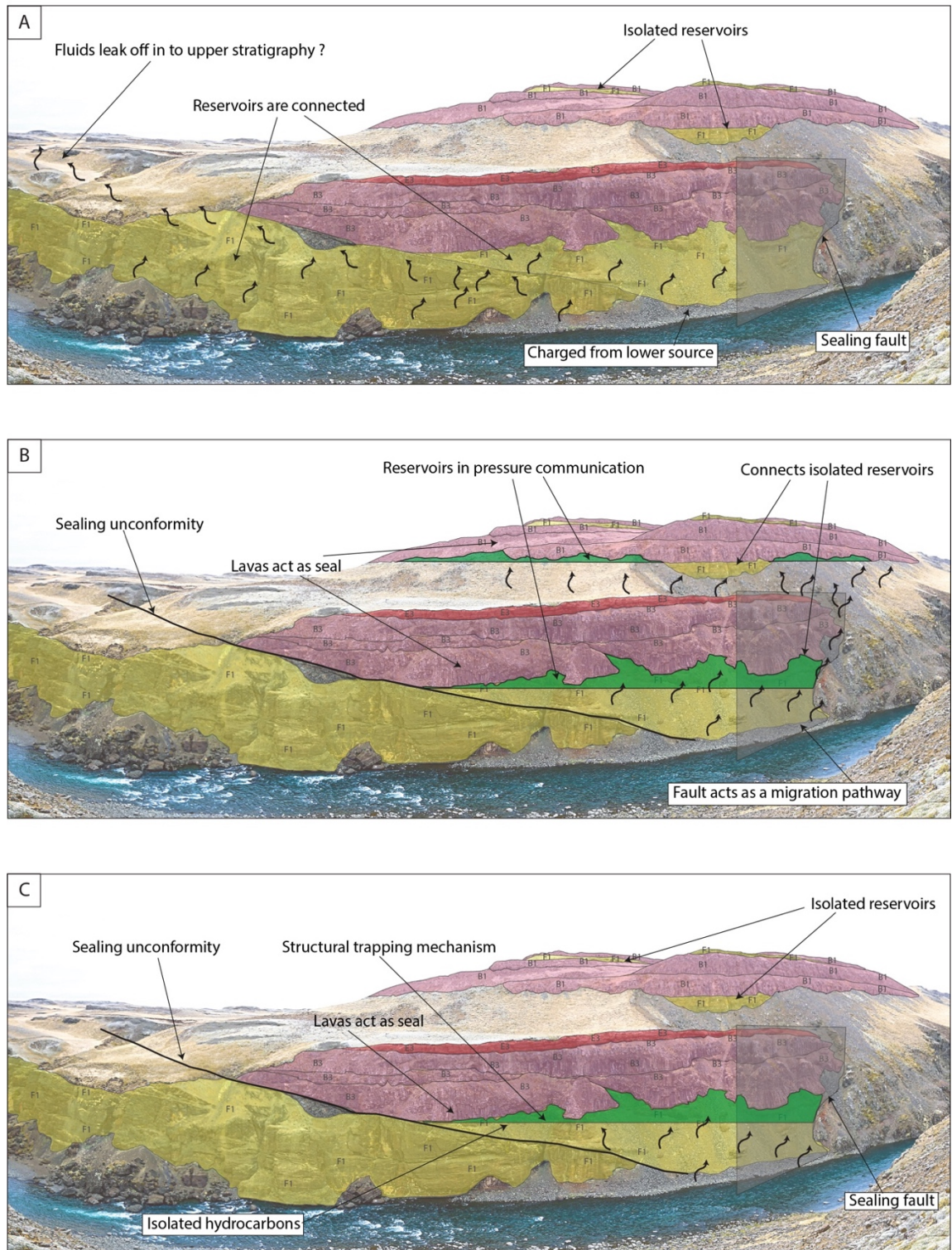


**Figure 9-32** Outcrop within the HF to be considered in the subsurface. The three different scenarios indicate how migration pathways may be affected by faulting and unconformities. In A, the unconformity between the two sandstone reservoirs is negligible and as a result fluids can migrate from lower in the stratigraphy between the two reservoirs. However this means that the fluids could potentially leak off as there is no top seal. In B, the unconformity is hypothesised to act as a side seal and the fault is not sealing, but instead, it acts as a migration pathway for fluids. The fluids would charge the lower reservoir unit and be trapped, before some migrate in to the overlying reservoir unit, connecting the two different reservoirs. In C, the unconformity and fault are both sealing, causing hydrocarbons to become trapped within the lower reservoir. This could happen in numerous places in the field area, creating isolated accumulations of hydrocarbons, making them difficult to produce.

## 9.7 The Hreppar Formation as an analogue

In order to fully understand volcanically dominated systems in terms of hydrocarbon exploration, many different formats of data need to be combined. Remote sensing data such as seismic, gravity/magnetic data should be combined with petrophysical data, core and field analogues to create a rounded view of the petroleum system. Volcanically dominated systems are incredibly complex as evidenced in the HF and fully understanding them requires time and the synthesis of a range of data sets. The Rosebank Field in the FSB was discovered in 2004 and at the time of writing is still going through an appraisal programme as it is not yet fully understood (Poppit et al, 2016).

In all hydrocarbon exploration activities it can be useful to examine onshore analogues to understand the large scale (km) to fine (mm) data (Bowman et al, 2016). This is particularly true in volcanically affected basins, such as the FSB. The HF is a good analogue for understanding elements of petroleum systems within volcanically dominated environments. The advantage of using a field analogue is that it enables the ground truthing of models of the subsurface and it is relatively cheap to acquire the data. In terms of the HF; it can inform models about the connectivity of reservoir units, how sediments move through volcanic dominated environments, how volcanic rocks interact with fluvial, glacial and lacustrine settings, the importance of structural controls on sedimentation and volcanism and allows us to understand heterogeneity within these types of environments. All of this data is invaluable when trying to understand a petroleum system in the subsurface as it reduces subsurface risk and uncertainty, validates interpretations and can be applied at every stage (i.e. exploration, appraisal, development, production and abandonment; Bowman et al, 2016, Vosgerau et al, 2016).

The studied area of the HF is ~16 km<sup>2</sup> and as a result is approaching the scale of a small field. The well spacing of the Rosebank Field has been superimposed on to the studied area of the HF (Figure 9-33) for a comparison between the two. In overall length of structures, the HF is ~half the size, indicating that features observed within the HF can potentially be directly compared with features identified in the offshore data of Rosebank and similar fields. The quantitative data presented in Figure 9-20, Figure 9-21, Figure 9-22 and Figure 9-24 starts to provide a basic, predictive model for volcano sedimentary settings. From these

data and the map insert, differing volcano sedimentary settings (onshore or offshore) can be compared and contrasted with the HF, e.g. thickness of volcanic system deposits and sedimentary deposits.

The data within these figures (Figure 9-20, Figure 9-21, Figure 9-22) highlights why an analogue such as the HF should be used in conjunction with remote sensing data. For instance 5.4 % of the lavas within the HF are >20 m thick, when this is combined with Figure 9-28 and Figure 9-29 it highlights the lack of detail observed within offshore data and what can and cannot be seen in seismic datasets, it is likely that 94.6% of the lava units within the HF would be unresolvable on seismic data. The average size of logged sandstone units within the HF are <1 m thick, these would be impossible to observe on offshore seismic datasets in volcano sedimentary settings. It is likely Figure 9-29 represents the quality of imaging within these areas. In order to understand these settings in detail and maximise hydrocarbon recovery, modelled data needs to be compared with real field data (Figure 9-34).

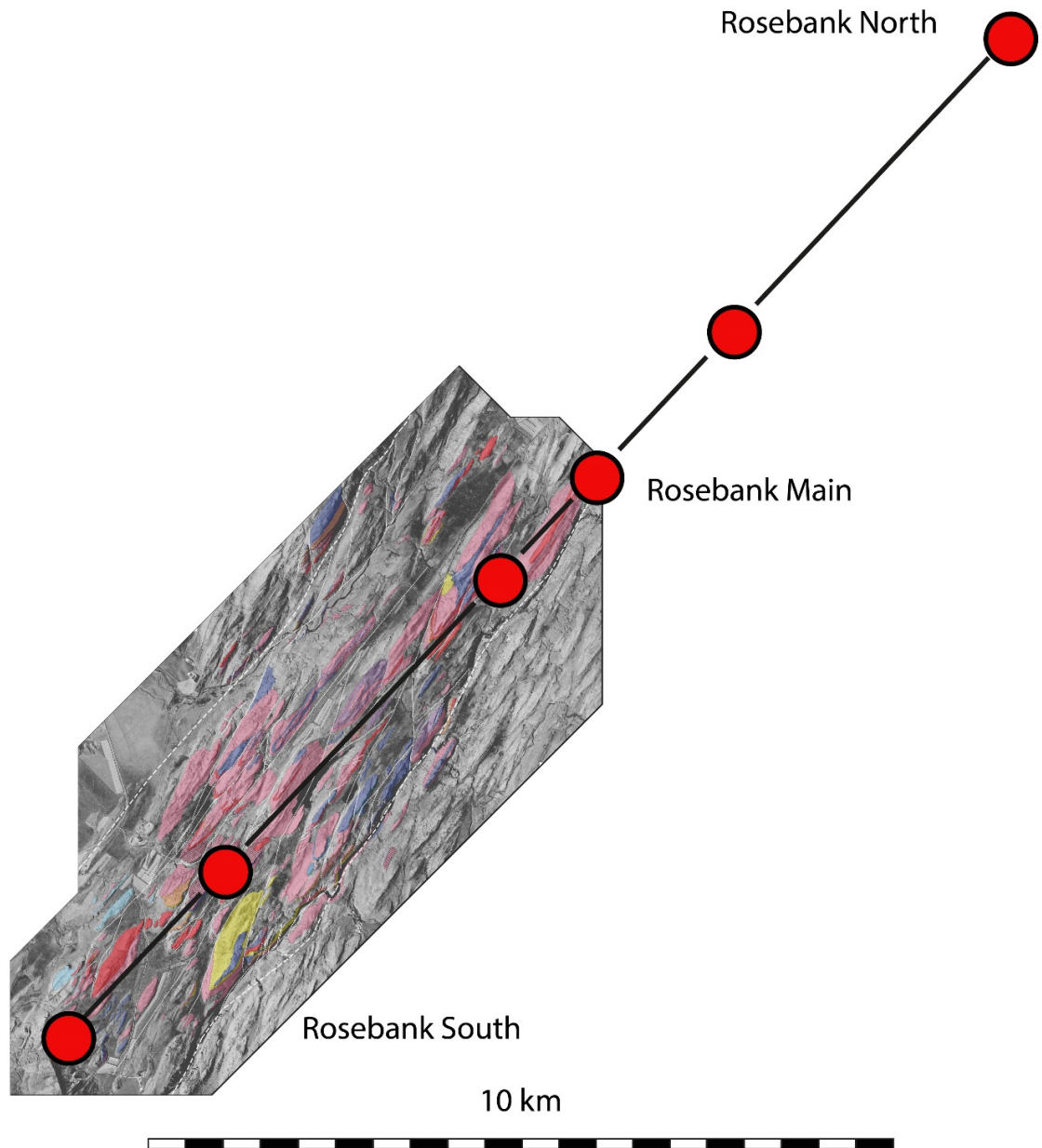


**Figure 9-33 Comparison of scale between the HF and the Rosebank well spacing in the FSB. The HF is approximately half the length of the Rosebank well spacing, suggesting that features observable within the HF could be present in the subsurface in the Rosebank Field.**

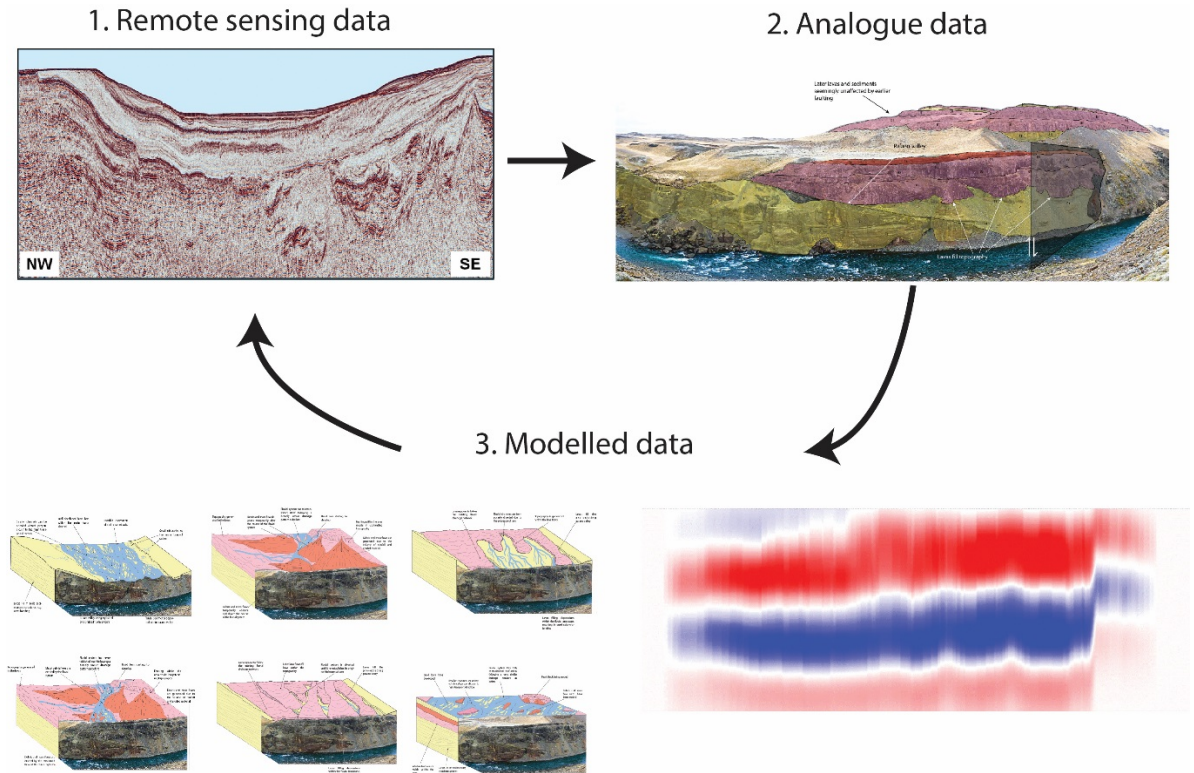


**Figure 9-34 Integration of data.** In order for exploration to be successful within volcanically dominated settings, all available data needs to be combined to create a coherent picture of the subsurface. Remote sensing data such as seismic data can initially be explored, but this needs to be compared with other data such as well data. There should then be a comparison with analogue data in order to compare and contrast various aspects of the prospect, such as connectivity of units. The analogue data should then be used to test the accuracy of models that have been created. All this data should then be fed back in to the remote sensing data, to further understand the prospect. The data can then be applied to exploration in similar areas.

## 9.8 Future exploration within volcanic dominated settings

Whilst exploration for hydrocarbons in volcanic dominated margins has numerous challenges associated with it, there is still a huge demand for oil and gas and as a result, exploration has to move to areas where exploration is more challenging in order to supply the demand; HP/HT areas, volcanic dominated environments, heavy oil to name a few. With volcanic dominated areas, it is important not to solely focus on the volcanics, but to understand how they may have positively or negatively interacted with the petroleum system.

Future exploration in volcanically dominated environments is targeting areas such as the UK Rockall Basin (Schofield et al, 2017), FSB in the UKCS 30<sup>th</sup> licensing round (2017), South Atlantic (Cameron et al, 1999; Jerram et al, 1999) and China (Wang

and Chen, 2015) (Figure 9-25). This exploration activity indicates that volcanic dominated environments continue to have the potential for hydrocarbon prospectively.

## 9.9 Conclusions

- Volcano sedimentary systems develop in a similar manner regardless of their location. The products of fluvial and volcanic systems (typically lavas and rivers) tend to occupy low lying topography, where it is easiest for them to flow.
- As the HF is Plio-Pleistocene in age, modern analogues in Iceland are generally comparable. This allows us to understand the processes which formed the HF in better detail and as a result, can also be applied to subsurface datasets.
- A tentative approach has been taken here to understand the spatial relationships between volcano sedimentary units within the HF. In doing so, this provides a basic predictive model which allows comparison between different volcano sedimentary settings. It also helps to quantitatively understand the HF.
- Hydrocarbon exploration within volcano sedimentary settings is particularly challenging, primarily due to the difficulties associated with imaging the subsurface beneath thick volcanic cover. In order to fully understand these settings in the subsurface, an analogue such as the HF has to be employed to ground truth models.

## 10 Conclusions and further work

The work in this project aims to inform and develop the current understanding of volcano-sedimentary settings and in doing so, aid hydrocarbon exploration in volcanic rifted margins. Volcanic rocks can affect all aspects of hydrocarbon systems and therefore, improve our understanding of how they develop and interact with other systems in 4D, will ultimately aid recovery of potential hydrocarbons. The work presented here on the HF at Flúðir demonstrates the variability in volcanic units; their thickness, geometries, lateral extent and degree of interaction with sediment.

By using the HF at Flúðir as a generic analogue of volcano sedimentary systems, each stage of hydrocarbon exploration from initial exploration to development and production can benefit from this work. The large scale elements of the HF at Flúðir, such as lateral connectivity of sedimentary units and volcanic units can aid with understanding the overall geometries of volcano sedimentary settings in the sub-surface. The study of the Stora Laxa river section can provide information on where reservoir units may occur and how these would develop with time. It will also aid understanding of how best to develop and produce a structurally complex, volcano sedimentary field. The work presented here on the HF at Flúðir also highlights the gap in information between the outcrop scale and the seismic scale, making it easy to identify where future works needs to be focussed and how best to do so.

### 10.1 Main findings of this work

This project has primarily focussed on field-based observations to better understand volcano sedimentary settings and their interpretation in hydrocarbon exploration. Field work has enabled detailed observations to be taken of the HF at Flúðir, such that complex sequences in volcano sedimentary settings can be understood at different scales.

Volcano sedimentary settings are complex and difficult to predict. Few studies have looked at the detailed architecture of these systems as a whole; however, by using the HF at Flúðir as a case study, the research presented here has highlighted important aspects of these systems:

- The development of the HF at Flúðir is strongly controlled by underlying structural geology of the system. This is important as it controls where fluvial drainage pathways occur, where lavas will flow and where water bodies develop. In order to understand the interaction between the volcanic and sedimentary systems there needs to be a good understanding of the structural evolution of the basin. In the case of the HF at Flúðir, the scale of the area is relatively small in terms of an offshore hydrocarbon field. If the HF was considered in offshore terms, the presence of so many volcanic units and the size of the area would inhibit accurate seismic imaging of the area, making it challenging to predict where reservoir intervals may occur. Further work needs to be done in order to accurately image smaller features in volcanic-dominated seismic data sets (see future work suggestion).
- Lavas will typically follow pre-existing lows within the topography. In environments where water plays a major role in the area, such as Iceland, the topographic lows are typically fluvial drainage pathways. In the HF, these are primarily controlled by the underlying structure and pre-existing volcanic units. As a result of lavas following these pathways, there is interaction with the underlying water-saturated sediment as the lavas and fluvial systems temporarily compete for accommodation space. This can generate peperite, pockets of hyaloclastite, pseudo pillows, and where lava enters water bodies such as lakes or the marine environment, pillows, hyaloclastite and reworked hyaloclastite can form depending on the environmental conditions. This can result in very irregular contacts between sedimentary units and volcanic units. As drainage pathways follow the topographic lows, this results in structural highs being avoided, which causes 'islands' (kipuka) of older geology being surrounded by new lava flows, until the lavas dominate the environment.
- If volcanic activity is significant, the drainage pathways can become dominated by lavas, reaching a point where they drainage pathways are eliminated. At this point, lavas will spread laterally, actively seeking topographic lows, until volcanic activity ceases. During volcanic quiescence, fluvial systems will generally re-establish in approximately the

same location, or parallel but off-flank, in which they previously occupied, resulting in the deposition of inter-lava sediments. However, the deposition of the lavas will control exactly where the new fluvial systems develop, due to the formation of topographic barriers that will divert these systems.

- The internal architecture of volcano-sedimentary environments is very heterogeneous and difficult to predict. This is due to many variable elements in a volcano sedimentary environment. Predicting where individual lithofacies may occur is very difficult even in an area like the HF, where the exposure is excellent, yet the underlying structure is so complex. Predicting lithofacies successions is easier, yet still remains a challenge. For instance, where lavas enter a water body, it is likely hyaloclastite, pillow lavas or reworked hyaloclastite will form, or even all three will form, yet predicting the extent of these is nearly impossible. However, if the underlying structure of the area is well known, then predicting, for instance, where water bodies and pillow lavas may form, is more tractable.
- Volcano sedimentary settings cannot be treated as simple layer-cake stratigraphies. They have complex architectures that are very heterogeneous and unpredictable, which makes working within these settings, offshore, difficult.
- The methods used in hydrocarbon exploration, such as seismic imaging and petrophysical analysis, are insufficient to fully understand the detail involved in volcano-sedimentary settings. Only the large-scale features in these environments are resolvable, making it challenging to understand aspects such as fluid flow. Facies models and forward models need to be refined in volcano-sedimentary settings to aid hydrocarbon exploration in these settings.

## 10.2 Further work

This project has been the first to examine the geology of the HF in detail and its use as an analogue for hydrocarbon exploration in volcano-sedimentary settings.

During this project, ideas for future work have arisen that would be complimentary to this project and could build upon the work that has been done here:

- Volcano sedimentary settings are very common, yet detailed case studies of individual areas are lacking. In order to understand these settings fully, more areas have to be studied. In doing so, this would enable areas to be compared and contrasted to determine which features of volcano-sedimentary settings are common and which are unique. This would involve characterizing an area through mapping, logging and modelling to determine how the area has evolved through geological time and in response to any potential underlying tectonic structure, fluvial regime, for example glacial and marine inputs. Comparing various localities in this style would provide a useful tool to model systems where very few data are available, and to develop end-member scenarios that may inform exploration and reservoir models.
- Hydrocarbon exploration typically involves using remote sensing tools to determine whether or not an area is prospective. These tools typically provide seismic and petrophysical data, yet their resolution of these is generally poor. Detailed forward-modelling of the outcrops such as those in the HF at Flúðir would bridge the gap between field data and offshore data, and also generate a database of seismic and petrophysical features of volcano sedimentary settings that could be used in hydrocarbon exploration.
- Combining the above two approaches in to one study, that examines synthetic seismic modelling of different volcano sedimentary environments, clearly has many benefits. These data could be combined with 3D photogrammetry to accurately create 3D models of the architectures of the volcano sedimentary environments. Detailed synthetic seismic data could be created for each of these models to then compare with real subsurface data. This would create a useful comparison of different areas, to again determine what is common and unique in volcano sedimentary environments.

# 11 Appendix

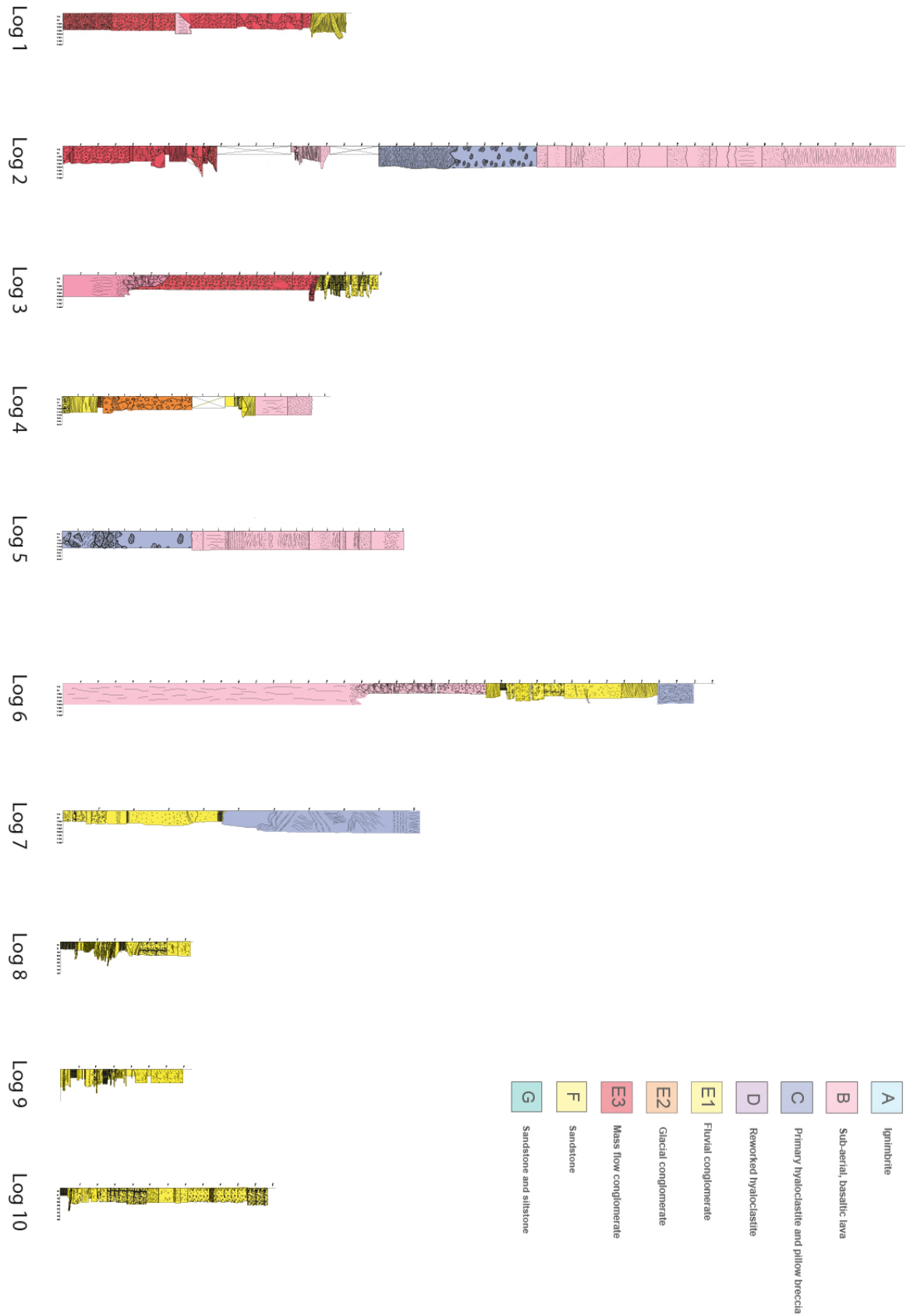


Figure 11-1 Graphic logs of the HF, 1-10.



Figure 11-2 Graphic logs of the HF, 11-20.



Figure 11-3 Graphic logs of the HF, 21-30.

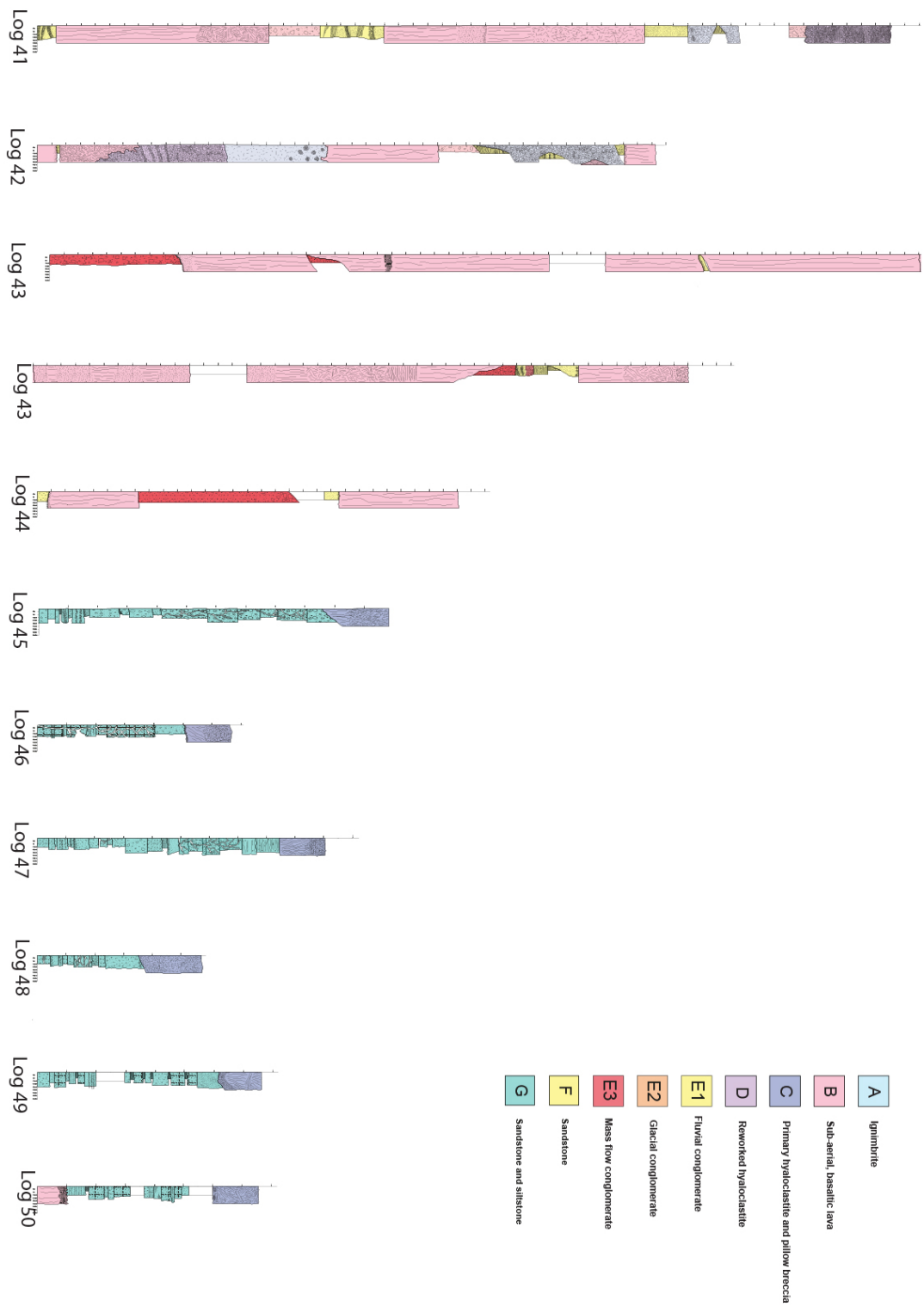


Figure 11-4 Graphic logs of the HF, 41-50.

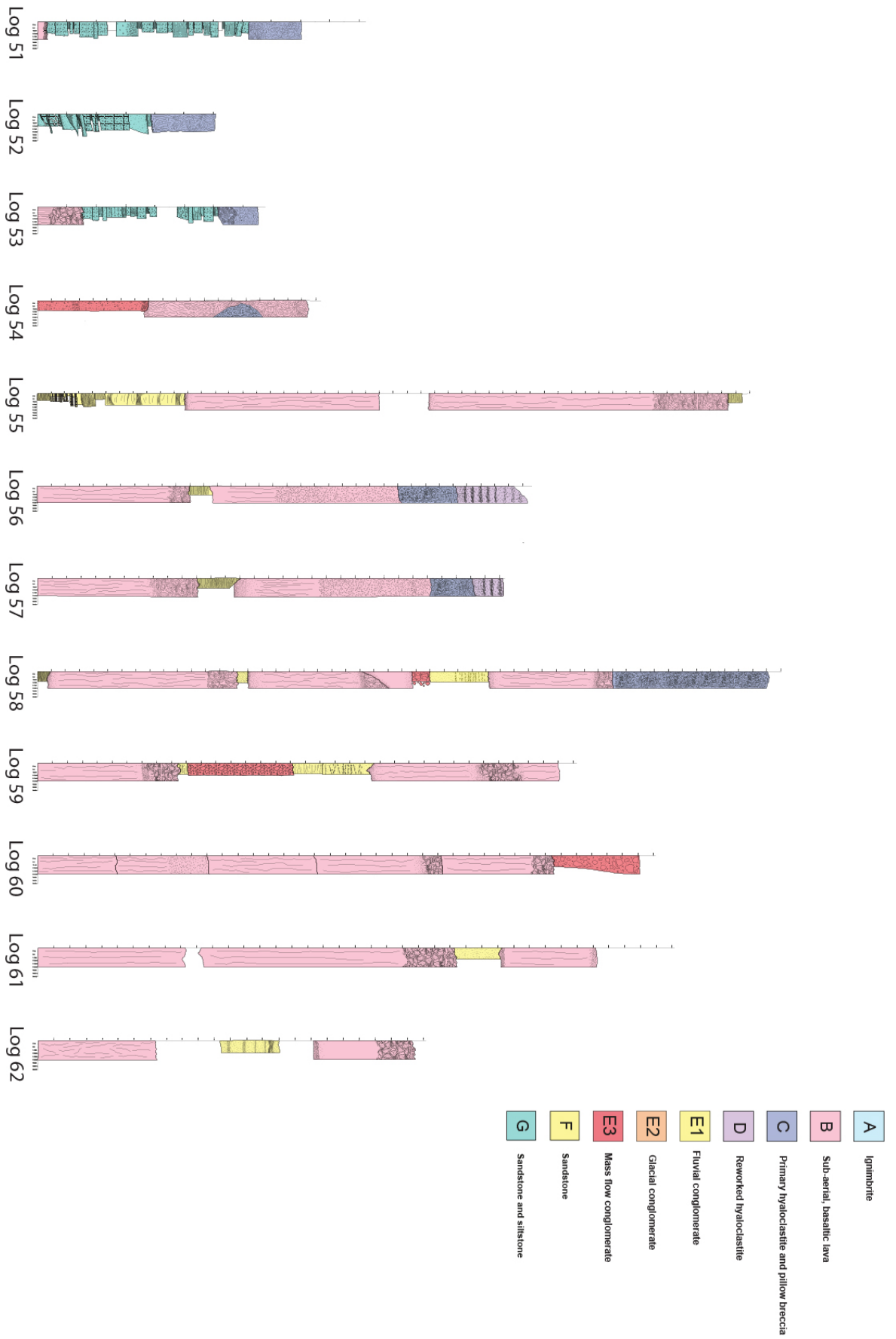


Figure 11-5 Graphic logs of the HF, 51-62.

## 12 References

Ashley, G., Shaw, J., and Smith, N., 1985, *Glacial Sedimentary Environments: SEPM*, Tulsa.

Ballantyne, C., 1991, Scottish landform examples – 2: The landslides of Trotternish, Isle of Skye: *Scottish Geographical Magazine*, v. 107, no. 2, p. 130-135.

Bennett, M. and Glasser, N., 2013, *Glacial geology: Ice sheets and landforms*, Wiley-Blackwell, Chichester.

Bennett, M., and Glasser, N., 2013, *Glacial geology*: Wiley-Blackwell, Chichester.

Bergerat, F., and Angelier, J., 2000, The South Iceland Seismic Zone: tectonic and sismotectonic analyses revealing the evolution from rifting to transform motion: *Journal of Geodynamics*, v. 29, no. 3-5, p. 211-231

Bergh, S. and Sigvaldason, G., 1991, Pleistocene mass-flow deposits of basaltic hyaloclastite on a shallow submarine shelf, South Iceland: *Bulletin of Volcanology*, v. 53, no. 8, p. 597-611

Biscardini, G., Morrison, R., Branson, D., and Del Maestro, A., 2017, 2017 Oil and Gas Trends. Adjusting business models to a period of recovery: PWC, 1-16

Bluck, B., 1974, Structure and directional properties of some valley sandur deposits in southern Iceland: *Sedimentology*, v. 21, no. 4, p. 533-554

Bondre, N., Duraiswami, R., and Dole, G., 2004, A brief comparison of lava flows from the Deccan Volcanic Province and the Columbia-Oregon Plateau Flood Basalts: Implications for models of flood basalt emplacement: *Journal of Earth System Science*, v. 113, no. 4, p. 809-817

Bourbié, T., Coussy, O., and Zinszner, B., 1987, *Acoustics of porous media*: Gulf, Houston.

Bowman, M., and Smyth, H., 2016, Reducing uncertainty and risk through field-based studies: Geological Society, London, Special Publications, v. 436, no. 1, p. 1-8

Branney, M. and Kokelaar, P., 1992, A reappraisal of ignimbrite emplacement: progressive aggradation and changes from particulate to non-particulate flow during emplacement of high-grade ignimbrite: *Bulletin of Volcanology*, v. 54, no. 6, p. 504-520

Branney, M. and Kokelaar, B., 2002, Pyroclastic density currents and the sedimentation of ignimbrites: Geological Society, London.

Breien, H., De Blasio, F., Elverhøi, A., and Høeg, K., 2008, Erosion and morphology of a debris flow caused by a glacial lake outburst flood, Western Norway: *Landslides*, v. 5, no. 3, p. 271-280

British Geological Survey, 1999, Classification of igneous rocks: BGS.

Brown, D. and Bell, B., 2006, Intrusion-induced uplift and mass wasting of the Palaeogene volcanic landscape of Ardnamurchan, NW Scotland: *Journal of the Geological Society*, v. 163, no. 1, p. 29-36

Brown, D. and Bell, B., 2007, Debris flow deposits within the Palaeogene lava fields of NW Scotland: evidence for mass wasting of the volcanic landscape during emplacement of the Ardnamurchan Central Complex: *Bulletin of Volcanology*, v. 69, no. 8, p. 847-868

Bryan, S., and Ferrari, L., 2013, Large igneous provinces and silicic large igneous provinces: Progress in our understanding over the last 25 years: *Geological Society of America Bulletin*, v. 125, no. 7-8, p. 1053-1078

Bubeck, A., Walker, R., Imber, J., Holdsworth, R., MacLeod, C., and Holwell, D., 2017, Rift zone-parallel extension during segmented fault growth: application to the evolution of the NE Atlantic: *Solid Earth Discussions*, p. 1-23

Cameron, N., Bate, R., Clure, V., and Benton, J., 1999, Oil and gas habitats of the South Atlantic: Introduction: Geological Society, London, Special Publications, v. 153, no. 1, p. 1-9,

Carrivick, J., and Tweed, F., 2013, Proglacial lakes: character, behaviour and geological importance: Quaternary Science Reviews, v. 78, p. 34-52

Cas, R. and Wright, J., 1987, Volcanic successions, modern and ancient: Allen & Unwin, London

Clifton, A., and Kattenhorn, S., 2006, Structural architecture of a highly oblique divergent plate boundary segment: Tectonophysics, v. 419, no. 1-4, p. 27-40

Collinson, J., 1996, Alluvial sediments, *in* Reading, H., Sedimentary Environments: Processes, Facies and Stratigraphy, Blackwell Science, Oxford, p. 37-82.

Costa, J., 1984, Physical geomorphology of debris flows., *in* Costa, J. and Fleischer, P., Developments and Applications in Geomorphology:, Springer Verlag, p. 268-317.

Costa, J., and Schuster, R., 1988, The formation and failure of natural dams: Geological Society of America Bulletin, v. 100, no. 7, p. 1054-1068,

Degraff, J. and Aydin, A., 1987, Surface morphology of columnar joints and its significance to mechanics and direction of joint growth: Geological Society of America Bulletin, v. 99, no. 5, p. 605,

Degraff, J., Long, P., and Aydin, A., 1989, Use of joint-growth directions and rock textures to infer thermal regimes during solidification of basaltic lava flows: Journal of Volcanology and Geothermal Research, v. 38, no. 3-4, p. 309-324,

Deloitte, 2015, Oil and Gas Reality Check 2015. A look at the top issues facing the oil and gas sector: Deloitte, 1-32 p.

Ebinghaus, A., Hartley, A., Jolley, D., Hole, M., and Millett, J., 2014, Lava-Sediment Interaction and Drainage-System Development In A Large Igneous

Province: Columbia River Flood Basalt Province, Washington State, U.S.A: *Journal of Sedimentary Research*, v. 84, no. 11, p. 1041-1063

Einarsson, P., 1991, Earthquakes and present-day tectonism in Iceland: *Tectonophysics*, v. 189, no. 1-4, p. 261-279

Einarsson, P., 2008, Plate boundaries, rifts and transforms in Iceland: *Jökull*, v. 58, p. 35-58.

Eiríksson, J., and Geirsdóttir, Á., 1991, A record of Pliocene and Pleistocene glaciations and climatic changes in the North Atlantic based on variations in volcanic and sedimentary facies in Iceland: *Marine Geology*, v. 101, no. 1-4, p. 147-159

Ellis, D., Stoker, M. S. 2014. The Faroe-Shetland Basin: a regional perspective from the Paleocene to the present day and its relationship to the opening of the North Atlantic Ocean. *Journal of the Geological Society, London, Special Publications*, **397**, 11-31.

Eyles, N., Eyles, C., and Miall, A., 1983, Lithofacies types and vertical profile models; an alternative approach to the description and environmental interpretation of glacial diamict and diamictite sequences: *Sedimentology*, v. 30, no. 3, p. 393-410

Farooqui, M., Hou, H., Li, G., Machin, N., Neville, T., Pal, A., Shrivastva, C., Wang, Y., Yang, F., Yin, C., Zhao, J., and Yang, X., 2009, Evaluating Volcanic Reservoirs: *Oilfield Review*, , no. 1, p. 36-47.

Fisher, R., 1961, Proposed classification of volcanoclastic sediments and rocks: *Geological Society of America Bulletin*, v. 72, no. 9, p. 1409

Fisher, R., 1984, Submarine volcanoclastic rocks: *Geological Society, London, Special Publications*, v. 16, no. 1, p. 5-27

Fitton, JG., Saunders, AD., Larsen, LM., Hardarson, BS., and Norry, MJ., 1998. Volcanic rocks from the southeast Greenland margin at 63°N: composition,

petrogenesis and mantle sources., *in* Saunders, AD., Larsen, HC. and SW, Wise.,(eds) Proceedings of the Ocean Drilling Project, Scientific Results, 152, p. 331-350.

Gallagher, J., and Dromgoole, P., 2007, Exploring below the basalt, offshore Faroes: a case history of sub-basalt imaging: *Petroleum Geoscience*, v. 13, no. 3, p. 213-225

Geirsdóttir, Á., and Eiríksson, J., 1994, Growth of an Intermittent Ice Sheet in Iceland during the Late Pliocene and Early Pleistocene: *Quaternary Research*, v. 42, no. 02, p. 115-130

Geoffroy, L., 2005, Volcanic passive margins: *Comptes Rendus Geoscience*, v. 337, no. 16, p. 1395-1408,

Gray, J., 2013, Petroleum prospectivity of the principal sedimentary basins on the United Kingdom Continental Shelf: Department of Energy and Climate Change.

Guilbaud, M., Self, S., Thordarson, T., and Blake, S., 2005, Morphology, surface structures, and emplacement of lavas produced by Laki, A.D. 1783-1784: Special Paper 396: Kinematics and dynamics of lava flows, p. 81-102

Holford, S., Schofield, N., Jackson, C., Green, P., and Duddy, I., 2013, Impacts of Igneous Intrusions on Source and Reservoir Potential in Prospective Sedimentary Basins Along the Western Australian Continental Margin, in *West Australia Basins Symposium*,.

Hon, K., Gansecki, C., and Kauahikaua, J., 2003, The Transition from 'A'ä to Pāhoehoe Crust on Flows Emplaced During the Pu'u 'Ö'ö-Kūpaianaha Eruption, *in* Heliker, C., Swanson, D. and Takahashi, T., The Pu ' u ' Ö ' ö-Kūpaianaha eruption of Kilauea Volcano, Hawai ' i: the first 20 years., USGS Professional Paper 1676, p. 89-103.

Hon, K., Kauahikaua, J., Denlinger, R., and Mackay, K., 1994, Emplacement and inflation of pahoehoe sheet flows: Observations and measurements of active lava

flows on Kilauea Volcano, Hawaii: Geological Society of America Bulletin, v. 106, no. 3, p. 351-370

Hungr, O., Evans, S., Bovis, M., and Hutchinson, J., 2001, A review of the classification of landslides of the flow type: Environmental & Engineering Geoscience, v. 7, no. 3, p. 221-238

Hurst, A., Scott, A., and Vigorito, M., 2011, Physical characteristics of sand injectites: Earth-Science Reviews, v. 106, no. 3-4, p. 215-246

Innes, J., 1983, Debris flows: Progress in Physical Geography, v. 7, no. 4, p. 469-501

Jerram, D., 2015, Hot Rocks and Oil: Are Volcanic Margins the New Frontier?: Elsevier R&D Solutions FOR OIL AND GAS,.

Jerram, D., and Widdowson, M., 2005, The anatomy of Continental Flood Basalt Provinces: geological constraints on the processes and products of flood volcanism: Lithos, v. 79, no. 3-4, p. 385-405

Jerram, D., Mountney, N., and Stollhofen, H., 1999, Facies architecture of the Etjo Sandstone Formation and its interaction with the Basal Etendeka Flood Basalts of northwest Namibia: implications for offshore prospectivity: Geological Society, London, Special Publications, v. 153, no. 1, p. 367-380

Jerram, D., Svensen, H., Planke, S., Polozov, A., and Torsvik, T., 2016, The onset of flood volcanism in the north-western part of the Siberian Traps: Explosive volcanism versus effusive lava flows: Palaeogeography, Palaeoclimatology, Palaeoecology, v. 441, p. 38-50

Kassab, M., and Weller, A., 2015, Study on P-wave and S-wave velocity in dry and wet sandstones of Tushka region, Egypt: Egyptian Journal of Petroleum, v. 24, no. 1, p. 1-11

Keszthelyi, L., and Self, S., 1998, Some physical requirements for the emplacement of long basaltic lava flows: *Journal of Geophysical Research: Solid Earth*, v. 103, no. B11, p. 27447-27464,

Keszthelyi, L., McEwen, A., and Thordarson, T., 2000, Terrestrial analogs and thermal models for Martian flood lavas: *Journal of Geophysical Research: Planets*, v. 105, no. E6, p. 15027-15049,

Koehn, D., Aanyu, K., Haines, S., and Sachau, T., 2008, Rift nucleation, rift propagation and the creation of basement micro-plates within active rifts: *Tectonophysics*, v. 458, no. 1-4, p. 105-116

Kristjánsson, L., Duncan, R., and Guðmundsson, Á., 2008, Stratigraphy, palaeomagnetism and age of volcanics in the upper regions of ÞJórsárdalur valley, central southern Iceland: *Boreas*, v. 27, no. 1, p. 1-13

Loizou, N., Liu, E., and Chapman, M., 2008, AVO analyses and spectral decomposition of seismic data from four wells west of Shetland, UK: *Petroleum Geoscience*, v. 14, no. 4, p. 355-368

Long, P. and Wood, B., 1986, Structures, textures, and cooling histories of Columbia River basalt flows: *Geological Society of America Bulletin*, v. 97, no. 9, p. 1144,

Lundin, E., and Doré, A., 2005, Fixity of the Iceland “hotspot” on the Mid-Atlantic Ridge: Observational evidence, mechanisms, and implications for Atlantic volcanic margins, *in* G.R, Foulger., J.H, Natland., D.C, Presnall. and D.L, Anderson., *Plates, Plumes and Paradigms*, Geological Society of America Special Papers, p. 627-651.

Lundin, E., and Doré, A., 2005, NE Atlantic break-up: a re-examination of the Iceland plume model and the Atlantic-Arctic linkage., *in* *Petroleum Geology: North-West Europe and Global Perspectives - Proceedings of the 6th Petroleum Geology Conference.*, Geological Society, London, p. 739-754.

- Lunt, I., Bridge, J., and Tye, R., 2004, A quantitative, three-dimensional depositional model of gravelly braided rivers: *Sedimentology*, v. 51, no. 3, p. 377-414
- Lyle, P. and Preston, J., 1998, The Influence of Eruptive Conditions on Joint Development in the Causeway Tholeiite Member of the Tertiary Antrim Lava Group, Northern Ireland: *Irish Journal of Earth Sciences*, v. 16, p. 19-32.
- Lyle, P., 2000, The eruption environment of multi-tiered columnar basalt lava flows: *Journal of the Geological Society*, v. 157, no. 4, p. 715-722,
- M. Church 1972. Baffin Island Sandurs: a study of Arctic fluvial Processes. Geological Survey of Canada Bulletin 216. 208 pp.,
- Macdonald, G., 1953, Pahoehoe, aa, and block lava: *American Journal of Science*, v. 251, no. 3, p. 169-191
- Macdonald, K., Fox, P., Alexander, R., Pockalny, R., and Gente, P., 1996, Volcanic growth faults and the origin of Pacific abyssal hills: *Nature*, v. 380, no. 6570, p. 125-129
- MacPhie, J., Doyle, M. and Allen, R. (1993). *Volcanic textures*. Hobart: ARC Centre of Excellence in Ore Deposits, University of Tasmania.
- Maizels, J., 1997, Jökulhlaup deposits in proglacial areas: *Quaternary Science Reviews*, v. 16, no. 7, p. 793-819, doi: 10.1016/s0277-3791(97)00023-1
- Marshall, P., Widdowson, M., and Murphy, D., 2016, The Giant Lavas of Kalkarindji: rubbly pāhoehoe lava in an ancient continental flood basalt province: *Palaeogeography, Palaeoclimatology, Palaeoecology*, v. 441, p. 22-37
- McPhie, J., Doyle, M., and Allen, R., 1993, *Volcanic Textures: a Guide to the Interpretation of Textures in Volcanic Rocks.*: Tasmania Centre for Ore Deposit and Exploration Studies, Hobart.

Menzies, M., Klemperer, S., Ebinger, C., and Baker, J., 2002, Characteristics of volcanic rifted margins: Special Paper 362: Volcanic Rifted Margins, p. 1-14

Miall, A., 1985, Architectural-element analysis: A new method of facies analysis applied to fluvial deposits: *Earth-Science Reviews*, v. 22, no. 4, p. 261-308

Millett, J., Wilkins, A., Campbell, E., Hole, M., Taylor, R., Healy, D., Jerram, D., Jolley, D., Planke, S., Archer, S. and Blischke, A. (2016). The geology of offshore drilling through basalt sequences: Understanding operational complications to improve efficiency. *Marine and Petroleum Geology*, 77, pp.1177-1192.

Mjelde, R., Breivik, A. J., Raum, T., Mittelstaedt, E., Ito, G., Faleide, J. I. 2008. Magmatic and tectonic evolution of the North Atlantic. *Journal of the Geological Society, London*, 165, p31-42.

Moy, D., and Imber, J., 2009, A critical analysis of the structure and tectonic significance of rift-oblique lineaments ('transfer zones') in the Mesozoic-Cenozoic succession of the Faroe-Shetland Basin, NE Atlantic margin: *Journal of the Geological Society*, v. 166, no. 5, p. 831-844

Muirhead, D., Bowden, S., Parnell, J., and Schofield, N., 2017, Source rock maturation owing to igneous intrusion in rifted margin petroleum systems: *Journal of the Geological Society*, p. jgs2017-011

Naylor, P., Bell, B., Jolley, D., Durnall, P. and Fredsted, R. (1999). Palaeogene magmatism in the Faeroe-Shetland Basin: influences on uplift history and sedimentation. In: *Petroleum Geology of Northwest Europe: Proceedings of the 5<sup>th</sup> Conference*. Geological Society, London, pp.545-558.

Nelson, C., Jerram, D., and Hobbs, R., 2009, Flood basalt facies from borehole data: implications for prospectivity and volcanology in volcanic rifted margins: *Petroleum Geoscience*, v. 15, no. 4, p. 313-324

Owen, A., Nichols, G., Hartley, A., Weissmann, G., and Scuderi, L., 2015, Quantification of a Distributive Fluvial System: The Salt Wash DFS of the Morrison Formation, SW U.S.A.: *Journal of Sedimentary Research*, v. 85, no. 5, p. 544-561

Passerini, P., Marcucci, M., Sguazzoni, G., and Pecchioni, E., 1997, Longitudinal strike-slip faults in oceanic rifting: a mesostructural study from western to southeastern Iceland: *Tectonophysics*, v. 269, no. 1-2, p. 65-89

Passey, S. and Bell, B., 2007, Morphologies and emplacement mechanisms of the lava flows of the Faroe Islands Basalt Group, Faroe Islands, NE Atlantic Ocean: *Bulletin of Volcanology*, v. 70, no. 2, p. 139-156,

Passey, S., 2009, Recognition of a faulted basalt lava flow sequence through the correlation of stratigraphic marker units, Skopunarfjørður, Faroe Islands, in Varming, T. and Ziska, H. Faroe Islands Exploration Conference: Proceeding of the 2<sup>nd</sup> Conference. *Annales Societatis Scientiarum Færoensis*, Tórshavn, 50, 2009:174-204.

Perregaard, J., and Schiener, E., 1979, Thermal alteration of sedimentary organic matter by a basalt intrusive (Kimmeridgian Shales, Milne Land, east Greenland): *Chemical Geology*, v. 26, no. 3-4, p. 331-343

Peterson, D. and Tilling, R., 1980, Transition of basaltic lava from pahoehoe to aa, Kilauea Volcano, Hawaii: Field observations and key factors: *Journal of Volcanology and Geothermal Research*, v. 7, no. 3-4, p. 271-293

Poppitt, S., Duncan, L., Preu, B., Fazzari, F., and Archer, J., 2015, The influence of volcanic rocks on the characterization of Rosebank Field - new insights from ocean-bottom seismic data and geological analogues integrated through interpretation and modelling, in *Petroleum geology of NW Europe: 50 years of learning- Proceedings of the 8th Petroleum Geology Conference*, Geological Society, London.

Rateau, R., Schofield, N., and Smith, M., 2013, The potential role of igneous intrusions on hydrocarbon migration, West of Shetland: *Petroleum Geoscience*, v. 19, no. 3, p. 259-272

Rawcliffe, H. and Brown, D., 2014, Lithofacies architecture of basaltic andesite lavas and their interaction with wet-sediment: Port a' Chroinn, Kerrera, NW Scotland: *Scottish Journal of Geology*, v. 50, no. 1, p. 49-55

Reading, H., 2002, *Sedimentary environments*: Blackwell Science, Oxford.

Reubi, O., Ross, P., and White, J., 2005, Debris avalanche deposits associated with large igneous province volcanism: An example from the Mawson Formation, central Allan Hills, Antarctica: *Geological Society of America Bulletin*, v. 117, no. 11, p. 1615

Rodriguez Monreal, F., Villar, H., Baudino, R., Delpino, D., and Zencich, S., 2009, Modeling an atypical petroleum system: A case study of hydrocarbon generation, migration and accumulation related to igneous intrusions in the Neuquen Basin, Argentina: *Marine and Petroleum Geology*, v. 26, no. 4, p. 590-605

Rowland, S., and Walker, G., 1990, Pahoehoe and aa in Hawaii: volumetric flow rate controls the lava structure: *Bulletin of Volcanology*, v. 52, no. 8, p. 615-628

Sassa, K., and Wang, G. Mechanism of landslide-triggered debris flows: Liquefaction phenomena due to the undrained loading of torrent deposits: *Debris-flow Hazards and Related Phenomena*, p. 81-104

Schmincke, H. and Swanson, D., 1967, Laminar Viscous Flowage Structures in Ash-Flow Tuffs from Gran Canaria, Canary Islands: *The Journal of Geology*, v. 75, no. 6, p. 641-644

Schofield, N., and Jolley, D., 2013, Development of intra-basaltic lava-field drainage systems within the Faroe-Shetland Basin: *Petroleum Geoscience*, v. 19, no. 3, p. 273-288

Schofield, N., and Jolley, D., 2013, Development of intra-basaltic lava-field drainage systems within the Faroe-Shetland Basin: *Petroleum Geoscience*, v. 19, no. 3, p. 273-288

Schofield, N., and Jolley, D., 2013, Development of intra-basaltic lava-field drainage systems within the Faroe-Shetland Basin: *Petroleum Geoscience*, v. 19, no. 3, p. 273-288

Schofield, N., Holford, S., Millett, J., Brown, D., Jolley, D., Passey, S., Muirhead, D., Grove, C., Magee, C., Murray, J., Hole, M., Jackson, C., and Stevenson, C., 2015, Regional magma plumbing and emplacement mechanisms of the Faroe-Shetland Sill Complex: implications for magma transport and petroleum systems within sedimentary basins: *Basin Research*, v. 29, no. 1, p. 41-63

Schofield, N., Jolley, D., Holford, S., Archer, S., Watson, D., Hartley, A., Howell, J., Muirhead, D., Underhill, J., and Green, P., 2017, Challenges of future exploration within the UK Rockall Basin: Geological Society, London, *Petroleum Geology Conference series*, p. PGC8.37

Schutter, S., 2003, Hydrocarbon occurrence and exploration in and around igneous rocks: Geological Society, London, *Special Publications*, v. 214, no. 1, p. 7-33

Schutter, S., 2003, Occurrences of hydrocarbons in and around igneous rocks, in Petford, N. and McCaffrey, K., *Hydrocarbons in Crystalline Rocks*, The Geological Society of London, London.

Self, S., Keszthelyi, L., and Thordarson, T., 1998, THE IMPORTANCE OF PĀHOEHOE: *Annual Review of Earth and Planetary Sciences*, v. 26, no. 1, p. 81-110

Self, S., Schmidt, A., and Mather, T., 2014, Emplacement characteristics, time scales, and volcanic gas release rates of continental flood basalt eruptions on Earth: *Geological Society of America Special Papers*, p. 319-337

Self, S., Thordarson, T., and Keszthelyi, L., 1997, Emplacement of Continental Flood Basalt Lava Flows, *in* Mahoney, J. and Coffin, F., Large Igneous Provinces: Continental, Oceanic, and Planetary Flood Volcanism, American Geophysical Union, Washington D.C.

Self, S., Thordarson, T., Keszthelyi, L., Walker, G., Hon, K., Murphy, M., Long, P., and Finnemore, S., 1996, A new model for the emplacement of Columbia River basalts as large, inflated Pahoehoe Lava Flow Fields: *Geophysical Research Letters*, v. 23, no. 19, p. 2689-2692,

Sigmundsson, F., Einarsson, P., Bilham, R., and Sturkell, E., 1995, Rift-transform kinematics in south Iceland: Deformation from Global Positioning System measurements, 1986 to 1992: *Journal of Geophysical Research: Solid Earth*, v. 100, no. B4, p. 6235-6248

Single, R., and Jerram, D., 2004, The 3D facies architecture of flood basalt provinces and their internal heterogeneity: examples from the Palaeogene Skye Lava Field: *Journal of the Geological Society*, v. 161, no. 6, p. 911-926

Skilling, I., White, J., and McPhie, J., 2002, Peperite: a review of magma-sediment mingling: *Journal of Volcanology and Geothermal Research*, v. 114, no. 1-2, p. 1-17

Smallwood, J., and White, R., 2002, Ridge-plume interaction in the North Atlantic and its influence on continental breakup and seafloor spreading: *Geological Society, London, Special Publications*, v. 197, no. 1, p. 15-37

Smellie, J., and Skilling, I., 1994, Products of subglacial volcanic eruptions under different ice thicknesses: two examples from Antarctica: *Sedimentary Geology*, v. 91, no. 1-4, p. 115-129

Stephens, T., Walker, R., Healy, D., Bubeck, A., England, R., and McCaffrey, K., 2017, Igneous sills record far-field and near-field stress interactions during volcano construction: Isle of Mull, Scotland: *Earth and Planetary Science Letters*, v. 478, p. 159-174

Syvitski, J., Jennings, A., and Andrews, J., 1999, High-Resolution Seismic Evidence for Multiple Glaciation across the Southwest Iceland Shelf: Arctic, Antarctic, and Alpine Research, v. 31, no. 1, p. 50

Tavani, S., Granado, P., Corradetti, A., Girundo, M., Iannace, A., Arbués, P., Muñoz, J. and Mazzoli, S. (2014). Building a virtual outcrop, extracting geological information from it, and sharing the results in Google Earth via OpenPlot and Photoscan: An example from the Khaviz Anticline (Iran). *Computers & Geosciences*, 63, pp.44-53.

Thordarson, T., 2012, Outline of Geology of Iceland, in Chapman Conference,.Thordarson, T. and Höskuldsson, A. (2014). *Iceland*. Edinburgh: Dunedin

Thordarson, T., and Höskuldsson, A., 2014, Iceland: Dunedin Academic, Edinburgh.

Thordarson, T., and Larsen, G., 2007, Volcanism in Iceland in historical time: Volcano types, eruption styles and eruptive history: *Journal of Geodynamics*, v. 43, no. 1, p. 118-152

Thordarson, T., and Self, S., 1998, The Roza Member, Columbia River Basalt Group: A gigantic pahoehoe lava flow field formed by endogenous processes?: *Journal of Geophysical Research: Solid Earth*, v. 103, no. B11, p. 27411-27445,

Van Gorp, W., Veldkamp, A., Temme, A., Maddy, D., Demir, T., van der Schriek, T., Reimann, T., Wallinga, J., Wijbrans, J., and Schoorl, J., 2013, Fluvial response to Holocene volcanic damming and breaching in the Gediz and Geren rivers, western Turkey: *Geomorphology*, v. 201, p. 430-448,

Vosgerau, H., Passey, S., Svennevig, K., Strunck, M., and Jolley, D., 2015, Reservoir architectures of interlava systems: a 3D photogrammetrical study of Eocene cliff sections, Faroe Islands: Geological Society, London, Special Publications, v. 436, no. 1, p. 55-73

Waite, R. (2007). Primary volcanoclastic rocks: COMMENT and REPLY: COMMENT. *Geology*, 35(1), pp.e141-e141.

Walker, G., 1971, Compound and simple lava flows and flood basalts: *Bulletin Volcanologique*, v. 35, no. 3, p. 579-590

Walker, G., 1993, Basaltic-volcano systems: Geological Society, London, Special Publications, v. 76, no. 1, p. 3-38

Walker, R., Holdsworth, R., Imber, J., and Ellis, D., 2012, Fault-zone evolution in layered basalt sequences: A case study from the Faroe Islands, NE Atlantic margin: *Geological Society of America Bulletin*, v. 124, no. 7-8, p. 1382-1393

Walker, R., Holdsworth, R., Imber, J., Faulkner, D., and Armitage, P., 2013, Fault zone architecture and fluid flow in interlayered basaltic volcanoclastic-crystalline sequences: *Journal of Structural Geology*, v. 51, p. 92-104

Walton, A., and Schiffman, P., 2003, Alteration of hyaloclastites in the HSDP 2 Phase 1 Drill Core 1. Description and paragenesis: *Geochemistry, Geophysics, Geosystems*, v. 4, no. 5, p. n/a-n/a,

Wang, P., and Chen, S., 2015, Cretaceous volcanic reservoirs and their exploration in the Songliao Basin, northeast China: *AAPG Bulletin*, v. 99, no. 03, p. 499-523

Watton, T., 2013, A multidisciplinary assessment of hyaloclastite deposits in petroleum systems using field studies, drill core, borehole image and wire-line log datasets [PhD]: Durham University.

Watton, T., Jerram, D., Thordarson, T., and Davies, R., 2013, Three-dimensional lithofacies variations in hyaloclastite deposits: *Journal of Volcanology and Geothermal Research*, v. 250, p. 19-33

Werner, R. and Schmincke, H., 1999, Englacial vs lacustrine origin of volcanic table mountains: evidence from iceland: *Bulletin of Volcanology*, v. 60, no. 5, p. 335-354

White, J. and Houghton, B. (2006). Primary volcanoclastic rocks. *Geology*, 34(8), p.677.

White, J. and Houghton, B. (2007). Primary volcanoclastic rocks: COMMENT and REPLY: REPLY. *Geology*, 35(1), pp.e142-e142.

White, J., and Riggs, N., 2009, Introduction: styles and significance of lacustrine volcanoclastic sedimentation, *in* White, J. and Riggs, N., *Volcanoclastic Sedimentation in Lacustrine Settings*, Science, p. 1-6.

White, J., McPhie, J., and Soule, S., 2000, Submarine Lavas and Hyaloclastite, *in* Sigurdsson, H., Bruce, H., Stephen, M., Hazel, R. and John, S., *Encyclopedia of Volcanoes*, Academic Press

Williamson, I., and Bell, B., 2012, The Staffa Lava Formation: graben-related volcanism, associated sedimentation and landscape character during the early development of the Palaeogene Mull Lava Field, NW Scotland: *Scottish Journal of Geology*, v. 48, no. 1, p. 1-46

Woodburn, N., Hardwick, A., Masoomzadeh, H., and Travis, T., 2014, Improved signal processing for sub-basalt imaging: Geological Society, London, *Special Publications*, v. 397, no. 1, p. 163-171

Wright, K., 2013, *Seismic Stratigraphy and Geomorphology of Palaeocene Volcanic Rocks, Faroe-Shetland Basin [PhD]: Durham University.*

Zielinski, T., and Van Loon, A., 2003, Pleistocene sandur deposits represent braidplains, not alluvial fans: *Boreas*, v. 32, no. 4, p. 590-61